GENETIC IDENTIFICATION AND BIOCHEMICAL CHARACTERIZATION OF XYLAN BACKBONE SYNTHASES IN ARABIDOPSIS AND POPLAR

by

CHANHUI LEE

(Under the Direction of Zheng-Hua Ye)

ABSTRACT

Xylan is the second most abundant polysaccharide in plant cell walls. However, its biosynthesis including the initiation and elongation of xylosyl backbone, side chain addition, and sugar modification, is still poorly understood. In an effort to identify xylan biosynthetic enzymes, we first profiled a number of upregulated genes during the process of the secondary cell wall formation. *PARVUS* was specifically expressed in the fibers and vessels, and its encoding protein was localized in the endoplasmic reticulum. Mutant phenotypes and structure analysis of xylans from the *parvus* mutant stems clearly showed its involvement in the biosynthesis of reducing end sequence of the xylan. Recent genetic and molecular studies in *Arabidopis* have shown that two proteins in glycosyltransferase (GT) 43 family, IRX9 and IRX14, are golgi-localized GTs, genetic defects of which result in a xylan deficient phenotype and a significant reduction in xylan chain length. In addition, the *in-vitro* activity assay with stem microsomes revealed that *irx9* and *irx14* mutants possess substantially lower xylosyltransferase activity compared with the wild type, suggesting their possible roles in xylan backbone polymerization. Comprehensive genetic analysis of the four Arabidopsis GT43 members provides evidence that all four Arabidopsis

GT43 members are involved in xylan biosynthesis and suggests that they form two functionally nonredundant groups essential for the normal elongation of xylan backbone. Multiple lines of evidence indicate that GTs involved in xylan biosynthesis are highly conserved between *Arabidopsis* and Poplar. Complementation studies revealed that PtrGT43 A/B/E are functional homologs of *Arabidopsis* IRX9, and PtrGT43 C/D are homologs of IRX14, forming two functionally nonredundant groups, which are required for the polymerization of xylan backbone. The studies presented here provide a wealth of genetic information that expands the knowledge of xylan biosynthesis.

INDEX WORDS: Arabidopsis, Poplar, Microsomes, Xylan, Glycosyltransferase, Xylan synthase, Secondary cell walls, Plant cell wall, Cell wall biosynthesis, *parvus*, *irregular xylem 9* (*irx9*), *irregular xylem 14* (*irx14*)

GENETIC IDENTIFICATION AND BIOCHEMICAL CHARACTERIZATION OF XYLAN BACKBONE SYNTHASES IN ARABIDOPSIS AND POPLAR

by

CHANHUI LEE

B.S., Chungnam National University, The Republic of Korea, 2003

M.S., Chungnam National University, The Republic of Korea, 2005

A Dissertation Submitted to the Graduate Faculty of The University of Georgia in Partial Fulfillment of the Requirements for the Degree

DOCTOR OF PHILOSOPHY

ATHENS, GEORGIA

2011

GENETIC IDENTIFICATION AND BIOCHEMICAL CHARACTERIZATION OF XYLAN BACKBONE SYNTHASES IN ARABIDOPSIS AND POPLAR

by

CHANHUI LEE

Major Professor: Zheng-Hua Ye

Committee: Michelle Momany
Carl M. Deom
Xiaoyu Zhang
Wolfgang Lukowitz

Electronic Version Approved:

Maureen Grasso

Dean of the Graduate School
The University of Georgia
May 2011

DEDICATION

To my wife and family for their love and support and my son, Hajoon Lee.

ACKNOWLEDGEMENTS

I am exceedingly fortunate to have Dr Zheng-Hua Ye as my major advisor during the past five years. He continues to influence me as a scientist and as a person. Without his willingness to help and support my projects, I would not have achieved this goal. I would like to thank all current and past members in the Ye lab, especially Ruiqin Zhong for giving me endless help and a warm heart. I would like to express many thanks to my committee members, Michelle Momany, Carl M. Deom, Xiaoyu Zhang, and Wolfgang Lukowitz, for their help, great comments and suggestions about my project. I would like to thank all departmental staff for their work, especially Susan Watkins and Kristin Meents. I would like to thank the greenhouse staff, Michael Boyd, Jeff, and Kevin Tarner for taking good care of our plants. I am also very grateful to Beth Richardson for her help and expertise on microscopic analysis and sample sectioning. All the resources of UGA, especially MALDI-TOF from Chemistry department, were great for my research and training. I would like to thank Dr Quincy Teng in EPA for NMR analysis. Finally, I acknowledge my family and friends, who provided unending love and support throughout this journey.

TABLE OF CONTENTS

LIST OF TABLES

LIST OF FIGURES

CHAPTER 1

INTRODUCTION AND LITERATURE REVIEW

One of the most distinctive features of plant cells is the deposition of walls outside the plasma membrane during cytokinesis. Since the structural framework of cell walls is mostly composed of a mixture of different polysaccharides, the final architecture of cell walls requires several enzymatic reactions including nucleotide sugar interconversion, polysaccharide biosynthesis, transport, and their assembly. Also, given the fact that the composition and amount of cell walls vary among cell types, the enzymatic reactions should be temporally and spatially controlled for the proper deposition and assembly of cell wall components in order for each cell type to perform its functional role. The cell wall is classified into two types, primary and secondary cell walls, primarily based on its location and polysaccharide composition. Whereas the primary cell wall is mainly composed of cellulose, xyloglucan, and pectin, thick secondary wall is made of cellulose, xylan, mannan, and lignin. With the exception of lignin, all other polymers are synthesized by the actions of glycosyltransferase (GT) that catalyze the attachment of activated donor sugars onto the acceptor substrates. *Arabidopsis* genome contains 445 GTs classified into 40 different families based on amino acid sequence similarity (CAZy; www.cazy.org/). Only a few of them are biochemically characterized in detail. Forward/reverse genetic studies demonstrated that mutation of some of GTs in several species resulted in the wide range of developmental phenotypes, including collapsed xylem, dwarfing, and sterility.

CELLULOSE BIOSYNTHESIS

Cellulose, β-1,4-linked glucose polymer without any substitution, is the most abundant biopolymer produced by vascular plants (Taylor, 2008). Cellulose in the cell wall of higher plants exists as a form of crystallized microfibrils, self-assembled and hydrogen-bonded β-1,4-glucan chains, to serve as a load-bearing network in which other hemicelluloses and pectin are cross-linked for the formation of rigid wall layers. Cellulose synthesizing machinery is located at the plasma membrane, where β-1,4-glucan chains are produced and coalesced to form microfibrils. This machinery has been visualized by freeze fracture electron microscopy and appeared as a hexameric rosette with a diameter of 25-30 nm (Kimura et al., 1999). Cellulose synthase (CesA) proteins originally identified from cotton cDNA on the basis of the sequence similarity with bacterial cellulose synthase belong to GT2 family with an inverting mechanism (Somerville, 2006). Genomic analysis indicate that there are 10 CesA genes in *Arabidopsis*, 12 in rice, 12 in maize, and 18 in *Populus* (Burn et al., 2002). All CesA proteins have a zinc-binding domain at the N-terminal and this domain is putatively responsible for protein-protein interaction. Genetic and molecular studies in *Arabidopsis* have provided the evidence that there are two different groups of CesA proteins required for the cellulose synthesis of primary (CesA1, CesA3, and CesA6) and secondary cell wall (CesA4, CesA7, and CesA8) (Mutwil et al., 2008). Immunoprecipitation experiment revealed that three secondary cell wall-specific CesA proteins appeared to form protein complex (Taylor et al., 2003). Current understanding of the processes of cellulose biosynthesis has been mainly obtained from forward/reverse genetics and transcript analysis. However, several aspects regarding biochemistry of cellulose biosynthesis still remain elusive.

Mutant complementation analysis and domain swapping studies have led to the conclusion that three non-redundant CesA genes are required for correct cellulose synthesis (Taylor, 2008). As seen in secondary-cell wall specific CesA proteins, interaction among three CesA proteins is essential for normal cellulose biosynthesis, although the interaction among primary cell wall CesA proteins has not been experimentally verified (Tanaka et al., 2003). Recent biochemical approach employing dual tagging system (Atanassov et al., 2009) has enabled successful purification of cellulose synthase complex from secondary cell wall and demonstrated that this complex is solely composed of three known secondary cell wall specific CesA proteins (CesA4, 7, and 8). Thus, it is highly plausible that the backbone chain polymerization of cellulose requires only three CesA proteins. However, the mechanism and enzymatic proteins involved in the initiation and termination of cellulose biosynthesis are poorly understood. Early biochemical analysis has failed to detect cellulose synthase activity in microsomes isolated from actively cellulose-synthesizing tissues (Somerville, 2006). Instead, a β-1,3-linked wound-response polysaccharide, callose, has been detected. Peng et al reported the biochemical evidence in cotton fiber that the lipid sitosterol-β-glucoside acts as a primer where glucose polymerization is initiated by CesA proteins (Peng et al., 2002). In this model, CesA proteins or unknown UDP-glucosyl transferase transfer glucose residues onto the lipid sitosterol-β-glucoside, forming lipid -linked oligosaccharides. The primer residue linked to oligo-glucose is then cleaved by Korrigan cellulase (Zuo et al., 2000). In vivo and in vitro experimental proofs are still lacking. Sucrose synthase and UDP-glucose pyrophosphorylase-mediated pathways have been shown to be essential for the direct production of UDP-glucose (Mutwil et al., 2008). Taken together, most, if not all, of genes involved in cellulose biosynthesis have been identified, and mutation of each gene results in the severe reduction of cellulose quantity, thereby leading to the

abnormal phenotypes in a number of developmental processes, particularly in vascular tissues. However, there is still huge lack of information regarding the detailed mechanism of its biosynthesis, including initiation, polymerization, and termination of glucan chains.

XYLOGLUCAN BIOSYNTHESIS

Xyloglucan in dicot plants is a hemicellulosic polysaccharide abundant only in primary cell wall, which is associated with cellulose microfibrils (Lerouxel et al., 2006). The association and dissociation between cellulose microfibrils and xyloglucan are developmentally regulated and appear to play the critical role during cell expansion. Xyloglucan has a main backbone of β-(1,4)-linked glucose and a side chain of α-1,6-linked xylose (Hoffman et al., 2005). Occasionally, the side chain is further substituted with α-(1,2)-fucose-β-(1,2)-galactose onto xylose residue. The pattern of side chain substitution contributes to the diversity of xyloglucan structure in different species and tissues. All the glycosyltransferases (GTs) responsible for the formation of XG side chain have been identified and biochemically examined (Lerouxel et al., 2006). Xyloglucan fucosyltransferase (XG FTase) has been initially isolated by protein purification from pea epicotyls, and activity assay of its *Arabidopsis* homolog (*AtFut1*) heterologously expressed in mammalian COS cells also showed XG FTase activity (Faik et al., 2000, 2002; Perrin et al., 1999). The biochemical data have been substantiated by the identification of *mur2* mutant that is deficient of XG fucose (Vanzin et al., 2002). Because this mutant is almost devoid of fucosylated xyloglucan found in the wild type, AtFUT1/MUR2 has been proposed as a principle XG FTase responsible for all XG fucosylation. MUR3 belonging to GT47 family has been shown to be a XG galatosyltransferase (GTase) (Madson et al., 2003). Structural analysis of XG from *mur3* mutant revealed the absence of two sugars (Galactose, Fucose) found in XG side chain, and activity assay of MUR3 expressed in *Pichia pastoris* demonstrated the enzymatic

activity that transfers galactose onto *mur3*-derived XG. XG xylosyltrasferase (XTase) in *Arabidopsis* has been identified on the basis of the sequence similarity with fenugreek XTase, belonging to GT34 family. Heterologuous expression of AtXT1 in *P.pastoris* confirmed that AtXT1 catalyzes the transfer of xylose form UDP-xylose onto β-1,4-linked glucose oligosaccharide acceptors (Faik et al., 2002). It has been predicted that xyloglucan backbone synthase might be a cellulose synthase like (CSL) protein due to the same structure of β-1,4-linked glucose polymer. This prediction coupled with transcriptional profiling of intensively XG-synthesizing nasturtium seed has led to the identification of XG backbone synthase in *Arabidopsis* (*AtCSLC4*), a member of CSLC gene (Cocuron et al., 2007). Although *in-vitro* activity of expressed AtCSLC4 protein has not been demonstrated, the observation that the β-1,4-linked glucose is produced in AtCSLC4 expressing *P. Pastoris* provides a strong evidence that AtCSLC4 is responsible for XG backbone synthase.

PECTIN BIOSYNTHESIS

Pectin is a structural component in plant cell walls as a galacturnonic acid (GalA)-rich polysaccharide, and its specific deposition in primary cell wall and the middle lamellar has been known to be associated with a number of growth/development-related processes as well as plant defense (O'Neill et al., 2004). Pectin is notorious for the most complex polymer whose biosynthesis requires at least sixty-seven enzymes. In general, pectin is structurally divided into three subclasses, homogalacturonan (HG), rhanogalacturonan I (RG-I), and -II. HG is a homopolymer of α-1,4-linked GalA , RG-I has a repeating backbone of α-1,2-Rha-α-1,4-GalA substituted with several number of oligosaccharides, and RG-II is the most complex pectin with at least eight α-1,4-linked GalA backbone decorated with twelve different sugars in different sugar linkages (Ridley et al., 2001; Mohnen, 2008). Pectin is synthesized, modified (methylation,

acetylation), and assembled in the Golgi as other hemicelluloses, but the detailed mechanism regarding biosynthesis and assembly is poorly understood since only few genes have been identified. Protein purification followed by peptide sequencing has led to the functional identification of an *Arabidopsis* pectin HG galacturonosyltransferase (AtGAUT1) that catalyzes the transfer GalA from UDP-GalA onto HG acceptors (Sterling et al., 2006). Two homologous genes in *Arabidopsis*, *RGXT1* and *RGXT2* belonging to GT77 family, have been identified, and enzyme activity assay with soluble forms of both protein expressed in insect cells confirmed that both encode α-1,3-xylosyltrasferase that transfers xylose onto fucose, a linkage only found in RG-II side chain (Egelund et al., 2006). Increasing number of genomic/proteomics information together with availabilities of diverse nucleotide sugars and acceptor oligosaccharides will greatly advance our understanding of pectin biosynthesis (Mohnen, 2008).

MANNAN BIOSYNTHESIS

Mannan polysaccharides account of less than 5 % of the dry mass of plant cell walls (Schroder et al., 2001). However, this polymer is the major non-cellulosic component in gymnosperm secondary cell wall (Popper, 2008). Structurally diverse mannan polysaccharides are found in the plant cell walls. The backbone of mannans and galactomannans is solely composed of β-(1,4)-linked mannose whereas mannose and glucose in a nonrepeating pattern have been identified in the backbone of galacto/glucomannans. The mannosyl residues in the backbone are substituted with α-(1,6)-linked galactose in galactomannans and galactoglucomannans. A significant amount of galacto/mannans is present in the seed of some legumes and palms, serving as storage carbohydrates (Buckeridge et al., 2000). Relatively small quantities of glucomannans exist in secondary cell walls of dicot plants and appear to associate non-covalently with cellulose microfibrils (Schroder et al., 2001). Three different

glycosyltransferases are required to complete the biosynthesis of mannan polysaccharides, two backbone synthases (mannan synthase and glucomannan synthase) and a galactosyltransferase for side chain addition. First enzyme identified was a galactosyltransferase from developing fenugreek seed endosperms, in which glucomannans are actively synthesized and accumulated (Edwards et al., 1999). Microsomes isolated from the fenugreek seed showed higher activity of galactosyltransferase onto exogenous mannose oligosaccharides. After protein sequencing, a gene encoding GT34 was heterologously expressed in *Pichia pastoris* and transgenic yeast exhibited high activity of galactosyltransferase. Mannan synthase first isolated from guar seeds is one of the Cellulose Synthase-Like A (CSLA) family (Dhugga et al., 2004). Later, systematic characterization of the biochemical function of a group of CSLA genes in *Arabidopsis* and rice by expressing in *Drosophila* Schneider 2 cells has revealed that CSLA2, 7, and 9 genes possess both mannan and glucomannan synthase activities (Liepman et al., 2005, 2007; Burton et al., 2006; Suzuki et al., 2006; Doblin et al., 2009). Also, several members of CSLA in Poplar were shown to encode both activities, suggesting conservation of enzymatic players of mannan biosynthesis in diverse plant species.

LIGNIN BIOSYNTHESIS

Lignin is a complex phenolic polymer primarily found in secondary wall-containing cell types such as vessels and fibers (Zhong and Ye, 2009). The presence of lignin imparts on cell walls the resistibility to both mechanical disruption and the action of cell wall hydrolases (Ralph, 2004). In addition, lignin is impregnated in cellulose and hemicelluloses matrix, providing increased mechanical strength and hydrophobicity. The biosynthesis of lignin is one of the most intensely characterized biosynthetic pathways in plant because of its abundance and economical importance (Boerjan et al., 2003). Lignin is a heteropolymer mainly made of three monolignols,

p-coumaryl alcohol, coniferyl alcohol, and sinapyl alcohol produced by the phenylpropanoid pathway. After synthesis in the cytoplasm, these monolignols are exported to the extracellular space and subsequently incorporated into the polymer by enzyme-mediated processes that remain poorly understood. Upon formation of the lignin polymer, these monolignols are referred to as final phenylpropanoid units, p-hydroxyphenyl (H), guaiacyl (G), and syringyl (S) lignin. The abundance and distribution of lignin vary among plant species and cell types. In general, G and S units are mainly found in angiosperms, whereas lignin of gymnosperms, ferns, and lycophytes is composed of G unit (Campbell and Sederoff, 1996; Zhong and Ye, 2009). Also, lignin polymer contains non-monolignol units, including ferulates, *p*-hydroxyphenyl, and coniferaldehyde (Ralph, 2004). The incorporation of ferulates to the lignin polymer contributes to the formation of crosslinks between lignin and hemicelluloses in secondary cell walls.

The overall reaction to synthesize three monolignols requires the sequential action of ten enzymes, which is well characterized (Boerjan et al., 2003; Rogers and Cambell, 2004)). Deamination of phenylalanine to cinnamic acid is mediated by an ammonia lyase (PAL). Following deamination, a cytochrome P450-dependent monooxygenase (C4H) hydroxylates the aromatic ring of cinnamic acid to form *p*-coumarate, which is then converted to *p*-coumaroyl CoA by an ATP-dependent CoA ligae (4CL). *p*-coumaryl alcohol is then produced from *p*-coumaroyl CoA by two oxidoreductase-mediated successive reductions (CCR and CAD). Coniferyl alcohol is synthesized by further enzymatic reactions including hydroxylation by C3′H, methylation by CCoAOMT, and finally two oxidoreductases (CCR and CAD) of each intermediate. Coniferaldehyde, an intermediate during coniferyl alcohol synthesis is subjected to another hydroxylation by F5H, resulting in the formation of 5-Hydroxyconfieraldehye. By the sequential actions by a methyltransferase (COMT) and CAD, sinapyl alcohol is produced. All of

genes involved in the monolignol biosynthesis have been identified and biochemically characterized (Humphreys and chapple, 2002; Rogers and Cambell, 2004; Vanholme et al., 2008). A diverse range of phenotypes including collapsed xylem, dwarfing, and developmental arrest at the early stage has been observed in the lignin-deficient mutants.

XYLAN BIOSYNTHESIS

Xylan is a predominant cell wall polymer in all higher plants, as well as some algae (Ebringerová and Heinze, 2000). Its tight association with cellulose microfibrils makes the whole framework of cell walls much stronger. Also, it has been reported that xylan is linked with lignin, pectin, and other hemicelluloses (Barakat et al., 2007). A recent investigation of lignin and carbohydrate complex formation revealed that, during cell wall assembly, non-covalent linkages are formed between xylan and α-carbon of the lignin monomer, and this interaction results in the formation of hydrophobic microdomain. The occurrence and structural diversity of xylan among species, and even in different tissues, indicate its importance in a range of fundamental processes of adaptation and development. Although most of the xylan found in plants commonly possess a backbone of β-(1,4)-linked D-xylosyl (Xyl) residues, several structural varieties primarily derive from different distributions and compositions of the side chain and any functional group substitution (Ebringerová and Heinze, 2000). The existence of side chains might be required to prevent the xylan polymer from self-assembling. Typically, xylan present in a primary cell wall is substituted with arabinose (Ara) and glucuronic acid (GlcA), whereas in a secondary cell wall, xylan has methyl GlcA and/or GlcA as a side chain.

The structure of xylan has been intensively studied in the past several decades because of its biological importance to plant development and commercial usefulness of xylan-derived products for humans and animals (Ebringerová and Heinze, 20001; Ebringerová, 2006).

Deacetylated xylan polymers can be isolated by alkali solution (NaOH and KOH), and a mild hydrolysis or xylanase treatment generates oligoxylosaccharides, that are subject to diverse analytical processes to identify the fine chemical structure. Since an alkali treatment can remove most of the acetyl groups heavily attached to xylosyl residues at O-3 and/or O-2, steam, thermochemical, and microwave oven treatments have been developed, and acetylated xylan has been successfully isolated from some tree species. With the exception of homoxylan, which is only found in some algae and whose backbone is composed of mixed β-(1,3)/ β-(1,4)-xylan, the backbone of all land plants is β-(1,4)-linked D-Xyl residues of approximately 100-200 degree of polymerization (DP) in length. Xylan is classified into four subgroups in terms of the different distributions and compositions of the side chain sugars and any functional group substitution: arabinoxylan (AX), (methyl)glucurono/arabinoxylan (M/GAX), and (methyl)glucuronoxylan (MGX) (12). Neutral AX is a primary component of grain tissues in crop plants and grasses. More than 30 % of AX has been reported in wheat bran, and about 13 % are present in whole grain flour made from barley and rye. The xylan backbones are substituted with α-L-arabinofuranose units (Araf) via α-(1,3) and/or α-(1,2) linkages in the ratio of 1:1.1-2 (This ratio will vary depending on the plant tissues and extraction methods). The existence of phenolic acids (ferulic and p-coumaric acid) esterifed to the O-5 of some Araf residues appears to provide some potential roles in covalent polysaccharide-polysaccharide or polysaccharide-protein interaction. In addition, another possible role of AX in cereal grain is to inhibit intercellular ice formation during winter time by enhancing the viscosity and the mechanical interference of the cell wall. M/GAX has been found in many tissues of monocot plants (straw, stems, stalks, and outer pericarp of grains), as well as non-lignified tissues in dicot plants. D-glucuronic acid (GlcA) and/or 4-O-methyl-a-D-glucuronic acid (4-O-Me-GlcA) residues are attached at the O-2 of

xylosyl residue (Xyl) (Fincher, 2009). The degree of (GlcA/4-O-Me-GlcA) and Araf substitution depends on the species and tissue types and show considerable variations in the range 3-9 (GlcA):10 (Xyl):1-10 (Araf). In dicots, including woody plants, all tissues undergoing secondary growth have xylan in the form of MGX. Whereas 30 % of GlcA is not methylated in non-woody plants, only methylated GlcA has been found in woody plants.

Although the fine structure of xylan from different species has been sufficiently resolved, the biosynthesis is poorly understood. Radio-isotope labeling experiments demonstrated that xylan biosynthesis takes place in the Golgi complex, and the polymers synthesized are exported outside of the plasma membrane (Fry, 2004). Activity assays have shown that proteins responsible for backbone elongation and the side chain (GlcA and Ara) addition are present in the Golgi fraction (Baydoun et al., 1983; Zeng et al., 2008). Recently, forward and reverse genetics coupled with functional genomics identified several glycosyltransferases (GTs), a group of enzymes that catalyze carbohydrate addition onto acceptor substrates, involved in xylan biosynthesis (Aspeborg et al., 2005; Brown et al., 2005, 2007, 2009; Persson et al., 2005; Zhong et al., 2005; Penan et al., 2007; Lee et al., 2007b, 2009b; Wu et al., 2009; Mortimer et al., 2010). On the basis of information obtained from protein homology search and mutant phenotypes of each GT, their possible roles have been predicted (Table 1.1).

Xylan biosynthesis, including different enzymatic actions for the backbone initiation and elongation, side chain and functional group additions, transportation of the polymer to the cell wall, and assembly with other cell wall components, is poorly understood (Ye et al., 2006; Brown et al., 2007). As mentioned earlier, polysaccharide labeling experiments and immunocytochemistry, as well as *in-vitro* activity assay with membrane microsomes from actively xylan-synthesing tissues, indicated that the formation of xylan structure takes place at

the inner face of Golgi membrane by a number of GTs and modifying enzymes. Furthermore, recently identified xylan-specific GTs in *Arabidopsis* demonstrated that all proteins, with the exception of PARVUS, are localized to the Golgi (Zhong et al., 2005; Pena et al., 2007; Lee et al., 2007b; Wu et al., 2009). Thus, as seen in other hemicelluloses (xyloglucan and mannan) and pectin, main events such as backbone polymerization and side chain addition occur at the Golgi complex. Given the fact that PARVUS is predominantly localized endoplasmic reticulum (ER), an unknown initial step of xylan biosynthesis might possibly occur at the ER (Lee et al., 2007b). It is generally believed that as other matrix polymers (xyloglucan and pectin), fully formed xylan polymers in the Golgi are packaged into vesicles, which are then exported to the apoplast along the actin cables (Taylor et al., 2008). Several xylan-deficient mutants that typically show similar phenotypes such as stunted growth and thin secondary cell walls have been genetically identified in *Arabidopsis* and all the mutated genes encode type II-GT in the same or different GT family (Brown et al., 2007). In-depth xylan structural analysis and activity assay with stem microsomes of each mutant proposed the possible role of each protein. To date, no xylan-deficient mutant and xylan-specific GTs have been found in monocot plants although recent bioinformatics using a number of expressed sequence tags (ESTs) in cereal and dicots have found some candidates for xylan synthase, arabinosyl, and feruloyl transferase (Fincher, 2009).

The similarity of backbone structures between cellulose and xylan such as glycosidic linkage (β-1,4) had led to the prediction that one or more of cellulose-synthase like (CSL) enzymes might be responsible for xylan xylosyltransferase (Richmond and Somerville, 2001; Lerouxel et al., 2006). Also, xylan xylosyltransferase would be type I GT (s) with multiple transmembrane helices to perform the processive action during polymerization. However, no xylan xylosyltransferase activity has been detected when recombinant CSL proteins are

heterologously expressed in *Drosophila* Schneider 2 cells (Liepman et al., 2005). Transcriptome studies in an effort to find secondary-cell wall specific genes in *Arabidopsis* and *poplar* uncovered several uncharacterized GTs with single transmembrane domain (Aspeborg et al., 2005; Brown et al., 2005). Thus, different from other hemicelluloses including xyloglucan and glucomannan whose backbone is polymerized by different members of Cellulose synthase like (CSL) gene family, xylan synthase might be non-CSL protein (s) (Lee et al., 2007a). Two proteins belonging to GT43 family, IRX9 and IRX14 have been implicated to be involved in xylan backbone elongation (Pena et al., 2007; Lee et al., 2007a, 2010; Brown et al., 2007;Wu et al., 2010). On the basis of the stereochemical outcome of the enzyme reactions, GT43 family is classified as a family with an inverting mechanism (the anomeric configuration of the product after the enzyme reaction can be inverted) (Lairson et al., 2008). To date, many GTs with inverting mechanism are involved in the β-linked polysaccharides such as cellulose, chitin, and hyaluronan. The implication of the involvement of two proteins (IRX9 and IRX14) in xylan backbone elongation is supported primarily by two experimental evidences: 1) microsomes isolated from each mutant stems exhibited greatly reduced ability to transfer UDP-xylose onto xylooligosaccharide acceptor compared to wild type 2) NMR study revealed that the chain length of *irx9* mutant GX is much shorter than that of WT while detailed GX structure of *irx14* has not been determined (Brown et al., 2007; Pena et al., 2007; Lee et al., 2007a). Our complementation study demonstrated that they are not functional homolog (non-redundant) since 35S promoter-driven IRX14 overexpression in *irx9* background, or vice versa, does not complement the mutant phenotypes (Lee et al., 2010). This result implies that these protein products IRX9 and IRX14 would be essential to make β-(1,4) xylose polymers in all tissues with a lignified secondary cell wall although *IRX14* expression pattern has not been well examined. Brown et al proposed that

similar to cellulose synthase complex, biosynthesis of the xylan backbone may require multiple enzymes or a multienzyme complex in which IRX9 and IRX14 may be part of it (Brown et al., 2007, 2009).

Another interesting observation regarding xylan structure is the existence of tetrasaccharide {β-D-Xyl-(1→3)-α-L-Rha-(1→2)-α-D-GalA-(1→4)-D-Xyl} at the reducing end of at least 80 % GX molecule in *Arabidopsis*, birch, spruce, and Poplar (Shimizu et al., 1976;Johansson and Samuelson, 1977; Andersson et al., 1983; Pena et al., 2007; Lee et al., 2009a). This reducing end sequence has not been found in monocot AX (Fincher, 2009). Conceivably, the reducing end sequence might serve as either primer or terminator during backbone elongation (Pena et al., 2007; York and O'Neill, 2008). Three GTs, FRA8, IRX8, and PARVUS appear to be involved in the biosynthesis of the reducing end sequences since genetic mutation of each of all three genes lead to a loss of the tetrasaccharide sequence (Zhong et al., 2005; Pena et al., 2007; Lee et al., 2007b)). The sugar linkage that the protein is responsible for has not yet been identified. Thus, additional biochemical characterization of each of them is imperative to clarify the exact function in the biosynthesis of the reducing end sequence.

Recently, two Golgi-localized GTs (GUX1 and GUX2) in GT8 family have been suggested to be required for the addition of both GlcA and MeGlcA onto xylan backbone (Mortimer et al., 2010). Substantial reduction of the Me(GlCA) frequency in the isolated xylan polymer was detected in the T-DNA mutants for *GUX1* and *GUX2*. In *gux1gux2* double mutant, no detectable xylan substitution was observed, and xylan glucuronyltransferase activity from stem microsomes was significantly reduced, although the thickness of xylem and fiber cell walls in stems is not affected. It appears that the abundance and chain length of xylan is not altered in *gux1gux2* double mutant, suggesting biosynthetic actions for backbone elongation and side chain

addition are not cooperative. The exact and direct biochemical function of these proteins remains to be determined.

Poplar has been used as a model for understanding tree biology due to the small genome size, rapid growth, close relatedness with other angiosperms, and routine transformation system (Bradshaw et al., 2000; Hawkins et al., 2003). Poplar is an excellent species particularly for studying wood formation. The large size of xylem cells permits detailed descriptive, physiological, molecular characterization of how the secondary cell wall is deposited. Similar to *Arabidopsis*, secondary cell walls in poplar are composed of cellulose, lignin, and glucuronoxylan (Mellerowicz and Sundberg., 2008). Comparison of transcriptional profiling of genes highly expressed during secondary cell wall formation in poplar and *Arabidopsis* indicated that cell wall biosynthetic genes involved in cellulose, mannan, and xylan biosynthesis and regulatory genes appear to be highly conserved between them (Aspeborg et al., 2005; Ye et al., 2006). The similarity of amino acid sequences indicates that some of poplar xylem-specific GTs, PoGT43B, GT47C, GT8D, and GT8/E are close homologs of *Arabidopsis* IRX9, FRA8, IRX8, and PARVUS, respectively, which are essential to glucuronoxylan biosynthesis. To determine if they are also involved in glucuronoxylan biosynthesis, each of poplar GTs was overexpressed in the respective xylan mutants (Zhou et al., 2006, 2007; Lee et al., 2009c). Detailed analysis of transgenic plants revealed that PoGT43B, GT47C, GT8D, and GT8/E are functional orthologs of *Arabidopsis* IRX9, FRA8, IRX8, and PARVUS, respectively. In situ hybridization revealed that those transcripts are present in the cell types undergoing secondary cell wall thickening. PoGT43B, GT47C, and GT8D are targeted to the Golgi whereas PoGT8/E are localized to ER. Downregulation of PoGT43B, GT47C, and GT8D mediated by *RNAi* in Poplar caused xylan-

deficient phenotypes (Lee et al., 2009a). Therefore, it is highly plausible that enzyme actions and overall processes of xylan biosynthesis might be conserved between Poplar and *Arabidopsis*.

REFERENCES

Atanassov, I.I., Pittman, J.K., and Turner, S.R. (2009). Elucidating the Mechanisms of Assembly and Subunit Interaction of the Cellulose Synthase Complex of Arabidopsis Secondary Cell Walls. J Biol Chem 284:3833-3841

Barakat, A., Winter, H., Rondeau-Mouro, C., Saake, B., Chabbert, B., and Cathala, B. (2007). Studies of xylan interactions and cross-linking to synthetic lignins formed by bulk and end-wise polymerisation: a model study of lignin carbohydrate complex formation. Planta 226:267–281.

Baydoun, E.A.H., Waldron, K.W., and Brett, C.T. (1983). The interaction of xylosyltransferase and glucuronyltransferase involved in glucuronoxylan synthesis in pea (Pisum sativum) epicotyls. Biochem J 257:853–858.

Boerjan, W., Ralph, J., and Baucher, M. (2003). Lignin biosynthesis. Annu. Rev. Plant Biol. 54, 519–546. (2000). Emerging model systems in plant biology: Poplar (Populus) as a model forest tree. J. Plant Growth Regul. 19:306–313.

Brown, D.M., Goubet, F., Wong, V.W., Goodacre, R., Stephens, E., Dupree, P., and Turner, S.R. (2007). Comparison of five xylan synthesis mutants reveals new insight into the mechanisms of xylan synthesis. Plant J 52:1154-1168.

Brown, D.M., Zeef, L.A.H., Ellis, J., Goodacre, R., and Turner, S.R. (2005). Identification of novel genes in Arabidopsis involved in secondary cell wall formation using expression profiling and reverse genetics. Plant Cell 17:2281–2295.

Brown, D.M., Zhang, Z., Stephens, E., Dupree, P., and Turner, S.R. (2009). Characterization

of IRX10 and IRX10-like reveals an essential role in glucuronoxylan biosynthesis in Arabidopsis. Plant J 57:732–746.

Brown, R.M. Cellulose structure and biosynthesis: what is in store for the 21st century?, J Polym Sci Pol Chem 42:487–495.

Burn, J.E., Hocart, C.H., Birch, R.J., Cork, A.C., and Williamson, R.E. (2002). Functional analysis of the cellulose synthase genes CesA1, CesA2, and CesA3 in Arabidopsis. Plant Physiol 129:797–807.

Campbell, M., and Sederoff, R. (1996). Variation in lignin content and composition: mechanisms of control and implications for the genetic improvement of plants. Plant Physiol 110:3-13.

Cocuron, J.C., Lerouxel, O., Drakakaki, G., Alonso, A.P., Liepman, A.H., Keegstra, K., Raikhel, N., and Wilkerson, C.G. (2007). A gene from the cellulose synthase-like C family encodes a β-1,4 glucan synthase. Proc Natl Acad Sci USA 104:8550–8555.

Ebringerová, A. (2006). Structural diversity and application potential of hemicelluloses. Macromolecular Symposia 232:1–12.

Ebringerová, A., and Heinze, T. (2000). Xylan and xylan derivatives—Biopolymers with valuable properties. I. Naturally occurring xylans structures, isolation procedures and properties. Macromol. Rapid Commun 21:542–556.

Egelund, J., Petersen, B.L., Motawia, M.S., Damager, I., Faik, A., Olsen, C.E., Ishii, T., Clausen, H., Ulvskov, P., and Geshi, N. (2006). Arabidopsis thaliana RGXT1 and RGXT2 encode Golgi-localized (1,3)-α-d-xylosyltransferases involved in the synthesis of pectic rhamnogalacturonan II. Plant Cell 18:2593–2607.

Faik, A., Bar-Peled, M., DeRocher, A.E., Zheng, W., Perrin, R.M., Wilkerson, C., Raikhel, N.V., and Keegstra, K. (2000). Biochemical characterization and molecular cloning of an α-1,2-

fucosyltransferase that catalyzes the last step of cell wall xyloglucan biosynthesis in pea. J Biol Chem 275:15082–15089.

Faik, A., Price, N.J., Raikhel, N.V., and Keegstra, K. (2002). An Arabidopsis gene encoding an α-xylosyltransferase involved in xyloglucan biosynthesis. Proc Natl Acad Sci USA 99:7797–7802.

Fincher, G.B. (2009). Revolutionary times in our understanding of cell wall biosynthesis and remodeling in the grasses. Plant Physiol 149:27–37.

Fry, S.C. (2004). Primary cell wall metabolism: tracking the careers of wall polymers in living plant cells. New Phytol 161 (3):642-675.

Hawkins, S., Leple, J.C., Cornu, D., Jouanin, L., and Pilate, G. (2003). Stability of transgene expression in poplar: a model forest tree species. Ann Forest Sci 60:427–438.

Hoffman, M., Jia, Z., Peña, M.J., Cash, M., Haper, A., Blackburn, A.R., Darvill, A., and York, W.S. (2005). Structural analysis of xyloglucans in the primary cell walls of plants in the subclass Asteridae. Carbohydr Res 340:1826–1840.

Humphreys, J.M., and Chapple, C. (2002). Rewriting the lignin roadmap. Curr. Opin. Plant Biol. 5:224–29.

Kimura, S., Laosinchai, W., Itoh, T., Cui, X., Linder, C.R., and Brown Jr, R.M. (1999). Immunogold labeling of rosette terminal cellulose-synthesizing complexes in the vascular plant Vigna angularis. Plant Cell 11:2075–2086.

Lee, C., O'Neill, M.A., Tsumuraya, Y., Darvill, A.G., and Ye, Z.H. (2007a). The irregular xylem9 mutant is deficient in xylan xylosyltransferase activity. Plant Cell Physiol 48:1624–1634.

Lee, C., Zhong, R., Richardson, E.A., Himmelsbach, D.S., McPhail, B.T., and Ye, Z.H. (2007b). The PARVUS Gene is Expressed in Cells Undergoing Secondary Wall Thickening and is Essential for Glucuronoxylan Biosynthesis. Plant Cell Physiol 48:1659-1672.

Lee, C., Teng, Q., Huang, W., Zhong, R., and Ye, Z.H. (2009a). Down-regulation of PoGT47C expression in poplar results in a reduced glucuronoxylan content and an increased wood digestibility by cellulase. Plant Cell Physiol 50:1075–1089.

Lee, C., Teng, Q., Huang, W., Zhong, R., and Ye, Z.H. (2009b). The F8H glycosyltransferase is a functional paralog of FRA8 involved in glucuronoxylan biosynthesis in Arabidopsis. Plant Cell Physiol 50:812–827.

Lee, C., Teng, Q., Huang, W., Zhong, R., and Ye, Z.H. (2009c). The poplar GT8E and GT8F glycosyltransferases are functional orthologs of Arabidopsis PARVUS involved in glucuronoxylan biosynthesis. Plant Cell Physiol 50:1982–1987.

Lee, C., Teng, Q., Huang, W., Zhong, R., and Ye, Z.H. (2010). The Arabidopsis family GT43 glycosyltransferases form two functionally nonredundant groups essential for the elongation of glucuronoxylan backbone. Plant Physiol. 153:526–541.

Lerouxel, O., Cavalier, D.M., Liepman, A.H., and Keegstra, K. (2006). Biosynthesis of plant cell wall polysaccharides—A complex process. Curr. Opin. Plant Biol 9:621–630.

Madson, M., Dunnand, C., Li, X.L., Vamzin, G.F., Caplan, J., Shoue, D.A., Carpita, N., and Reiter, W.D. (2003). The MUR3 gene of Arabidopsis encodes a xyloglucan galactosyltransferase that is evolutionarily related to animal exostosins. Plant Cell 15:1662–1670.

Mellerowicz, E.J., and Sundberg, B. (2008). Wood cell walls: biosynthesis, developmental dynamics and their implications for wood properties. Curr Opin Plant Biol. 11:293–300.

Mohnen, D. (2008) Pectin structure and biosynthesis. Curr. Opin. Plant Biol 11:266–277.

Mutwil, M., Debolt, S., and Persson, S. (2008). Cellulose synthesis: a complex complex. Curr Opin Plant Biol 11:252–257.

O'Neille, M.A., Ishii, T., Albersheim, P., and Darvill, A.G. (2004). Rhamnogalacturonan II: structure and function of a borate cross-linked cell wall pectic polysaccharide. Annu Rev Plant Biol 55:109–139.

Pena, M.J., Zhong, R., Zhou, G.-K., Richardson E.A., O'Neill, M.A., Darvill, A.G., York, W.S., and Ye, Z.H. (2007) Arabidopsis irregular xylem8 and irregular xylem9: implications for the complexity of glucuronoxylan biosynthesis. Plant Cell 19:549–563.

Peng, L., Kawagoe, Y., Hogan, P., and Delmer, D. (2002). Sitosterol-β-glucoside as primer for cellulose synthesis in plants. Science 295:147–150.

Perrin, R.M., DeRocher, A.E., Bar-Peled, M., Zeng, W., Norambuena, L., Orellana, A., Raikhel, N.V., and Keegstra, K. (1999). Xyloglucan fucosyltransferase, an enzyme involved in plant cell wall biosynthesis. Science 284:1976–1979.

Ralph, J. (2004). Lignins: natural polymers from oxidative coupling of 4-hydroxyphenyl propanoids. Phytochem. Rev 3:29–60.

Ridley, D.L., O'Neill, M.A., and Mohnen, D. (2001). Pectins: structure, biosynthesis, and oligogalacturonide-related signaling. Phytochemistry 57:929–967.

Rogers, L.A., and Campbell, M.M. (2004). The genetic control of lignin deposition during plant growth and development. New Phytol 164:17–30.

Somerville, C. (2006). Cellulose synthesis in higher plants. Annu Rev Cell Dev Biol 22:53–78.

Sterling, J.D., Atmodjo, M.A., Inwood, S.E., Kolli, K., Quigley, H.F., Hahn, M.G., and Mohnen, D. (2006). Functional identification of an Arabidopsis pectin biosynthetic homogalacturonan galacturonosyltransferase. Proc Natl Acad Sci USA 103:5236–5241.

Tanaka, K., Murata, K., Yamazaki, M., Onosato, K., Miyao, A., and Hirochika, H. (2003). Three distinct rice cellulose synthase catalytic subunit genes required for cellulose synthesis in the secondary wall. Plant Physiol 133:73–83.

Taylor, N.G. (2008). Cellulose biosynthesis and deposition in higher plants. New Phytol 178:239–252.

Taylor, N.G., Gardiner, J.C., Whiteman, R., and Turner, S.R. (2004). Cellulose synthesis in the Arabidopsis secondary cell wall. Cellulose 11:329–338.

Taylor, N.G., Howells, R.M., Huttly, A.K., Vickers, K., and Turner, S.R. (2003). Interactions among three distinct CesA proteins essential for cellulose synthesis. Proc. Natl. Acad. Sci. U. S. A. 100:1450-1455

Taylor, N.G., Laurie, S., and Turner, S.R. (2000). Multiple cellulose synthase catalytic subunits are required for cellulose synthesis in Arabidopsis. Plant Cell 12:2529–2540.

Vanholme, R., Morreel, K., Ralph, J., and Boerjan, W. (2008). Lignin engineering. Curr.Opin. Plant Biol 11:278-85.

Vanzin, G.F., Madson, M., Carpita, N.C., Raikhel, N.V., Keegstra, K., and Reiter, W.D. (2002). The mur2 mutant of Arabidopsis thaliana lacks fucosylated xyloglucan because of a lesion in fucosyltransferase AtFUT1. Proc Natl Acad Sci USA 99:3340–3345.

Vogel, J. (2008). Unique aspects of the grass cell wall. Curr. Opin. Plant Biol. 11:301–307.

Wu, A.M., Rihouey, C., Seveno, M., Ho¨rnblad, E., Singh, S.K., Matsunaga, T., Ishii, T., Lerouge, P., and Marchant, A. (2009). The Arabidopsis IRX10 and IRX10-LIKE

glycosyltransferases are critical for glucuronoxylan biosynthesis during secondary cell wall formation. Plant J 57:718–731.

Ye, Z.H., York, W.S., and Darvill, A.G. (2006). Important new players in secondary wall synthesis. Trends Plant Sci. 11:162–164.

York, W.S., and O'Neill, M.A. (2008). Biochemical control of xylan biosynthesis: which end is up?. Curr. Opin. Plant Biol. 11:258–265.

Zeng, W., Chatterjee, M.,and Faik, A. (2008). UDP-xylose-stimulated glucuronyltransferase activity in wheat microsomal membranes: characterization and role in glucurono(arabino)xylan biosynthesis. Plant Physiol 147:78–91.

Zhong, R., Pena, M.J., Zhou, G.-K., Nairn, C.J., Wood-Jones, A., Richardson, E.A., Morrison, W.H., Darvill, A.G., York, W.S., and Ye, Z.H. (2005). The FRA8 gene, which encodes a putative glucuronyltransferase, is essential for normal secondary wall synthesis. Plant Cell 17:3390–3408.

Zhong, R., and Ye, Z.H. (2007). Regulation of cell wall biosynthesis. Curr. Opin. Plant Biol. 10: 564–572.

Zhong. R., and Ye, Z.H. (2009) Transcriptional regulation of lignin biosynthesis. Plant Signaling & Behavior 4:1028-1034.

Zuo, J., Niu, Q.W, Nishizawa, N., Wu, Y., Kost, B., and Chua, N.H. (2000). KORRIGAN, an Arabidopsis endo-1,4-β-glucanase, localizes to the cell plate by polarized targeting and is essential for cytokinesis. Plant Cell 12:1137–1152.

Table 1. 1. Glycosyltransferases involved in the xylan biosynthesis of *Arabidopsis*

Protein name (GT family)	Protein localization	Mutant				Predicted function
		SCW thickness	Reducing end sequence	Xylan chain length	XylT activity	
FRA8 (GT47)	Golgi	Thin	Reduced	80	Unaltered	α-Rha transferese
IRX8 (GT8)	Golgi	Thin	Reduced	125	Unaltered	α-GalA transferase
IRX9 (GT43)	Golgi	Thin	Unaltered	28	Reduced	Xylan synthase
IRX14 (GT43)	Golgi	Thin	Unaltered	Reduced	Reduced	Xylan synthase
PARVUS (GT8)	ER	Thin	Reduced	N/A	Unaltered	An unknown initial step in the biosynthesis of reducing end sequence

Data derived from Zhong et al., 2005, Pena et al., 2007, Brown et al., 2007, and Lee et al., 2007b. Xylan chain length of the *Arabidopsis* wild type is 93. N/A, not available

CHAPTER 2

THE IRREGULAR XYLEM9 MUTANT IS DEFICIENT IN XYLAN XYLOSYLTRANSFERASE ACTIVITY[1]

---

[1]Lee, C., O'Neill, M.A., Tsumuraya, Y., Darvill, A.G., and Ye, Z.H. (2007). Plant Cell Physiology 48:1624–1634. Reprinted here with permission of publisher.

ABSTRACT

Xylan is the second most abundant polysaccharide in dicot wood, thus elucidating xylan biosynthetic pathway is required to understand the mechanisms controlling wood formation. Genetic and chemical studies in *Arabidopsis* have implicated three genes, *FRAGILE FIBER8* (*FRA8*), *IRREGULAR XYLEM8* (*IRX8*) and *IRREGULAR XYLEM9* (*IRX9*), in the biosynthesis of glucuronoxylan (GX), but the biochemical functions of the encoded proteins are not known. In this study, we determined the effect of the *fra8*, *irx8* and *irx9* mutations on the activities of xylan xylosyltransferase (XylT) and glucuronyltransferase (GlcAT). We show that microsomes isolated from the stems of wild-type *Arabidopsis* exhibit XylT and GlcAT activities in the presence of exogenous 1,4-linked β-D-xylooligomers. Xylooligomers ranging in size from 2 to 6 can be used as acceptors by XylT to form xylooligosaccharides with up to 12 xylosyl residues. We provide evidence that the *irx9* mutation results in a substantial reduction in XylT activity but has no discernible effect on GlcAT activity. In contrast, neither XylT nor GlcAT activity is affected by *fra8* and *irx8* mutations. Our results provide biochemical evidence that the *irx9* mutation results in a deficiency in xylan XylT activity, thus leading to a defect in the elongation of xylan backbone.

INTRODUCTION

Wood is of immense importance in human life as it is used for construction, pulping and paper-making, and has considerable value as a renewable source of biomass for biofuel production. Understanding the biosynthetic pathways that lead to the formation of wood will allow us to rationally design strategies to produce wood with improved properties by altering plant secondary cell wall composition.

Cellulose, xylan and lignin are the major components of dicot wood. Nevertheless the biosynthetic pathways leading to the formation of xylan is poorly understood. Xylan is composed of a linear backbone of 1,4-linked β-D-xylosyl residues, of which about 10% are substituted with α-D-glucuronic acid (GlcA), 4-*O*-methyl- α-D-glucuronic acid (MeGlcA), and/or arabinose (Ebringerová and Heinze, 2000). Xylans are classified based on the nature of the side chains: (methyl)glucuronoxylan (GX), arabinoxylan, or glucuronoarabinoxylan. GX is the predominant xylan present in dicot wood, whereas arabinoxylan and glucuronoarabinoxylan are the most abundant hemicelluloses in grass cell walls (Ebringerová and Heinze, 2000). GX from birch, spruce and *Arabidopsis* have been shown to contain a distinct glycosyl sequence →4)-β-D-Xyl*p*-(1→4)-β-D-Xyl*p*-(1→3)-α-L-Rha*p*-(1→2)-α-D-Gal*p*A-(1→4)-D-Xyl*p* at the reducing end (Shimizu et al., 1976; Johansson and Samuelson, 1977; Anderson et al. 1983; Pena et al., 2007). Thus, GX biosynthesis is likely to involve glycosyltransferases responsible for the formation of the backbone and the reducing end sequence, as well as enzymes that add and modify side chains. The isolation and functional characterization of genes encoding xylan biosynthetic enzymes is a critical step toward increasing our understanding of xylan biosynthesis.

Numerous enzyme activities associated with xylan biosynthesis, including xylosyltransferase (XylT), glucuronosyltransferase (GlcAT), methyltransferase, and

arabinosyltransferase have been described (Dalessandro and Northcote, 1981; Baydoun et al., 1983 and 1989; Suzuki et al., 1991; Porchia and Scheller, 2000; Kuroyama and Tsumuraya, 2001; Gregory et al., 2002; Porchia et al., 2002; Urahara et al., 2004). Microsomes isolated from wheat seedlings and barley endosperms contain XylT activity that adds up to five xylosyl residues to exogenous xylooligomer acceptors (Kuroyama and Tsumuraya, 2001; Urahara et al., 2004). However, in other studies the XylT was reported to transfer xylose to high molecular weight endogenous acceptors present in the microsomal preparations (Dalessandro and Northcote, 1981; Baydoun et al., 1983; Suzuki et al., 1991; Porchia and Scheller, 2000; Gregory et al., 2002). Gregory et al. (2002) partially purified a XylT activity-associated 50-kD polypeptide from French bean. However, no secondary wall xylan biosynthetic enzymes have been purified to homogeneity and biochemically characterized, nor have their corresponding genes been identified.

Recent molecular and genetic studies have provided strong evidence that three *Arabidopsis* genes, *FRAGILE FIBER8* (*FRA8*), *IRREGULAR XYLEM8* (*IRX8*), and *IRX9* (Brown et al., 2005; Persson et al., 2005; Zhong et al., 2005; Bauer et al., 2006; Pena et al., 2007; Persson et al., 2007) as well as their respective poplar homologs, *PoGT47C*, *PoGT8D* and *PoGT43B* (Aspeborg et al., 2005; Zhou et al., 2006 and 2007), have roles in secondary cell wall GX biosynthesis. FRA8, IRX8 and IRX9 encode putative glycosyltransferases belonging to families GT47, GT8 and GT43, respectively. These genes are expressed in cells undergoing secondary wall thickening and their encoded proteins are localized in Golgi (Zhong et al., 2005; Pena et al., 2007; Zhou et al., 2006 and 2007), the known site of GX biosynthesis. Mutations of the *FRA8, IRX8* and *IRX9* genes cause a substantial reduction in the GX content of secondary walls. Structural analysis of the GX in the *fra8* and *irx8* mutants revealed a decrease in the

number of GX chains and a decrease in the amount of GlcA residues together with the near absence of the GalA-containing glycosyl sequence at the GX reducing end. These results suggest that FRA8 and IRX8 are involved in the biosynthesis of the glycosyl sequence at the reducing end of GX or in the addition of GlcA side chains. In contrast, the *irx9* mutation leads to an increase in the number of GX chains but a substantial reduction in GX chain length as well as in the number of GlcA side chains. These results have led to the suggestion that IRX9 is a xylan synthase (Pena et al., 2007). However, no XylT activity has been detected using recombinant IRX9 (Pena et al., 2007). Thus, the possibility cannot be discounted that the shortened GX chemotype in *irx9* may result from a defect in the addition of side chains, thereby resulting in reduced GX chain elongation (Pena et al., 2007). Indeed, previous studies have led to the suggestion that GX biosynthesis requires the cooperative actions of XylT and GlcAT (Baydoun et al., 1983).

In this report, we show that microsomes from wild-type *Arabidopsis* stems exhibit XylT and GlcAT activities in the presence of exogenous xylooligomers. We present biochemical data demonstrating that the *irx9* mutation results in a substantial reduction in XylT activity but has no discernible effect on GlcAT activity. The *fra8* and *irx8* mutations have no discernible effects on the activities of XylT and GlcAT. Our data is consistent with the notion that IRX9 is the XylT that is responsible for the normal elongation of the GX backbone. This is the first report showing a deficiency of a xylan biosynthetic enzyme in mutants defective in xylan biosynthesis.

RESULTS

Biochemical properties of XylT activity in microsomes of wild-type stems

To investigate the effects of the *fra8*, *irx8* and *irx9* mutations on XylT and GlcAT activities, we first established conditions for the assay of these enzymes and for studying their

biochemical properties. We found XylT activity in microsome preparations from wild-type *Arabidopsis* inflorescence stems in which a large amount of xylan is synthesized. XylT activity was dependent on the presence of exogenous Xyl_6. No XylT activity was detected without the addition of exogenous acceptors. The transfer of radiolabeled Xyl from UDP-[^{14}C]-Xyl to Xyl_6 was dependent on Xyl_6 concentration (Fig. 2.1A) with an apparent K_m value of 10.6 mM and V_{max} of 21.8 pmol/min/mg protein. The XylT activity was both time- and protein-concentration-dependent (Fig. 2.1B, C). The optimal pH for the XylT activity was around 6.5 (Fig. 2.1D) and its optimal temperature about 10 to 20 ^{o}C (Fig. 2.1E). UDP-GlcA stimulated the XylT activity up to 30% (Fig. 2.1F), probably because the addition of GlcA side chains by the GlcAT activity may increase the solubility of the elongated xylooligomers, which could further be used as acceptors for the XylT activity.

It has been shown that microsomes isolated from wheat and barley can use xylooligomers with different length as acceptors (Kuroyama and Tsumuraya, 2001; Urahara et al., 2004). We next investigated the effectiveness of xylooligomers with different lengths as acceptors for the XylT activity (Fig. 2.2). The monomer Xyl_1-AA was not an acceptor for Xyl transfer (Fig. 2.2B). A low level of Xyl transfer was obtained using Xyl_2-AA as an acceptor. The XylT activity readily transferred Xyl residues to acceptors ranging from Xyl_3 to Xyl_6 (Fig. 2.2D, F, G, H), resulting in the synthesis of xylooligosaccharides with a size up to Xyl_{12}.

To find out whether longer reaction time can lead to the production of longer xylooligosaccharides by the XylTase activity, we did a time course study using Xyl_4-AA as acceptors. Up to seven xylosyl residues were added to Xyl_4-AA with a 2-hr incubation, leading to the production of a population of xylooligosaccharides ranging from Xyl_5 to Xyl_{11} (Fig. 2.3A).

Prolonged incubation (5 - 8 hr) did not result in the formation of xylooligosaccharides longer than Xyl_{12} but did cause a gradual increase in the proportions of Xyl_9 to Xyl_{11} (Fig. 2.3A to C).

We used enzymatic treatment and matrix assisted laser desorption time of flight mass spectrometry (MALDI-TOF-MS) analyses to confirm that the reaction products formed by reacting Xyl_4-AA and UDP-Xyl with microsomes were 1,4-linked β–D–xylooligosacchrides. MALDI-TOF-MS gave masses (*m/z* 822, 954, 1086, 1218, 1350, 1482 and 1614) for products that differed by 132 Da (Fig. 2.4). A series of oligosaccharides that differ by an incremental mass of 132 is consistent with the sequential addition of pentosyl residues to Xyl_4-AA (Fig. 2.4). Endo-β-(1,4)-xylanase and exo-β-(1,4)-xylosidase treatment of the XylT-generated products resulted in hydrolysis of the Xyl_n-AA oligomers to di- or tri-xylooligomer (Fig. 2.5). These results confirm that the XylT-generated products were composed of 1,4-linked β-D-xylosyl residues.

Biochemical properties of GlcAT activity in microsomes of wild-type stems

We found that microsomes isolated from *Arabidopsis* inflorescence stems also exhibited GlcAT activity in the presence of an exogenous 1,4-β-D-xylohexose (Xyl_6). The transfer of radiolabeled GlcA from UDP-[^{14}C]-GlcA to Xyl_6 was shown to be dependent on Xyl_6 concentration (Fig. 2.6A) with an apparent K_m value of 10.8 mM and V_{max} of 114.6 pmol/min/mg protein. The GlcATase activity was time- and protein concentration-dependent (Fig. 2.6B, C). The optimal pH for GlcAT activity was about 6.5 (Fig. 2.6D), with substantial activity over a temperature range of 10 to 37 ^{o}C (Fig. 2.6E). Addition of UDP-Xyl in the reaction mixture did not stimulate GlcAT activity; instead high concentrations (0.5 – 5mM) of UDP-Xyl inhibited its activity (Fig. 2.6F).

GlcAT and XylT activities in the fra8, irx8 and irx9 mutants

We next investigated the effects of the *fra8, irx8 and irx9* mutations on XylT and GlcAT activities. Inflorescence stems were again used to determine the relative enzyme activities in wild type and mutant plants as these tissues have the highest XylT and GlcAT activities (Fig. 2.7). Because FRA8, IRX8 and IRX9 proteins were previously shown to be targeted to Golgi (Zhong et al., 2005; Pena et al., 2007) and the microsomes we prepared was enriched with the activity of inosine diphosphatase (Lait and Zwiazek, 2001), a Golgi marker enzyme (data not shown), we reasoned that FRA8, IRX8 and IRX9 proteins were present in microsome preparations and therefore it was appropriate to use microsomal preparations to study the effects of the *fra8, irx8 and irx9* mutations on XylT and GlcAT activities. GlcAT activity was somewhat elevated in the microsomal preparations of three mutants compared with the wild type (Fig. 2.8A). XylT activity was also elevated in the *fra8* and *irx8* mutants. The elevation of the GlcAT and XylT activities could be due to a compensatory effect caused by the mutations. However, XylT activity was substantially reduced in the *irx9* mutant compared with the wild type (Fig. 2.8B). A time course analysis of the transfer of radiolabeled xylosyl residues from UDP-[^{14}C]-Xyl onto the xylooligomer acceptor demonstrated that much less label was incorporated by *irx9* microsomes than wild-type microsomes (Fig. 2.8C), a result that is consistent with IRX9 being involved with xylan synthesis. XylT activity in *irx9* plants was returned to near-normal levels by complementation of the mutant with the wild-type *IRX9* gene or its poplar homolog, *PoGT47B* gene (Fig. 2.8D). Taken together these results provide strong evidence that IRX9 has a role in the synthesis of the xylan backbone of secondary wall GX.

To investigate in greater detail the effect of the *irx9* mutation on the elongation of xylooligosaccharides, we compared the number of xylosyl residues added onto the Xyl_6-AA acceptor by wild-type and *irx9* microsomes. With wild type microsomes, Xyl_6-AA was elongated

within 2 hr to a mixture of xylooligosaccharides ranging from Xyl_7-AA to Xyl_{12}-AA, with Xyl_7-AA to Xyl_9-AA predominating (Fig. 2.9A). After 5-hr of reaction time, the peaks of Xyl_{10}-AA to Xyl_{12}-AA were elevated, whereas those of Xyl_6-AA to Xyl_8-AA were diminished (Fig. 2.9B). In contrast, in the *irx9* mutant, Xyl_6-AA was only elongated to a mixture of Xyl_7-AA to Xyl_9-AA, and even after 5-hr of reaction time Xyl_7-AA remained the predominant peak (Fig. 2.9C, D). These results indicate that the *irx9* mutation reduces the XylT activity, thereby causing a substantial decrease in the transfer of xylosyl residues onto the xylooligomers.

DISCUSSION

It was previously proposed that cellulose synthase-like (Csl) genes might encode enzymes for the biosynthesis of hemicelluloses (Richmond and Somerville, 2001). Indeed, members of Csl gene families CslC, CslA and CslF have been shown to synthesize the backbones of xyloglucan (Cocuron et al., 2007), glucomannan (Dhugga et al., 2004; Liepman et al., 2005), and (1,3;1,4)-β-D-glucan (Burton et al., 2006), respectively. However, gene(s) involved in the biosynthesis of the xylan backbone have remained elusive. No recombinant Csl proteins have been shown to have XylT activity (Liepman et al., 2005), nor has transcription profiling analysis revealed correlations between xylan biosynthesis and the expression of Csl genes, with the exception of CslA, during wood formation (Aspeborg et al., 2005). Our demonstration that IRX9 is required for normal XylT activity as well as normal elongation of xylan chains provides the first biochemical evidence that a glycosyltransferase other than a Csl protein is involved in the biosynthesis of the xylan backbone.

The irx9 mutation causes a deficiency in the transfer of xylosyl residues onto xylooligomer acceptors

The *irx9* mutation causes a number of changes in GX structure, including a decreased ratio of GlcA to MeGlcA residues, an increased number of GX chains, and a substantial reduction in GX chain length (Pena et al., 2007). The findings that the GX chain number increases and its length decreases in the *irx9* mutant suggest that the primary effect of the *irx9* mutation may be on the elongation of GX chains rather than on the initiation of GX biosynthesis. However, the *irx9* mutation also decreases the ratio of GlcA to MeGlcA residues on the GX. Thus, it is equally possible that IRX9 is involved in the transfer of GlcA residues on the GX, and that a defect in GlcA transfer may itself lead to an attenuation of GX chain elongation (Pena et al., 2007). Our biochemical data showed that the *irx9* mutation has no discernible effect on GlcAT activity, thereby limiting the possibility that IRX9 is required for GlcAT activity. Instead, our study demonstrated that the *irx9* mutation causes a reduction in XylT activity. The decreased XylT activity in the *irx9* mutant results in a reduced ability to transfer xylosyl residues onto xylooligomer acceptors, leading to the formation of much shorter xylooligosaccharides than wild type plants (Fig. 2.9). This finding is consistent with the chemical analysis showing that the degree of polymerization of GX is reduced from 93 in the wild type to 28 in the *irx9* mutant (Pena et al., 2007). Thus, our study provides compelling evidence that the decreased GX chain length caused by the *irx9* mutation is due to a deficiency in XylT activity.

It is important to note that the *irx9* mutation does not completely eliminate the XylT activity. Because the T-DNA insertion (SALK_058238) in the *irx9* mutant disrupts an *IRX9* exon that encodes part of the putative catalytic domain, *irx9* is presumably a null mutant. Therefore, the low level of XylT activity remained in the *irx9* mutant is likely contributed by its functional homolog(s), which may also result in a limited elongation of xylan backbone.

The *fra8* and *irx8* mutations do not affect GlcAT and XylT activities

A previous study demonstrated that *fra8* and *irx8* mutants synthesize GX that is nearly devoid of the reducing end glycosyl sequence →4)-β-D-Xyl*p*-(1→4)-β-D-Xyl*p*-(1→3)-α-L-Rha*p*-(1→2)-α-D-Gal*p*A-(1→4)-D-Xyl*p*, indicating that FRA8 and IRX8 are involved in the biosynthesis of this sequence. However, the *fra8* and *irx8* mutations also cause a reduction in both the number of GX chains and the ratio of GlcA to MeGlcA residues in the GX (Zhong et al., 2005; Pena et al., 2007; Persson et al., 2007). Therefore, the results of genetic and chemical analyses do not exclude the possibility that FRA8 and IRX8 are involved in the transfer of GlcA residues onto xylan backbone. Our biochemical data provide evidence that the *fra8* and *irx8* mutations do not result in a reduction in XylT or GlcAT activities, which suggest that FRA8 and IRX8 have no direct roles in the transfer of GlcA residues onto the xylan backbone or in the elongation of the xylan backbone by addition of xylosyl residues. The results of our study support the proposal that the FRA8 and IRX8 glycosyltransferases are involved in the biosynthesis of the glycosyl sequence at the GX reducing end (Pena et al., 2007).

The XylT and GlcAT activities in Arabidopsis microsomes require exogenous xylooligomers as acceptors

Xylan XylT activities have been identified in sycamore, poplar, pea, wheat, barley, zinnia, and French bean (Dalessandro and Northcote, 1981; Baydoun et al., 1983; Suzuki et al., 1991; Porchia and Scheller, 2000; Kuroyama and Tsumuraya, 2001; Gregory et al., 2002). In most of cases, the XylT activity was detected without the addition of exogenous acceptors suggesting that these XylTs use microsome-associated endogenous acceptors or that these enzymes do not require an acceptor. Indeed, a detergent-solubilized, and partially purified XylT fraction has been reported to have XylT activity in the absence of exogenous acceptors (Gregory et al., 2002). However, exogenous xylooligomer acceptors are required for XylT activities in the

microsomes of asparagus (Feingold et al., 1959), wheat (Kuroyama and Tsumuraya, 2001) and barley (Urahara et al., 2004). It is not known whether the discrepancy on the requirement of exogenous acceptors is due to the difference of microsome preparations or the nature of XylTs from different species. In any case, it is clear that with *Arabidopsis* microsomes, exogenous xylooligomers are required for the XylT activity and that a xylooligomer as short as xylotriose or xylotetraose is sufficient to be an acceptor for the transfer of xylosyl residues.

The GlcAT activity in the *Arabidopsis* microsomes was also found to require exogenous xylooligomers as an acceptor suggesting the presence of a GlcAT that transfers GlcA onto preformed xylooligomers. No GlcA was transferred in the absence of an exogenous xylooligomer acceptor indicating that the microsome preparations contain little if any endogenous acceptors for GlcAT. The addition of exogenous UDP-Xyl to the reaction mixture did not increase the amount of GlcA incorporated. Because the Xyl_6 acceptor used is elongated to Xyl_{12} by the XylT activity, this indicates that no additional GlcA residues are transferred to the elongated xylooligomers by the GlcAT activity. This is consistent with the reported normal distribution of GlcA residues along the xylan backbone, which is typically about one GlcA residues for every 10 xylosyl residues (Ebringerová and Heinze, 2000). Our finding that the GlcAT activity can transfer GlcA onto preformed xylooligomers is in contrast to the previous report showing that pea epicotyl microsomes can only add GlcA onto nascent xylan but not onto preformed xylan (Baydoun et al., 1989). This discrepancy may be due to our use of xylooligomers rather than newly synthesized xylan polysaccharides as acceptors.

In summary, our study demonstrates that IRX9 is required for the normal XylT activity. Previous attempts to demonstrate XylT activity using recombinant IRX9 protein have been unsuccessful (Pena et al., 2007). Thus, it is essential to design strategies to further biochemically

characterize IRX9. A complete description of the biochemical properties of IRX9 together with IRX8, FRA8, and other yet to be identified proteins involved in xylan biosynthesis will undoubtedly lead to a better understanding of the biosynthetic pathway of xylan, the second most abundant polysaccharide produced by woody plants.

MATERIALS AND METHODS

Plant materials

Wild-type *Arabidopsis* (ecotype Columbia), *fra8* (Zhong et al., 2005), *irx8* (SALK_008642), *irx9* (SALK_058238), *irx9*-complemented with wild-type IRX9 (Pena et al., 2007), and *irx9*-compelemented with PoGT43B (Zhou et al., 2007) plants were grown in a greenhouse. Inflorescence stems, roots, leaves used for microsome isolation were collected from 6-week-old plants, and seedlings used for microsome isolation were two weeks old.

Enzymes and chemicals

Endo-β-xylanase M6 and xylooligomers (Xyl_2 to Xyl_6) were purchased from Megazyme (Wicklow, Ireland). Xylose, UDP-GlcA, anthranilic acid, and β-xylosidase were from Sigma (St. Louis, MO, USA). UDP-Xyl was from CarboSource Service (Athens, GA, USA; supported in part by NSF-RCN grant #0090281). UDP-[^{14}C]-Xyl (specific activity, 264 mCi/mmol) and UDP-[^{14}C]-GlcA (specific activity, 300 mCi/mmol) were from American Radiolabeled Chemical (St. Louis, MO, USA). Toyopearl HW-40 was from Tosoh Bioscience (Montgomeryville, PA, USA).

Anthranilic acid labeling of xylooligomers

Xylose and xylooligomers (Xyl_2 to Xyl_6) were labeled at their reducing termini with anthranilic acid (AA) according to Ishii et al. (2002). Briefly, oligosaccharides were reacted for 2 hr at 65 ^{o}C with 0.2 M AA in 20 mM sodium acetate, pH 5.5, containing 1M $NaBH_3CN$. The reaction was terminated by the addition of 10 mM ammonium acetate (pH 7.0), and the AA-

labeled oligosaccharides were separated from AA and $NaBH_3CN$ by chromatography on a column (1.5 x 100 cm) of Toyopearl HW-40F and eluted with 10 mM ammonium acetate (pH 7.0). The A_{254nm} of the eluant was monitored and the UV-positive fractions containing the AA-labeled xylose and xylooligomers were pooled and lyophilized.

Assay of GlcAT and XylT activities by radiolabeling

Microsomes were isolated and the GlcAT and XylT activities were determined following the procedures by Kuroyama and Tsumuraya (2001). Briefly, plant materials were homogenized with a mortar and pestle in the grinding solution (50 mM Hepes-NaOH, pH 7.3, 0.4 M sucrose, 10 μg/ml aprotinin and 10 μg/ml leupeptin). After centrifugation at 3,000 *g* for 15 min to remove debris, the supernatant was further centrifuged at 100,000 *g* for 1 hr. The pellets containing the microsomes were re-suspended in the buffer containing 50 mM Hepes-NaOH (pH 7.3) and 0.4 M sucrose, and stored at –80 ^{o}C. The protein concentration of microsomal fraction was measured using the BioRad protein assay kit with BSA as the standard protein. For assay of GlcAT activity, 100 μg of microsomes were incubated with the reaction mixture (a total volume of 30 μl) containing 50 mM Hepes-KOH, pH 6.8, 5 mM $MnCl_2$, 1 mM DTT, 0.5% Triton X-100, 0.2 μg/μl Xyl_6, and UDP-[^{14}C]-GlcA (0.1 μCi). After incubation at 21 ^{o}C for various times, the reaction was stopped by addition of the termination solution (0.3 M acetic acid containing 20 mM EGTA). For assay of XylT activity, 100 μg of microsomes were incubated with the reaction mixture (a total volume of 30 μl) containing 50 mM Hepes-KOH, pH 6.8, 5 mM $MnCl_2$, 1 mM DTT, 0.5% Triton X-100, 0.1 mM cold UDP-Xyl, 0.2 μg/μl Xyl_6, and UDP-[^{14}C]-Xyl (0.1 μCi). After incubation at 21 ^{o}C for various times, the reaction was stopped by addition of the termination solution. The radiolabeled xylooligosaccharides were separated from UDP-[^{14}C]-Xyl by paper chromatography according to Ishikawa et al. (2000). The terminated reaction mixture

was spotted onto a strip of Whatmann 3MM paper and developed with 95% ethanol:1M ammonium acetate (2:1, v/v) as the solvent. The radiolabeled xylooligosaccharides are retained at the original spot, whereas UDP-[^{14}C]-Xyl moved along with the solvent. The spot containing the radiolabeled xylooligosaccharides was cut out, sonicated in 0.1N NaOH, and the amount of radioactivity present was determined with a PerkinElmer scintillation counter (Waltham, MA, USA). The activity of inosine diphosphatase in microsomes was determined according to Lait and Zwiazek (2001).

Assay of XylT activity using Xyl_n-AA as acceptors and HPLC analysis of Xyl_n-AA

XylT activity with Xyl_n-AA acceptors was carried out in a reaction mixture (a total volume of 30 μl) containing 50 mM Hepes-KOH, pH 6.8, 5 mM $MnCl_2$, 1 mM DTT, 0.5% Triton X-100, 0.1 mM cold UDP-Xyl, 0.5 mM Xyl_n-AA, and 200 μg of microsomes. After incubation at 21 ^{o}C for various times, the reaction was terminated with 0.1 M acetic acid, and filtered with an Amicon Ultrafree-MC filter (0.22 μm). The products formed were analyzed by reversed-phase HPLC analysis. HPLC was performed with an Agilent 1100 series LC system and a Shimadzu RF-10A_{XL} fluorescence detector (Ex_{320nm}, Em_{420nm}). The incorporated Xyl_n-AA products were separated using a Luna C18 (5 μm) column (250 mm long, 4.6 mm i.d.). The column was eluted at 0.5 ml/min with aq 80% methanol containing 0.02% (v/v) trifluoroacetic acid (0 - 5 min) followed by a gradient to 100% methanol over 45 min.

Treatment of xylooligosaccharides with β-xylanase and β-xylosidase

The XylT activity reaction using Xyl_n-AA acceptors as described above was terminated by heating at 100 ^{o}C for 3 min. The reaction mixture (a total volume of 30 μl) was centrifuged at 12,000 g for 5 min and the supernatant was saved for treatment with β-xylanase and β-xylosidase. The supernatant (10 μl) was mixed with 50 mM sodium acetate, pH 6.0 (30 μL)

containing β-xylanase (4.5 units) or β-xylosidase (0.005 units) and incubated for 6 hr at 37 ^{o}C. The reaction was terminated with 0.1 M acetic acid, and subjected to reverse-phase HPLC analysis.

Matrix-Assisted Laser-Induced/Ionization-Time-Of-Flight Mass Spectrometry (MALDI-TOF MS)

The AA-labeled xylooligosaccharides from the XylT-catalyzed reactions were analyzed by MALDI-TOF mass spectrometry using a Hewlett-Packard LDI 1700 XP spectrometer operated in the positive-ion mode with an accelerating voltage of 30 kV, an extractor voltage of 9 kV, and a source pressure of approx 8 x 10^{-7} torr. The enzyme reaction mixture was mixed with an equal volume of water (200 μL) and then applied to a Strata C-18 solid phase extraction cartridge (3 mL, Phenomenex) that had been pre-washed with methanol and then with water. The cartridge was eluted with water (5 mL) and then with 60% methanol (5 mL) to elute the Xyl_n-AA oligomers. The solution was concentrated to dryness under a flow of air and the residue dissolved in water (100 μL). A portion (1 μL) of the solution was mixed with the MALDI matrix (1 μL, 0.1 M 2,5-dihydroxbenzoic acid and 0.03 M 1-hydroxyisoquinoline in 50% acetonitrile) and dried on the stainless steel target plate. Spectra are the average of at least 100 laser shots.

ACKNOWLEDGMENTS

We thank Nicholas S. Hill for use of his lyophilizer, and the reviewers for their constructive comments and suggestions. This work was supported by grants from the U.S. Department of Energy-Bioscience Division (Grant DE-FG02-03ER15415 to Z.-H. Y. and Grants DE-FG05-93ER20097 and DE-FG02-96ER20220 to M.A.O. and A.G.D.).

REFERENCES

Andersson, S.-I., Samuelson, O., Ishihara, M. and Shimizu, K. (1983) Structure of the reducing end-groups in spruce xylan. *Carbohydr. Res.* 111: 283-288.

Aspeborg, H., Schrader, J., Coutinho, P.M., Stam, M., Kallas, A., Djerbi, S., Nilsson, P., Denman, S., Amini, B., Sterky, F., Master, E., Sandberg, G., Mellerowicz, E., Sundberg, B., Henrissat, B. and Teeri, T.T. (2005) Carbohydrate-Active Enzymes Involved in the Secondary Cell Wall Biogenesis in Hybrid Aspen. *Plant Physiol.* 137: 983-997.

Bauer, S., Vasu, P., Persson, S., Mort, A.J. and Somerville, C.R. (2006) Development and application of a suite of polysaccharide-degrading enzymes for analyzing plant cell walls. *Proc. Natl. Acad. Sci. USA.* 103: 11417-11422.

Baydoun, E.A.-H., Usta, J.A.-R., Waldron, K.W. and Brett, C.T. (1989) A methyltransferase involved in the biosynthesis of 4-*O*-methylglucuronoxylan in etiolated pea epicotyls. *J. Plant Physiol.* 135: 81-85.

Baydoun, E.A.-H., Waldron, K.W. and Brett, C.T. (1983) The interaction of xylosyltransferase and glucuronyltransferase involved in glucuronoxylan synthesis in pea (*Pisum sativum*) epicotyls. *Biochem. J.* 257: 853-858.

Brown, D.M., Zeef, L.A.H., Ellis, J., Goodacreb, R. and Turner, S.R. (2005) Identification of novel genes in *Arabidopsis* involved in secondary cell wall formation using expression profiling and reverse genetics. *Plant Cell* 17: 2281-2295.

Burton, R.A., Wilson, S.M., Hrmova, M., Harvey, A.J., Shirley, N.J., Medhurst, A., Stone, B.A., Newbigin, E.J., Bacic, A. and Fincher, G.B. (2006) Cellulose synthase-like CslF genes mediate the synthesis of cell wall (1,3;1,4)-β-D-glucans. *Science* 311:1940-1942.

Cocuron, J.C., Lerouxel, O., Drakakaki, G., Alonso, A.P., Liepman, A.H., Keegstra, K., Raikhel, N. and Wilkerson, C.G. (2007) A gene from the cellulose synthase-like C family encodes a β-1,4 glucan synthase. *Proc. Natl. Acad. Sci. USA* 104: 8550-8555.

Dalessandro, G. and Northcote, D.H. (1981) Increase of xylan synthetase activity during xylem differentiation of the vascular cambium of sycamore and poplar trees. *Planta* 151: 61-67.

Dhugga, K.S., Barreiro, R., Whitten, B., Stecca, K., Hazebroek, J., Randhawa, G.S., Dolan, M., Kinney, A.J., Tomes, D., Nichols, S. and Anderson, P. (2004) Guar seed β-mannan synthase is a member of the cellulose synthase super gene family. *Science* 303: 363-366.

Ebringerová, A. and Heinze, T. (2000) Xylan and xylan derivatives-biopolymers with valuable properties, 1. Naturally occurring xylans structures, isolation procedures and properties. *Macromol. Rapid Commun.* 21: 542-556.

Gregory, A.C.E., Smith, C., Kerry, M.E., Wheatley, E.R. and Bolwell, G.P. **(**2002) Comparative subcellular immunolocation of polypeptides associated with xylan and callose synthases in French bean (*Phaseolus vulgaris*) during secondary wall formation. *Phytochemistry* 59: 249-259.

Ishii, T., Ichita, J., Matsue, H., Ono, H. and Maeda, I. (2002) Fluorescent labeling of pectic oligosaccharides with 2-aminobenzamide and enzyme assay for pectin. *Carbohydr. Res.* 337: 1023-1032.

Ishikawa, M., Kuroyama, H., Takeuchi, Y. and Tsumuraya, Y. (2000) Characterization of pectin methyltransferase from soybean hypocotyls. *Planta* 210: 782-791.

Johansson, M.H. and Samuelson, O. (1977) Reducing end groups in birch xylan and their alkaline degradation. *Wood Sci. Technol.* 11: 251-263.

Kuroyama, H. and Tsumuraya, Y. (2001) A xylosyltransferase that synthesizes β-(1->4)-xylans in wheat (*Triticum aestivum* L.) seedlings. *Planta* 213: 231-240.

Lait, C.G. and Zwiazek, J.J. (2001) A calcium-binding protein with similarity to serum albumin localized to the ER-Golgi network and cell walls of spinach (*Spinacia oleracea*). *Physiol. Plant.* 112: 460-469.

Lerouxel, O., Cavalier, D.M., Liepman, A.H. Keegstra, K. (2006) Biosynthesis of plant cell wall polysaccharides - a complex process. *Curr. Opin. Plant Biol.* 9: 621-630.

Liepman, A.H., Wilkerson, C.G. and Keegstra, K. (2005) Expression of cellulose synthase-like (*Csl*) genes in insect cells reveals that *CslA* family members encode mannan synthases. *Proc. Natl. Acad. Sci. USA* 102: 2221-2226.

Pena, M.J., Zhong, R., Zhou, G.-K., Richardson, E.A., O'Neill, M.A., Darvill, A.G., York, W.S. and Ye, Z.-H. (2007) *Arabidopsis irregular xylem8* and *irregular xylem9*: Implications for the complexity of glucuronoxylan biosynthesis. *Plant Cell* 19: 549-563.

Persson, S., Caffall, K.H., Freshour, G., Hilley, M.T., Bauer, S., Poindexter, P., Hahn, M.G., Mohnen, D. and Somerville, C. (2007) The *Arabidopsis irregular xylem8* mutant is deficient in glucuronoxylan and homogalacturonan, which are essential for secondary cell wall integrity. *Plant Cell* 19: 237-255.

Persson, S., Wei, H., Miline, J., Page, G.P. and Somerville, C.R. (2005) Identification of genes required for cellulose synthesis by repression analysis of public microarray data sets. *Proc. Natl. Acad. Sci. USA* 102: 8633-8638.

Porchia, A.C. and Scheller, H.V. (2000) Arabinoxylan biosynthesis: identification and partial characterization of β-1,4-xylosyltransferase from wheat. *Physiol. Plant.* 110: 350-356.

Porchia, A.C., Sorensen, S.O. and Scheller, H.V. (2002) Arabinoxylan biosynthesis in wheat. Characterization of arabinosyltransferase activity in Golgi membranes. *Plant Physiol.* 130: 432-441.

Richmond, T.A. and Somerville, C.R. (2001) Integrative approaches to determining Csl function. *Plant Mol. Biol.* 47: 131-143.

Shimizu, K., Ishihara, M. and Ishihara, T. (1976) Hemicellulases of brown rotting fungus, *Tyromyces palustris*. II. The oligosaccharides from the hydrolysate of a hardwood xylan by the intracellular xylanase. *Mokuzai Gaikkashi.* 22: 618-625.

Suzuki, K., Ingold, E., Sugiyama, M. and Komamine, A. (1991) Xylan synthase activity in isolated mesophyll cells of *Zinnia elegans* during differentiation to tracheary elements. *Plant Cell Physiol.* 32: 303-306.

Urahara, T., Tsuchiya, K., Kotake, T., Tohno-oka, T., Komae, K., Kawada, N. and Tsumuraya, Y. (2004) A β-(1→4)-xylosyltransferase involved in the synthesis of arabinoxylans in developing barley endosperms. *Physiol. Plant.* 122: 169-180.

Zhong, R., Pena, M.J., Zhou, G.-K., Nairn, C.J., Wood-Jones, A., Richardson, E.A., Morrison, W.H., Darvill, A.G., York, W.S. and Ye, Z.-H. (2005) *Arabidopsis Fragile Fiber8*, which encodes a putative glucuronyltransferase, is essential for normal secondary wall synthesis. *Plant Cell* 17: 3390-3408.

Zhou, G.K., Zhong, R., Richardson, E.A., Himmelsbach, D.S., McPhail, B.T., and Ye, Z.-H. (2007). Molecular characterization of PoGT8D and PoGT43B, two secondary wall-associated glycosyltransferases in poplar. *Plant Cell Physiol.* 48: 689-699.

Zhou, G.K., Zhong, R., Richardson, E.A., Morrison, W.H. 3rd., Nairn, C.J,. Wood-Jones, A. and Ye, Z.-H. (2006) The poplar glycosyltransferase GT47C is functionally conserved with *Arabidopsis Fragile Fiber8. Plant Cell Physiol.* 47:1229-1240.

Figure 2.1. Biochemical properties of the XylT activity in microsomes from *Arabidopsis* stems. Microsomes were incubated with UDP-[^{14}C]-Xyl and Xyl_6 for 20 min unless otherwise indicated, and the XylT activity was measured by counting the radioactivity (CPM) present in the reaction products. All assays were repeated twice and the data are means ± SE. (A) Dependence of the XylT activity on the concentration of Xyl_6 acceptor. (B) Time course of the transfer of radiolabeled Xyl onto the Xyl_6 acceptor by the XylT activity. Note that the XylT activity is linear in the first 40 min and reached maximum after 100-min incubation under the assay conditions used. (C) The XylT activity is protein concentration-dependent. (D) Effect of pH on the XylT activity. (E) Effect of temperature on the XylT activity. (F) Effect of UDP-GlcA on the XylT activity.

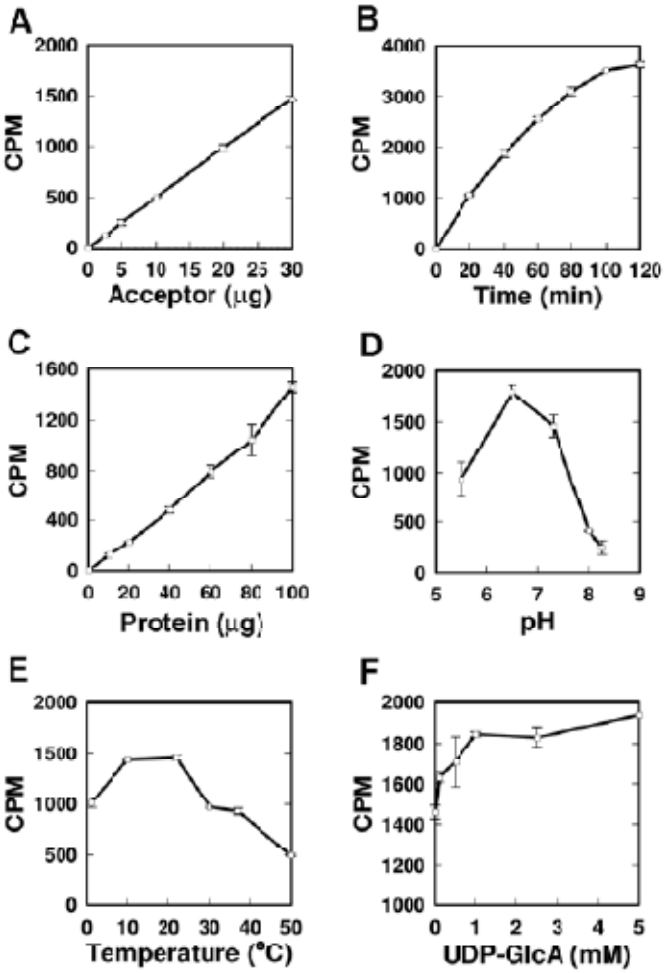
A
CPM
2000
1500
1000
500
0
0 5 10 15 20 25 30
Acceptor (μg)
B
CPM
4000
3000
2000
1000
0
0 20 40 60 80 100 120
Time (min)
C
CPM
1600
1200
800
400
0
0 20 40 60 80 100
Protein (μg)
D
CPM
2000
1500
1000
500
0
5 6 7 8 9
pH
E
CPM
2000
1500
1000
500
0
0 10 20 30 40 50
Temperature (°C)
F
CPM
2000
1800
1600
1400
1200
1000
0 1 2 3 4 5
UDP-GlcA (mM)

Figure 2.2. Xylooligomers of different length as acceptors for the XylT activity. Microsomes were incubated with UDP-Xyl and the fluorescent acceptors Xyl_1-AA (B), Xyl_2-AA (C), Xyl_3-AA (D), Xyl_4-AA (F), Xyl_5-AA (G), or Xyl_6-AA (H) for 5 hr, and the reaction products were analyzed by reverse-phase HPLC for separation and detection of the fluorescent xylooligosaccharides. A chromatogram of standard $Xyl_{1\text{-}6}$-AA is shown in (A) and (E) for reference. The XylT activity can transfer xylosyl residues onto xylooligomers as short as xylobiose.

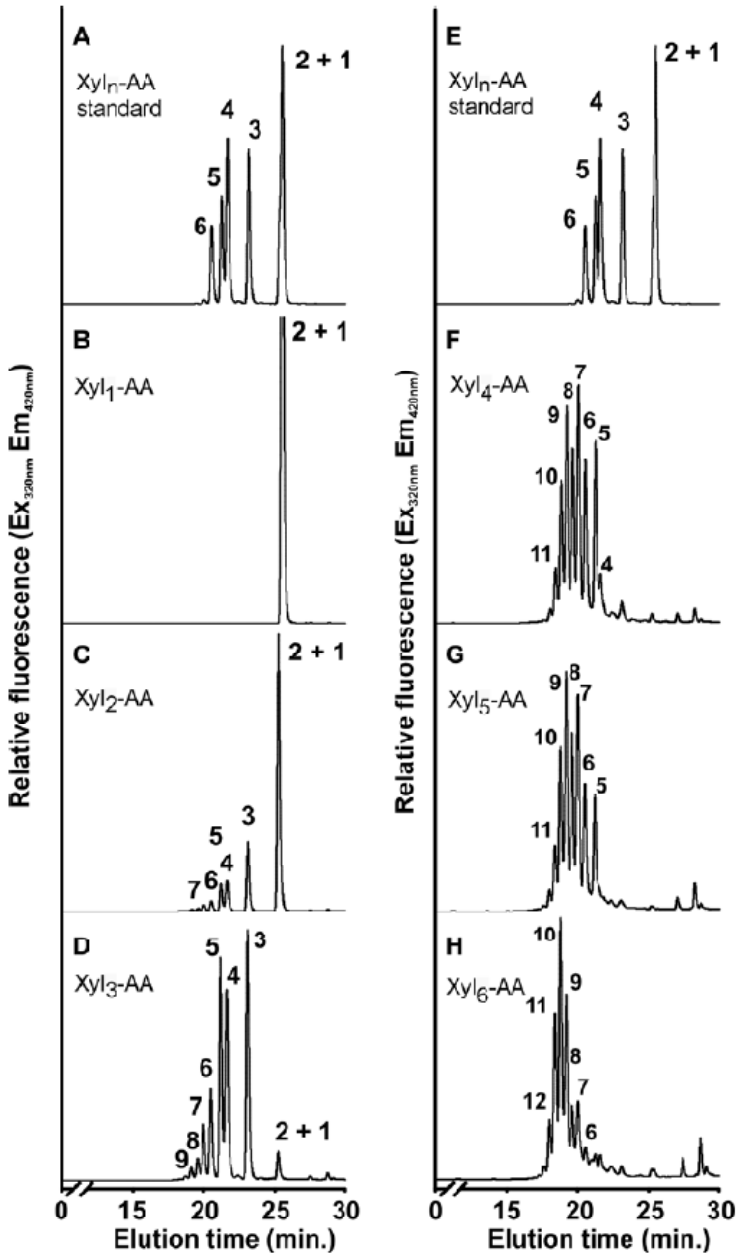
A
Xyl$_n$-AA standard
2 + 1
4
3
5
6
B
Xyl$_1$-AA
2 + 1
C
Xyl$_2$-AA
2 + 1
5
3
4
7
6
D
Xyl$_3$-AA
5
3
4
6
7
8
9
2 + 1
E
Xyl$_n$-AA standard
2 + 1
4
3
5
6
F
Xyl$_4$-AA
7
8
9
6
5
10
11
4
G
Xyl$_5$-AA
9
8
7
10
6
5
11
H
Xyl$_6$-AA
10
11
9
8
12
7
6
Relative fluorescence (Ex$_{320nm}$ Em$_{420nm}$)
Relative fluorescence (Ex$_{320nm}$ Em$_{420nm}$)
0
15
20
25
30
Elution time (min.)
0
15
20
25
30
Elution time (min.)

Figure 2.3. Successive transfer of xylosyl residues onto the acceptors by the XylT activity. Microsomes were incubated with UDP-Xyl and the fluorescent Xyl_4-AA acceptor for 2 hr (A), 5 hr (B) and 8 hr (C), and the reaction products were analyzed by reverse-phase HPLC. The XylT activity is able to successively elongate Xyl_4 up to Xyl_{12}.

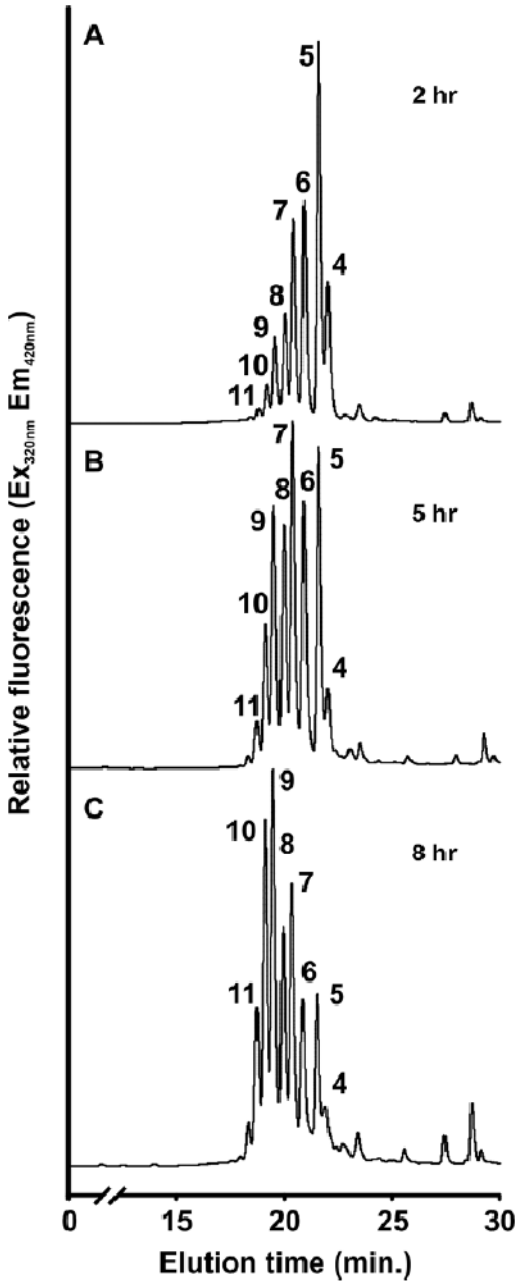
A
2 hr
5
6
7
4
8
9
10
11
B
5 hr
7
8
6
5
9
10
4
11
C
8 hr
9
10
8
7
6
11
5
4
0
15
20
25
30
Elution time (min.)
Relative fluorescence (Ex320nm Em420nm)

Figure 2.4. MALDI TOF mass spectrum of the XylT-catalyzed reaction products. Microsomes were incubated with UDP-Xyl and the acceptor Xyl_4-AA, and the reaction products were purified and analyzed by MALDI TOF MS. Inset shows the chemical structure of Xyl_n-AA. A series of ions with a mass increment of 132 D corresponding to one xylosyl residue were observed in the spectrum. These ions correspond to AA-labeled oligosaccharides $[Xyl_n\text{-AA} + Na]^+$ composed of 5 to 11 Xyl residues.

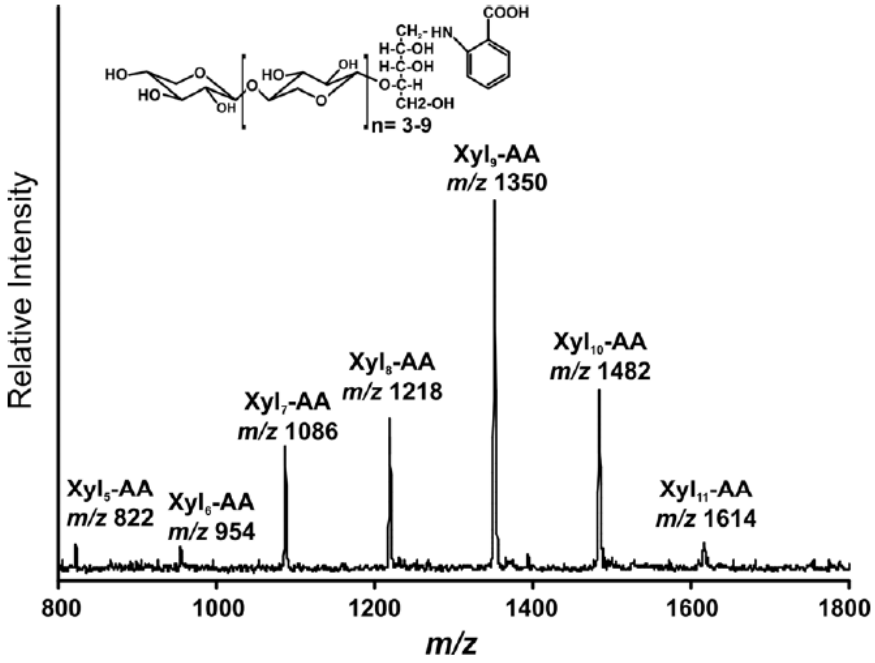
Relative Intensity
m/z
800
1000
1200
1400
1600
1800
n= 3-9
Xyl5-AA
m/z 822
Xyl6-AA
m/z 954
Xyl7-AA
m/z 1086
Xyl8-AA
m/z 1218
Xyl9-AA
m/z 1350
Xyl10-AA
m/z 1482
Xyl11-AA
m/z 1614

Figure 2.5. Degradation of the XylT-catalyzed reaction products by endo-β-(1,4)-xylanase and exo-β-(1,4)-xylosidase. Microsomes were incubated with UDP-Xyl and the fluorescent Xyl_4-AA acceptor, and the reaction products were digested with endo-β-(1,4)-xylanase (B) or exo-β-(1,4)-xylosidase (C). The reaction products with (B, C) and without (A) enzymatic digestion were analyzed by reverse-phase HPLC. Treatment of the reaction products with β-(1,4)-xylanase and exo β-(1,4)-xylosidase results in their degradation into Xyl_1 to Xyl_3, indicating that the reaction products have β-(1,4)-linkage.

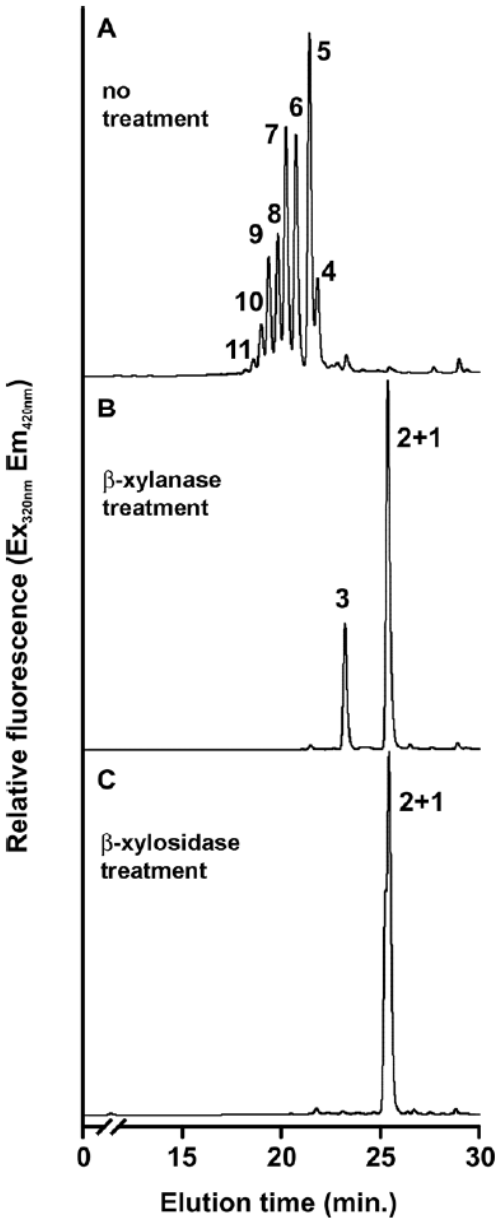
A
no
treatment
5
6
7
8
9
4
10
11
B
β-xylanase
treatment
2+1
3
C
β-xylosidase
treatment
2+1
Relative fluorescence (Ex320nm Em420nm)
0
15
20
25
30
Elution time (min.)

Figure 2.6. Biochemical properties of the GlcAT activity in microsomes from *Arabidopsis* stems. Microsomes were incubated with UDP-[^{14}C]-GlcA and Xyl_6 for 20 min unless otherwise indicated, and the GlcAT activity was measured by counting the radioactivity (CPM) of the reaction products. All assays were repeated twice and the data are means ± SE. (A) Dependence of the GlcAT activity on the concentration of Xyl_6 acceptor. (B) Time course of the transfer of radiolabeled GlcA onto the Xyl_6 acceptor by the GlcAT activity. Note that the GlcAT activity is linear in the first 30 min and reached maximum after 80-min incubation under the assay conditions used. (C) The GlcAT activity is protein concentration-dependent. (D) Effect of pH on the GlcAT activity. (E) Effect of temperature on the GlcAT activity. (F) Effect of UDP-Xyl on the GlcAT activity.

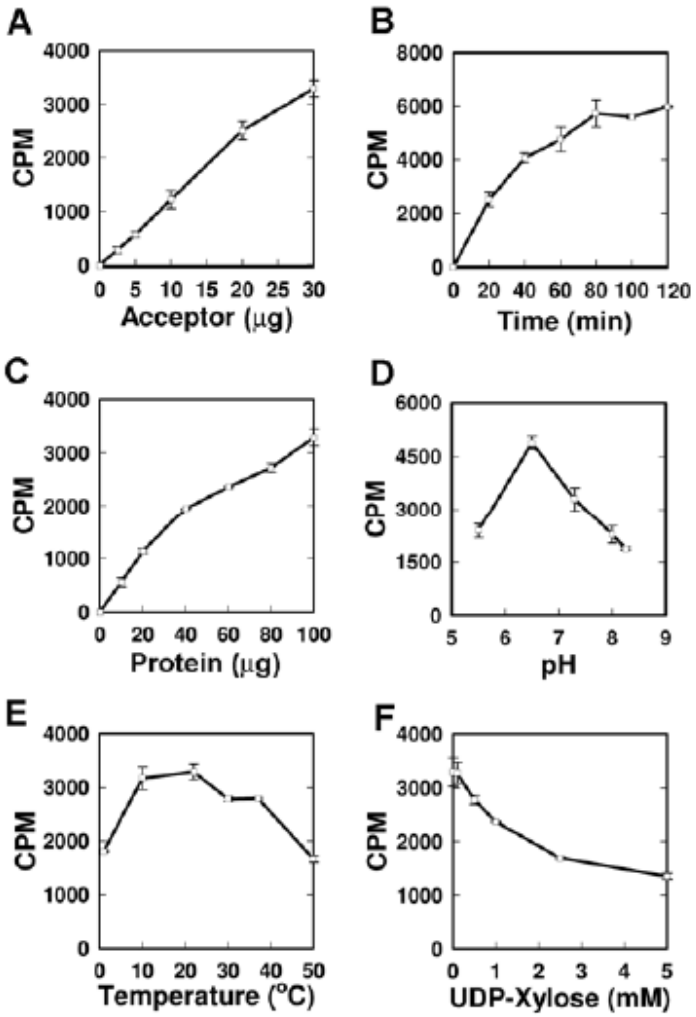
A
CPM
4000
3000
2000
1000
0
0 5 10 15 20 25 30
Acceptor (μg)
B
CPM
8000
6000
4000
2000
0
0 20 40 60 80 100 120
Time (min)
C
CPM
4000
3000
2000
1000
0
0 20 40 60 80 100
Protein (μg)
D
CPM
6000
4500
3000
1500
0
5 6 7 8 9
pH
E
CPM
4000
3000
2000
1000
0
0 10 20 30 40 50
Temperature (°C)
F
CPM
4000
3000
2000
1000
0
0 1 2 3 4 5
UDP-Xylose (mM)

Figure 2.7. The XylT and GlcAT activities in different *Arabidopsis* organs. Microsomes isolated from stems, seedlings, roots and leaves were incubated with UDP-[^{14}C]-Xyl and Xyl_6 for 20 min, and the XylT activity was measured by counting the radioactivity (CPM) of the reaction products. All assays were repeated twice and the data are means ± SE. The middle and bottom parts of stems exhibited the highest XylT and GlcAT activities.

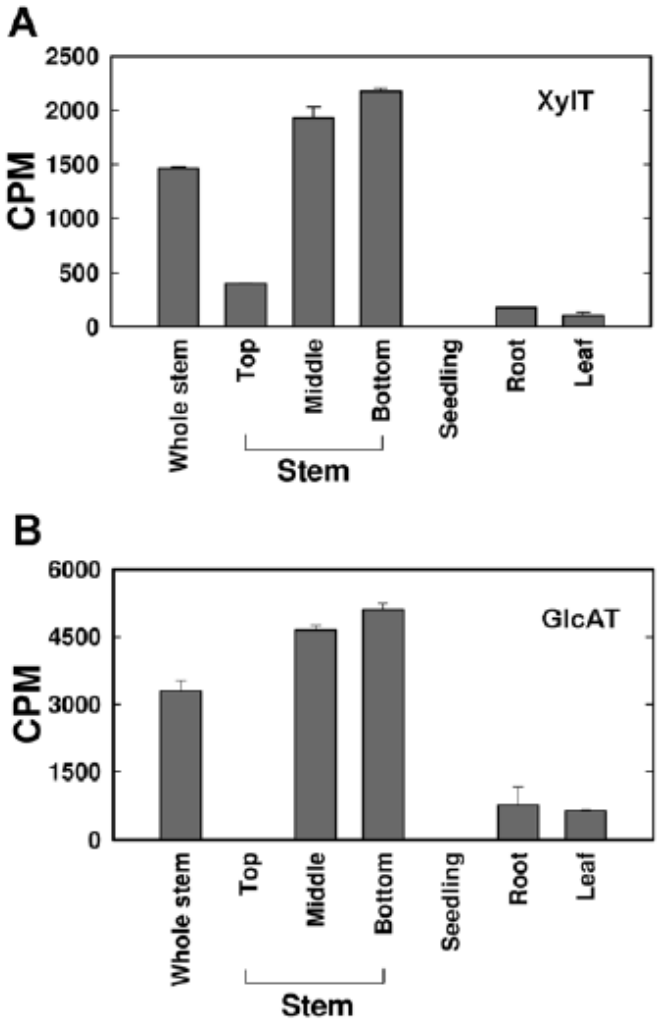
A
2500
2000
1500
1000
500
0
CPM
XylT
Whole stem
Top
Middle
Bottom
Seedling
Root
Leaf
Stem
B
6000
4500
3000
1500
0
CPM
GlcAT
Whole stem
Top
Middle
Bottom
Seedling
Root
Leaf
Stem

Figure 2.8. The XylT and GlcAT activities in the stems of wild type, *irx9*, *irx8* and *fra8*. Microsomes isolated from the wild type and mutants were incubated with Xyl_6 and UDP-[^{14}C]-GlcA or UDP-[^{14}C]-Xyl for 20 min unless otherwise indicated, and the GlcAT and XylT activities were measured by counting the radioactivity (CPM) of the reaction products. All assays were repeated twice and the data are means ± SE. (A) GlcAT activity in the *irx9*, *irx8* and *fra8* mutants compared with the wild type. (B) XylT activity in the *irx9*, *irx8* and *fra8* mutants compared with the wild type. Note that the XylT activity was drastically reduced in the *irx9* mutant but slightly increased in the *irx8* and *fra8* mutants. (C) Time course of the XylT activity in the wild type and the *irx9* mutant. The XylT activity in *irx9* remained low even after 2-hr incubation. (D) Complementation of *irx9* with the *Arabidopsis* IRX9 or its poplar homolog PoGT43B restored the XylT activity.

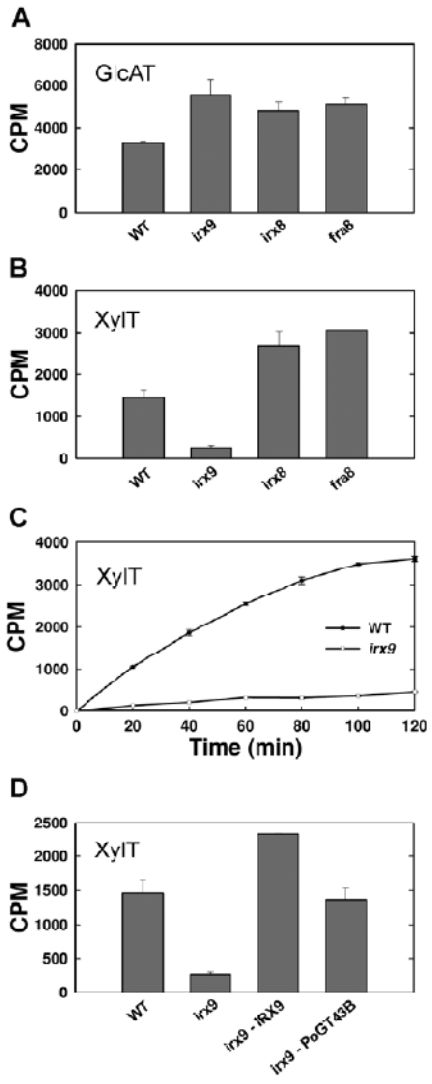
A
GlcAT
CPM
8000
6000
4000
2000
0
WT
irx9
irx8
fra8
B
XylT
CPM
4000
3000
2000
1000
0
WT
irx9
irx8
fra8
C
XylT
CPM
4000
3000
2000
1000
0
0
20
40
60
80
100
120
Time (min)
WT
irx9
D
XylT
CPM
2500
2000
1500
1000
500
0
WT
irx9
irx9 - IRX9
irx9 - PoGT43B

Figure 2.9. Deficiency in the transfer of xylosyl residues onto xylooligomer acceptors in the *irx9* mutant. Microsomes from the wild type (A, B) and *irx9* (C, D) were incubated with UDP-Xyl and the fluorescent Xyl_6-AA acceptor for 2 hr (A, C) and 5 hr (B, D), and the reaction products were analyzed by reverse-phase HPLC. Note that the XylT activity in the wild type transferred up to 6 xylosyl residues onto the acceptors, whereas only up to three xylosyl residues were transferred by the XylT activity in *irx9*.

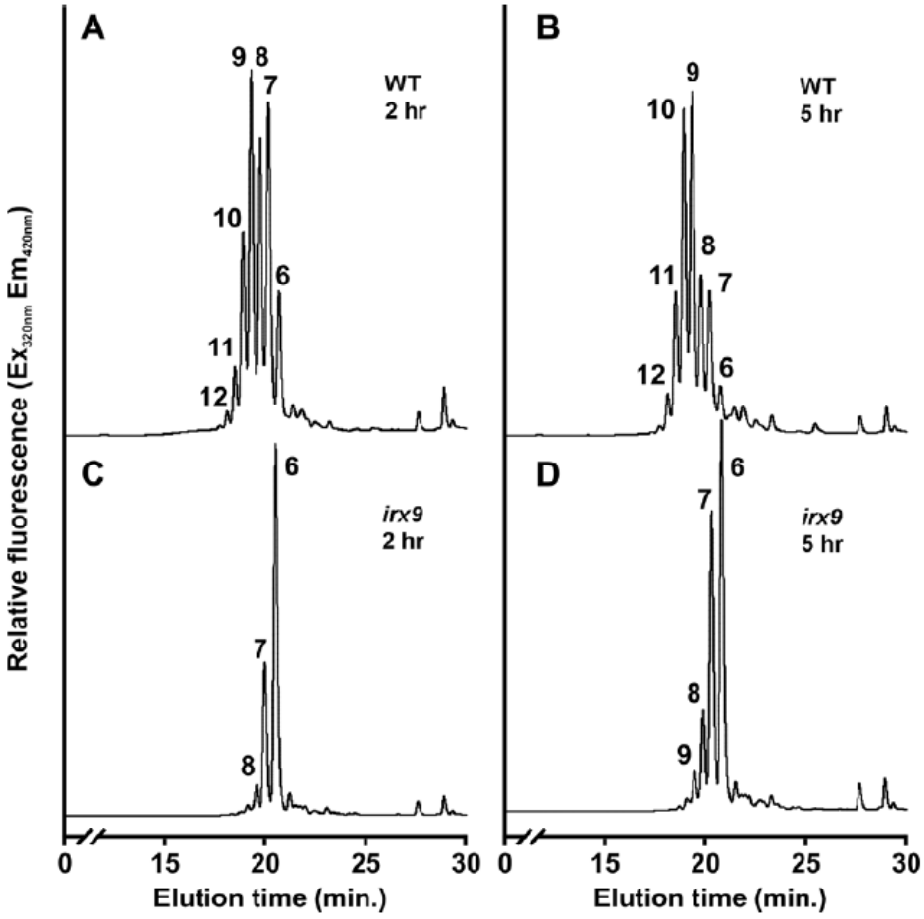
A
B
C
D
WT
2 hr
WT
5 hr
irx9
2 hr
irx9
5 hr
Relative fluorescence (Ex320nm Em420nm)
Elution time (min.)
Elution time (min.)
0
15
20
25
30

CHAPTER 3

THE *PARVUS* GENE IS EXPRESSED IN CELLS UNDERGOING SECONDARY WALL THICKENING AND ESSENTIAL FOR GLUCURONOXYLAN BIOSYNTHESIS[1]

[1] Lee, C., Zhong, R., Richardson, E.A., Himmelsbach, D.S., McPhail, B.T., and Ye, Z.-H. (2007). Plant Cell Physiology 43: 1659-1672. Selected as a cover page. Reprinted here with permission of publisher.

ABSTRACT

Xylan together with cellulose and lignin are the three major components of secondary walls in wood and elucidation of the biosynthetic pathway of xylan is of importance for potential modification of secondary wall composition to produce wood with improved properties. So far, three *Arabidopsis* glycosyltransferases, FRAGILE FIBER8, IRREGULAR XYLEM8 and IRREGULAR XYLEM9, have been implicated in glucuronoxylan (GX) biosynthesis. In this study, we demonstrate that PARVUS, which is a member of family GT8, is required for the biosynthesis of the tetrasaccharide primer sequence, β-D-Xyl-(1→3)-α-L-Rha-(1→2)-α-D-GalA-(1→4)-D-Xyl, located at the reducing end of GX. The *PARVUS* gene is expressed during secondary wall biosynthesis in fibers and vessels, and its encoded protein is predominantly localized in the endoplasmic reticulum. Mutation of the *PARVUS* gene leads to a drastic reduction in secondary wall thickening and GX content. Structural analysis of GX using 1H NMR spectroscopy revealed that the *parvus* mutation causes a loss of the tetrasaccharide primer sequence at the reducing end of GX and an absence of glucuronic acid side chains in GX. Activity assay showed that the xylan xylosyltransferase and glucuronyltransferase activities were not affected in the *parvus* mutant. Together, these findings implicate a possible role of PARVUS in the initiation of biosynthesis of the GX tetrasaccharide primer sequence and provide novel insights into the mechanisms of GX biosynthesis.

INTRODUCTION

Cellulose, xylan and lignin are the three principal components of dicot wood. Because of the importance of wood in human life, it is imperative to elucidate the mechanisms involved in the biosynthesis and regulation of wood components. Knowledge gained from such studies will potentially allow us to modify cell wall composition on the basis of our needs, such as engineering walls more suitable for biofuel production. Although the biosynthetic genes for cellulose and lignin have been well characterized, our understanding of genes involved in xylan biosynthesis is limited.

Xylan is composed of a linear backbone of (1,4)-linked β-D-xylosyl (Xyl) residues with an average degree of polymerization from 90 to 120 (Johansson and Samuelson, 1977; Pena et al., 2007). About 10% of Xyl residues on the backbone are substituted with α-D-glucuronic acid (GlcA), 4-*O*-methyl-α-D-glucuronic acid (MeGlcAT), and/or α-D-arabinose at *O*-2 and/or *O*-3, and the Xyl residues may be acetylated on C-2 or C-3 (Ebringerová and Heinze, 2000). Based on the nature of substitutions, xylan is typically named (methyl)glucuronoxylan (GX), which is the main hemicellulose in dicot wood, arabinoxylan and glucuronoarabinoxylan, which are the most abundant hemicelluloses in grass cell walls (Ebringerová and Heinze, 2000). The biosynthesis of the xylan backbone and its side chains requires at least five types of enzymes, including xylosyltransferases (XylT), glucuronyltransferases (GlcAT), arabinosyltransferases, methyltransferases, and acetyltransferases. The activities of XylT, GlcAT, arabinosyltransferase, and methyltransferases involved in xylan biosynthesis have been biochemically studied in a number of plant species (Dalessandro and Northcote, 1981; Baydoun et al., 1983 and 1989; Suzuki et al., 1991; Porchia and Scheller, 2000; Kuroyama and Tsumuraya, 2001; Gregory et al., 2002; Porchia et al., 2002; Urahara et al., 2004). Recently, the *IRREGULAR XYLEM9* (*IRX9*)

gene, which encodes a putative glycosyltransferase (GT) belonging to family GT43 (Coutinho et al., 2003), has been found to be essential for normal xylan backbone biosynthesis. The *IRX9* gene is expressed in cells undergoing the biosynthesis of secondary walls including GX, and its encoded protein is localized in Golgi, where GX is synthesized (Pena et al., 2007). Mutation of the *IRX9* gene causes a reduction in GX level (Brown et al., 2005; Bauer et al., 2006) as well as a substantial decrease in GX chain length (Pena et al., 2007). The defective GX chain elongation caused by the *irx9* mutation is correlated with a deficiency in xylan XylT activity (Lee et al., 2007). IRX9 is the first GT known to be required for normal xylan XylT activity. Both genetic and biochemical analyses suggest that IRX9 is a putative xylan synthase required for GX backbone elongation (Pena et al., 2007; Lee et al., 2007). The poplar GT43A/B, which is a homolog of IRX9 and expressed during wood formation (Aspeborg et al., 2005), is also likely responsible for GX backbone elongation in the secondary walls of wood because PoGT43B can functionally complement the GX and XylTase deficiency caused by the *irx9* mutation (Zhou et al., 2007; Lee et al., 2007).

In addition to the β-(1,4)-linked D-Xyl residues in the backbone, the reducing end of GX from birch, spruce and *Arabidopsis* has been found to contain a distinct tetrasaccharide primer sequence β-D-Xyl-(1→3)-α-L-Rha-(1→2)-α-D-GalA-(1→4)-D-Xyl (Shimizu et al., 1976; Johansson and Samuelson, 1977; Anderson et al. 1983; Pena et al., 2007). Conceivably, at least four additional GTs are required for the biosynthesis of the tetrasaccharide primer sequence. So far, two GT genes, *FRAGILE FIBER8* (*FRA8*) and *IRX8*, which encode proteins belonging to GT families 47 and 8 (Coutinho et al., 2003), respectively, have been implicated in the biosynthesis of the tetrasaccharide primer sequence at the GX reducing end. Both *FRA8* and *IRX8* are specifically expressed in cells undergoing secondary wall biosynthesis, and their encoded

proteins are localized in Golgi (Zhong et al., 2005b; Pena et al., 2007). Mutations of the *FRA8* and *IRX8* genes result in a reduction in GX level (Brown et al., 2005; Zhong et al., 2005b; Pena et al., 2007; Persson et al., 2007) and a near absence of the tetrasaccharide primer sequence, indicating that FRA8 and IRX8 are involved in the biosynthesis of the tetrasaccharide primer sequence at the GX reducing end (Pena et al., 2007). Because family GT47 enzymes to which FRA8 belongs have inverting mechanisms and catalyze the formation of β-glycosidic linkages using α-linked nucleotide sugars or vice-versa, FRA8 was proposed to catalyze the β-linkage of Xyl to *O*3 of rhamnose using UDP-α-D-Xyl as a substrate or the α-linkage of rhamnose to *O*2 of galacturonic acid (GalA) using UDP-β-L-rhamnose (Pena et al., 2007). Since family GT8 enzymes of which IRX8 is a member have retaining mechanisms and typically catalyze the formation of α-glycosidic linkages using α-linked nucleotide sugars, IRX8 was proposed to catalyze the α-linkage of GalA to *O*4 of the reducing Xyl residue of the tetrasaccharide primer sequence (Pena et al., 2007). The poplar GT47C, which is a homolog of FRA8 and expressed during wood formation, is also likely involved in the biosynthesis of the tetrasaccharide primer sequence at the reducing end of GX in secondary walls of wood (Zhou et al., 2006).

As described above, three GT genes have been implicated in various steps of GX biosynthesis. However, at least nine different enzymes are required for the biosynthesis of GX, arabinoxylan and glucuronoarabinoxylan. To further our understanding of the xylan biosynthetic pathway, it is necessary to identify and characterize additional xylan biosynthetic genes. In this study, we report that the *PARVUS* gene, which encodes a protein belonging to family GT8, is another GT required for GX biosynthesis. We show that the *PARVUS* gene is expressed during secondary wall biosynthesis and its encoded protein is localized in the endoplasmic reticulum (ER). We demonstrate that mutation of the *PARVUS* gene leads to a reduction in GX content and a loss of

the tetrasaccharide primer sequence at the GX reducing end. Considering the fact that PARVUS is associated with ER, it is tempting to propose that PARVUS is involved in the first transfer of the reducing Xyl residue of the tetrasaccharide primer sequence at the GX reducing end to an unknown acceptor at ER.

RESULTS

Expression of the PARVUS gene is associated with secondary wall thickening

The interfascicular fibers of *Arabidopsis* inflorescence stems deposit a large amount of cellulose, xylan and lignin in secondary walls, which have been used as a model for studying genes involved in secondary wall biosynthesis (Zhong et al., 2001 and 2005b; Pena et al., 2007). To find genes responsible for xylan biosynthesis, we analyzed GTs that were up-regulated during secondary wall thickening using interfascicular fibers isolated by laser microdissection (Zhong et al., 2006). In this report, we studied the function of a putative GT gene, At1g19300, which was induced during secondary wall thickening of fibers. The At1g19300 gene is a member of GT family 8 (Coutinho et al., 2003) and was previously named *PARVUS/GLZ1/GATL1* (Lao et al., 2003; Shao et al., 2004; Sterling et al., 2006) and proposed to be involved in pectin biosynthesis (Lao et al., 2003; Lerouxel et al., 2006). We have found that the *PARVUS* gene is highly expressed in fibers and xylem cells undergoing secondary wall thickening but not in parenchymatous pith cells (Fig. 3.1A). At the organ level, the *PARVUS* gene is predominantly expressed in stems in which abundant secondary wall-containing fibers and xylem cells are produced (Fig. 3.1B). In addition, the expression of the *PARVUS* gene was shown to be co-induced with three known xylan biosynthetic genes, *FRA8*, *IRX8* and *IRX9*, by overexpression of MYB46 (Fig. 3.1C), which results in ectopic deposition of secondary walls (Zhong et al., 2007a). Moreover, its expression was down-regulated together with *FRA8*, *IRX8* and *IRX9* in

SND1/NST1 RNAi lines (Fig. 3.1D), which exhibit a loss of secondary wall thickening in fiber cells (Zhong et al., 2007b). Therefore, we reasoned that PARVUS is likely involved in the biosynthesis of a secondary wall component, such as GX, rather than pectin as previously proposed.

We next performed *in situ* mRNA localization to investigate the developmental expression pattern of the *PARVUS* gene in *Arabidopsis* stems and roots. In rapidly elongating internodes in which protoxylem is the only secondary wall-containing tissue present, the *PARVUS* mRNA signal was seen in the developing vessels of the protoxylem (Fig. 3.2A). At this stage, interfascicular fiber cells are undergoing rapid elongation and no secondary wall thickening is evident (Ye et al., 2002). Concomitantly, no *PARVUS* mRNA signal was seen in interfascicular fiber cells (Fig. 3.2A). In nonelongating internodes in which secondary wall thickening is evident in interfascicular fibers, strong *PARVUS* mRNA signal was detected in interfascicular fiber cells in addition to developing vessels and xylary fibers in metaxylem (Fig. 3.2B). The *PARVUS* mRNA signal was also observed in developing vessels and xylary fibers in secondary xylem of roots (Fig. 3.2C). The control stem section hybridized with the sense *PARVUS* RNA probe did not show any positive signals (Fig. 3.2D). These results demonstrate that the *PARVUS* gene is specifically expressed in cells undergoing secondary wall thickening, including interfascicular fibers, vessels, and xylary fibers. The secondary wall-associated expression pattern of the *PARVUS* gene revealed in this study differs from that reported in a previous study, which employed the promoter-GUS reporter gene analysis and showed its expression in almost all cell types in stems (Shao et al., 2004). It is apparent that the promoter used in the expression study lacks some regulatory elements required for the endogenous gene expression.

The PARVUS protein is associated with the endoplasmic reticulum

The PARVUS protein is predicted to have a hydrophobic signal peptide sequence at the N-terminus (Fig. 3.3A; Lao et al., 2003) by both protein hydropathy analysis and the prediction of protein sorting signals and localization sites program (PSORT; http://psort.ims.u-tokyo.ac.jp/). To examine the subcellular localization of the PARVUS protein, we co-expressed yellow fluorescent protein (YFP)-tagged PARVUS with a cyan fluorescent protein (CFP)-tagged ER marker and a Golgi marker in carrot (*Daucus carota*) protoplasts and studied their colocalization patterns. It was found that the fluorescent signals of PARVUS-YFP displayed a network-like pattern, which clearly overlapped with the localization pattern of the ER marker (Fig. 3.3D to G). In contrast, the network-like signals of PARVUS-YFP displayed apparent differences from the punctate localization pattern of FRA8-CFP (Fig. 3.3H to K) that is known to be localized in Golgi (Zhong et al., 2005a) although some overlap of signals was observed. The control protoplasts expressing YFP alone had fluorescent signals distributed throughout the cytoplasm (Fig. 3.3B, C). These results indicate that the PARVUS protein is predominantly associated with ER.

Mutation of the PARVUS gene causes a severe reduction in secondary wall thickening of fibers and vessels

The finding that the *PARVUS* gene is specifically expressed in cells undergoing secondary wall thickening suggests that it is likely involved in secondary wall biosynthesis. To find out whether the *PARVUS* gene is essential for secondary wall thickening, we obtained a homozygous T-DNA insertion knockout line of *PARVUS* (SALK_045368; obtained from ABRC, Columbus, OH, USA)) for examination of stem strength and wall thickness of fibers and vessels. The homozygous T-DNA knockout plants were smaller in rosette size and their stems exhibited a dwarf phenotype, which is identical to the previously reported observations for *parvus* mutations

(Lao et al., 2003; Shao et al., 2004). It was found that mutation of the *PARVUS* gene led to a severe reduction in the mechanical strength of stems compared with the wild type (Fig. 3.4A). Examination of fibers and vessels in stems and roots revealed that the wall thickness of fibers and vessels in the *parvus* mutant was drastically decreased compared with the wild type (Fig. 3. 4B to G). It was apparent that the vessels in the *parvus* mutant exhibited a collapsed phenotype, which is most likely caused by the reduced wall strength as observed in other known secondary wall defective mutants (Brown et al., 2005; Zhong et al., 2005b; Persson et al., 2005). Transmission electron microscopy showed that the wall thickness of interfascicular fibers, vessels and xylary fibers was reduced by 50 to 66% compared with the wild type (Fig. 3.5; Table 3.1). These results suggest that PARVUS is required for normal secondary wall thickening in both fibers and vessels.

Mutation of the PARVUS gene results in a reduction in GX content in stems and a loss of LM10 antibody labeling of xylan in secondary walls of fibers and vessels

The observation that PARVUS is associated with ER indicates that it is involved in the biosynthesis of a non-cellulosic polysaccharide. Because the major non-cellulosic polysaccharide in secondary walls of *Arabidopsis* fibers and vessels is GX, we postulate that PARVUS might play a role in GX biosynthesis. To investigate which secondary wall components are affected by the *parvus* mutation, we first analyzed the composition of total cell walls isolated from stems and found that the amount of xylose and glucose, which are the respective main components of GX and cellulose, was reduced by 46.7% and 23.5%, respectively, compared with the wild type (Table 3.2). No significant alterations were seen in the amount of other cell wall neutral sugars, including mannose, galactose, arabinose, rhamnose and fucose. Further composition analysis of 1 N and 4 N KOH extracts of cell walls from stems of wild type and *parvus* showed that the most

drastically reduced sugar content was xylose (Table 3.3). Because the xylose in 1 N and 4 N KOH extracts of *Arabidopsis* stems primarily comes from GX (Zhong et al., 2005b), these findings strongly suggest that PARVUS is involved in GX biosynthesis. The reduction in cellulose content in the *parvus* mutant is likely due to an indirect effect, which has also been observed in three other known xylan deficient mutants (Brown et al., 2005; Zhong et al., 2005b). The *parvus* mutation has previously been shown to reduce the xylose content in leaf cell walls, which was attributed to an indirect effect due to its presumed role in pectin biosynthesis (Lao et al., 2003). Because PARVUS is a GT believed to be involved in polysaccharide synthesis but unlikely in lignin synthesis, we did not analyze the possible effect of its mutation on lignin alterations.

To substantiate the role of PARVUS in GX biosynthesis, we next examined the effect of the *parvus* mutation on GX deposition by immunolocalization using monoclonal antibody LM10 that binds to 4-*O*-methylglucuronoxylan (McCartney et al., 2005). Immunolabeling of wild-type stem and root sections showed intensive fluorescent signals in the walls of interfascicular fibers and xylem cells including vessels and xylary fibers (Fig. 3.6A, D), all of which are known to contain abundant GX in secondary walls. In contrast, almost no fluorescent signals were observed in the secondary wall-containing tissues in *parvus* stems and roots (Fig. 3.6B, E). Expression of the wildtype *PARVUS* gene in the *parvus* mutant restored the xylan signals to the wild-type level in all secondary wall-containing tissues in stems and roots (Fig. 3.6C, F). These results demonstrate that PARVUS is required for the normal biosynthesis and deposition of GX in secondary walls of fibers and vessels.

The parvus mutation leads to an absence of nonmethylated GlcA side chains in GX

To determine whether mutation of the *PARVUS* gene affects the GX structure, the KOH solubilized GX from stems of wild type and the *parvus* mutant was digested with endoxylanase and the acidic xylooligosaccharides produced by the digestion were analyzed by matrix-assisted laser-desorption ionization time-of-flight mass spectrometry (MALDI-TOF MS). MALDI-TOF MS of the wild-type acidic xylooligosacchrides revealed two major ion peaks [M + Na]+ at mass to-charge ratios (*m/z*) of 743 and 759 (Fig. 3.7A), which are attributed to xylooligosaccharides with four Xyl residues substituted with one non-methylated α-D-GlcA or one 4-*O*-Me-α-D-GlcA, respectively (Fig. 3.7C; Zhong et al., 2005b). The xylooligosaccharides bearing 4-*O*-Me-α-D-GlcA side chains are more abundant than those bearing α-D-GlcA side chains, which is a typical pattern observed in the GX of wild-type *Arabidopsis* (Zhong et al., 2005b). In contrast, the MALDI-TOF spectrum of *parvus* acidic xylooligosacchrides contains only the ion peak at *m/z* of 759 (Fig. 3.7B). The *parvus* mutant lacked the ion with *m/z* of 745 that is attributed to xylotetrasaccharides substituted with one nonmethylated α-D-GlcA. The MALDI-TOF analysis demonstrates that the *parvus* mutation results in a loss of α-D-GlcA side chains in GX.

The *parvus* mutation causes a loss of the tetrasaccharide primer sequence located at the reducing end of GX

The *Arabidopsis* GX contains a tetrasaccharide primer sequence located at the reducing end, which differs from the GX backbone (Pena et al., 2007). Previous study showed that FRA8 and IRX8 are required for the biosynthesis of this tetrasaccharide primer sequence (Pena et al., 2007). To further investigate the roles of PARVUS in GX biosynthesis, we examined whether the *parvus* mutation affects the biosynthesis of the tetrasaccharide primer sequence using NMR spectrometry. The ^{1}H-NMR spectrum of wild-type acidic xylooligosaccharides contained anomeric resonances of H1 and H5 of α-D-GlcA and H1 of branched β-D-Xyl residues bearing

an α-D-GlcA residue as well as H1 and H5 of 4-*O*-Me-α-D-GlcA residues and H1 of branched β-D-Xyl residues bearing a 4-*O*-Me-α-D-GlcA residue (Fig. 3.8A). The spectrum also includes resonances of H1 of α-Xyl and β-Xyl residues at the reducing ends of oligoxylosaccharides and H1 of unbranched β-Xyl residues (Fig. 3.8A). Furthermore, the resonances assigned to the tetrasaccharide primer sequence β-D-Xyl-(1→3)-α-L-Rha-(1→2)-α-D-GalA-(1→4)-D-Xyl that is located at the reducing end of GX was apparent in the spectrum of wild-type acidic xylooligosaccharides (Fig. 3.8A). These resonances include H1 of α-D-GalA, H1 of α-L-Rha, H1 of 3-linked β-D-Xyl, H4 of α-D-GalA, and H2 of α-L-Rha. The observed 1H-NMR spectrum of wild-type acidic xylooligosaccharides is the same as that previously reported for wild-type *Arabidopsis* acidic xylooligosaccharides (Zhong et al., 2005; Pena et al., 2007). Examination of the 1H-NMR spectrum of *parvus* acidic xylooligosaccharides showed an apparent lack of resonances of H1 of α-D-GalA, H1 of α-L-Rha, H1 of 3-linked β-DXyl, H4 of α-D-GalA, and H2 of α-L-Rha, which are assigned to the tetrasaccharide primer sequence β-D-Xyl-(1→3)-α-L-Rha-(1→2)-α-D-GalA-(1→4)-D-Xyl that is located at the reducing end of GX (Fig. 3.8B). In addition, the resonances assigned to H1 and H5 of α-D-GlcA and H1 of branched β-D-Xyl residues bearing an α-D-GlcA residue were absent in *parvus* (Fig. 3.8B), which is consistent with the MALDI-TOF data (Fig. 3.7). These results demonstrate that the *parvus* mutation leads to a loss of the tetrasaccharide primer sequence at the GX reducing end, which suggests that PARVUS is involved in the biosynthesis of the tetrasaccharide primer sequence.

The xylan xylosyltransferase and glucuronyltransferase activities are not affected by *parvus* mutation

To investigate whether the reduced GX content and altered GX structure were caused by a reduction in xylan xylosyltransferase (XylT) or glucuronyltransferase (GlcAT) activities, we performed comparative analysis of their activities using microsomes isolated from wild-type and *parvus* stems. It was found that there was no decrease in the XylT and GlcAT activities in the *parvus* mutant; instead they were elevated compared with the wild type (Fig. 3.9). The elevation of XylT and GlcAT activities was also observed in three other xylan deficient mutants, *fra8*, *irx8* and *irx9* (Lee et al., 2007), probably due to a compensatory effect caused by these mutations. These results suggest that PARVUS is not required for the normal activities of xylan XylT and GlcAT.

DISCUSSION

Xylan is the second most abundant polysaccharide in dicot wood and thus understanding its biosynthetic pathway is of importance for rationally modifying secondary wall composition to produce wood with improved properties. At least nine different enzymes are needed in the multiple steps of xylan biosynthesis, including the initiation and elongation of xylan backbone, and addition and modification of xylan side chains. So far, one GT, IRX9, has been demonstrated to be required for normal xylan XylT activity and normal elongation of the xylan chain, and two other GTs, FRA8 and IRX8, have been shown to be required for the biosynthesis of the tetrasaccharide primer sequence at the reducing end of GX. Our identification of PARVUS as another GT essential for the biosynthesis of the tetrasaccharide primer sequence at the reducing end of GX marks another important step toward the elucidation of the complex process of xylan biosynthesis.

***PARVUS* is expressed during secondary wall biosynthesis and its encoded protein is associated with the endoplasmic reticulum**

Gene expression analyses revealed that the *PARVUS* gene is expressed predominantly in cells undergoing secondary wall thickening (Figs. 3.1 and 3.2), a pattern similar to that of three other known xylan biosynthetic genes (Zhong et al., 2005b; Pena et al., 2007; Persson et al., 2007). The secondary wall-associated expression pattern indicates that PARVUS is unlikely involved in the biosynthesis of a primary wall component, such as pectin, because there is little pectin present in secondary walls (Willats et al., 2001). The previous notion that PARVUS might be involved in pectin biosynthesis was primarily based on its sequence homology to other members of family GT8, QUASIMODO1 (Bouton et al., 2001) and GAUT1 (Sterling et al., 2006), and no genetic or biochemical data are available to substantiate such a proposed function. As discussed below, the secondary wall-associated expression pattern of PARVUS is consistent with its essential role in the biosynthesis of GX in secondary walls. The poplar GT8E/F, which is a close homolog of PARVUS, has also been shown to be expressed during wood formation (Aspeborg et al., 2005). PARVUS was found to be predominantly localized in ER, a localization pattern different from that of other known xylan biosynthetic enzymes, FRA8, IRX8 and IRX9, which are located in Golgi (Zhong et al., 2005b; Pena et al., 2007). This difference is consistent with the sequence analysis showing that whereas FRA8, IRX8 and IRX9 are type II membrane proteins, PARVUS is predicted to contain a hydrophobic signal peptide sequence but no transmembrane helices. The ER localization of PARVUS suggests that it catalyzes a step that is different from FRA8, IRX8 and IRX9 in GX biosynthesis.

PARVUS is likely involved in the initiation of the biosynthesis of the GX tetrasaccharide primer sequence at the endoplasmic reticulum

Structural analysis of GX from the *parvus* mutant clearly demonstrates that PARVUS is involved in the biosynthesis of the tetrasaccharide primer sequence at the reducing end of GX. Thus,

PARVUS joins FRA8 and IRX8 in the list of GTs required for the synthesis of the tetrasaccharide sequence. Based on their catalytic mechanisms, FRA8 has previously been proposed to catalyze the transfer of Xyl to rhamnose or rhamnose to GalA, whereas IRX8 was proposed to transfer GalA to the reducing Xyl residue at the GX reducing end (Pena et al., 2007). Because PARVUS belongs to family GT8 in which known members have retaining catalytic mechanisms and it is phylogenetically related to IRX8, it is possible that PARVUS and IRX8 function redundantly in catalyzing the addition of α-D-GalA to *O*4 of the reducing Xyl residue at the GX reducing end using UDP-α-D-GalA as a sugar donor. However, the fact that PARVUS is predominantly localized in ER and IRX8 in Golgi suggests that PARVUS catalyzes an enzymatic step earlier than IRX8 in the GX biosynthetic pathway. One appealing hypothesis is that PARVUS is involved in the initiation of the tetrasaccharide primer biosynthesis by catalyzing the transfer of the reducing Xyl residue onto an unknown acceptor in ER. This scenario bears analogy with the biosynthesis of animal glycosaminoglycans. It has been shown that the biosynthesis of animal glycosaminoglycans requires a tetrasaccharide primer sequence, and the synthesis of the primer is initiated in ER by transferring of the reducing Xyl residue to protein and the subsequent steps of the tetrasaccharide primer synthesis occur in Golgi (Prydz and Dalen, 2000). Previous study has shown that GX is covalently attached to protein (Crosthwaite et al., 1994). Thus, it is possible that the GX tetrasaccharide primer synthesis is initiated in ER where PARVUS might catalyze the transfer of the reducing Xyl residue to protein, which is then transported to Golgi where subsequent additions of sugar residues are catalyzed by IRX8, FRA8 and other uncharacterized GTs. It was previously proposed that the tetrasaccharide sequence at the reducing end of GX might function as a primer or as a chain terminator for GX biosynthesis (Pena et al., 2007). Our finding that PARVUS is predominantly localized in ER and

required for the synthesis of the tetrasaccharide sequence at the reducing end of GX favors the tetrasaccharide sequence as a primer for GX biosynthesis.

PARVUS is essential for the biosynthesis of normal amount of GX and GlcA side chains

In addition to a loss of the tetrasaccharide sequence at the reducing end of GX, the *parvus* mutation also leads to a reduction in GX content and a loss of GlcA side chains. These phenotypes, which are also observed in three other xylan mutants, *fra8*, *irx8* and *irx9* (Brown et al., 2005; Zhong et al., 2005b; Bauer et al., 2006; Pena et al., 2007; Persson et al., 2007), are likely an indirect effect caused by the defects in the biosynthesis of the tetrasaccharide primer sequence. As proposed above, the tetrasaccharide sequence most likely functions as a primer for xylan backbone elongation, and thus a disruption in the biosynthesis of the primer sequence by the *parvus* mutation leads to an inhibition of GX biosynthesis. The loss of GlcA but not methylated GlcA side chains in GX could be explained by the saturation mechanism (Zhong et al., 2005; Pena et al., 2007). Because GlcA is methylated after it is transferred onto the GX backbone (Baydoun et al., 1989), it is possible that in wild type, the methyltransferase activity could not keep up with the rate of GlcA addition and thus a proportion of GlcA side chains are not methylated. In contrast, the GX biosynthesis rate is greatly reduced in the *parvus* mutant, and thus the available methyltransferase activity could sufficiently methylate all GlcA side chains. This is consistent with the activity data showing that the *parvus* mutation does not affect the GlcAT activity (Fig. 3.9).

In summary, our study reveals an essential role of PARVUS in GX biosynthesis in secondary walls. We have demonstrated that PARVUS is required for the biosynthesis of the tetrasaccharide primer sequence, β-D-Xyl-(1→3)-α-L-Rha-(1→2)-α-D-GalA-(1→4)-D-Xyl, located at the reducing end of GX. Based on our findings, we propose that PARVUS is involved

in the initiation of the biosynthesis of the tetrasaccharide sequence, which functions as a primer for subsequent GX biosynthesis. Our work provides foundation knowledge for further dissecting the mechanisms involved in the initiation of GX biosynthesis.

MATERIALS AND METHODS

Gene expression analysis

For analysis of gene expression in different cell types, interfascicular fiber cells, xylem cells and pith cells from inflorescence stems of 6-week-old *Arabidopsis* plants were isolated using the PALM microlaser system (PALM Microlaser Technologies, Bernried, Germany) and used for RNA isolation and amplification as described (Zhong et al., 2006). For analysis of gene expression in different organs, total RNA was isolated from leaves, roots, stems, and flowers of 6-week-old *Arabidopsis* plants using a Qiagen RNA isolation kit (Valencia, CA, USA). For quantitative PCR analysis, total RNA was treated with DNase I and used for first strand cDNA synthesis. The first strand cDNA was then used as template for real-time quantitative PCR analysis using gene specific primers (5'-gtacacgtcacgcatcgaagag-3' and 5'-agaatccaacgcgaacggcgtttg-3') with the QuantiTect SYBR Green PCR Kit (Clontech, Mountain View, CA, USA). The relative mRNA levels were determined by normalizing the PCR threshold cycle number of each gene with that of the *EF1α* reference gene. The expression level of each gene in the wild-type control or in the sample with the lowest expression level was set to 1 and the data were the average of three replicates.

In situ localization of mRNAs

Wild-type *Arabidopsis* inflorescence stems were used for *in situ* mRNA localization as described (McAbee et al., 2005). Tissues were fixed in 2.5% formaldehyde and 0.5% glutaraldehyde and then embedded in paraffin. Ten-micrometer-thick sections were cut, mounted onto slides, and

hybridized with digoxygenin-labeled *PARVUS* antisense RNA probe synthesized using the DIG RNA labeling mix (Roche, Mannheim, Germany). The *PARVUS* cDNA sequence used for RNA probe synthesis was PCR-amplified using gene-specific primers (5'-ccgacgcttcttccttacgag-3' and 5'-ggtttaatcaaaccggcaaaaacc-3') and this sequence shows no significant homology with other GTs. The hybridization and washing conditions used only allowed specific hybridization of the RNA probe to the *PARVUS* mRNA. The hybridization signals were detected with alkaline phosphatase-conjugated antibodies against digoxigenin and subsequent color development with alkaline phosphatase substrates.

Subcellular localization of fluorescent protein-tagged proteins

The colocalization of fluorescent protein-tagged PARVUS with the Golgi and ER markers was carried out in carrot protoplasts as described (Zhong et al., 2005a). The PARVUS cDNA was fused in frame with the yellow fluorescent protein (YFP) cDNA and ligated between the cauliflower mosaic virus 35S promoter and the nopaline synthase terminator in a high copy vector. The fusion protein thus generated will have the YFP tag at the C-terminus. The PARVUS-YFP construct was co-transfected into carrot protoplasts together with cyan fluorescent protein (CFP)-tagged FRA8, a protein known to be localized in Golgi (Zhong et al., 2005a) or with a CFP-tagged ER marker that was generated by fusing an *Arabidopsis* chitinase signal peptide to the N-terminus and an HDEL sequence to the C-terminus of CFP (Batoko et al., 2000). After 20-hr incubation, the transfected protoplasts were examined for yellow and cyan fluorescent signals using a Leica TCs SP2 spectral confocal microscope.

Immunolocalization of xylan

Basal stem internodes and roots of 10-week-old plants were fixed with 2% glutaraldehyde

in phosphate buffered saline (PBS), dehydrated through a gradient of ethanol, and then embedded in LR White Resin (Electron Microscopy Sciences, Fort Washington, PA, USA). One-micrometerthick sections were cut with a microtome and incubated with the LM10 monoclonal antibody, which recognizes glucuronoxylan (Plantprobes, Leeds, UK; McCartney et al., 2005) and then with fluorescein isothiocyanate-conjugated secondary antibodies. The fluorescence-labeled sections were observed using a Leica TCs SP2 spectral confocal microscope. Images from single optical sections were collected and processed with Adobe Photoshop.

Breaking force measurement

The main inflorescence of 10-week-old wild type *Arabidopsis* and *parvus* plants were divided into three equal segments, which were measured for their breaking force using a digital force/length tester (Model DHT4-50; Larson System, Minneapolis, MN, USA). The breaking force (g) was calculated as the force needed to break apart a stem segment (Zhong et al., 1997).

Histology

Basal stem internodes and roots of 10-week-old plants were fixed with 2% glutaraldehyde in PBS at 4oC overnight. After fixation, tissues were postfixed in 1% (v/v) OsO4, dehydrated through a gradient of ethanol, embedded in Spurr's resin (Electron Microscopy Sciences), and then subjected to sectioning with a microtome (Burk et al., 2006). One-micrometer-thick sections were stained with toluidine blue for light microscopy. For transmission electron microscopy, 85-nm thick sections were stained with uranyl acetate and lead citrate, and visualized using a Zeiss EM 902A transmission electron microscope.

Cell wall isolation and extraction

Inflorescence stems of 10-week-old plants were collected for cell wall isolation. Stems were ground into fine powder in liquid nitrogen with a motar and pestle, homogenized sequentially in

70% ethanol and 100% acetone with a polytron. The resulting cell wall residues were dried in a vacuum oven at 60oC. The wall preparations were subsequently subjected to sequential extractions with ammonium acetate (50 mM, 24 h), 1 N KOH containing 1% (w/v) NaBH4 (24 hr), and 4 N KOH containing 1% (w/v) NaBH4 (24 hr) according to Zhong et al. (2005b). The 1N and 4 N KOH soluble extracts were passed through a glass-fiber filter, neutralized to pH 6.0 with glacial acetic acid, dialyzed in a dialysis tubing (3,500 Mr cutoff; Fisher Scientific, Pittsburgh, PA, USA) against deionized water, and lyophilized.

Cell wall composition analysis

Cell wall sugars (as alditol acetates) were determined following the procedure described by Hoebler et al. (1989). Briefly, cell walls were incubated with 70% sulfuric acid at 37ºC for 60 minutes followed by addition of inositol as the internal standard and dilution with water to 2N sulfuric acid. After heating for 120 minutes at 100ºC, the solution was cooled and treated with 25% ammonium solution. After reduction with sodium borohydride in dimethyl sulfoxide, the solution was heated for 90 minutes at 40ºC, followed by sequential treatment with glacial acetic acid, acetic anhydride, 1-methylimidazole, dichloromethane, and water. The organic layer containing the alditol acetates of the hydrolyzed cell wall sugars was washed three times with water, and sugars were analyzed on an Agilent 6890N gas-liquid chromatography (Wilmington, DE, USA) equipped with a 30 m x 0.25 mm (i.d.) silica capillary column DB 225 (Alltech Assoc., Deerfield, IL, USA).

Generation of xylooligosaccharides with β-endo-xylanase

The 1 N and 4 N KOH solubilized wall preparations were digested with β-xylanase M6 (Megazyme, Wicklow, Ireland) for generation of xylooligosaccharides as described (Zhong et al., 2005b). The released xylooligosaccharides were desalted and separated by size-exclusion

chromatography on a Sephadex G-25 column (100 x 2.5 mm). Fractions containing the oligosaccharides were determined by the phenol-sulfuric assay (DuBois et al., 1956), pooled and lyophilized.

Matrix-assisted laser-desorption ionization time-of-flight mass spectrometry (MALDI-TOF MS)

The acidic xylooligosaccharides released from β-xylanase digestion were analyzed using a MALDI-TOF mass spectrometer operated in the positive-ion mode with an accelerating voltage of 30 kV, an extractor voltage of 9 kV, and a source pressure of approximately 8 x 10-7 torr. The aqueous sample was mixed (1:1, v/v) with the MALDI matrix (0.2 M 2,5-dihydroxbenzoic acid and 0.06 M 1-hydroxyisoquinoline in 50% acetonitrile) and dried on the stainless steel target plate. Spectra are the average of 100 laser shots.

^{1}H-NMR spectroscopy

NMR spectra of the acidic xylooligosaccharides from β-xylanase digestion were recorded at 298 K with an NMR spectrometer. Chemical shifts were measured relative to internal acetone at δ 2.225. The ^{1}H-NMR assignments were done by comparison with the NMR spectra data for *Arabidopsis* acidic xylooligosaccharides (Zhong et al., 2005b; Pena et al., 2007) and further confirmed by two-dimensional gCOSY, HSQC, HMBC, and TOCSY spectra.

Assay of GlcAT and XylT activities

Microsomes were isolated and the GlcAT and XylT activities were determined following the procedures by Kuroyama and Tsumuraya (2001). For assay of GlcAT activity, 100 μg of microsomes were incubated with the reaction mixture (a total volume of 30 μl) containing 50 mM Hepes-KOH, pH 6.8, 5 mM MnCl2, 1 mM DTT, 0.5% Triton X-100, 0.2 μg/μl Xyl6 (Megazyme), and UDP-[14C]-GlcA (0.1 μCi; American Radiolabeled Chemical, St. Louis, MO,

USA). For assay of XylT activity, 100 μg of microsomes were incubated with the reaction mixture (a total volume of 30 μl) containing 50 mM Hepes-KOH, pH 6.8, 5 mM MnCl2, 1 mM DTT, 0.5% Triton X-100, 0.1 mM cold UDP-Xyl (CarboSource Service, Athens, GA, USA; supported in part by NSF-RCN grant #0090281), 0.2 μg/μl Xyl6, and UDP-[14C]-Xyl (0.1 μCi; American Radiolabeled Chemical). After incubation at 21 oC for 20 min, the reactions were stopped by addition of the termination solution (0.3 M acetic acid containing 20 mM EGTA). The radiolabeled xylooligosaccharides were separated from UDP-[14C]-Xyl or UDP-[14C]-GlcA by paper chromatography according to Ishikawa et al. (2000), and the incorporation of radiolabeled Xyl or GlcA onto xylooligosaccharides was determined with a PerkinElmer scintillation counter (Waltham, MA, USA).

ACKNOWLEDGMENTS

We thank N.S. Hill for his help on the lyophilization of samples, M.A. O'Neill for his suggestions on GX analysis, and the editor and the reviewers for their comments and suggestions. C.H. Lee was partly supported by Korea Science and Engineering Foundation (Grant # KRF-2005-215-F00002). This work was supported by a grant from the U.S. Department of Energy-Bioscience Division (Grant # DE-FG02-03ER15415).

REFERENCES

Andersson, S.-I., Samuelson, O., Ishihara, M. and Shimizu, K. (1983) Structure of the reducing end-groups in spruce xylan. *Carbohydr. Res.* 111: 283-288.

Aspeborg, H., Schrader, J., Coutinho, P.M., Stam, M., Kallas, A., Djerbi, S., Nilsson, P., Denman, S., Amini, B., Sterky, F., Master, E., Sandberg, G., Mellerowicz, E., Sundberg, B., Henrissat, B. and Teeri, T.T. (2005) Carbohydrate-Active Enzymes Involved in the Secondary Cell Wall Biogenesis in Hybrid Aspen. *Plant Physiol.* 137: 983-997.

Batoko, H., Zheng, H.-Q., Hawes, C. and Moore, I. (2000) A Rab1 GTPase is required for transport between the endoplasmic reticulum and Golgi apparatus and for normal Golgi movement in plants. *Plant Cell* 12: 2201-2217.

Bauer, S., Vasu, P., Persson, S., Mort, A.J. and Somerville, C.R. (2006) Development and application of a suite of polysaccharide-degrading enzymes for analyzing plant cell walls. *Proc. Natl. Acad. Sci. USA.* 103: 11417-11422.

Baydoun, E.A.-H., Usta, J.A.-R., Waldron, K.W. and Brett, C.T. (1989) A methyltransferase involved in the biosynthesis of 4-*O*-methylglucuronoxylan in etiolated pea epicotyls. *J. Plant Physiol.* 135: 81-85.

Baydoun, E.A.-H., Waldron, K.W. and Brett, C.T. (1983) The interaction of xylosyltransferase and glucuronyltransferase involved in glucuronoxylan synthesis in pea (*Pisum sativum*) epicotyls. *Biochem. J.* 257: 853-858.

Bouton, S., Leboeuf, E., Mouille, G., Leydecker, M.-T., Talbotec, J., Grainier, F., Lahaye, M., Höfte, H. and Truong, H.-N. (2002) *QUASIMODO1* encodes a putative membrane-bound glycosyltransferase required for normal pectin synthesis and cell adhesion in *Arabidopsis*. *Plant Cell* 14: 2577-2590.

Brown, D.M., Zeef, L.A.H., Ellis, J., Goodacreb, R. and Turner, S.R. (2005) Identification of novel genes in *Arabidopsis* involved in secondary cell wall formation using expression profiling and reverse genetics. *Plant Cell* 17: 2281-2295.

Burk, D.H., Zhong, R., Morrison, W.H.III and Ye, Z.-H. (2006) Disruption of cortical microtubules by overexpression of green fluorescent protein-tagged α-tubulin 6 causes a marked reduction in cell wall synthesis. *J. Integr. Plant Biol.* 48: 85-98.

Coutinho, P.M., Deleury, E., Davies, G.J. and Henrissat, B. (2003) An evolving hierarchical family classification for glycosyltransferases. *J. Mol. Biol.* 328: 307-317.

Crosthwaite, S.K., MacDonald, F.M., Baydoun, E.A.-H. and Brett, C.T. (1994) Properties of a protein-linked glucuronxylan formed in the plant Golgi apparatus. *J. Exp. Bot.* 45: 471-475.

Dalessandro, G. and Northcote, D.H. (1981) Increase of xylan synthetase activity during xylem differentiation of the vascular cambium of sycamore and poplar trees. *Planta* 151: 61-67.

DuBois, M., Gilles, K.A., Hamilton, J.K., Rebers, P.A. and Smith, F. (1956) Colorimtric method for determination of sugars and related substances. *Anal. Chem.* 28: 350-356.

Ebringerová, A. and Heinze, T. (2000) Xylan and xylan derivatives-biopolymers with valuable properties, 1. Naturally occurring xylans structures, isolation procedures and properties. *Macromol. Rapid Commun.* 21: 542-556.

Gregory, A.C.E., Smith, C., Kerry, M.E., Wheatley, E.R. and Bolwell, G.P. **(**2002) Comparative subcellular immunolocation of polypeptides associated with xylan and callose synthases in French bean (*Phaseolus vulgaris*) during secondary wall formation. *Phytochemistry* 59: 249-259.

Hoebler, C., Barry, J.L., David, A. and Delort-Laval, J. (1989) Rapid acid-hydrolysis of plant cell wall polysaccharides and simplified quantitative determination of their neutral monosaccharides by gas-liquid chromatography. *J. Ag. Food Chem.* 37: 360-367.

Ishikawa, M., Kuroyama, H., Takeuchi, Y. and Tsumuraya, Y. (2000) Characterization of pectin methyltransferase from soybean hypocotyls. *Planta* 210: 782-791.

Johansson, M.H. and Samuelson, O. (1977) Reducing end groups in birch xylan and their alkaline degradation. *Wood Sci. Technol.* 11: 251-263.

Kuroyama, H. and Tsumuraya, Y. (2001) A xylosyltransferase that synthesizes β-(1->4)-xylans in wheat (*Triticum aestivum* L.) seedlings. *Planta* 213: 231-240.

Lao, N.T., Long, D., Kiang, S., Coupland, G., Shoue, D.A., Carpita, N.C. and Kavanagh, T.A. (2003) Mutation of a family 8 glycosyltransferase gene alters cell wall carbohydrate composition and causes a humidity-sensitive semi-sterile dwarf phenotype in *Arabidopsis*. *Plant Mol. Biol.* 53: 687-701.

Lee, C., O'Neill, M.A., Tsumuraya, Y., Darvill, A.G. and Ye, Z.-H. (2007) The *irregular xylem9* mutant is deficient in xylan xylosyltransferase activity. *Plant Cell Physiol* (doi:10.1093/pcp/pcm135).

Lerouxel, O., Cavalier, D.M., Liepman, A.H. and Keegstra, K. (2006) Biosynthesis of plant cell wall polysaccharides - a complex process. *Curr. Opin. Plant Biol.* 9: 621-630.

McAbee, J.M., Kuzoff, R.K. and Gasser, C.S. (2005) Mechanisms of derived unitegmy among impatiens species. *Plant Cell* 17: 1674-1684.

McCartney, L., Marcus, S.E. and Knox, J.P. (2005) Monoclonal antibodies to plant cell wall xylans and arabinoxylans. *J. Histochem. Cytochem.* 53: 543-546.

Pena, M.J., Zhong, R., Zhou, G.-K., Richardson, E.A., O'Neill, M.A., Darvill, A.G., York, W.S. and Ye, Z.-H. (2007) *Arabidopsis irregular xylem8* and *irregular xylem9*: Implications for the complexity of glucuronoxylan biosynthesis. *Plant Cell* 19: 549-563.

Persson, S., Caffall, K.H., Freshour, G., Hilley, M.T., Bauer, S., Poindexter, P., Hahn, M.G., Mohnen, D. and Somerville, C. (2007) The *Arabidopsis irregular xylem8* mutant is deficient in glucuronoxylan and homogalacturonan, which are essential for secondary cell wall integrity. *Plant Cell* 19: 237-255.

Persson, S., Wei, H., Miline, J., Page, G.P. and Somerville, C.R. (2005) Identification of genes required for cellulose synthesis by repression analysis of public microarray data sets. *Proc. Natl Acad. Sci. USA* 102: 8633-8638.

Porchia, A.C. and Scheller, H.V. (2000) Arabinoxylan biosynthesis: identification and partial characterization of β-1,4-xylosyltransferase from wheat. *Physiol. Plant.* 110: 350-356.

Porchia, A.C., Sorensen, S.O. and Scheller, H.V. (2002) Arabinoxylan biosynthesis in wheat. Characterization of arabinosyltransferase activity in Golgi membranes. *Plant Physiol.* 130: 432-441.

Prydz, K. and Dalen, K.T. (2000) Synthesis and sorting of proteoglycans. *J. Cell Sci.* 11: 193-205. Shao, M., Zheng, H., Hu, Y., Liu, D., Jang, J.-C., Ma, H. and Huang, H. (2004) The *GAOLAOZHUANGREN1* gene encodes a putative glycosyltransferase that is critical for normal development and carbohydrate metabolism. *Plant Cell Physiol.* 45: 1453-1460.

Shimizu, K., Ishihara, M. and Ishihara, T. (1976) Hemicellulases of brown rotting fungus, *Tyromyces palustris*. II. The oligosaccharides from the hydrolysate of a hardwood xylan by the intracellular xylanase. *Mokuzai Gaikkashi.* 22: 618-625.

Sterling, J.D., Atmodjo, M.A., Inwood, S.E., Kumar Kolli V.S., Quigley, H.F., Hahn, M.G. and Mohnen, D. (2006) Functional identification of an *Arabidopsis* pectin biosynthetic homogalacturonan galacturonosyltransferase. *Proc. Natl. Acad. Sci. USA* 103: 5236-5241.

Suzuki, K., Ingold, E., Sugiyama, M. and Komamine, A. (1991) Xylan synthase activity in isolated mesophyll cells of *Zinnia elegans* during differentiation to tracheary elements. *Plant Cell Physiol.* 32: 303-306.

Urahara, T., Tsuchiya, K., Kotake, T., Tohno-oka, T., Komae, K., Kawada, N. and Tsumuraya, Y. (2004) A β-(1→4)-xylosyltransferase involved in the synthesis of arabinoxylans in developing barley endosperms. *Physiol. Plant.* 122: 169-180.

Willats, W.G.T., McCartney, L., Mackie, W. and Knox, J.P. (2001) Pectin: cell biology and prospects for functional analysis. *Plant Mol. Biol.* 47: 9-27.

Ye, Z.-H., Freshour, G., Hahn, M.G., Burk, D.H. and Zhong, R. (2002) Vascular development in *Arabidopsis*. *Int. Rev. Cytol*. 220: 225-256.

Zhong, R., Burk, D.H., Nairn, C.J., Wood-Jones, A., Morrison, W.H.III and Ye, Z.-H. (2005a) Mutation of SAC1, an *Arabidopsis* SAC domain phosphoinositide phosphatase, causes alterations in cell morphogenesis, cell wall synthesis, and actin organization. *Plant Cell* 17: 1449-1466.

Zhong, R., Burk, D.H. and Ye, Z.-H. (2001) Fibers. A model for studying cell differentiation, cell elongation, and cell wall biosynthesis. *Plant Physiol.* 126: 477-479.

Zhong, R., Demura, T. and Ye, Z.-H. (2006) SND1, a NAC domain transcription factor, is a key regulator of secondary wall synthesis in fibers of *Arabidopsis*. *Plant Cell* 18: 3158-3170.

Zhong, R., Pena, M.J., Zhou, G.-K., Nairn, C.J., Wood-Jones, A., Richardson, E.A., Morrison, W.H., Darvill, A.G., York, W.S. and Ye, Z.-H. (2005b) *Arabidopsis Fragile Fiber8*,

which encodes a putative glucuronyltransferase, is essential for normal secondary wall synthesis. *Plant Cell* 17: 3390-3408.

Zhong, R., Richardson, E.A. and Ye, Z.-H. (2007a) The MYB46 transcription factor is a direct target of SND1 and regulates secondary wall biosynthesis in *Arabidopsis*. *Plant Cell* (doi/10.1105/tpc.107.053678).

Zhong, R., Richardson, E.A. and Ye, Z.-H. (2007b) Two NAC domain transcription factors, SND1 and NST1, function redundantly in regulation of secondary wall synthesis in fibers of *Arabidopsis*. *Planta* 225: 1603-1611.

Zhong, R., Taylor, J.J. and Ye, Z.-H. (1997) Disruption of interfascicular fiber differentiation in an *Arabidopsis* mutant. *Plant Cell* 9: 2159-2170.

Zhou, G.K., Zhong, R., Richardson, E.A., Himmelsbach, D.S., McPhail, B.T., and Ye, Z.-H.(2007). Molecular characterization of PoGT8D and PoGT43B, two secondary wall-associated glycosyltransferases in poplar. *Plant Cell Physiol.* 48: 689-699.

Zhou, G.K., Zhong, R., Richardson, E.A., Morrison, W.H. 3rd., Nairn, C.J,. Wood-Jones, A. and Ye, Z.-H. (2006) The poplar glycosyltransferase GT47C is functionally conserved with *Arabidopsis Fragile Fiber8. Plant Cell Physiol.* 47:1229-1240.

Table 3.1. Wall thickness of fibers and vessels in the stems and roots of wild-type and *parvus* mutant plants

Sample	Interfascicular Fibers	Stem		Root	
		Vessels	Xylary fibers	Vessels	Xylary fibers
Wild Type	2.10±0.36	1.01±0.09	0.71±0.18	1.16±0.14	0.78±0.21
parvus	0.71±0.21	0.45±0.15	0.36±0.07	0.54±0.18	0.27±0.10

Wall thickness was measured from transmission electron micrographs of fibers and vessels. Data are means (μm) ± SE from 20 cells.

Table 3. 2. Monosaccharide composition of cell walls from the stems of wild-type and *parvus* plants

Sample	Glucose	Xylose	Mannose	Galactose	Arabinose	Rhamnose	Fucose
Wild type	306±26	122±4	20.7±0.6	14.9±2.4	13.7±1.7	8.0±1.0	2.5±0.6
parvus	234±22	65±5	25.2±0.5	18.3±0.7	17.4±1.7	5.0±0.6	1.6±0.3

Cell wall residues used for composition analysis were prepared from stems of 10-week-old plants. Data are means (mg/g dry cell wall) ± SE of three independent assays.

Table 3.3. Monosaccharide composition of 1 N and 4 N KOH extracts from the cell walls of wild-type and *parvus* plants

Cell wall sample	Xylose	Mannose	Galactose	Arabinose	Rhamnose	Fucose	Glucose
1N KOH extract							
Wild type	44.5±10.5	0.7±0.1	3.5±0.4	3.2±0.7	2.7±0.7	0.6±0.1	11.4±0.6
parvus	9.9±0.5	1.4±0.1	4.9±0.4	4.5±0.4	2.8±0.2	0.5±0.2	6.9±0.1
4N KOH extract							
Wild type	30.2±4.0	8.6±0.5	6.6±0.7	2.8±0.3	2.3±0.2	2.1±0.2	16.2±1.0
parvus	13.2±1.6	7.8±1.1	4.8±0.6	2.2±0.2	1.4±0.1	1.4±0.1	12.2±1.5

Cell walls were extracted sequentially with 1 N and 4 N KOH and the alkali-soluble extracts were used for monosaccharide composition analysis. Data are means (mg/g dry cell wall) ± SE of two independent assays.

Figure 3.1. Expression analysis of the *PARVUS* gene by real-time quantitative PCR. Error bars represent SE of three replicates. (A) The *PARVUS* gene is highly expressed in interfascicular fibers and xylem cells but absent in pith cells. The cells used for expression analysis were lasermicrodissected from *Arabidopsis* stem sections. (B) The *PARVUS* gene exhibits predominant expression in stems undergoing secondary wall thickening. (C) The expression of *PARVUS* together with three other secondary wall biosynthetic genes, *FRA8*, *IRX8* and *IRX9,* is induced by MYB46 overexpression, which results in ectopic deposition of secondary walls. (D) The expression of *PARVUS*, *FRA8*, *IRX8* and *IRX9* is down-regulated in SND1/NST1 RNAi lines, which exhibit a loss of secondary wall thickening in fiber cells.

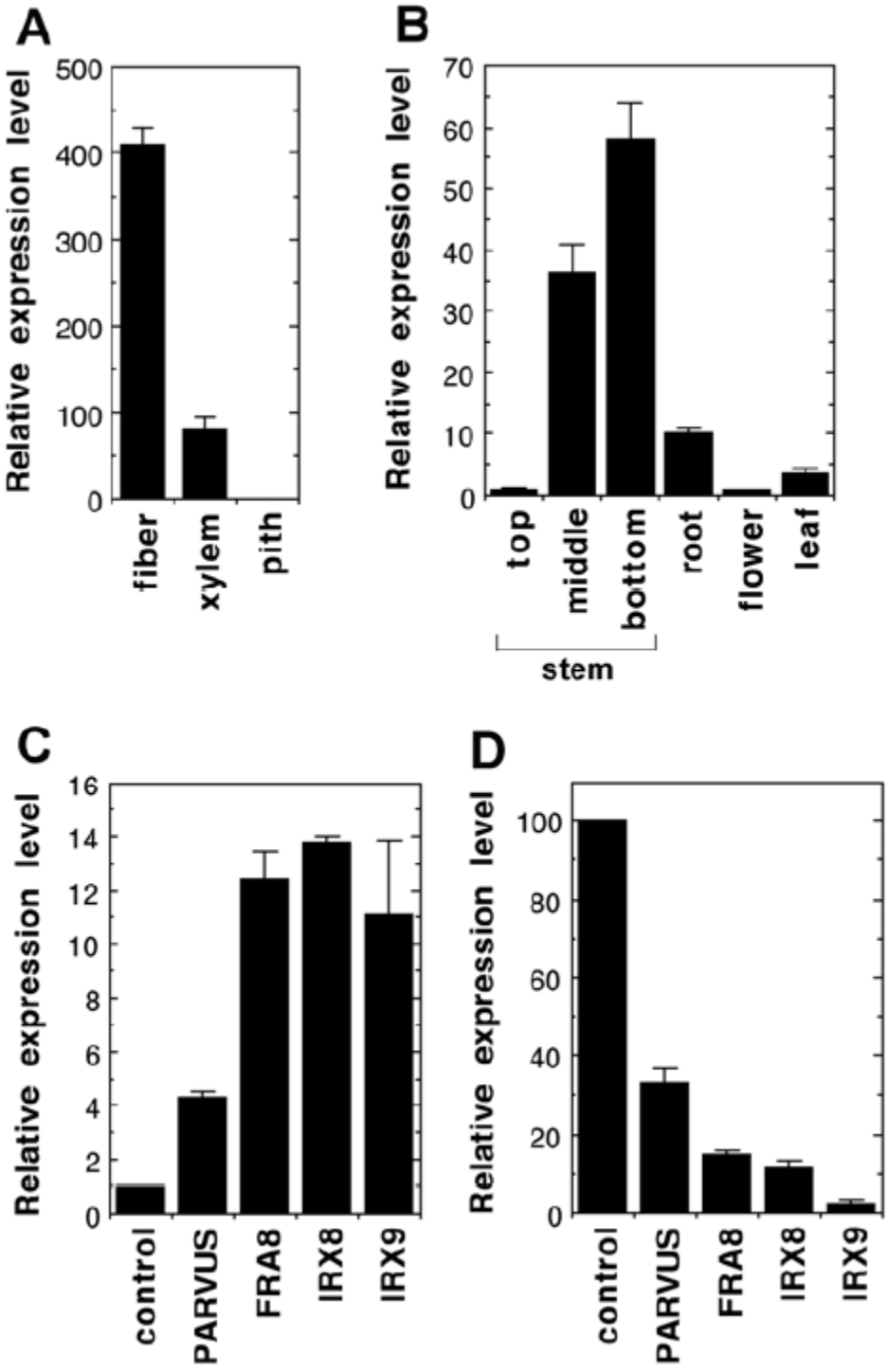
A
Relative expression level
500
400
300
200
100
0
fiber
xylem
pith
B
Relative expression level
70
60
50
40
30
20
10
0
top
middle
bottom
root
flower
leaf
stem
C
Relative expression level
16
14
12
10
8
6
4
2
0
control
PARVUS
FRA8
IRX8
IRX9
D
Relative expression level
100
80
60
40
20
0
control
PARVUS
FRA8
IRX8
IRX9

Figure 3.2. In situ hybridization analysis of the *PARVUS* mRNA in *Arabidopsis* stems and roots. Cross sections of stems and roots of wild-type plants were hybridized with digoxigenin-labeled *PARVUS*antisense (A-C) or sense (D) RNA probe, and subsequently detected with alkaline phosphateconjugated antibodies. The hybridization signals are shown as purple color. (A) Cross section of the elongating part of a stem showing the predominant expression of *PARVUS* in developing vessels (arrows). (B) Cross section of the non-elongating part of a stem showing the expression of *PARVUS* in interfascicular fibers, xylary fibers (arrow) and developing vessels (arrowheads), all of which undergoing extensive secondary wall thickening. (C) Cross section of a root showing the predominant expression of *PARVUS* in the developing secondary xylem. (D) A control section of the non-elongating part of a stem hybridized with the sense *PARVUS* probe showing the absence of hybridization signals. if, interfascicular fiber; mx, metaxylem; px, protoxylem; sx secondary xylem. Bars = 204 μm.

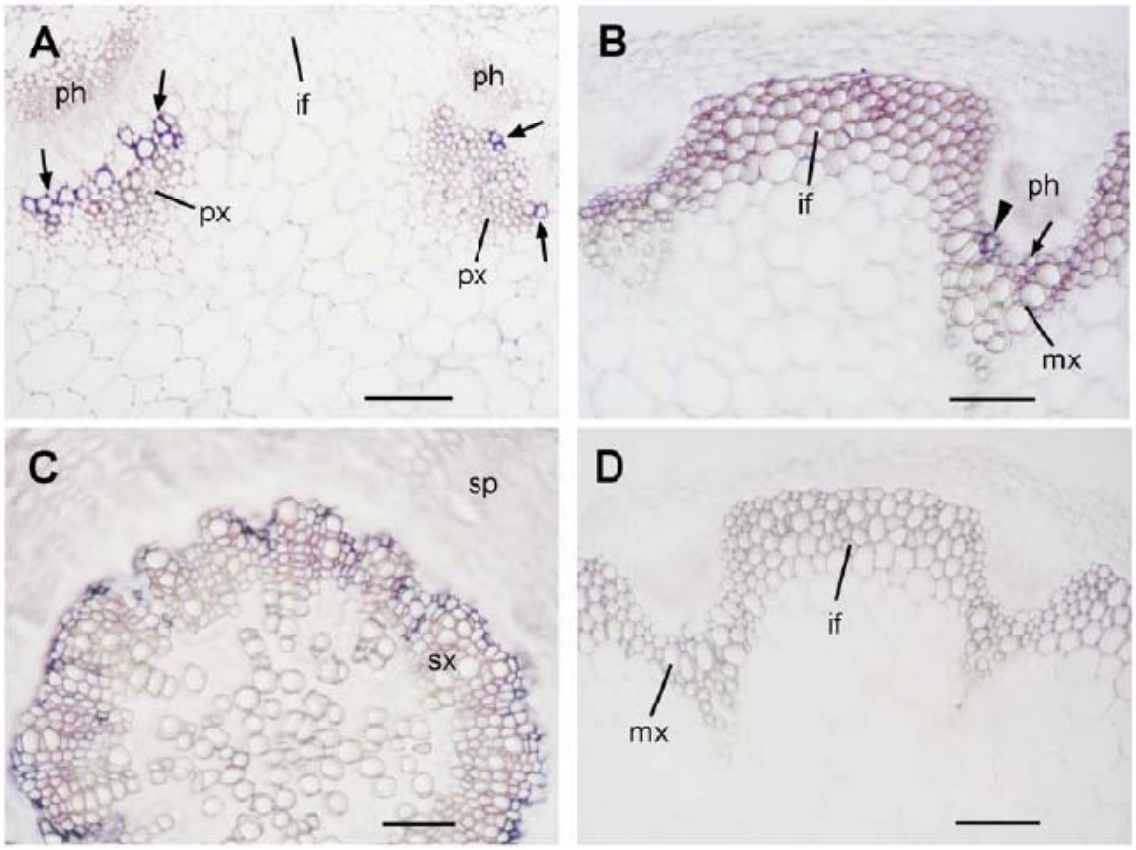
A
ph
if
ph
px
px
B
if
ph
mx
C
sp
sx
D
if
mx

Figure 3.3. Subcellular localization of the PARVUS protein. Yellow fluorescent protein (YFP)-tagged PARVUS together with cyan fluorescent protein (CFP)-tagged subcellular organelle markers were co-expressed in carrot protoplasts, and their fluorescent signals were visualized with a laser confocal microscope. (A) Hydropathy plot of the PARVUS protein showing the presence of a signal peptide sequence at the N terminus. (B) and (C) Differential interference contrast (DIC) image (B) and the corresponding fluorescent signals (C) of a carrot protoplast expressing YFP alone. (D-G) DIC image (D) and the corresponding PARVUS-YFP signals (E), ER-CFP signals (F) and the merged image (G) of a carrot cell expressing PARVUS-YFP and the ER marker ERCFP. Note the close superimposition of PARVUS-YFP and ER-CFP signals. (H-K) DIC image (H) and the corresponding PARVUS-YFP signals (I), FRA8-CFP signals (J) and the merged image (K) of a carrot cell expressing PARVUS-YFP and the Golgi-localized FRA8-CFP. Note the differences between the network localization pattern of PARVUS-YFP and the punctate pattern of FRA8-CFP. Bars = 35 μm.

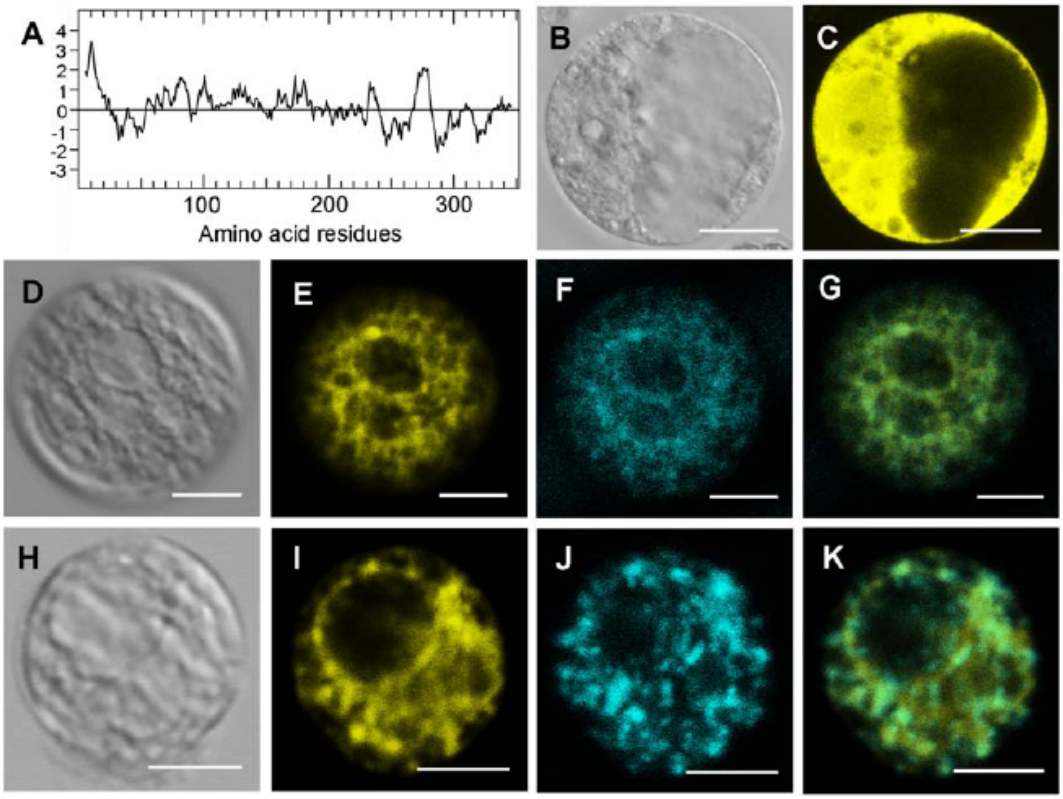
A
4
3
2
1
0
-1
-2
-3
100
200
300
Amino acid residues
B
C
D
E
F
G
H
I
J
K

Figure 3.4. Mutation of the *PARVUS* gene results in a dramatic reduction in stem strength and wall thickness of fibers and vessels. Inflorescence stems of 10-week-old plants were used for breaking strength measurement, and the bottom internodes and roots were sectioned for examination of fibers and vessels. (A) Breaking force measurement showing a drastic reduction in stem strength in the *parvus* mutant compared with the wild type. Error bars represent SE of measurements of 20 plants. (B) and (C) Cross sections of stems showing vascular bundles of the wild type (B) and *parvus* mutant (C). Note that the vessels in the *parvus* mutant are severely deformed (arrows). (D) and (E) Cross sections of interfascicular regions of stems showing the drastically reduced fiber wall thickness in *parvus* (E) compared with the wild type (D). (F) and (G) Cross sections of roots showing the thin-walled vessels and fibers in secondary xylem in the *parvus* mutant (F) compared with the wild type (G). Note the severely deformed vessels in the *parvus* mutant (arrows). co, cortex; if, interfascicular fiber; ph, phloem; ve, vessel; xf, xylary fiber. Bars = 141 μm.

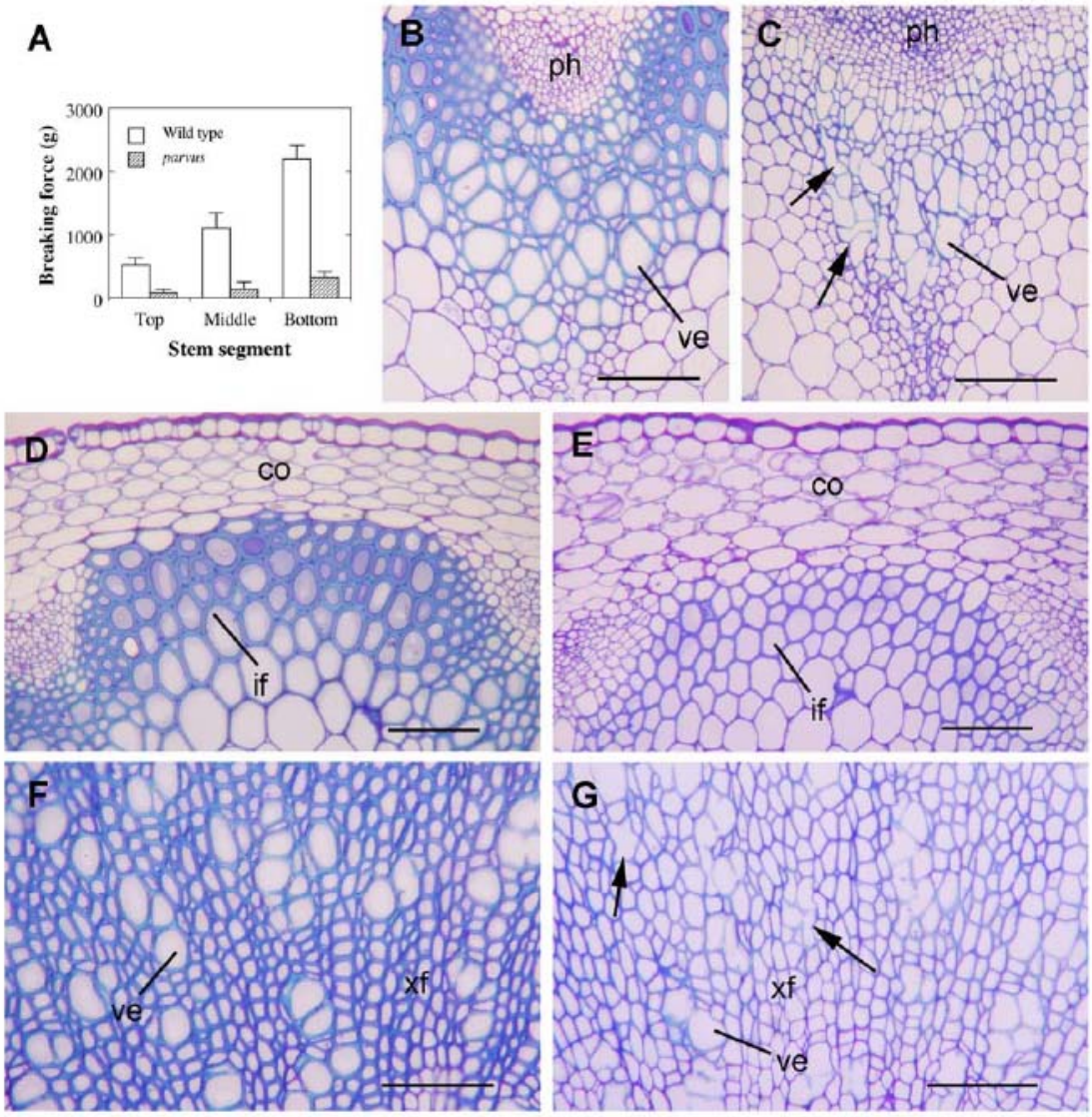
A
Breaking force (g)
3000
2000
1000
0
Wild type
parvus
Top
Middle
Bottom
Stem segment
B
ph
ve
C
ph
ve
D
co
if
E
co
if
F
ve
xf
G
xf
ve

Figure 3.5. Transmission electron microscopy of secondary walls of fibers and vessels in the *parvus* mutant. (A) and (B) Interfascicular fiber cells of stems showing their thin walls in *parvus* (B) compared with the wild type (A). (C) and (D) Vessels and xylary fibers of stems showing their thin walls in *parvus* (D) compared with the wild type (C). Note the deformation of vessels. (E) and (F) Vessels and xylary fibers in root secondary xylem showing their thin walls in *parvus* (F) compared with the wild type (E). Note the deformation of vessels. ve, vessel; xf, xylary fiber. Bars = 7.9 μm.

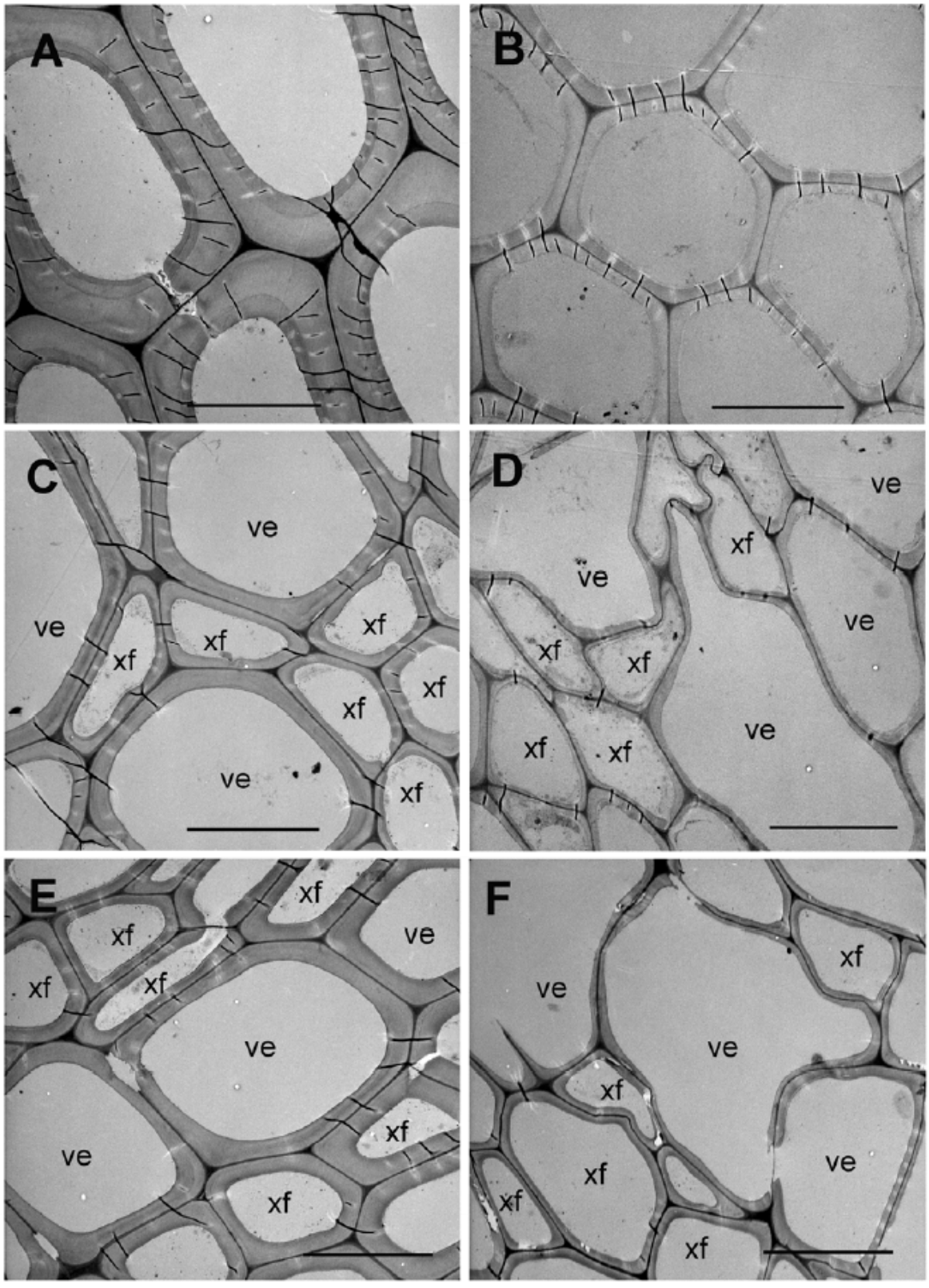
A
B
C
ve
ve
xf
xf
xf
xf
xf
ve
xf
D
ve
xf
ve
ve
xf
xf
ve
xf
xf
E
xf
xf
ve
xf
xf
ve
ve
xf
xf
F
xf
ve
ve
xf
xf
ve
xf
xf

Figure 3.6. Immunodetection of xylan in fibers and vessels of *parvus* stems and roots. Stem and root sections were probed with the monoclonal antibody LM10 that was generated against plant cell wall (1,4)-β-D-xylan. Xylan signals were detected with fluorescein isothiocyanate-conjugated secondary antibodies and visualized with a laser confocal microscope. (A) to (C) Xylan immunofluorescent signals in stem sections of the wild type (A), *parvus* mutant (B), and *parvus* complemented with the wild-type *PARVUS* gene (C). Note the absence of xylan signals in the walls of interfascicular fibers and xylem in the *parvus* mutant compared with the wild type. (D) to (F) Xylan immunofluorescent signals in root sections of the wild type (D), *parvus* mutant (E), and *parvus* complemented with the wild-type *PARVUS* gene (F). Note the absence of xylan signals in the walls of secondary xylem in the *parvus* mutant. if, interfascicular fiber, sx, secondary xylem; xy, xylem. Bars = 159 μm.

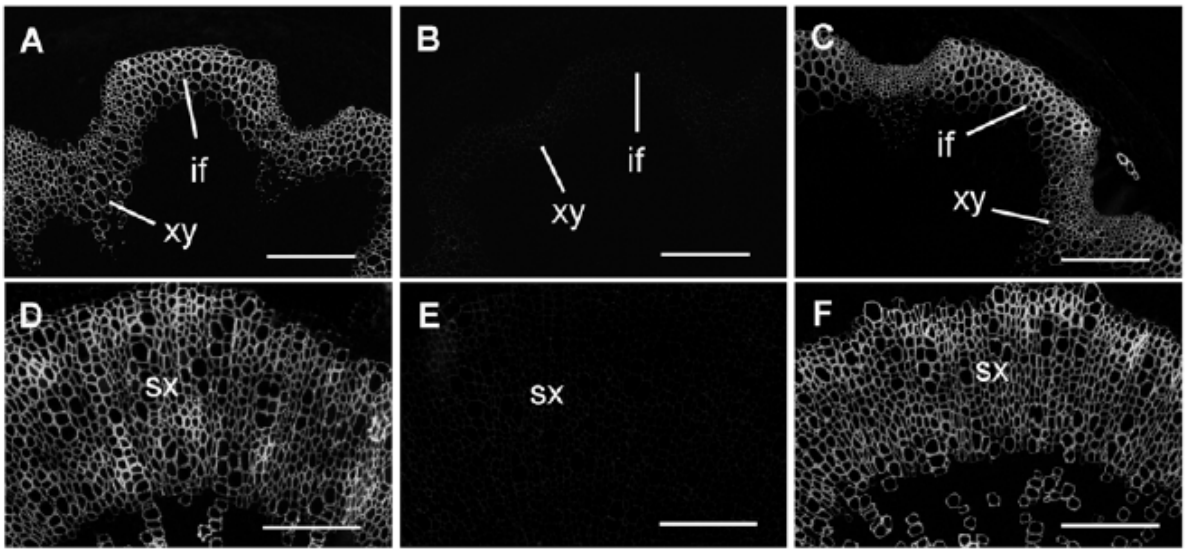
A
if
xy
B
if
xy
C
if
xy
D
sx
E
sx
F
sx

Figure 3.7. MALDI-TOF mass spectra of acidic xylooligosaccharides generated by β-endoxylanase digestion of GX from the stems of the wild type (A) and *parvus* mutant (B). The ions at *m/z* 743 and 759 correspond to xylooligosaccharides composed of four Xyl residues bearing a nonmethylated GlcA residue (X4G) and a methylated GlcA residue (X4M), respectively (C). Note the absence of the ion at *m/z* 743 corresponding to X4G in the *parvus* mutant.

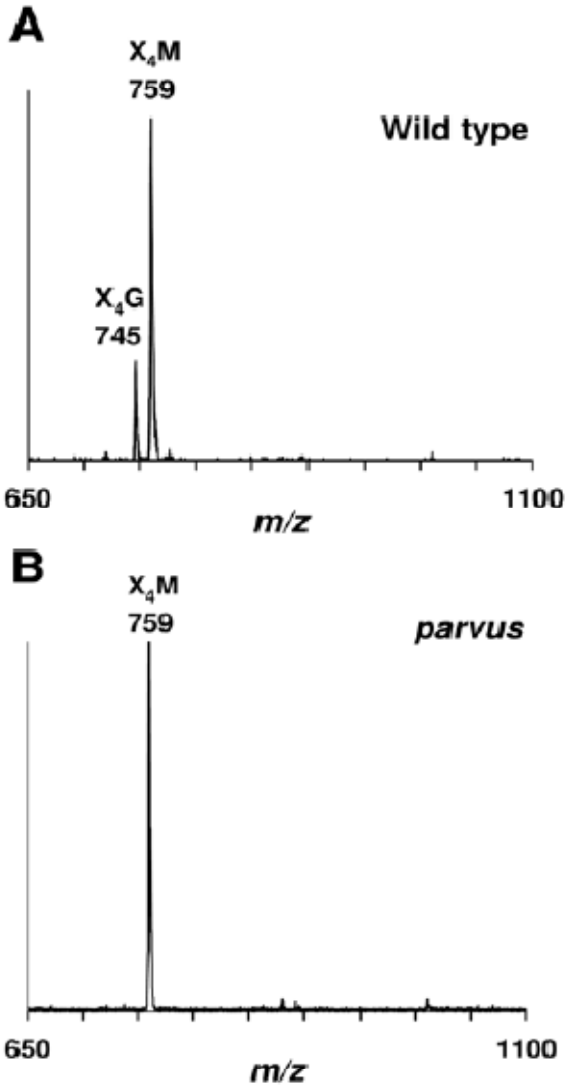

C

X_4G:

β-D-Xyl-(1→4)-β-D-Xyl-(1→4)-β-D-Xyl-(1→4)-D-Xyl

2

↑

1

α-D-GlcA

X_4M:

β-D-Xyl-(1→4)-β-D-Xyl-(1→4)-β-D-Xyl-(1→4)-D-Xyl

2

↑

1

4-*O*-Me-α-D-GlcA

Figure 3.8. Anomeric region of the ^{1}H-NMR spectra of xylooligosaccharides generated by β-endoxylanase digestion of GX from wild type (A) and *parvus* (B) stems. Resonances are labeled with the position of the assigned proton and the identity of the residue containing that proton. G denotes the resonance of H1 of branched β-Xyl residues bearing an α-GlcA side chain. M denotes the resonance of H1 of branched β-Xyl residues bearing a 4-*O*-Me-α-GlcA side chain. The resonances of H5 of 4-*O*-Me-α-GlcA in *parvus* are shifted relative to those of the wild type. It is apparent that compared with the wild type, the *parvus* mutant lacks the resonances of H1 of α-DGalA, H1 of α-L-Rha, H1 of 3-linked β-D-Xyl, H4 of α-D-GalA and H2 of α-L-Rha from the tetrasaccharide primer sequence located at the reducing end of GX as well as the resonances of H1 and H5 of α-GlcA residues, and H1 of branched β-Xyl residues bearing an α-GlcA residues.

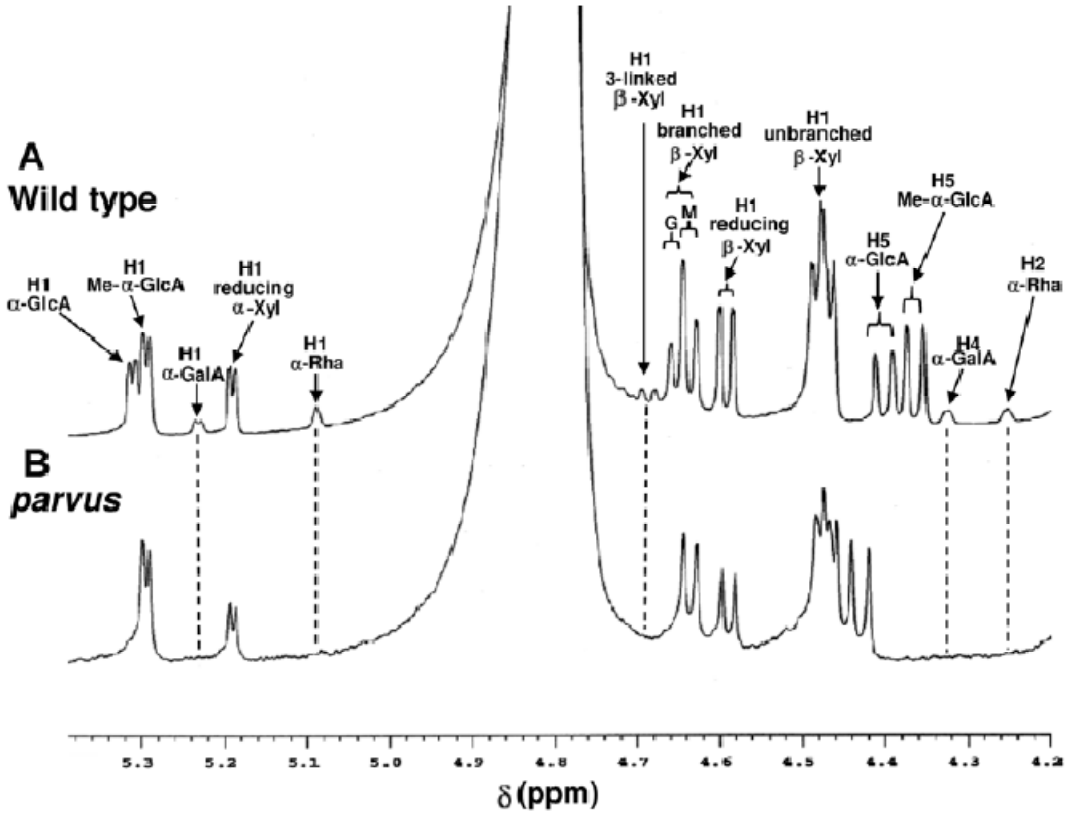
A
Wild type
B
parvus
H1
α-GlcA
H1
Me-α-GlcA
H1
α-GalA
H1
reducing
α-Xyl
H1
α-Rha
H1
3-linked
β-Xyl
H1
branched
β-Xyl
H1
unbranched
β-Xyl
G
M
H1
reducing
β-Xyl
H5
α-GlcA
H5
Me-α-GlcA
H4
α-GalA
H2
α-Rha
5.3
5.2
5.1
5.0
4.9
4.8
4.7
4.6
4.5
4.4
4.3
4.2
δ (ppm)

Figure 3.9. The XylT and GlcAT activities in the stems of the wild type and *parvus* mutant. Microsomes isolated from the stems of the wild type and *parvus* mutant were incubated with Xyl6 and UDP-[14C]-Xyl or UDP-[14C]-GlcA, and the XylT and GlcAT activities were detected by counting the radioactivity (CPM) of the reaction products. Error bars represent SE of two separate assays. (A) XylT activity in the *parvus* mutant compared with the wild type. (B) GlcAT activity in the *parvus* mutant compared with the wild type.

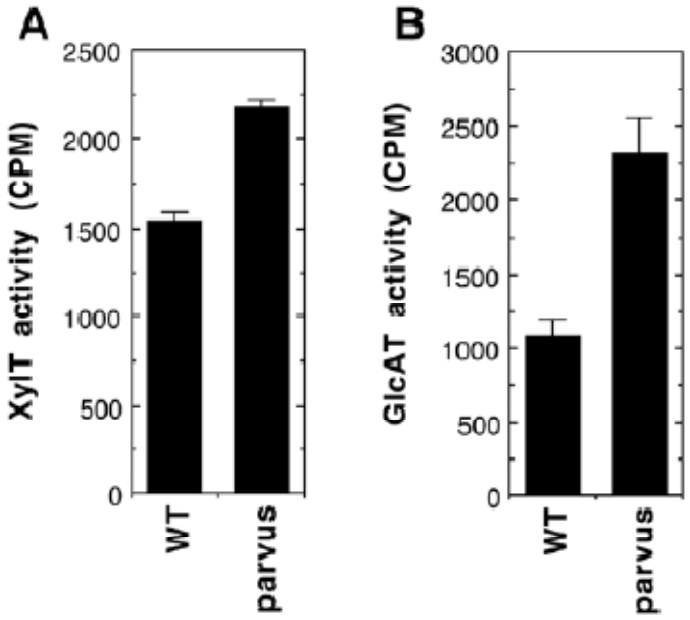
A
XylT activity (CPM)
2500
2000
1500
1000
500
0
WT
parvus
B
GlcAT activity (CPM)
3000
2500
2000
1500
1000
500
0
WT
parvus

CHAPTER 4

THE ARABIDOPSIS FAMILY GT 43 GLYCOSYLTRANSFERASES FORM TWO FUNCTIONALLY NON-REDUNDANT GROUPS ESSENTIAL FOR THE ELONGATION OF GLUCURONOXYLAN BACKBONE[1]

[1]Lee, C., Teng, Q., Huang, W., Zhong, R., and Ye, Z.-H. (2010). Plant Physiology 153:526-541.

ABSTRACT

There exist four members of family GT43 glycosyltransferases in the Arabidopsis genome and mutations of two of them, IRX9 or IRX14, have previously been shown to cause a defect in glucuronoxylan (GX) biosynthesis. However, it is currently unknown whether IRX9 and IRX14 perform the same biochemical function and whether the other two GT43 members are also involved in GX biosynthesis. In this report, we performed comprehensive genetic analysis of the functional roles of the four Arabidopsis GT43 members in GX biosynthesis. The I9H (IRX9 homolog) and I14H (IRX14 homolog) genes were shown to be specifically expressed in cells undergoing secondary wall thickening and their encoded proteins were targeted to the Golgi, where GX is synthesized. Overexpression of I9H but not IRX14 or I14H rescued the GX defects conferred by the irx9 mutation, whereas overexpression of I14H but not IRX9 or I9H complemented the GX defects caused by the irx14 mutation. Double mutant analyses revealed that I9H functioned redundantly with IRX9 and that I14H was redundant with IRX14 in their functions. In addition, double mutations of IRX9 and IRX14 were shown to cause a loss of secondary wall thickening in fibers and a much more severe reduction in GX amount than their single mutants. Together, these results provide genetic evidence demonstrating that all four Arabidopsis GT43 members are involved in GX biosynthesis and suggest that they form two functionally non-redundant groups essential for the normal elongation of GX backbone.

INTRODUCTION

Secondary walls constitute the bulk of cellulosic biomass produced by vascular plants. Cellulosic biomass in the form of fibers and wood is an important raw material for a myriad of industrial uses, such as timber, pulping, paper-making, and textiles. Due to the dwindling of non-renewable fossil fuels and the detrimental effects of burning fossil fuels on the global environment, there has been an urgent call to develop alternative renewable energy sources and the lignocellulosic biomass from plants is considered to be an attractive renewable source for biofuel production (Somerville, 2006). However, lignocellulosic biomass is recalcitrant to the enzymatic conversion of cellulose into sugars because cellulose is embedded in a complex mixture of polysaccharides and lignin polymers that block the accessibility of degrading enzymes. It has been shown that reduction of lignin and xylan by chemical or enzymatic treatment or by the transgenic approach reduces the recalcitrance of the lignocellulosic biomass to saccharification (Himmel et al., 2007; Chen and Dixon et al., 2007; Lee et al., 2009a). Therefore, a complete understanding of how individual components of lignocellulosic biomass are biosynthesized will potentially allow us to design novel strategies for genetic modification of cell wall composition, hence reduction in biomass recalcitrance to biofuel production.

Xylan is the main hemicellulose that cross-links with cellulose in the secondary walls of dicot plants (Carpita and McCann, 2000). It is made of a linear backbone of β-(1,4)-linked xylosyl residues, about 10% of which are attached with side chains of single residues of glucuronic acid (GlcA) and/or 4-*O*-methylglucuronic acid (MeGlcA) via α-(1,2)-linkages. The backbone xylosyl residues may also be substituted with arabinosyl and acetyl groups. Based on the nature of the side chains, xylan is generally grouped as (methyl)glucuronoxylan (GX), which is the main hemicellulose in dicots, and arabinoxylan and glucuronoarabinoxylan, which are the

most abundant hemicelluloses in grass cell walls (Ebringerová and Heinze, 2000). In addition to the xylosyl backbone, the reducing end of xylan from birch (*Betula verrucosa*), spruce (*Picea abies*), Arabidopsis, and poplar (*Populus alba X tremula*) contains a unique tetrasaccharide sequence β-D-Xyl*p*-(1→3)-α-L-Rha*p*-(1→2)-α-D-Gal*p*A-(1→4)-D-Xyl*p* (Shimizu et al., 1976; Johansson and Samuelson, 1977; Andersson et al., 1983; Pena et al., 2007; Lee et al., 2009).

The biosynthesis of xylan requires multiple glycosyltransferases and other modifying enzymes. Early biochemical studies revealed the activities of xylosyltransferases, glucuronosyltransferases, arabinosyltransferases, methyltransferases, and acetyltransferases that are likely involved in the biosynthesis of xylan (Baydoun et al., 1983 and 1989; Kuroyama and Tsumuraya, 2001; Gregory et al., 2002; Porchia et al., 2002; Urahara et al., 2004; Zeng et al., 2008). However, none of the genes corresponding to these xylan biosynthetic enzymes have been identified. Recent molecular and genetic studies in Arabidopsis and poplar have led to the identification of a number of glycosyltransferases that are essential for GX biosynthesis. Among them, several members of the families GT47 and GT8 from Arabidopsis (FRA8, F8H, IRX8, and PARVUS) and poplar (GT47C, GT8D, and GT8E/8F) are implicated in the biosynthesis of the GX reducing end sequence (Aspeborg et al., 2005; Zhong et al., 2005; Brown et al., 2005 and 2007; Zhou et al., 2006 and 2007; Pena et al., 2007; Persson et al., 2007; Lee et al., 2007b, 2009b and 2009c). These glycosyltransferase genes are specifically expressed in vessels and fibers and their encoded proteins are targeted to Golgi where GX is synthesized except for PARVUS and GT8E/8F that are predominantly located in the endoplasmic reticulum (Lee et al., 2007b and 2009c). Mutations of the Arabidopsis *FRA8*, *IRX8*, and *PARVUS* genes all led to a near loss of the reducing end tetrasaccharide sequence and a reduction in GX amount (Brown et al., 2007;

Pena et al., 2007; Lee et al., 2007), indicating their essential roles in the biosynthesis of the GX reducing end sequence although their exact enzymatic activities are still unknown.

The genetic studies have also identified roles of two members of family GT43 glycosyltransferases, IRX9 and IRX14, from Arabidopsis and GT43B from poplar in the biosynthesis of the GX xylosyl backbone (Brown et al., 2007; Pena et al., 2007; Zhou et al., 2007). The expression of *IRX9* has been shown to be associated with cells undergoing secondary wall biosynthesis and its encoded protein is targeted to the Golgi. Mutation of the *IRX9* gene causes a drastic reduction in xylan xylosyltransferase activity (Brown et al., 2007; Lee et al., 2007) and concomitantly a substantial decrease in the GX chain length and GX amount (Pena et al., 2007). Mutation of *IRX14* was shown to result in a reduction in the GX level and the xylosyltransferase activity (Brown et al., 2007). In addition, two functionally redundant glycosyltransferases IRX10 and IRX10-like, which belong to family GT47, were also demonstrated to be required for the normal GX level and xylan xylosyltransferase activity, suggesting their involvement in the biosynthesis of the GX xylosyl backbone (Brown et al., 2009; Wu et al., 2009).

In this report, we performed comprehensive molecular and genetic studies of the roles of all members of the Arabidopsis family GT43 glycosyltransferases in GX biosynthesis. We show that like *IRX9*, the other three GT43 members, *I9H* (IRX9 homolog), *IRX14* and *I14H* (IRX14 homolog), are expressed in secondary wall-containing cells and their encoded proteins are targeted to the Golgi. We have found that the GX defects in the *irx9* mutant can be rescued by overexpression of I9H but not IRX14 and I14H. Similarly, overexpression of I14H but not IRX9 and I9H is able to complement the GX defects caused by the *irx14* mutation. Furthermore, genetic analysis of an array of double mutants revealed redundant and non-redundant roles of

GT43 members in GX biosynthesis. Our findings demonstrate that the Arabidopsis family GT43 glycosyltransferases form two functionally non-redundant groups essential for the normal elongation of GX backbone.

RESULTS

Family GT43 glycosyltransferase genes are expressed in cells undergoing secondary wall thickening

The previous findings that two members of the Arabidopsis family GT43 glycosyltransferases are involved in GX biosynthesis raised a question as to whether other GT43 members perform a similar function. There exist four GT43 members, IRX9 (At2g37090), I9H (IRX9 homolog; At1g27600), IRX14 (At4g36890), and I14H (IRX14 homolog; At5g67230), in the Arabidopsis genome. Among them, IRX14 and I14H share the highest sequence similarity (81.1%), and I9H shares a relatively higher sequence similarity with IRX9 than with IRX14 and I14H (Fig. 4.1, A and B). Phylogenetic analysis further indicates that IRX14 and I14H are more closely related to each other than to IRX9 and I9H, and vice versa (Fig. 4.1C). IRX9 was previously shown to be specifically expressed in vessels and fibers (Pena et al., 2007), but the expression patterns of other GT43 members are not known. Quantitative PCR analysis showed that *I9H* was ubiquitously expressed in all organs examined, whereas *IRX14* and *I14H* were preferentially expressed in the inflorescence stems (Fig. 4.1D). Further expression analysis in the isolated cells from stems revealed that *I9H*, *IRX14*, and *I14H* were preferentially expressed in xylem and/or interfascicular fibers, the cell types undergoing secondary wall thickening (Fig. 4.1E). We next tested whether the expression of *I9H*, *IRX14*, and *I14H* was regulated by SND1, a master transcriptional switch activating the biosynthetic pathways of xylan, cellulose, and lignin (Zhong et al., 2006 and 2007). It was found that their expression was reduced in the

SND1/NST1 RNAi lines and that SND1 overexpression induced the expression of *I9H* and *IRX14* (Fig. 4.1F).

We further examined the expression patterns of *I9H, IRX14,* and *I14H* in transgenic Arabidopsis plants using the β-glucuronidase (GUS) reporter gene. Consistent with the quantitative PCR analysis, these genes were found to be specifically expressed in interfascicular fibers and xylem cells in the inflorescence stems (Fig. 4.2, A, B, D, E, G and H). In the roots, *IRX14* and *I14H* were expressed in both developing vessels and xylary fibers in the secondary xylem (Fig. 4.2, F and I), whereas *I9H* expression was only evident in developing vessels but not in xylary fibers (Fig. 4.2C). These expression studies demonstrate a close association of *I9H* and *I14H* with cells undergoing secondary wall thickening, suggesting their possible involvement in secondary wall biosynthesis.

Family GT43 glycosyltransferases are targeted to the golgi

IRX9 was previously demonstrated to reside in the Golgi (Pena et al., 2007), but the subcellular locations of other GT43 members have not yet been examined. Sequence analysis of I9H, IRX14, and I14H using the TMHMM2.0 program for prediction of transmembrane helices in proteins (http://www.cbs.dtu.dk/service/TMHMM-2.0/) predicts that they are membrane proteins with a single (I9H and IRX14) or double (I14H) transmembrane helices (Fig. 4.3, A to C). To study their actual subcellular locations, yellow fluorescent protein (YFP)-tagged GT43 members were co-expressed with cyan fluorescent protein (CFP)-tagged FRA8 in carrot (*Daucus carota*) cells. Examination of the fluorescent signals revealed that I9H, IRX14, and I14H exhibited a punctate distribution, a pattern matched with FRA8 (Fig. 4.3, F to Q) that is known to be localized in the Golgi (Zhong et al., 2005). The control cells expressing YFP alone showed

signals throughout the cytoplasm (Fig. 4.3, D and E). These results demonstrate that I9H, IRX14, and I14H are Golgi-localized proteins.

Overexpression of I9H but not IRX14 and I14H complements the *irx9* mutant defects

Previous genetic studies showed that mutation of either *IRX9* or *IRX14* caused a partial reduction in the xylosyltransferase activity and GX content (Brown et al., 2007; Lee et al., 2007; Pena et al., 2007), which may be due to functional compensation by other GT43 members. To test this possibility, we investigated whether the defects caused by either *irx9* or *irx14* could be rescued by overexpression of GT43 members driven by the cauliflower mosaic virus (CaMV) 35S promoter. One of the prominent phenotypes of *irx9* was the weakened stem strength due to the reduced secondary wall thickness (Fig. 4.4, A and B). Overexpression of I9H and IRX9 in the *irx9* mutant effectively restored the stem breaking strength and the secondary wall thickness of fibers to the wild-type levels (Fig. 4.4, A, C, D, and G), indicating that I9H is a functional homolog of IRX9. It was noted that not all I9H-complemented *irx9* plants exhibited the same breaking strength as that of the wild type, which is likely due to the variation of the degree of complementation among different individuals. In contrast, overexpression of IRX14 and I14H did not complement the stem strength and secondary wall thickness defects conferred by *irx*9 (Fig. 4.4, A, E and F).

The reduced secondary wall thickness in *irx9* was previously found to be caused by GX defects, including a decrease in GX level, a loss of non-methylated GlcA, and a reduced GX chain length (Pena et al., 2007). Analysis of the GX content revealed that I9H overexpression in the *irx9* mutant restored the cell wall xylose level to that of the wild type (Table 4.1), indicating that excess I9H could complement the loss of IRX9 to restore the GX level. It should be noted that similar to *fra8*, *irx9* and *irx14* cause not only a reduction in xylose but also a reduction in

glucose, which might be attributed to an indirect impediment of cellulose synthesis caused by a reduction in GX (Zhong et al., 2005). The observed increase in the levels of some other cell wall sugars might be simply due to the relative decrease in the levels of cellulose and GX or an increased synthesis of other wall polysaccharides in response to the reduced level of cellulose, a phenotype commonly observed in cellulose-deficient mutants (Fagard et al., 2000; His et al., 2001). Overexpression of GT43 members in *irx9* also resulted in a change in the levels of other sugars in addition to xylose, which might reflect the complexity of cell wall metabolism. The structure of GX in the complemented plants was examined by analyzing the acidic xylooligosaccharides using matrix-assisted laser-desorption ionization time-of-flight mass spectrometry (MALDI-TOF MS). Acidic xylooligosaccharides from the wild type contain two prominent ion peaks $[M+Na]^+$ at mass-to-charge ratios (*m/z*) of 745 and 759, which correspond to xylotetrasaccharides substituted with one GlcA and one MeGlcA, respectively (Fig. 4.5A). The loss of GlcA side chains caused by the *irx9* mutation (Fig. 4.5B) was rescued by overexpression of I9H and IRX9 (Fig. 4.5, C and D) but not by IRX14 and I14H (Fig. 4.5, E and F).

The structure of GX from the complemented plants was further analyzed using nuclear magnetic resonance (NMR) spectroscopy. The resonances that are assigned to the GX reducing end tetrasaccharide sequence, β-D-Xyl-(1→3)-α-L-Rha-(1→2)-α-D-GalA-(1→4)-D-Xyl, include H1 of α-D-GalA, H1 of α-L-Rha, H1 of 3-linked β-D-Xyl, H4 of α-D-GalA, and H2 of α-L-Rha (Pena et al., 2007). It was previously found that the resonances for the GX reducing end tetrasaccharide sequence in *irx9* were highly elevated compared with those of the wild type, which is caused by a significant reduction in the GX chain length and thereby a relative increase in the ratio of the GX reducing end sequence over the backbone xylosyl residues (Pena et al.,

2007). It was evident that overexpression of I9H but not IRX14 and I14H in *irx9* restored the resonance intensity for the GX reducing end tetrasaccharide sequence to the wild-type level (Fig. 4.6; Table 4.3), indicating that excess I9H is sufficient to complement the GX chain length defect conferred by *irx9*. Consistent with the MALDI-TOF MS results showing that I9H overexpression restores the α-D-GlcA side chains in GX (Fig. 4.5), the resonances assigned to H1 of α-D-GlcA residues, which were absent in *irx9*, were restored to the wild-type level in the I9H-complemented *irx9* plants (Fig. 4.6).

The restoration of GX level and structure in I9H-complemented *irx9* plants was accompanied by a partial rescue of the GX xylosyltransferase activity (Fig. 4.7A). Overexpression of IRX14 and I14H did not restore the xylosyltransferase activity in the *irx9* mutant. It was interesting to note that overexpression of IRX9 in *irx9* led to an increased xylosyltransferase activity compared with the wild type. Together, these results suggest that I9H can perform the same biochemical function as IRX9 in the biosynthesis of GX backbone and that they are functionally distinct from IRX14 and I14H.

Overexpression of I14H but not IRX9 and I9H complements the *irx14* mutant defects

Our finding that overexpression of IRX14 and I14H does not complement the *irx9* mutant defects prompted us to test whether IRX14 and I14H form another pair of functional homologs involved in GX backbone biosynthesis. It was found that overexpression of I14H and IRX14 but not IRX9 and I9H in the *irx14* mutant rescued the defects in the stem strength, secondary wall thickness, the GX level, the GlcA side chains, and the GX xylosyltransferase activity (Fig. 4.4, A, H to M; Fig. 4.5, G to L; Fig. 4.7; Table 4.1). The *irx14* mutation was previously shown to cause a reduction in the GX level (Brown et al., 2007), but it is unknown whether the GX chain length is affected in the mutant. NMR analysis showed that similar to those in *irx9*, the resonances for

the GX tetrasaccharide reducing end sequence in *irx14* were highly increased compared to those in the wild type (Fig. 4.6), indicating that the GX chain length in *irx14* is significantly reduced (Table 4.3). Overexpression of I14H in *irx14* apparently restored the resonance signals for the GX tetrasaccharide reducing end sequence to the wild-type level, indicating its ability to complement the GX chain length defect conferred by *irx14* (Fig. 4.6; Table 4.3). These results demonstrate that I14H and IRX14 form another group of functional homologs involved in GX biosynthesis.

Double mutant analysis reveals redundant roles of GT43 members in GX biosynthesis

The findings that *I9H* is expressed in the same cell types as *IRX9* and excess I9H is able to complement the *irx9* mutant defects indicate that they function redundantly in GX biosynthesis. Likewise, I14H might function redundantly with IRX14 in GX biosynthesis. To test these hypotheses, we generated an array of double mutants with all possible combinations of the GT43 members and examined their effects on plant growth and GX biosynthesis. Although the *irx9* or *irx14* mutant exhibited a reduction in stem strength, secondary wall thickness, and the GX level (Brown et al., 2007; Pena et al., 2007), T-DNA insertion mutation of *I9H* or *I14H* alone did not have any discernable effects (Figs. 4.8 and 9; Table 4.2). However, homozygous double mutations of *IRX9* and *I9H* led to a strong retardation of plant growth (Fig. 3.8D). Even after prolonged growth (4 months), no inflorescence stems grew out from the rosettes, which prevented us from further analysis of the double homozygous mutants. The double mutant that is homozygous for *irx9* and heterozygous for *i9h (+/-)* did grow out short inflorescence stems after prolonged growth. Examination of the *irx9 i9h (+/-)* inflorescence stems revealed that the interfascicular fibers had thinner walls (Figs. 4.8J and 4.9F) than did *irx9* (Figs. 4.8F and 4.9B). In addition, cell wall composition analysis showed that the xylose content in *irx9 i9h (+/-)* was

more severely reduced than that in *irx9* (Table 4.2). These results demonstrate that IRX9 and I9H play redundant roles in GX biosynthesis and secondary wall thickening.

Similar to *irx9 i9h*, double homozygous mutations of *IRX14* and *I14H* cause a much stronger effect on plant growth compared with *irx14* (Fig. 4.8D). The *irx14 i14h* grew out short inflorescence stems, allowing us to examine the secondary wall thickening and the GX level. The *irx14 i14h* stems had little secondary wall thickening in the interfascicular fibers (Figs. 4.8O and 4.9K) and a much lower xylose content (Table 4.2) than those of *irx14* (Figs. 4.8H and 4.9D). The double mutant that is homozygous for *irx14* and heterozygous for *i14h (+/-)* also had a more severe retardation in plant growth compared with *irx14* (Fig. 4.8D).

We next examined the plant growth and secondary wall thickening in the double mutants, including *irx9 i14h*, *i9h irx14*, and *i9h i14h*. The plant growth (Fig. 4.8D) and secondary wall thickening phenotypes of the *irx9 i14h* (Figs. 4.8L and 4.9H) and the *i9h irx14* (Figs. 4.8M and 4.9I) double mutants were similar to those of *irx9* (Figs. 4.8F and 4.9B) and *irx14* (Figs. 4.8H and 4.9D), respectively. Cell wall composition analysis revealed that the xylose content in *irx9 i14h* had a slight reduction compared with *irx9*, whereas the xylose content in *i9h irx14* was similar to that in *irx14* (Table 4.2). Although no significant alterations in plant growth and secondary wall thickening were seen in the *i9h i14h* double mutant (Figs. 4.8D, 8N and 4.9J) compared with the wild type (Figs. 4.8E and 4.9A), the xylose content in *i9h i14h* was slightly reduced (Table 4.2).

We further investigated the effects of double mutations of *IRX9* and *IRX14* on plant growth and GX biosynthesis. Both *irx9 irx14* and *irx9 irx14 (+/-)* exhibited strong retardation in plant growth (Fig. 4.8D). The *irx9 irx14* plants grew out small inflorescence stems after 6-month growth, and examination of these stems revealed the absence of discernable secondary walls in

the interfascicular fibers (Figs. 4.8K and 4.9G), a phenotype much more severe than that in the *irx9* (Fig. 4.8F) or *irx14* (Fig. 4.8H) single mutant. Further cell wall composition analysis of *irx9 irx14* stems revealed a drastic reduction in the xylose content (Table 4.2), indicating a more severe effect on GX biosynthesis than the *irx9* or *irx14* mutation alone.

The results from these comprehensive genetic analyses demonstrate that all four GT43 members are involved in GX biosynthesis although IRX9 and IRX14 play major roles. Together with the mutant complementation studies, our findings suggest that the family GT43 glycosyltransferases form two functionally non-redundant groups, IRX9 together with I9H and IRX14 together with I14H, both of which are essential for GX biosynthesis.

DISCUSSION

IRX9 and IRX14 function non-redundantly in the elongation of GX backbone

Our findings that IRX9 can not functionally complement the loss of IRX14 and vice versa suggest that IRX9 and IRX14 are two functionally non-redundant GT43 members essential for GX biosynthesis. Considering the fact that both IRX9 and IRX14 are required for the elongation of GX backbone (Pena et al., 2007; Fig. 4.6), it is reasonable to propose that IRX9 and IRX14 function cooperatively in the elongation of GX backbone. Such a cooperative function might have important implications in understanding the biochemical mechanism of GX backbone biosynthesis. The GX backbone is composed of β-(1,4)-linked xylosyl residues, and its biosynthesis needs to overcome a steric problem because each xylosyl residue is flipped nearly 180^{o} with respective to its neighboring residues. Similar to a model proposed for cellulose biosynthesis in which two glycosyltransferase activities operate cooperatively from opposite sites to add cellobiosyl units to the β-(1,4)-glucan chain (Carpita and Vergara, 1998), the biosynthesis of GX backbone might also require two enzyme activities that operate in such a mechanism.

Although their exact biochemical functions await further investigation, IRX9 and IRX14 are strong candidates for such two glycosyltransferase activities involved in the elongation of the β-(1,4)-xylan chain. This hypothesis is consistent with the facts that mutation of either *irx9* or *irx14* results in a defect in the GX chain length and a reduction in the xylosyltransferase activity and that IRX9 and IRX14 are non-redundant in their functions.

Redundancy of family GT43 genes in GX biosynthesis

We have demonstrated that I9H and I14H are redundant in function with IRX9 and IRX14, respectively based on the following lines of evidence. First, all four GT43 members are expressed in the same cell types that undergo secondary wall thickening (Fig. 4.2) and their proteins are targeted into the Golgi (Fig. 4.3), where GX is synthesized. Second, overexpression of I9H and I14H can effectively rescue the GX defects, including the GX chain length, caused by the mutations of *IRX9* and *IRX14*, respectively (Figs. 4.4 to 6; Tables 4.1 and 4.3). Third, double mutation of *IRX9* and *I9H* results in a more severe defect in the GX level and a strong retardation of plant growth and likewise, double mutation of *IRX14* and *I14H* leads to similar phenotypes (Fig. 4.8; Table 4.2). Together, these results suggest that IRX9 and I9H are a pair of functional homologs and IRX14 and I14H are another pair of functional homologs. This finding explains the early observations that the *irx9* or *irx14* mutant only exhibits partial reductions in GX content and secondary wall thickness (Brown et al., 2005 and 2007; Pena et al., 2007). However, the *i9h* or *i14h* mutation alone does not cause any GX defects, indicating that IRX9 and IRX14 are functionally dominant in GX biosynthesis in vivo. The gene redundancy appears to be common in GX biosynthesis in Arabidopsis. For example, FRA8 and F8H are a pair of redundant genes required for GX reducing end sequence biosynthesis (Lee et al., 2009b), and IRX10 and IRX10-L are another pair involved in GX backbone biosynthesis (Brown et al., 2009; Wu et al., 2009).

In both of these cases, single mutation of FRA8 or IRX10 results in a defect in GX biosynthesis but single mutation of its homolog does not. Double mutations of these genes, either *FRA8* and *F8H* or *IRX10* and *IRX10-L*, cause a strong retardation in plant growth, a phenotype that is also observed in the double mutants, *irx9 i9h* and *irx14 i14h*. Since GX is a critical component required for cross-linking cellulose microfibrils in secondary walls, gene redundancy in GX biosynthesis likely presents an evolutionary advantage to safeguard the proper making of secondary walls, which are the key structure of vessels essential for water transport in the plant body.

Genes involved in GX backbone biosynthesis

It was previously proposed that some of the cellulose synthase-like (CSL) genes might encode xylan synthase (Richmond and Somerville, 2001), which is congruent with the findings that several hemicellulose backbones, such as xyloglucan β-1,4-glucan (Cocuron et al., 2007), β-1,4-mannan (Dhugga et al., 2004; Liepman et al., 2005), and β-(1,3;1,4)-mix-linked glucan (Burton et al., 2006), are synthesized by members of the CSL gene families. However, no recombinant CSL proteins were shown to exhibit any xylan synthase activity (Liepman et al., 2005). Transcription profiling analysis of wood formation in poplar revealed no correlations between secondary wall synthesis and the expression of CSL genes with the exception of the CSLA (a mannan synthase) gene (Aspeborg et al., 2005; Suzuki et al., 2006). Although mutation of CSLD5 has been reported to cause a decrease in xylosyltransferase activity and xylan immunolabeling, the CSLD5 gene is not expressed in cells undergoing secondary wall thickening and thus the observed phenotypes were considered to be indirect (Bernal et al., 2007). Therefore, genes responsible for the biosynthesis of GX backbone remain elusive. Because GT43 members are specifically expressed in cells undergoing secondary wall thickening and GX

biosynthesis (Pena et al., 2007; Fig. 4.2) and IRX9 and IRX14 are required for the normal GX xylosyltransferase activity and the normal elongation of GX chains (Brown et al., 2007; Lee et al., 2007; Pena et al., 2007; Fig. 4.6), GT43 members are apparently strong candidates for GX xylosyltransferases or part of the complexes required for the xylosyltransferase activities. However, an attempt of assaying the xylosyltransferase activity of recombinant IRX9 proteins was not successful (Pena et al., 2007). Our finding that IRX9 and IRX14 are non-redundant in function suggests that expression of both IRX9 and IRX14 would be required for the GX xylosyltransferase activity. Furthermore, the recent finding that IRX10 and IRX10-L are also required for the normal GX xylosyltransferase activity (Brown et al., 2009; Wu et al., 2009) indicates that the biosynthesis of GX backbone is much more complicated than expected. As suggested previously, a complex composed of multiple glycosyltransferases and other proteins might be involved in GX backbone synthesis (Pena et al., 2007). Further biochemical characterization of GT43 members together with other players will be necessary to unravel the biochemical process of GX biosynthesis.

MATERIALS AND METHODS

Plant growth conditions

Plants were grown in a greenhouse under 14-h-light/10-h-dark cycles. Common garden potting soil was used for growing plants with biweekly application of plant fertilizers.

Gene expression analysis

Total RNA from *Arabidopsis thaliana* (ecotype Columbia) plants was isolated with a Qiagen RNA isolation kit (Qiagen). The organs used were from 7-week-old plants grown in a greenhouse. RNA from different cell types (interfascicular fibers, xylem, and pith cells) was isolated and amplified as described previously (Zhong et al., 2006). First strand cDNA was

synthesized from total RNA treated with DNase I and then used as a template for real-time quantitative PCR analysis with the QuantiTect SYBR Green PCR kit (Clontech). The PCR primers for *I9H* are 5'-tccaggagacatcatttatagagc-3' and 5'-ctatttcatagttatgagagcctg-3', those for *IRX14* are 5'- aagatcaaatgccattatcccaag-3' and 5'-tcagtttctttcttgatgcttagacga-3', and those for *I14H* are 5'- cctggctggatcataaagtcacc-3' and 5'-tcagctagttgctgacactttgac-3'. The relative expression level was calculated by normalizing the PCR threshold cycle number of each gene with that of the *EF1α* reference gene. The data were the average of three biological replicates. RT-PCR was applied to examine the transcript level in the GT43 mutants as described previously (Zhong et al., 2005). The expression of the *EF1α* gene was used as an internal control for determining the RT-PCR amplification efficiency among different samples.

GUS reporter gene analysis

To ensure the inclusion of all sequences required for the expression of the endogenous genes, the *I9H, IRX14, or I14H* gene containing a 3-kb 5' upstream sequence, the entire coding region, and a 2-kb 3' downstream sequence was used for the GUS reporter gene analysis. The GUS reporter gene was inserted in frame right before the stop codon of these genes and then cloned into the binary vector pBI101 (Clontech) to create the GUS reporter constructs. The constructs were transformed into wild-type *Arabidopsis* plants by the agrobacterium-mediated transformation (Bechtold and Bouchez 1994) to generate the GUS reporter transgenic plants. Inflorescence stems and roots from 7-week-old first generation of the transgenic plants were examined for the GUS activity as described previously (Zhong et al. 2005). At least 30 independent transgenic plants were tested and a consistent GUS staining pattern was observed for each GUS reporter construct.

Subcellular localization

The subcellular localization of I9H, IRX14, and I14H was performed by co-transfecting yellow fluorescent protein (YFP)-tagged fusion proteins and the cyan fluorescent protein (CFP)-tagged Golgi marker (FRA8) into carrot (*D. Carota*) protoplasts (Liu et al. 1994). The full-length cDNAs of *I9H*, *IRX14*, and *I14H* were fused in frame with the *YFP* cDNA and ligated between the CaMV 35S promoter and the nopaline synthase terminator in pBI221 (Clontech). Fluorescence signals in transfected protoplasts were visualized using a Leica TCs SP2 spectral confocal microscope (Leica Microsystems). At least 20 fluorescence-positive protoplasts were examined and the same subcellular localization pattern was observed for each construct. Images were saved and processed with Adobe Photoshop Version 7.0 (Adobe Systems).

Complementation of the *irx9* and *irx14* mutants

The full-length cDNAs of GT43 members driven by the CaMV 35S promoter were cloned into the pGPTV binary vector. The constructs were introduced into the Arabidopsis *irx9* or *irx14* mutant by the agrobacterium-mediated transformation (Bechtold and Bouchez, 1994). Transgenic plants were selected on hygromycin, and the first generation of transgenic plants was used for breaking strength and anatomical analyses. Basal parts of the main inflorescence of 10-week-old plants were measured for the breaking force using a digital force/length tester (Zhong et al., 1997). The breaking force was calculated as the force needed to break apart a stem segment. For each construct, at least 96 transgenic plants were generated and examined.

Histology

Tissues were fixed in 2% formaldehyde and embedded in Low Viscosity (Spurr's) resin (Electron Microscopy Sciences) as described (Burk et al. 2006). For light microscopy, 1-µm-thick sections were cut with a microtome and stained with toluidine blue. For transmission electron microscopy, 85-nm-thick sections were cut, post-stained with uranyl acetate and lead

citrate, and observed using a Zeiss EM 902A transmission electron microscope (Carl Zeiss). For each construct, stems from at least 8 transgenic plants (first generation) with representative phenotypes were sectioned and representative data were shown.

Cell wall sugar composition analysis

Inflorescence stems from at least 20 independent lines of Arabidopsis plants were used for cell wall isolation according to Zhong et al. (2005). Cell wall sugars (as alditol acetates) were determined following the procedure described by Hoebler et al. (1989). The alditol acetates of the hydrolyzed cell wall sugars were analyzed on an Agilent 6890N gas-liquid chromatography (Wilmington) equipped with a 30 m x 0.25 mm (i.d.) silica capillary column DB 225 (Alltech Assoc.).

Matrix-Assisted Laser-Desorption Ionization Time-of-Flight Mass Spectrometry (MALDI-TOF MS)

Xylooligosaccharides were prepared by digestion of 4 N KOH solubilized wall preparations with β-xylanase M6 (Megazyme) as described (Zhong et al., 2005). The acidic xylooligosaccharides were analyzed using a MALDI-TOF mass spectrometer operated in the positive-ion mode with an accelerating voltage of 30 kV, an extractor voltage of 9 kV, and a source pressure of approximately 8 x 10^{-7} torr. The aqueous sample was mixed (1:1, v/v) with the MALDI matrix (0.2 M 2,5-dihydroxbenzoic acid and 0.06 M 1-hydroxyisoquinoline in 50% acetonitrile) and dried on the stainless steel target plate. Spectra are the average of 100 laser shots.

^{1}H-NMR spectroscopy

NMR spectra of the acidic xylooligosaccharides from β-xylanase digestion were acquired at 20 ^{o}C on a Varian Inova 600 MHz spectrometer (599.7 MHz, ^{1}H) using a 5 mm cryogenic

triple resonance probe (Varian). All NMR samples were prepared using 100% D_2O in 3 mm standard NMR tube. ^1H chemical shifts were referenced to DSS (2,2-dimethyl-2-silapentane-5-sulfonate sodium salt). For all experiments, 64 transients were collected using a spectral width of 6,000 Hz and an acquisition time of 5-seconds. The residual water resonance was suppressed by a 1-second presaturation pulse at a field strength of 40 Hz. 1D spectra were processed using MestReC (MestreC Research) with 0.2-Hz apodization followed by zero-filling to 128 k points. The ^1H NMR assignments were done by comparison with the NMR spectra data for *Arabidopsis* acidic xylooligosaccharides (Zhong et al., 2005; Peña et al., 2007).

Assay of xylosytransferase activity

Microsomes were isolated from the inflorescence stems of at least four individual 8-week-old plants for each genotype following the procedure of Kuroyama and Tsumuraya (2001) and stored at -80^{o}C until used. For assay of the xylosyltransferase activity, microsomes (100 μg per 30 μl reaction) were incubated with the reaction mixture containing 50 mM HEPES-KOH, pH 6.8, 5 mM $MnCl_2$, 1 mM dithiothritol, 0.5% Triton X-100, 0.1 mM cold UDP-Xyl (CarboSource Service), 0.2 μg/μl Xyl_6 (Megazyme) and UDP-[^{14}C]Xyl (0.1 μCi; American Radiolabeled Chemical). The reaction products were separated from UDP-[^{14}C]Xyl by paper chromatography according to Ishikawa et al. (2000) and counted for the amount of radioactivity with a PerkinElmer scintillation counter.

Accession numbers

The *Arabidopsis* Genome Initiative locus identifiers for the Arabidopsis genes investigated in this study are IRX9 (At2g37090), I9H (At1g27600), IRX14 (At4g36890), and I14H (At5g67230).

ACKNOWLEDGMENTS

We thank the ABRC (Columbus, OH) for the T-DNA knockout lines of *IRX9*, *I9H*, *IRX14*, and *I14H*, and the editor and the reviewers for their constructive comments and suggestions. This work was supported by grants from the U.S. Department of Energy-Bioscience Division (DE-FG02-03ER15415 to Z.H.Y.), and the U.S. EPA Office of Research and Development and the U.S. EPA Office of Science Council Policy (Q.T.). This work has been subjected to review by the National Exposure Research Laboratory and approved for publication. Approval does not signify that the contents reflect the views of the Agency, nor does mention of trade names or commercial products constitute endorsement or recommendation for use.

REFERENCES

Andersson S-I, Samuelson O, Ishihara M, Shimizu K (1983) Structure of the reducing end-groups in spruce xylan. Carbohydr Res 111: 283-288

Aspeborg H, Schrader J, Coutinho PM, Stam M, Kallas A, Djerbi S, Nilsson P, Denman S, Amini B, Sterky F, Master E, Sandberg G, Mellerowicz E, Sundberg B, Henrissat B, Teeri TT (2005) Carbohydrate-Active Enzymes Involved in the Secondary Cell Wall Biogenesis in Hybrid Aspen. Plant Physiol 137: 983-997

Baydoun EA-H, Usta JA-R, Waldron KW, Brett CT (1989) A methyltransferase involved in the biosynthesis of 4-*O*-methylglucuronoxylan in etiolated pea epicotyls. J Plant Physiol 135: 81-85

Baydoun EA-H, Waldron KW, Brett CT (1983) The interaction of xylosyltransferase and glucuronyltransferase involved in glucuronoxylan synthesis in pea (*Pisum sativum*) epicotyls. Biochem J 257: 853-858

Bechtold N, Bouchez D (1994) In planta *Agrobacterium*-mediated transformation of adult *Arabidopsis thaliana* plants by vacuum infiltration. In Gene Transfer to Plants, Potrykus, I., Spangenberg, G., eds (Berlin:Springer-Verlag), pp. 19-23

Bernal AJ, Jensen JK, Harholt J, Sørensen S, Moller I, Blaukopf C, Johansen B, de Lotto R, Pauly M, Scheller HV, Willats WG (2007) Disruption of ATCSLD5 results in reduced growth, reduced xylan and homogalacturonan synthase activity and altered xylan occurrence in Arabidopsis. Plant J 52: 791-802

Brown DM, Goubet F, Wong VW, Goodacre R, Stephens E, Dupree P, Turner SR (2007) Comparison of five xylan synthesis mutants reveals new insight into the mechanisms of xylan synthesis. Plant J 52: 1154-1168

Brown DM, Zeef LAH, Ellis J, Goodacreb R, Turner SR (2005) Identification of novel genes in *Arabidopsis* involved in secondary cell wall formation using expression profiling and reverse genetics. Plant Cell 17: 2281-2295

Brown DM, Zhang Z, Stephens E, Dupree P, Turner SR (2009) Characterization of IRX10 and IRX10-like reveals an essential role in glucuronoxylan biosynthesis in *Arabidopsis*. Plant J 57: 732-746

Burk DH, Zhong R, Morrison WHIII, Ye Z-H (2006) Disruption of cortical microtubules by overexpression of green fluorescent protein-tagged α-tubulin 6 causes a marked reduction in cell wall synthesis. J Integr Plant Biol 48: 85-98

Burton RA, Wilson SM, Hrmova M, Harvey AJ, Shirley NJ, Medhurst A, Stone BA, Newbigin EJ, Bacic A, Fincher GB (2006) Cellulose synthase-like CslF genes mediate the synthesis of cell wall (1,3;1,4)-β-D-glucans. Science 311: 1940-1942

Carpita N, McCann M (2000) The cell wall. In Biochemistry and Molecular Biology of Plants, B.B. Buchanan, W. Gruissem, R.L. Jones, eds (Rockville, Maryland: American Society of Plant Physiologists), pp. 52-108

Carpita N, Vergara C (1998) A recipe for cellulose. Science 279: 672-673

Chen F, Dixon RA (2007) Lignin modification improves fermentable sugar yields for biofuel production. Nat Biotechnol 25: 759-761

Cocuron JC, Lerouxel O, Drakakaki G, Alonso AP, Liepman AH, Keegstra K, Raikhel N, Wilkerson CG (2007) A gene from the cellulose synthase-like C family encodes a β-1,4 glucan synthase. Proc Natl Acad Sci USA 104: 8550-8555

Dhugga KS, Barreiro R, Whitten B, Stecca K, Hazebroek J, Randhawa GS, Dolan M, Kinney AJ, Tomes D, Nichols S, Anderson P (2004) Guar seed β-mannan synthase is a member of the cellulose synthase super gene family. Science 303: 363-366

Ebringerová A, Heinze T (2000) Xylan and xylan derivatives-biopolymers with valuable properties. 1. Naturally occurring xylans structures, isolation procedures and properties. Macromol Rapid Commun 21: 542-556

Fagard M, Desnos T, Desprez T, Goubet F, Refregier G, Mouille G, McCann M, Rayon C, Vernhettes S, Höfte H (2000) *PROCUSTE1* encodes a cellulose synthase required for normal cell elongation specifically in roots and dark-grown hypocotyls of Arabidopsis. Plant Cell 12: 2409-2423

Gregory ACE, Smith C, Kerry ME, Wheatley ER, Bolwell GP (2002) Comparative subcellular immunolocation of polypeptides associated with xylan and callose synthases in French bean (*Phaseolus vulgaris*) during secondary wall formation. Phytochemistry 59: 249-259

Himmel ME, Ding SY, Johnson DK, Adney WS, Nimlos MR, Brady JW, Foust TD (2007) Biomass recalcitrance: engineering plants and enzymes for biofuels production. Science 315: 804-807

His I, Driouich A, Nicol F, Jauneau A, Höfte H (2001) Altered pectin composition in primary cell walls of korrigan, a dwarf mutant of Arabidopsis deficient in a membrane-bound endo-1,4-β-glucanase. Planta 212: 348-358

Hoebler C, Barry JL, David A, Delort-Laval J (1989) Rapid acid-hydrolysis of plant cell wall polysaccharides and simplified quantitative determination of their neutral monosaccharides by gas-liquid chromatography. J Ag Food Chem 37: 360-367

Ishikawa M, Kuroyama H, Takeuchi Y, Tsumuraya Y (2000) Characterization of pectin methyltransferase from soybean hypocotyls. Planta 210: 782-791

Johansson MH, Samuelson O (1977) Reducing end groups in birch xylan and their alkaline degradation. Wood Sci Technol 11: 251-263

Kuroyama H, Tsumuraya Y (2001) A xylosyltransferase that synthesizes β-(1->4)-xylans in wheat (*Triticum aestivum* L.) seedlings. Planta 213: 231-240

Lee C, O'Neill MA, Tsumuraya Y, Darvill AG, Ye Z-H (2007a) The *irregular xylem9* mutant is deficient in xylan xylosyltransferase activity. Plant Cell Physiol 48: 1624-1634

Lee C, Teng Q, Huang W, Zhong R, Ye Z-H (2009a). Down-regulation of PoGT47C expression in poplar results in a reduced glucuronoxylan content and an increased wood digestibility by cellulase. Plant Cell Physiol 50: 1075-1089

Lee C, Teng Q, Huang W, Zhong R, Ye Z-H (2009b) The F8H glycosyltransferase is a functional paralog of FRA8 involved in glucuronoxylan biosynthesis in Arabidopsis. Plant Cell Physiol 50: 812-827

Lee C, Teng Q, Huang W, Zhong R, Ye Z-H (2009c) The poplar GT8E and GT8F glycosyltransferases are functional orthologs of Arabidopsis PARVUS involved in glucuronoxylan biosynthesis. Plant Cell Physiol 50: 1982-1987

Lee C, Zhong R, Richardson EA, Himmelsbach DS, McPhail BT, Ye Z-H (2007b) The *PARVUS* gene is expressed in cells undergoing secondary wall thickening and is essential for glucuronoxylan biosynthesis. Plant Cell Physiol 48: 1659-1672

Liepman AH, Wilkerson CG, Keegstra K (2005) Expression of cellulose synthase-like (*Csl*) genes in insect cells reveals that *CslA* family members encode mannan synthases. Proc Natl Acad Sci USA 102: 2221-2226

Liu ZB, Ulmasov T, Shi X, Hagen G, Guilfoyle TJ (1994) Soybean GH3 promoter contains multiple auxin-inducible elements. Plant Cell 6: 645-657

Page RDM (1996) TREEVIEW: An application to display phylogenetic trees on personal computers. Computer Appl Biosci 12: 357-358

Pena MJ, Zhong R, Zhou G-K, Richardson EA, O'Neill MA, Darvill AG, York WS, Ye Z-H (2007) *Arabidopsis irregular xylem8* and *irregular xylem9*: Implications for the complexity of glucuronoxylan biosynthesis. Plant Cell 19: 549-563

Persson S, Caffall KH, Freshour G, Hilley MT, Bauer S, Poindexter P, Hahn MG, Mohnen D, Somerville C (2007) The *Arabidopsis irregular xylem8* mutant is deficient in glucuronoxylan and homogalacturonan, which are essential for secondary cell wall integrity. Plant Cell 19: 237-255

Porchia AC, Sorensen SO, Scheller HV (2002) Arabinoxylan biosynthesis in wheat. Characterization of arabinosyltransferase activity in Golgi membranes. Plant Physiol 130: 432-441

Richmond TA, Somerville CR (2001) Integrative approaches to determining Csl function. Plant Mol Biol 47: 131-143

Shimizu K, Ishihara M, Ishihara T (1976) Hemicellulases of brown rotting fungus, *Tyromyces palustris*. II. The oligosaccharides from the hydrolysate of a hardwood xylan by the intracellular xylanase. Mokuzai Gaikkashi 22: 618-625

Somerville C (2006) The billion-ton biofuel vision. Science 312: 1277

Suzuki S, Li L, Sun Y-H, Chiang VL (2006) The cellulose synthase gene superfamily and biochemical functions of xylem-specific cellulose synthase-like genes in *Populus trichocarpa*. Plant Physiol 142: 1233-1245

Thompson JD, Higgins DG, Gibson TJ (1994) CLUSTAL W: improving the sensitivity of progressive multiple sequence alignment through sequence weighting, position-specific gap penalties and weight matrix choice. Nuc Acids Res 22: 4673-4680

Urahara T, Tsuchiya K, Kotake T, Tohno-oka T, Komae K, Kawada N, Tsumuraya Y (2004) A β-(1→4)-xylosyltransferase involved in the synthesis of arabinoxylans in developing barley endosperms. Physiol Plant 122: 169-180

Wu AM, Rihouey C, Seveno M, Hörnblad E, Singh SK, Matsunaga T, Ishii T, Lerouge P, Marchant A (2009) The *Arabidopsis* IRX10 and IRX10-LIKE glycosyltransferases are critical for glucuronoxylan biosynthesis during secondary cell wall formation. Plant J 57: 718-731

Zeng W, Chatterjee M, Faik A (2008) UDP-Xylose-stimulated glucuronyltransferase activity in wheat microsomal membranes: characterization and role in glucurono(arabino)xylan biosynthesis. Plant Physiol 147: 78-91

Zhong R, Demura T, Ye Z-H (2006) SND1, a NAC domain transcription factor, is a key regulator of secondary wall synthesis in fibers of Arabidopsis. Plant Cell 18: 3158-3170

Zhong R, Pena MJ, Zhou G-K, Nairn CJ, Wood-Jones A, Richardson EA, Morrison WH, Darvill AG, York WS, Ye Z-H (2005) Arabidopsis *Fragile Fiber8*, which encodes a putative glucuronyltransferase, is essential for normal secondary wall synthesis. Plant Cell 17: 3390-3408

Zhong R, Richardson EA, Ye Z-H (2007) Two NAC domain transcription factors, SND1 and NST1, function redundantly in regulation of secondary wall synthesis in fibers of Arabidopsis. Planta 225: 1603-1611

Zhong R, Taylor JJ, Ye Z-H (1997) Disruption of interfascicular fiber differentiation in an Arabidopsis mutant. Plant Cell 9: 2159-2170

Zhou GK, Zhong R, Richardson EA, Himmelsbach DS, McPhail BT, Ye Z-H (2007) Molecular characterization of PoGT8D and PoGT43B, two secondary wall-associated glycosyltransferases in poplar. Plant Cell Physiol 48: 689-699

Zhou GK, Zhong R, Richardson EA, Morrison WH, Nairn CJ. Wood-Jones A, Ye Z-H (2006) The poplar glycosyltransferase GT47C is functionally conserved with Arabidopsis *Fragile Fiber8.* Plant Cell Physiol 47: 1229-1240

Table 4.1. Monosaccharide composition of cell walls from inflorescence stems of wild type, *irx9*, *irx14*, and the *irx9* and *irx14* plants overexpressing GT43 members

Sample	Xylose	Glucose	Mannose	Galactose	Arabinose	Rhamnose
Wild type	**108.7 ± 4.6**	412.1 ± 4.7	18.9 ± 1.3	17.5 ± 1.3	12.6 ± 2.2	11.1 ± 1.2
irx9	**60.8 ± 0.3**	337.9 ± 0.4	39.0 ± 0.1	38.4 ± 1.3	28.6 ± 0.2	16.4 ± 0.6
irx9 + IRX9	**91.6 ± 3.1**	370.4 ± 3.0	19.1 ± 3.2	16.7 ± 0.8	16.7 ± 0.9	14.9 ± 0.9
irx9 + I9H	**107.4 ± 2.8**	446 ± 3.8	24.1 ± 0.9	18.2 ± 0.8	18.2 ± 0.6	12.7 ± 0.6
irx9 + IRX14	**60.2 ± 5.9**	366.9 ± 35.0	44.2 ± 5.0	25.8 ± 3.4	28.8 ± 3.2	19.3 ± 2.9
irx9 + I14H	**52.7 ± 11.6**	393.7 ± 42.2	43.1 ± 5.6	24.9 ± 3.6	23.9 ± 2.2	16.4 ± 1.2
irx14	**49.4 ± 5.0**	334 ± 8.4	23.6 ± 0.7	32.9 ± 2.9	12.0 ± 1.5	12.2 ± 0.9
irx14 + IRX9	**45.9 ± 3.9**	338.5 ± 11.7	23.6 ± 2.2	28.6 ± 0.8	13.7 ± 1.3	17.1 ± 0.8
irx14 + I9H	**56.0 ± 2.0**	372.1 ± 9.6	31.5 ± 2.6	29.1 ± 0.2	14.6 ± 0.1	18.2 ± 0.9
irx14 + IRX14	**98.5 ± 4.3**	385.4 ± 3.8	27.7 ± 1.3	24.9 ± 1.4	13.9 ± 0.2	12.7 ± 0.8
irx14 + I14H	**96.9 ± 1.2**	397.5 ± 6.0	18.0 ± 1.3	22.7 ± 3.3	11.5 ± 0.1	15.2 ± 0.2

The wall residues for cell wall composition analysis were prepared from stems. The data are means (mg/g dry cell wall) ± SE of duplicate assays.

Table 4.2. Monosaccharide composition of cell walls from inflorescence stems of wild type and GT43 mutants

Sample	Xylose	Glucose	Mannose	Galactose	Arabinose	Rhamnose
Wild type	**110.4 ± 1.4**	402.0 ± 0.2	18.0 ± 0.4	14.6 ± 0.2	11.0 ± 0.2	11.7 ± 0.4
irx9	**57.2 ± 0.3**	336.9 ± 0.4	35.1 ± 0.1	39.9 ± 1.3	23.8 ± 0.2	13.9 ± 0.6
i9H	**106.6 ± 3.8**	418.1 ± 4.5	17.5 ± 0.7	13.9 ± 0.6	9.0 ± 0.1	10.4 ± 0.1
irx14	**59.5 ± 2.1**	346.5 ± 7.5	24.6 ± 2.5	16.2 ± 1.3	11.2 ± 0.1	10.9 ± 0.5
i14h	**102.3 ± 4.8**	391.8 ± 7.6	17.9 ± 2.3	15.1 ± 1.1	10.3 ± 0.5	10.6 ± 0.5
irx9 i9h(+/-)	**40.2 ± 1.1**	329.7 ± 8.4	40.4 ± 2.1	43.4 ± 1.4	35.8 ± 1.1	19.4 ± 2.0
irx9 irx14	**26.5 ± 0.5**	292.4 ± 5.3	20.2 ± 4.8	49.3 ± 3.4	26.0 ± 1.9	12.1 ± 0.2
irx9 i14h	**49.2 ± 1.7**	337.9 ± 13.4	30.6 ± 1.5	23.1 ± 1.8	15.2 ± 1.3	13.7 ± 0.9
i9h irx14	**59.3 ± 3.9**	358.0 ± 15.7	25.7 ± 2.9	15.6 ± 1.7	11.2 ± 0.5	11.9 ± 0.3
i9h i14h	**94.2 ± 21.9**	366.7 ± 24.3	12.6 ± 0.4	12.3 ± 1.0	8.9 ± 0.4	9.5 ± 0.5
irx14 i14h	**29.1 ± 1.8**	251.7 ± 11.1	24.3 ± 1.8	26.9 ± 2.2	19.3 ± 1.1	13.9 ± 0.6

The wall residues for cell wall composition analysis were prepared from stems. The data are means (mg/g dry cell wall) ± SE of duplicate assays.

Table 4.3. Relative abundance of the reducing end tetrasaccharide sequence and side chains, and the degree of polymerization of GX from the wild type and GT43 mutants overexpressing various GT43 members

Sample	Frequency of occurrence of GlcA and MeGlcA side chains[a]	Relative abundance of the reducing end tetrasaccharide sequence[b]	Average DP[c]
Wild type	21.6%	100%	93.0
irx9	21.3%	31.9%	29.7
irx9 + IRX9	20.3%	88.1%	81.9
irx9 + I9H	19.0%	79.2%	73.7
irx9 + IRX14	20.3%	23.1%	21.5
irx9 + I14H	20.8%	34.0%	31.6
irx14	22.0%	37.6%	35.0
irx14 + IRX9	23.4%	40.9%	38.0
irx14 + I9H	23.3%	40.9%	38.0
irx14 + IRX14	21.5%	70.3%	65.4
irx14 + I14H	20.4%	82.3%	76.5

[a]The frequency of occurrence of the GlcA and MeGlcA side chains was calculated from the ratios of the NMR resonance of the branched β-Xyl to that of total β-Xyl.

[b]The relative abundance of the reducing end tetrasaccharide sequence was determined from the ratios of the NMR resonance of the reducing end sequence to that of the branched β-Xyl. The abundance of the reducing end tetrasaccharide sequence in the wild type was taken as 100%.

[c]The average degree of polymerization (DP) was calculated based on the ratios of relative abundance of the reducing end sequence of a given sample to that of the wild type. The average DP of the wild type was taken as 93 (Pena et al., 2007).

Figure 4.1. Sequence comparison and expression analysis of family GT43 members. (A) Amino acid sequence alignment of the four Arabidopsis GT43 proteins. The numbers shown at the left of each sequence are the positions of amino acid residues in the corresponding proteins. Identical and similar residues are shaded with black and gray, respectively. (B) Percentage of identity and similarity of GT43 proteins. (C) Phylogenetic relationship of Arabidopsis GT43 members. The GT43 sequences were aligned using the ClustlW program (Thompson et al., 1994) and the phylogenetic tree was displayed using the TREEVIEW program (Page, 1996). The 0.1 scale denotes 10% change, and the bootstrap values are presented in percentages at the nodes. (D) Quantitative PCR analysis of the expression of *I9H*, *IRX14*, and *I14H* in different Arabidopsis organs. The highest expression level in an organ was set to 100. (E) Quantitative PCR analysis of the expression of *I9H*, *IRX14*, and *I14H* in pith cells, xylem cells, and interfascicular fibers that were laser-microdissected from wild-type Arabidopsis stems. The expression level in pith cells was taken as 1. (F) Quantitative PCR analysis of the expression of *I9H*, *IRX14*, and *I14H* in the SND1 overexpressors (SND1-OE) (left panel) and SND1/NST1 RNAi lines (right panel). The expression of each gene in the wild type was used as a control. Error bars in (D) to (F) denote SE of three biological replicates.

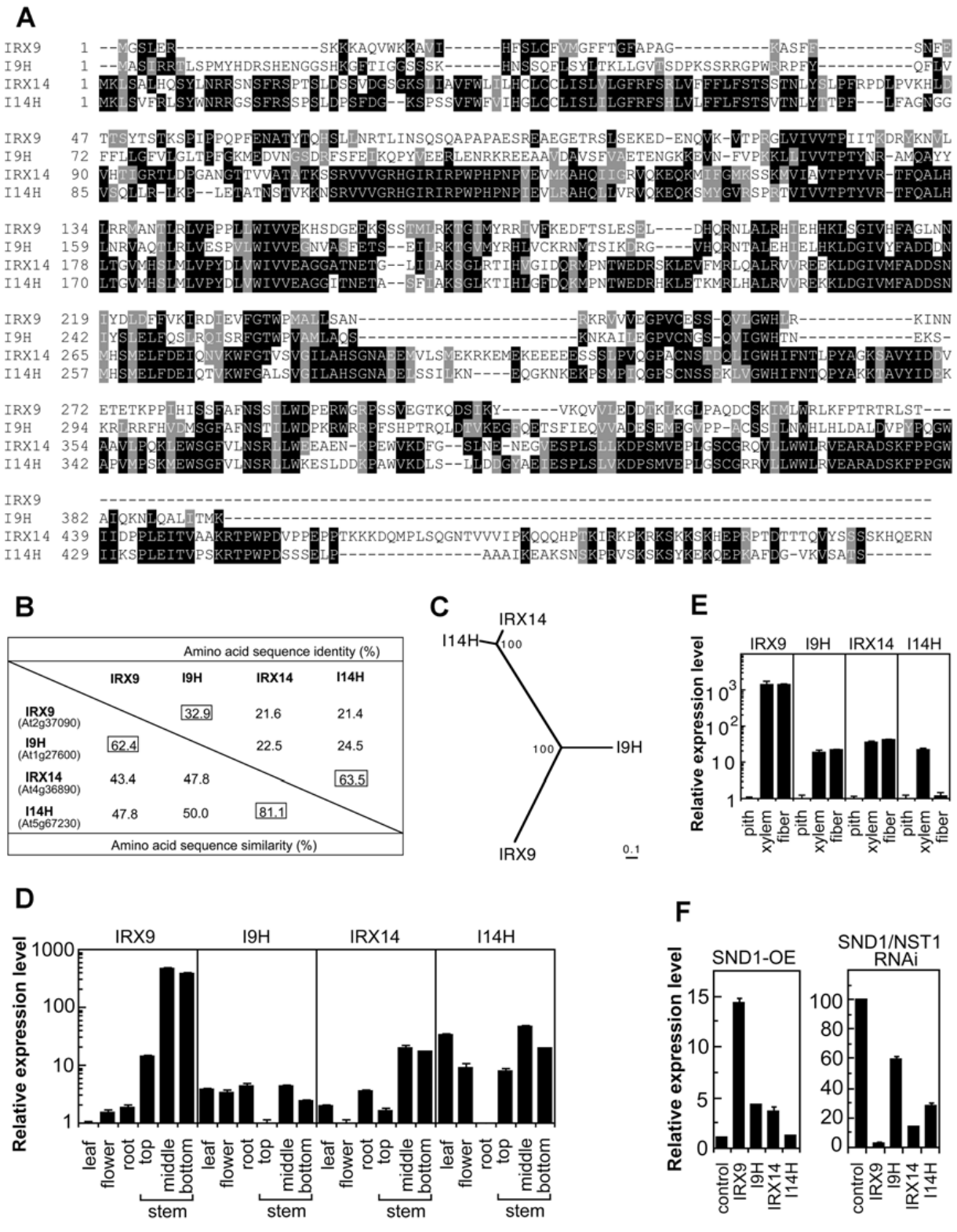
A
IRX9
I9H
IRX14
I14H
B
Amino acid sequence identity (%)
IRX9
I9H
IRX14
I14H
IRX9 (At2g37090)
I9H (At1g27600)
IRX14 (At4g36890)
I14H (At5g67230)
32.9
21.6
21.4
62.4
22.5
24.5
43.4
47.8
63.5
47.8
50.0
81.1
Amino acid sequence similarity (%)
C
IRX14
I14H
100
100
I9H
IRX9
0.1
E
Relative expression level
IRX9
I9H
IRX14
I14H
pith
xylem
fiber
D
Relative expression level
IRX9
I9H
IRX14
I14H
leaf
flower
root
top
middle
bottom
stem
F
SND1-OE
SND1/NST1 RNAi
Relative expression level
control
IRX9
I9H
IRX14
I14H

Figure 4.2. Expression patterns of *I9H*, *IRX14*, and *I14H* in elongating and non-elongating internodes of inflorescence stems, and roots. Cross sections of stems and roots from transgenic Arabidopsis plants expressing the *I9H*, *IRX14*, and *I14H* genes fused with the GUS reporter genes were stained for the GUS activity (shown as blue). if, interfascicular fiber; ve, vessels; xf, xylary fiber; xy, xylem. Bar in (A) = 130 μm in (A) to (I).

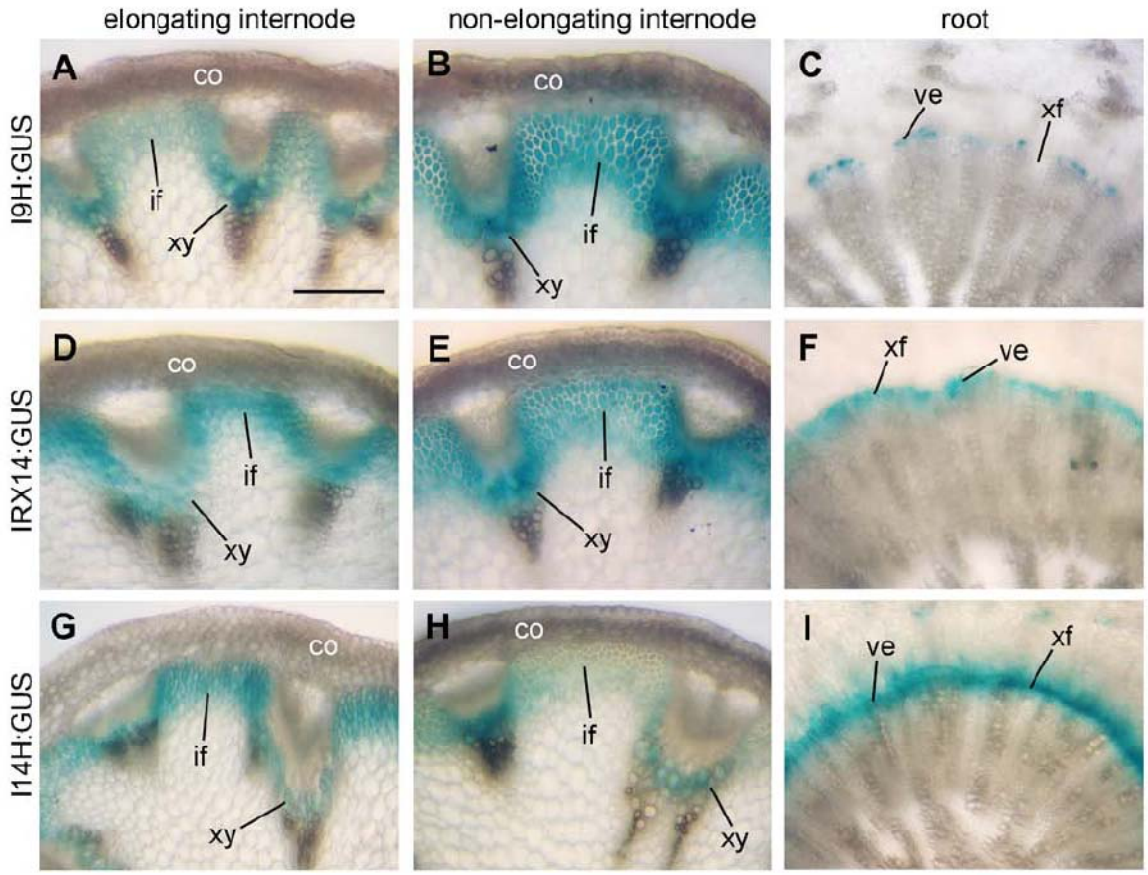
elongating internode
non-elongating internode
root
I9H:GUS
IRX14:GUS
I14H:GUS
A
B
C
D
E
F
G
H
I
co
if
xy
ve
xf

Figure 4.3. Subcellular localization of I9H, IRX14, and I14H. Fluorescent protein-tagged fusion proteins were expressed in carrot protoplasts, and the signals were visualized with a laser confocal microscope. (A) to (C) I9H, IRX14, and I14H are membrane proteins as predicted by the TMHMM2.0 program. Inside, the cytoplasmic side of the membrane; outside, the noncytoplasmic side of the membrane. (D) and (E) A carrot protoplast (D; differential interference contrast image) expressing YFP alone showing the fluorescent signals throughout the cytoplasm (E). (F) to (I) A carrot protoplast (F) co-expressing I9H-YFP (G) and the Golgi-localized FRA8-CFP (H). (J) to (M) A carrot protoplast (J) co-expressing IRX14-YFP (K) and FRA8-CFP (L). (N) to (Q) A carrot protoplast (N) co-expressing I14H-YFP (O) and FRA8-CFP (P). Note the colocalization of I9H-YFP (I), IRX14-YFP (M), and I14H-YFP (Q) with the Golgi marker FRA8-CFP.

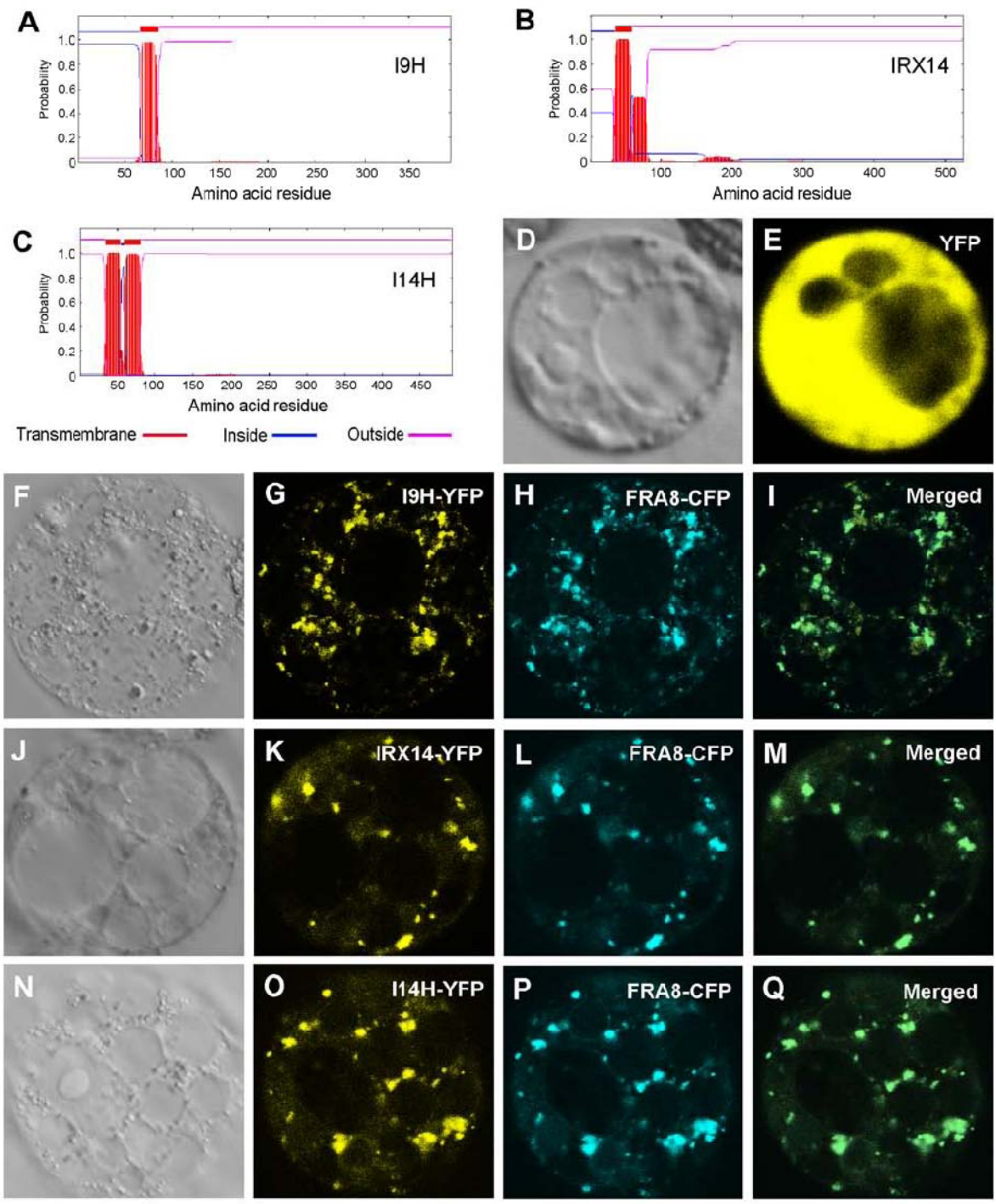
A
I9H
Probability
Amino acid residue
B
IRX14
Probability
Amino acid residue
C
I14H
Probability
Amino acid residue
Transmembrane
Inside
Outside
D
E
YFP
F
G
I9H-YFP
H
FRA8-CFP
I
Merged
J
K
IRX14-YFP
L
FRA8-CFP
M
Merged
N
O
I14H-YFP
P
FRA8-CFP
Q
Merged

Figure 4.4. Complementation of the *irx9* and *irx14* mutants by overexpression of GT43 members. The full-length cDNAs of the four Arabidopsis GT43 members driven by the CaMV 35S promoter were introduced into *irx9* or *irx14* and the bottom parts of inflorescence stems of 10-week-old transgenic overexpressors were examined for the stem breaking strength (A) and the secondary wall thickness in interfascicular fibers (B to M). Bar in (B) = 5.4 μm in (B) to (M). (A) Measurement of the breaking strength of stems of the wild type, *irx9*, *irx14*, and the mutants overexpressing GT43 members. Each bar represents the breaking force of the inflorescence stem of individual plants. It was evident that the stem breaking strength of *irx9* was restored by overexpression of IRX9 or I9H and that of *irx14* was restored by overexpression of IRX14 or I14H. (B) to (M) Transmission electron microscopy showing the restoration of the secondary wall thickness of the interfascicular fibers in the stems of the *irx9* mutant by overexpression of IRX9 and I9H, and that of the *irx14* mutant by overexpression of IRX14 and I14H.

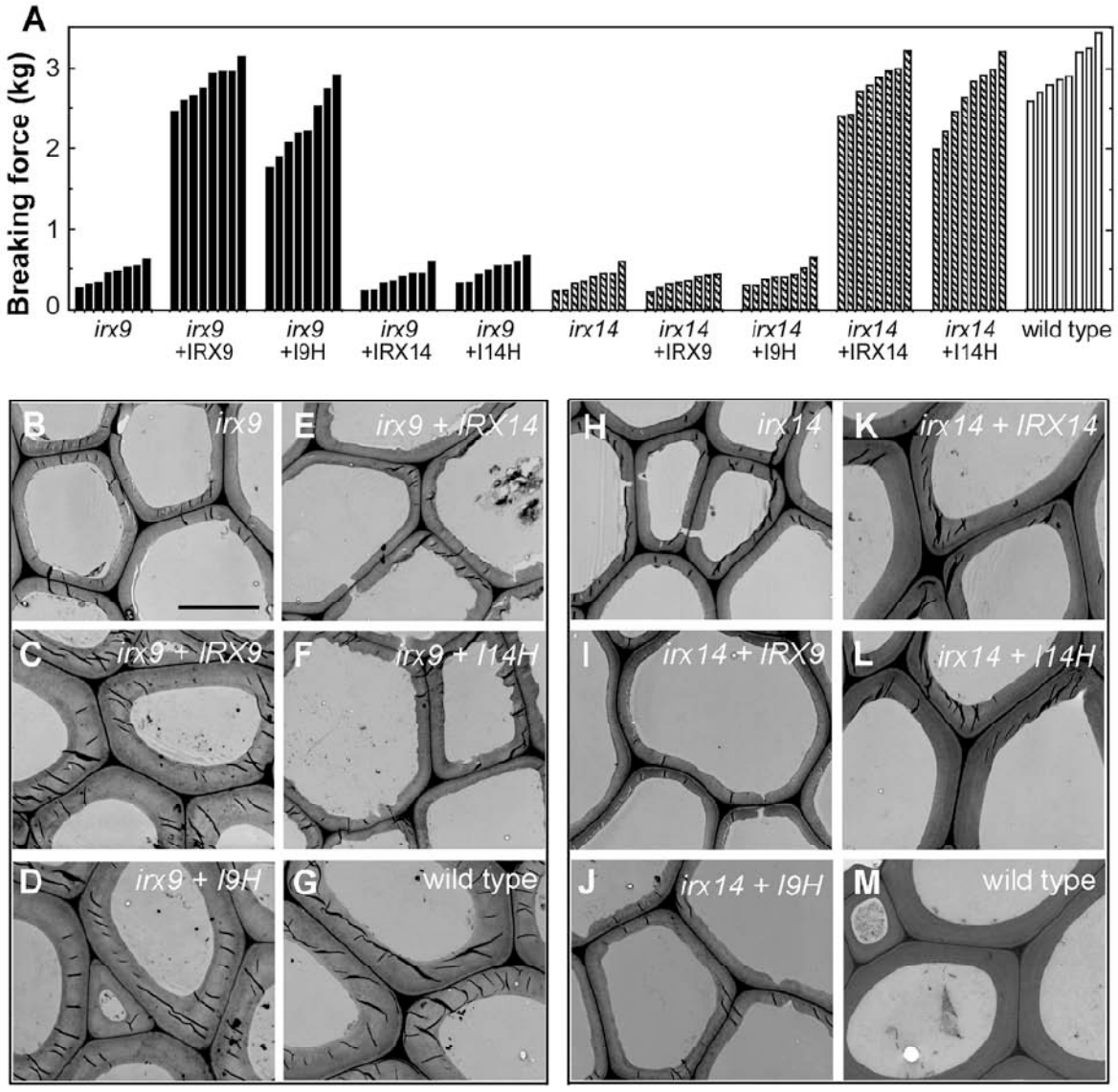
A
Breaking force (kg)
0
1
2
3
irx9
irx9 +IRX9
irx9 +I9H
irx9 +IRX14
irx9 +I14H
irx14
irx14 +IRX9
irx14 +I9H
irx14 +IRX14
irx14 +I14H
wild type
B irx9
C irx9 + IRX9
D irx9 + I9H
E irx9 + IRX14
F irx9 + I14H
G wild type
H irx14
I irx14 + IRX9
J irx14 + I9H
K irx14 + IRX14
L irx14 + I14H
M wild type

Figure 4.5. MALDI-TOF mass spectra of acidic xylooligosaccharides generated by β-endoxylanase digestion of GX from the stems of the wild type, *irx9*, *irx14*, and the mutants overexpressing GT43 members. The ions at *m/z* 745 and 759 correspond to xylotetrasaccharides bearing a GlcA residue (X_4G) or a methylated GlcA residue (X_4M). The ion at *m/z* 781 corresponds to the doubly sodiated X_4M. Note that the missing ion at *m/z* 745 corresponding to X_4G in *irx9* was restored by overexpression of IRX9 or I9H and that in *irx14* was restored by overexpression of IRX14 or I14H.

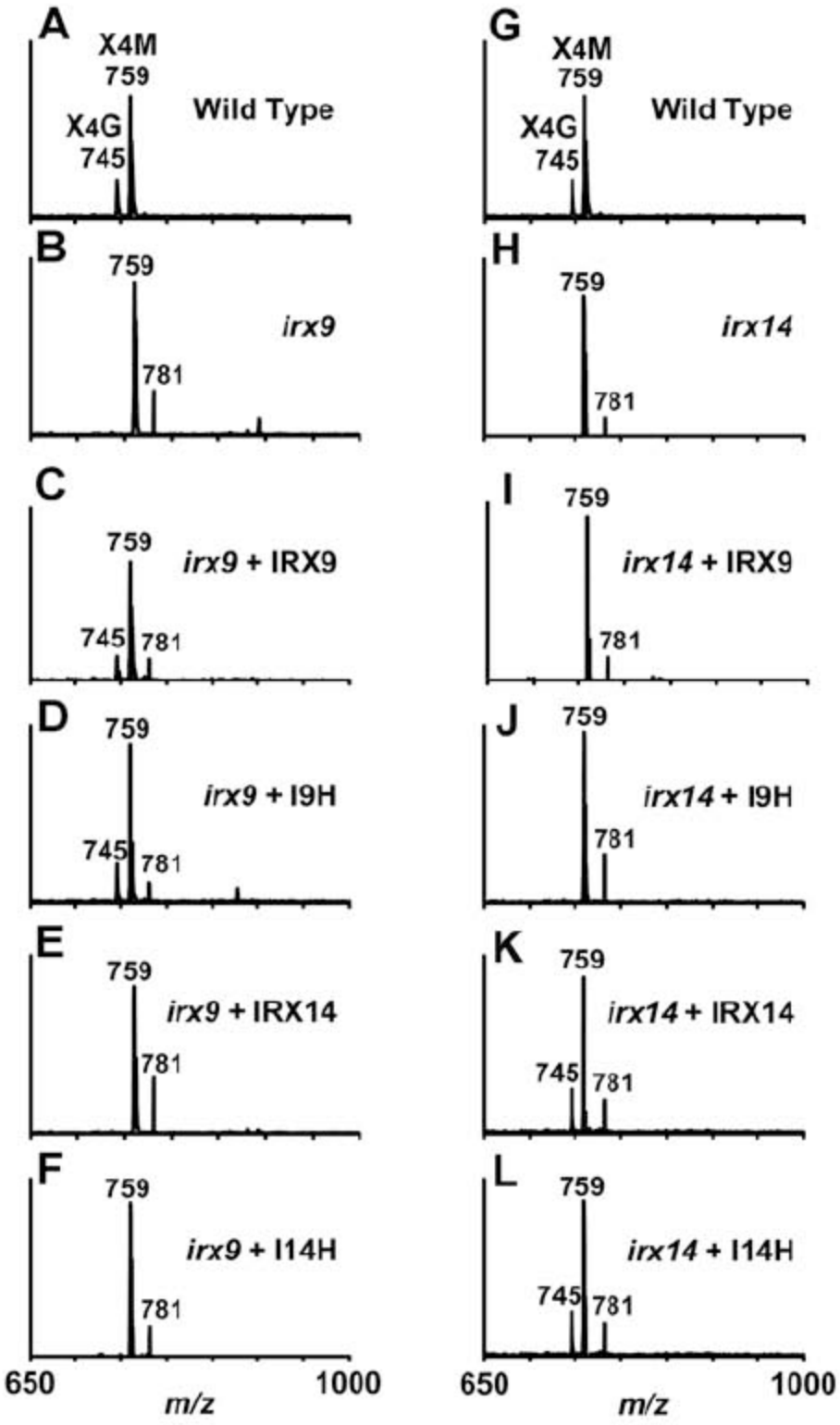
A
X4M
759
X4G
745
Wild Type
B
759
irx9
781
C
759
irx9 + IRX9
745
781
D
759
irx9 + I9H
745
781
E
759
irx9 + IRX14
781
F
759
irx9 + I14H
781
650
1000
m/z
G
X4M
759
X4G
745
Wild Type
H
759
irx14
781
I
759
irx14 + IRX9
781
J
759
irx14 + I9H
781
K
759
irx14 + IRX14
745
781
L
759
irx14 + I14H
745
781
650
1000
m/z

Figure 4.6, ^{1}H-NMR spectra of acidic xylooligosaccharides generated by β-endoxylanase digestion of GX from the stems of the wild type, *irx9*, *irx14*, and the mutants overexpressing GT43 members. Resonances are labeled with the position of the assigned proton and the identity of the residue containing that proton. Note the restoration of the resonance of H1 of α-GlcA in *irx9* complemented with IRX9 and I9H and in *irx14* complemented with IRX14 and I14H (arrows). The resonances of H1 of α-D-GalA, H1 of α-L-Rha, H1 of 3-linked β-D-Xyl, H4 of α-D-GalA, and H2 of α-L-Rha are from the GX reducing end tetrasaccharide sequence. Note the elevated relative resonance intensity of the GX reducing end tetrasaccharide sequence in *irx 9* and *irx14* and the reduction in its resonance intensity in *irx9* complemented with IRX9 and I9H and in *irx14* complemented with IRX14 and I14H. The doublet resonance peak at 4.39 ppm in the wild type is assigned to H5 α-GlcA and that at 4.35 ppm is assigned to H5 Me-α-GlcA. The resonance shift of H5 proton in other samples is likely attributed to its high sensitivity to a slight variation of pH and concentration of the samples because of its close proximity to the carboxyl group. A similar cause may lead to a slight resonance shift of H1 and H4 α-GalA. HDO, hydrogen deuterium oxide.

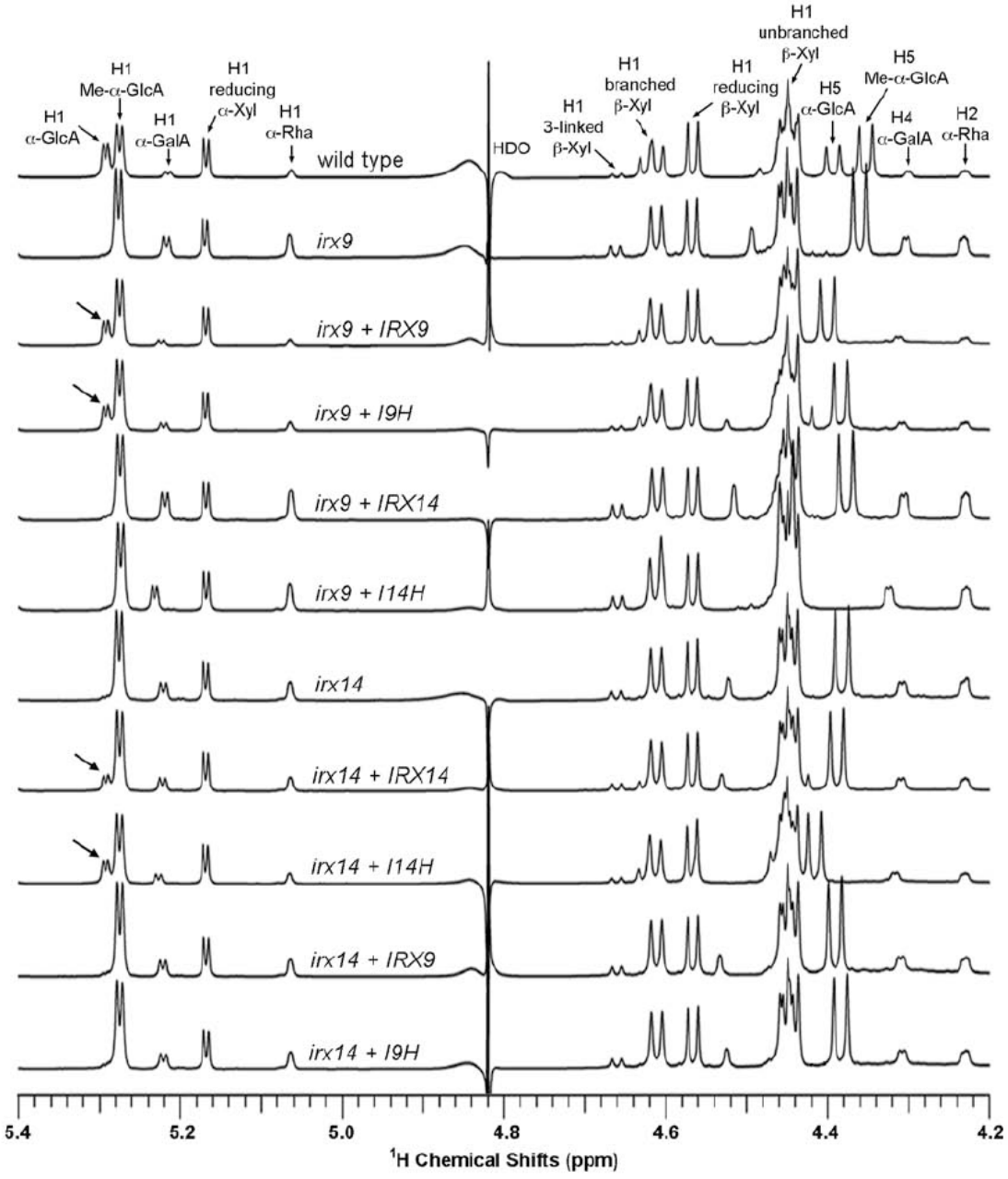
H1
α-GlcA
H1
Me-α-GlcA
H1
α-GalA
H1
reducing
α-Xyl
H1
α-Rha
wild type
HDO
H1
3-linked
β-Xyl
H1
branched
β-Xyl
H1
reducing
β-Xyl
H1
unbranched
β-Xyl
H5
α-GlcA
H5
Me-α-GlcA
H4
α-GalA
H2
α-Rha
irx9
irx9 + IRX9
irx9 + I9H
irx9 + IRX14
irx9 + I14H
irx14
irx14 + IRX14
irx14 + I14H
irx14 + IRX9
irx14 + I9H
5.4
5.2
5.0
4.8
4.6
4.4
4.2
¹H Chemical Shifts (ppm)

Figure 4.7. Time course of the xylosyltransferase activity in the wild type, *irx9*, *irx14*, and the mutants overexpressing GT43 members. (A) Overexpression of I9H or IRX9 but not IRX14 or I14H in *irx9* rescued the deficiency in the xylosyltransferase activity caused by the *irx9* mutation. Note the increased xylosyltransferase activity in *irx9* overexpressing IRX9. (B) Overexpression of I14H or IRX14 but not IRX9 or I9H in *irx14* rescued the deficiency in the xylosyltransferase activity caused by the *irx14* mutation.

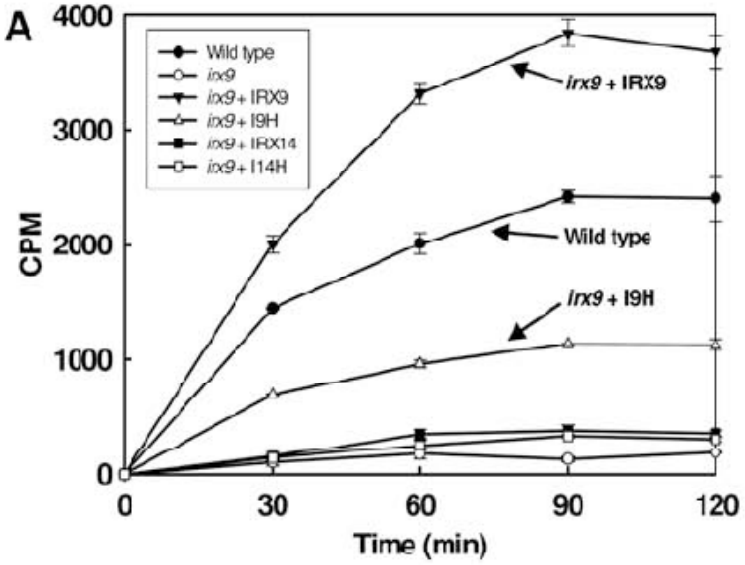
A
4000
3000
2000
1000
0
CPM
0
30
60
90
120
Time (min)
Wild type
irx9
irx9 + IRX9
irx9 + I9H
irx9 + IRX14
irx9 + I14H
irx9 + IRX9
Wild type
irx9 + I9H

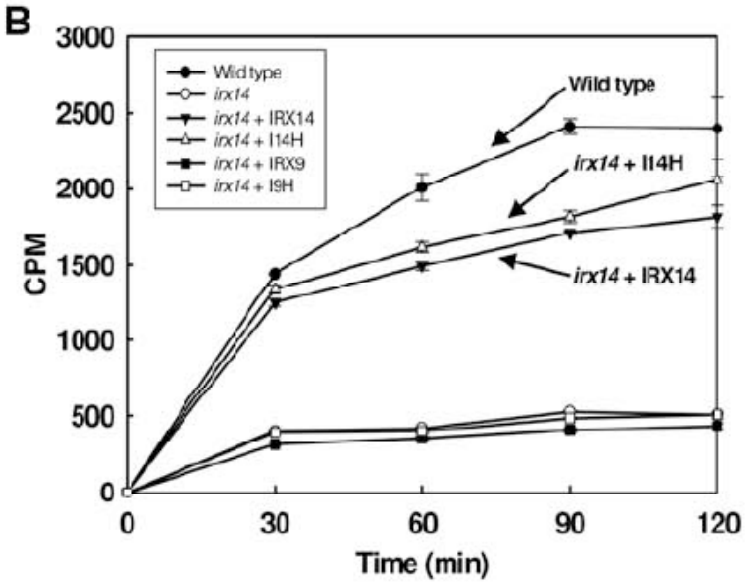
B
3000
2500
2000
1500
1000
500
0
CPM
0
30
60
90
120
Time (min)
Wild type
irx14
irx14 + IRX14
irx14 + I14H
irx14 + IRX9
irx14 + I9H
Wild type
irx14 + I14H
irx14 + IRX14

Figure 4.8. Effects of single and double mutations of GT43 members on plant growth and fiber wall thickening. (A) Diagrams showing the sites of T-DNA insertions in the *I9H* and *I14H* genes. (B) PCR identification of homozygous *i9h* and *i14h* mutants. T-DNA indicates the amplified DNA fragment with a T-DNA left border primer and an *I9H* or *I14H* primer flanking the T-DNA insertion site. Endogenous indicates the amplified *I9H* or *I14H* DNA fragment with primers spanning the T-DNA insertion site. (C) Breaking strength measurement showing that the stem strength of *i9h* and *i14h* is similar to that of the wild type. Each bar represents the breaking force of the inflorescence stem of individual plants. (D) Morphology of 10-week-old single and double GT43 mutants. Insets show the enlarged images of the rosette plants of *irx9 i9h* and *irx9 irx14*. (E) to (O) Cross sections of stems showing the interfascicular fibers in single and double GT43 mutants. Note the extremely thin fiber walls in *irx9 irx14* and *irx14 i14h*. The bottom parts of inflorescence stems of 10-week-old plants except for *irx9 i9h (+/-)* and *irx9 irx14*, which were from 4-month and 6-month old plants, respectively, were sectioned and stained with toluidine blue for anatomy. if, interfascicular fiber. Bar in (E) = 65 μm for (E) to (O).

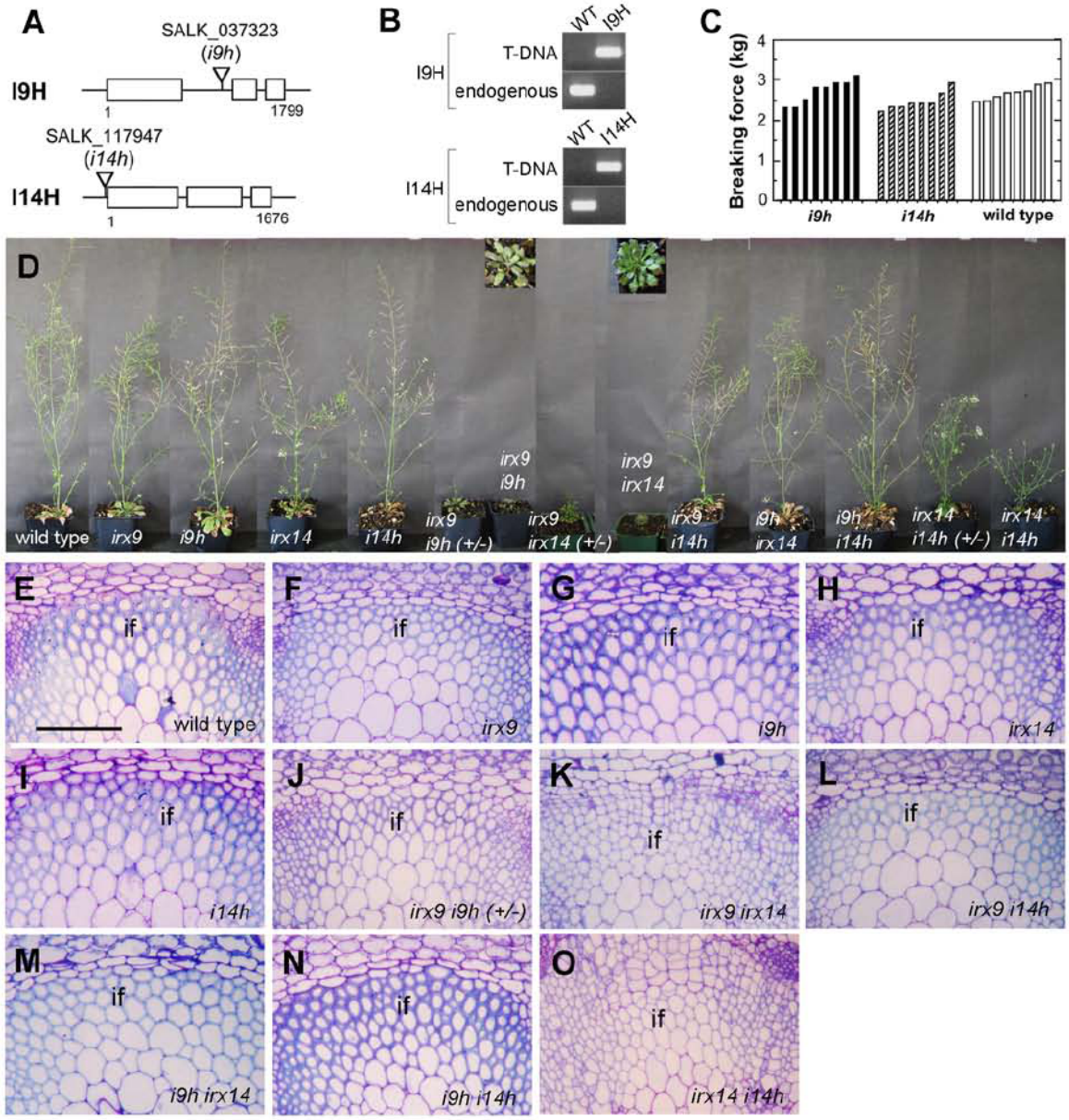
A
SALK_037323
(i9h)
I9H
1
1799
SALK_117947
(i14h)
I14H
1
1676
B
WT
I9H
T-DNA
endogenous
I9H
WT
I14H
T-DNA
endogenous
I14H
C
Breaking force (kg)
0
1
2
3
4
i9h
i14h
wild type
D
wild type
irx9
i9h
irx14
i14h
irx9
i9h (+/-)
irx9
i9h
irx9
irx14 (+/-)
irx9
irx14
irx9
i14h
i9h
irx14
i9h
i14h
irx14
i14h (+/-)
irx14
i14h
E
if
wild type
F
if
irx9
G
if
i9h
H
if
irx14
I
if
i14h
J
if
irx9 i9h (+/-)
K
if
irx9 irx14
L
if
irx9 i14h
M
if
i9h irx14
N
if
i9h i14h
O
if
irx14 i14h

Figure 4.9. Transmission electron micrographs of the cell walls of interfascicular fibers in the stems of the wild type and GT43 mutants. The bottom parts of the inflorescence stems of 10-week-old plants except for *irx9 i9h (+/-)* and *irx9 irx14*, which were from 4-month and 6-month old plants, respectively, were examined for fiber wall thickness. Bar in (A) = 7.2 μm for (A) to (K).

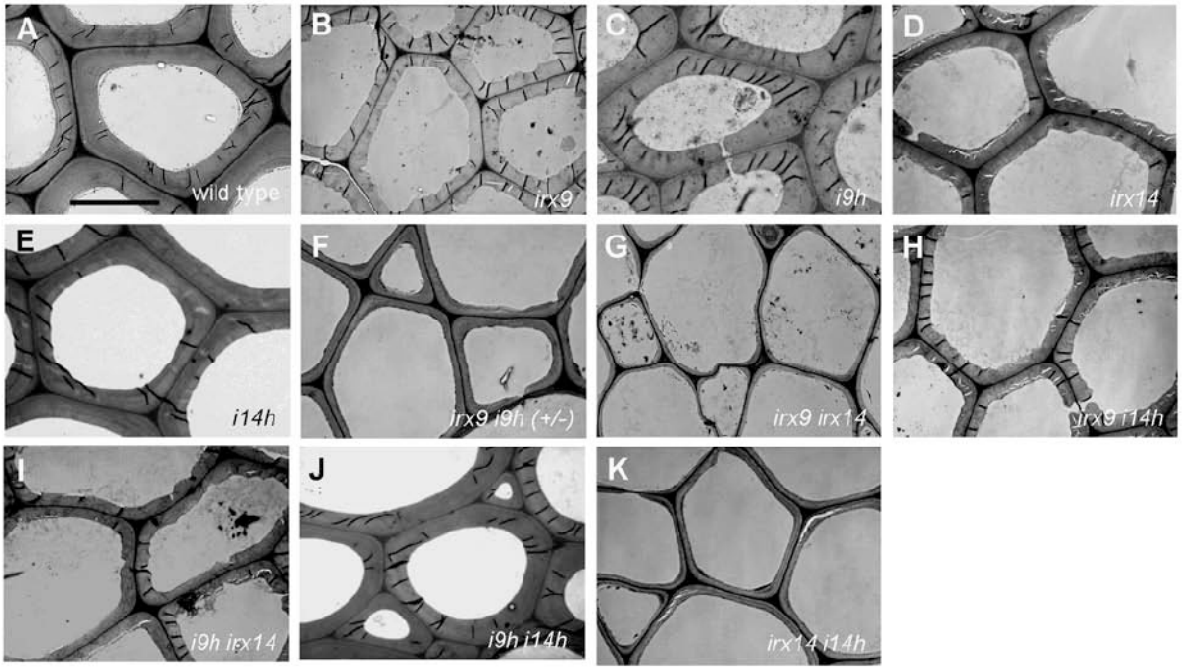
A
wild type
B
irx9
C
i9h
D
irx14
E
i14h
F
irx9 i9h (+/-)
G
irx9 irx14
H
irx9 i14h
I
i9h irx14
J
i9h i14h
K
irx14 i14h

CHAPTER 5

MOLECULAR DISSECTION OF XYLAN BIOSYNTHESIS DURING WOOD FORMATION IN POPLAR[1]

[1]Lee, C., Teng, Q., Zhong, R., and Ye, Z.-H. Mol. Plant (submitted)

ABSTRACT

Xylan, being the second most abundant polysaccharide in dicot wood, is considered to be one of the factors contributing to wood biomass recalcitrance for biofuel production. To better utilize wood as biofuel feedstock, it is crucial to functionally characterize all the genes involved in xylan biosynthesis during wood formation. In this report, we investigated roles of poplar families GT43 and GT8 glycosyltransferases in xylan biosynthesis during wood formation. There exist seven GT43 genes in the genome of poplar (Populus trichocarpa), five of which, namely PtrGT43A, PtrGT43B, PtrGT43C, PtrGT43D, and PtrGT43E, were shown to be highly expressed in the developing wood and their encoded proteins were localized in the Golgi. Comprehensive genetic complementation coupled with chemical analyses demonstrated that overexpression of PtrGT43A/B/E but not PtrGT43C/D was able to rescue the xylan defects conferred by the Arabidopsis irx9 mutant, whereas overexpression of PtrGT43C/D but not PtrGT43A/B/E led to a complementation of the xylan defects in the Arabidopsis irx14 mutant. The essential roles of poplar GT43 members in xylan biosynthesis was further substantiated by RNAi downregulation of GT43B in the hybrid poplar (Populus alba x tremula) leading to reductions in wall thickness and xylan content in wood, and an elevation in the abundance of the xylan reducing end sequence. Wood digestibility analysis revealed that cellulase digestion released more glucose from the wood of poplar GT43B RNAi lines than the control wood, indicating a decrease in wood biomass recalcitrance. Furthermore, RNAi downregulation of another poplar wood-associated glycosyltransferase, PoGT8D, was shown to cause decreases in wall thickness and xylan content as well as in the abundance of the xylan reducing end sequence. Together, these findings demonstrate that the poplar GT43 members form two functionally nonredundant groups, i.e., PtrGT43A/B/E as functional orthologs of Arabidopsis IRX9 and

PtrGT43C/D as functional orthologs of Arabidopsis IRX14, all of which are involved in the biosynthesis of xylan backbones, and that the poplar GT8D is essential for the biosynthesis of the xylan reducing end sequence.

INTRODUCTION

Wood as the most abundant biomass produced by land plants is indispensible to our daily lives. Wood not only provides abundant raw materials for energy, construction, paper-making, and many other industrial uses, but also has recently been considered to be an attractive source for biofuel production (Carroll and Somerville, 2009). There has been a long history of active research in wood biology in the hope of better utilizing this abundant, renewable biomass for our ever-expanding needs (Plomion et al., 2001). Although wood is well characterized anatomically and chemically, our understanding of the genes participating in wood formation is still in infancy and only a small number of wood-associated genes from tree species have been characterized functionally (Mellerowicz and Sundberg, 2008). Further investigation of the functions of genes involved in wood formation in tree species is necessary in order to provide foundation knowledge for genetic improvement of wood quantity and quality.

Previous transcriptome profiling of genes expressed during wood formation have revealed a number of regulatory and biosynthetic genes that are likely involved in the biosynthesis of wood components, including cellulose, hemicellulose (xylan and glucomannan), and lignin (Aspeborg et al., 2005; Prassinos et al., 2005; Andersson-Gunneras et al., 2006; Bedon et al., 2007; Pavy et al., 2008; Wilkins et al., 2009; Grant et al., 2010; Zhong et al., 2010a and 2010b). Noteworthy is the transcriptome analysis of the secondary wall thickening zone in poplar wood that identified 25 wood-associated glycosyltransferses (GTs) (Aspeborg et al., 2005). Among these GTs, four (CesA1, CesA2, CesA3 and CesA9) are cellulose synthases (Joshi et al.,

2004) and one (GT2A) is a mannan synthase (Suzuki et al., 2006; Liepman et al., 2007). A number of other poplar wood-associated GTs, including GT47C, GT43B, and GT8E/F, have recently been demonstrated to be involved in the biosynthesis of xylan, the second most abundant polysaccharide in wood.

In poplar wood, xylan is made of a linear chain of β-1,4-linked xylosyl residues with a degree of polymerization around 120 (Jacobs and Dahlman, 2001). Some of the xylosyl residues in the xylan backbone are substituted by α-1,2-linked 4-*O*-methylglucuronic acid residues and acetylated at C-2 or C-3 (Timell, 1967). As in other woody species, the reducing end of xylan in poplar contains a unique tetrasaccharide sequence consisting of β-D-Xyl*p*-(1→3)-α-L-Rha*p*-(1→2)-α-D-Gal*p*A-(1→4)-B-Xyl*p* (Shimizu et al., 1976; Johansson and Samuelson, 1977; Andersson et al., 1983; Pena et al., 2007; Lee et al., 2009). Complementation studies have shown that poplar GT47C and GT8E/F are functional orthologs of the *Arabidopsis thaliana* FRA8 (Zhong et al., 2005) and PARVUS (Lee et al., 2007b), respectively, which are involved in the biosynthesis of the xylan reducing end sequence (Zhou et al., 2006; Lee et al., 2009c). The essential role of poplar GT47C in xylan biosynthesis has been demonstrated directly by RNA interference (RNAi) analysis showing that downregulation of PoGT47C expression causes reductions in both xylan content and the abundance of the xylan reducing end sequence (Lee et al., 2009a). Complementation study has also revealed that the poplar GT43B is a functional ortholog of the *Arabidopsis* IRX9 participating in the elongation of xylan backbone (Zhou et al., 2007). The functional roles of the remaining poplar wood-associated GTs identified by Asprborg et al. (2005) have not been analyzed experimentally. Elucidation of the functions of all wood-associated GTs will help unravel the complex process of wood formation.

In the *Arabidopsis* genome, there exist four GT43 genes, all of which have been shown to be involved in xylan biosynthsis (Brown et al., 2007; Pena et al., 2007; Keppler and Showalter, 2010; Lee et al., 2010; Wu et al., 2010). Genetic studies have revealed that the *Arabidopsis* GT43 members form two functionally non-redundant groups, IRX9/I9H and IRX14/I14H, that are required for the normal elongation of xylan backbone (Lee et al., 2010). The poplar (*Populus trichocarpa*) genome contains seven GT43 genes (Tuskan et al., 2006), namely *PtrGT43A-G*, of which only *GT43B* was previously shown to be implicated in xylan biosynthesis (Zhou et al., 2007). In this report, we show that three additional poplar GT43 members, *PtrGT43C/D/E*, are specifically expressed in developing secondary xylem and their encoded proteins are targeted into Golgi where xylan is synthesized. We demonstrate by complementation analysis that PtrGT43A/B/E are functional ortholgs of the *Arabidopsis* IRX9, whereas PtrGT43C/D are functional ortholgs of the *Arabidopsis* IRX14. Furthermore, we show that RNA interference (RNAi) downregulation of *GT43B* expression in poplar leads to a defect in xylan biosynthesis and a reduction in wood recalcitrance to cellulase digestion. We also reveal that RNAi downregulation of the expression of *GT8D* in poplar causes a reduction in xylan content and a decrease in the abundance of the xylan reducing end sequence. Our studies provide direct evidence showing that the poplar GT43 members form two functionally distinct groups involved in the elongation of xylan backbone and that the poplar GT8D participates in the biosynthesis of the xylan reducing end sequence during wood formation.

RESULTS

Poplar GT43 genes are expressed in developing secondary xylem

There exist seven GT43 genes in the genome of *Populus trichocarpa* (Tuskan et al., 2006). Besides the wood-associated *PtrGT43A/B*, which are close homologs of *IRX9* (Aspeborg

et al., 2005), the other five GT43 genes, namely *PtrGT43C/D/E/F/G*, show less sequence similarity to *IRX9*. Phylogenetic analysis revealed that PtrGT43C/D are closely related to IRX14 and I14H (also named IRX14L), whereas PtrGT43E/F/G are more closely grouped together with I9H (also named IRX9L) (Fig. 5.1A). Previous transcriptome analysis showed that *PtrGT43A-E* but not *PtrGT43F/G* are highly expressed during wood formation (http://www.bar.utoronto.ca/efppop/cgi-bin/efpWeb.cgi; Wilkins et al., 2009), indicating that they might be involved in the biosynthesis of wood components. Therefore, we decided to perform functional analysis to elucidate the functions of these wood-associated GT43 genes.

We first employed in situ mRNA hybridization approach to examine the cell-type level expression pattern of GT43 genes in the developing wood of *Populus trichocarpa*. It was found that strong hybridization signals for *PtrGT43A/C/E* were detected not only in developing vessels and fibers in secondary xylem but also in ray parenchyma cells (Fig. 5.1B to D). Hybridization signals were also evident in phloem fibers. Since *PtrGT43A/B* are duplicated genes with high sequence identity (87%), the probe for *PtrGT43A* was able to recognize both *PtrGT43A* and *PtrGT43B* transcripts. Similarly, *PtrGT43C/D* are duplicated genes with high sequence identity (86%), the probe for *PtrGT43C* recognized both *PtrGT43C* and *PtrGT43D* transcripts. The control sections hybridized with the sense probes did not show any positive signals in developing xylem (Fig. 5.1F). These results demonstrate that these poplar GT43 genes are expressed in vessels, fibers and ray parenchyma cells in developing secondary xylem, an expression pattern similar to genes known to be involved in xylan biosynthesis in poplar (Zhou et al., 2006 and 2007).

To further substantiate their involvement in the biosynthesis of wood components, we determined the subcellular locations of these poplar GT43 proteins. Poplar GT43B was

previously shown to be targeted to the Golgi (Zhou et al., 2007). Sequence analysis using the TMHMM2.0 program for the prediction of transmembrane helices in proteins (http://www.cbs.dtu.dk/service/TMHMM-2.0/) predicted that these poplar GT43 proteins are typical type II membrane proteins containing one or two transmembrane helices (Fig. 5.2A to D). Subcellular localization studies using fluorescence protein tagging in carrot protoplasts demonstrated that the GT43 proteins were co-localized with FRA8 (Fig.5.2G to V), a family GT47 glycosyltransferase known to be located in the Golgi (Zhong et al., 2005). The control protoplasts expressing YFP alone showed a uniform distribution of fluorescent signals throughout the cytoplasm (Fig. 5.2E and F). These results indicate that these poplar GT43 proteins are located in the Golgi where non-cellulosic polysaccharides, such as xylan, are synthesized.

Expression of PtrGT43A/B/E but Not PtrGT43C/D rescues the *irx9* mutant phenotypes

The results from gene expression and protein subcellular localization analyses suggest that similar to poplar GT43B, other poplar GT43 members are also likely involved in the biosynthesis of xylan during wood formation. To test this hypothesis, we examined the ability for poplar GT43 genes to complement the xylan defects conferred by the *Arabidopsis irx9* mutant. The *irx9* inflorescence stems exhibited a strong reduction in their mechanical strength due to a defect in secondary wall thickening in xylem and interfascicular fibers (Brown et al., 2005; Pena et al., 2007). Complementation analysis revealed that overexpression of PtrGT43A/B/E in *irx9* effectively restored the stem mechanical strength to the wild-type level, whereas overexpression of PtrGT43C/D did not (Fig. 5.3A). Examination of xylem and interfascicular fibers in stems further showed that overexpression of PtrGT43A/B/E but not PtrGT43C/D complemented the

collapsed vessel and reduced secondary wall thickening phenotypes caused by the *irx9* mutation (Fig. 5.3B to I and 5.4A to H).

To find out whether the restored secondary wall phenotype was due to complementation of the xylan defects in *irx9*, we analyzed the xylan content and structure in the PtrGT43-complemented *irx9* plants. The *irx9* mutant is deficient in xylose content caused by the reduced chain length of xylan backbone (Pena et al., 2007). Cell wall composition analysis demonstrated that overexpression of PtrGT43A/B/E but not PtrGT43C/D significantly restored the xylose content close to the wild-type level (Table 5.1). Further analysis of xylan structure showed that the loss of the glucuronic acid (GlcA) side chains conferred by *irx9* was restored by overexpression of PtrGT43A/B/E but not PtrGT43C/D (Fig. 5.5A to H).

We next examined the xylan chain length in *irx9* with the overexpression of GT43 members. The *irx9* mutation leads to a reduction in xylan chain length from an average of 93 in the wild type to 30, thereby resulting in a relative increase in the abundance of the reducing end sequence as revealed by nuclear magnetic resonance spectroscopy (NMR) (Pena et al., 2007; Figure 5.6). Analysis of the xylan structure using NMR showed a significant reduction in the relative abundance of the reducing end sequence due to a restoration of the xylan chain length in *irx9* with the overexpression of PtrGT43A/B/E but not PtrGT43C/D (Fig. 5.6; Table 5.2). Consistent with the restored chain length, overexpression of PtrGT43A/B/E partially complemented the defective xylosyltransferase activity conferred by the *irx9* mutation (Fig. 5.7A). Taken together, these chemical and structural analyses indicate that PtrGT43A/B/E are functional orthologs of IRX9 and they are involved in the biosynthesis of xylan backbone.

Expression of PtrGT43C/D but not PtrGT43A/B/E rescues the *irx14* mutant phenotypes

PtrGT43C/D are more closely related to the *Arabidopsis* IRX14 instead of IRX9 based on the phylogenetic analysis (Fig. 5.1A), which may explain why PtrGT43C/D failed to rescue the *irx9* mutant phenotypes. To find out whether PtrGT43C/D are functional orthologs of IRX14, we overexpressed them in the *irx14* mutant. Comprehensive histological, chemical and biochemical analyses of the transgenic plants demonstrated that PtrGT43C/D but not PtrGT43A/B/E complemented the *irx14* mutant phenotypes, including the restoration of vessel morphology (Fig. 5.3J to 5.3Q), secondary wall thickness (Fig. 5.4I to 5.4P), stem mechanical strength (Fig. 5.3A), xylan content (Table 5.1), GlcA side chains (Fig. 5.5I to 5.5P), xylan chain length (Fig. 5.6; Table 5.2), and xylosyltransferase activity (Fig. 5.7B). It was interesting to note that although overexpression of PtrGT43E did not rescue the xylan deficient phenotypes conferred by the *irx14* mutation, it partially restored the xylosyltransferase activity (Fig. 5.7B). Together with the results from the *irx9* complementation test, these data indicate that the poplar GT43 members are involved in xylan biosynthesis and they form two functionally distinct groups, i.e., PtrGT43A/B/E as IRX9 functional orthologs, and PtrGT43C/D as IRX14 functional orthologs.

Downregulation of the expression of Poplar *GT43B* and *GT8D* results in defects in xylan biosynthesis in poplar

We further investigated the effects of downregulation of the expression of *PoGT43B* and *PoGT8D* on xylan biosynthesis in the hybrid poplar *Populus alba* x *tremula*. PoGT43B was previously shown to be a functional ortholog of *Arabidopsis* IRX9 by complementation study and PoGT8D is an ortholog of *Arabidopsis* IRX8 that is known to be involved in the biosynthesis of the xylan reducing end sequence, but their functional roles in wood formation in poplar have not been studied (Zhou et al., 2007). We generated and examined over 40 transgenic poplar RNAi lines for downregulation of expression of *PoGT43B* or *PoGT8D*. Quantitative PCR

analysis revealed that the transgenic poplar plants expressing *PoGT43B* RNAi transcripts exhibited a significant reduction in the expression level of *PoGT43A/B* and that those expressing *PoGT8D* RNAi transcripts had a severe reduction in the expression level of *PoGT8D* and its duplicated gene, *PoGT8D-2* (Fig. 5.8A). Examination of the wood of transgenic poplar plants showed that RNAi downregulation of the expression of *PoGT43B* and *PoGT8D* caused defects in wood cell structure and morphology, i.e., a deformation of vessel shapes (Fig. 5.8B to 5.8F) and a reduction in the wall thickness of fibers (Fig. 5.9A to 5.9E). These results indicate that PoGT43B and PoGT8D are required for the normal development of secondary walls and the mechanical strength of vessels.

To find out whether the observed secondary wall defects in *PoGT43B* and *PoGT8D* RNAi lines were correlated with alterations in xylan content and structure, we isolated wood cell walls from the RNAi lines. Cell wall composition analysis demonstrated that the xylose content was significantly reduced in both *PoGT43B*- and *PoGT8D*-RNA lines compared with the control (Table 5.3), indicating that RNAi downregulation of the expression of *PoGT43B* and *PoGT8D* causes a defect in xylan biosynthesis. This conclusion was further substantiated by the immunolocalization of xylan with the xylan monoclonal antibody LM10 showing that the xylan signals were reduced in the walls of wood cells but not phloem fiber cells in the *PoGT8D* RNAi lines (Fig. 5.10C). No drastic reduction in xylan signals was observed in the *PoGT43B* RNAi lines (Fig. 5.10B), which is consistent with the observation in the *Arabidopsis irx9* mutant (Pena et al., 2007). It was noticed that the amount of some other monosaccharides, noticeably arabinose, was also altered in both *PoGT43B* and *PoGT8D* RNAi lines (Table 5.3), which could be a result of indirect effects on primary wall biosynthesis in ray parenchyma cells of wood.

In addition to the reduction in xylan amount, RNAi downregulation of the expression of *PoGT43B* and *PoGT8D* also caused a change in xylan chain length or the abundance of its reducing end sequence (Fig. 5.11). NMR spectroscopic analysis demonstrated that the resonance signals for the xylan reducing end sequence in the *PoGT43B* RNAi lines were elevated compared to those in the control (Fig. 5.11; Table 5.4). This phenomenon is similar to that observed in the *Arabidopsis irx9* mutant (Pena et al., 2007), which is caused by the shortening of chain length of the xylan backbone, thus leading to a relative elevation in the signals for the reducing end sequence. In contrast, the resonance signals for the xylan reducing end sequence in the *PoGT8*D RNAi lines were decreased compared to those in the control (Fig. 5.11; Table 5.4), an observation similar to that in the *Arabidopsis irx8* mutant due to a defect in the biosynthesis of the xylan reducing end sequence.

To find out whether defects in xylan biosynthesis affected the synthesis of other wall components, we analyzed lignin composition in the wood of the wild type and transgenes. It was found that the amount of extractable guaiacyl lignin in the *PoGT43B* RNAi lines was significantly reduced, whereas that in the *PoGT8*D RNAi lines was slightly affected compared with the control (Table 5.5). A similar but milder reduction in the amount of syringyl lignin was also detected. These results indicate that alterations in xylan biosynthesis negatively impact the deposition of lignin polymers in transgenic wood.

Increased cellulose digestibility by cellulase in the *PoGT43B* RNAi lines

Lignin and xylan were considered to be critical factors contributing to the recalcitrance of biomass for the conversion of cellulose to fermental sugars (Himmel et al., 2007). To find out whether RNAi downregulation of the expression of *PoGT43B* and *PoGT8D* had any effects on the recalcitrance of wood, we determined the digestibility of wood cell walls by cellulase. To do

so, wood cell walls were incubated with cellulase and the released glucose was quantitatively determined. The results showed that more glucose was released from wood cell walls of *PtrGT43B* RNAi lines but no change from those of *PtrGT8D* RNAi lines compared to those of the control (Fig. 5.12), demonstrating that the alterations in xylan content and structure in *PtrGT43B* RNAi lines lead to an increased digestibility of wood cell walls by cellulase.

DISCUSSION

Glycosyltransferase families are classified based on their amino acid sequence similarity rather than on their uses of common acceptors and/or donors (Campbell et al., 1997). Therefore, members in the same GT family may perform different biochemical activities. One such example is family GT47 comprising of 39 members (Zhong and Ye, 2003), several of which have been demonstrated to be involved in the biosynthesis of different cell wall polysaccharides, such as xylan (Zhong et al., 2005; Brown et al., 2005, 2007 and 2009; Pena et al., 2007; Wu et al., 2009), xyloglucan (Madson et al., 2003), and pectin (Harholt et al., 2006). Furthermore, FRA8 and IRX10, two phylogenetically closely-related members of GT47 (Zhong and Ye, 2003), have distinct roles in xylan biosynthesis; FRA8 being involved in the biosynthesis of the xylan reducing end sequence (Pena et al., 2007) and IRX10 being required for the normal biosynthesis of xylan backbone (Brown et al., 2009). Thus, genetic and biochemical studies are necessary to assign the biochemical functions of different glycosyltransferases in a particular GT family. In this study, we performed functional characterization of five poplar wood-associated family GT43 members and revealed that they form two functionally distinct groups involved in the biosynthesis of xylan backbone. Our study enriches the understanding of family GT43 glycosyltransferases and their roles in xylan biosynthesis during wood formation.

Our findings that the five poplar wood-associated GT43 members are able to complement the xylan defects conferred by the *irx9* or *irx14* mutation provide genetic evidence that these five poplar GT43 members are involved in the xylan backbone biosynthesis during wood formation. Furthermore, the complementation study has demonstrated that these poplar GT43 members form two functionally non-redundant groups, PtrGT43A/B/E as functional orthologs of IRX9 and PtrGT43C/D as functional orhtologs of IRX14. The remaining two members, PtrGT43F/G, which have little expression in developing wood, are phylogenetically grouped together with *Arabidopsis* I9H (Fig. 5.1A) and likely have the same biochemical functions as IRX9/I9H. It has previously been proposed that IRX9 and IRX14 are two xylosyltransferases that function cooperatively in the elongation of β-(1,4)-xylan chain and such a cooperative mechanism, which is similar to that proposed for cellulose biosynthesis (Carpita and Vergara, 1998), may be essential to overcome the steric problem for the transfer of each xylosyl residue because one xylosyl residue is flipped nearly 180^{o} with respective to its neighboring residue (Lee et al., 2010). The finding that PtrGT43A/B/E and PtrGT43C/D are functional orthologs of IRX9 and IRX14, respectively, indicates that the biochemical mechanism for xylan biosynthesis is well conserved between herbaceous *Arabidopsis* and woody trees, both of which employing two functionally non-redundant groups of GT43 members for the elongation of the xylan backbone.

It is interesting to note that although overexpression of PtrGT43C/D and PtrGT43E in *irx9* and *irx14*, respectively, did not complement the defects in xylan structure, their overexpression caused a slight elevation in xylosyltransferase activity (Fig. 5.7). Assuming that GT43 members are xylosyltransferases, one possible explanation for this phenomenon is that their overexpression leads to an increase in the addition of a single xylosyl residue onto the exogenous acceptor, thereby an elevated xylosyltransferase activity in the *in vitro* assay.

However, this elevated xylosyltransferase activity could not overcome the steric problem for the successive transfer of xylosyl residues with different orientation next to each other, thus unable to result in normal elongation of the xylan backbone. So far, it is still unknown whether GT43 members themselves possess xylosyltransferase activity or are accessory enzymes required for xylosyltransferase activity. Although an early attempt to detect xylosyltransferase activity using recombinant IRX9 protein in yeast cells was unsuccessful (Pena et al., 2007), available evidence from genetic and biochemical analyses in both *Arabidopsis* and poplar favor the hypothesis that GT43 members are xylosyltransferases responsible for the elongation of xylan backbone. The findings that two functionally non-redundant groups of GT43 members are involved in the elongation of xylan backbone in both *Arabidopsis* and poplar indicate that at least these two groups of GT43 members are required for future attempts of uncovering the identity of long-sought xylan synthase.

In addition to the finding that poplar GT43 members are involved in the elongation of xylan backbone, our study demonstrates that another poplar wood-associated GT, PoGT8D, is required for the biosynthesis of the xylan reducing end sequence. RNAi downregulation of *PoGT8D* expression was shown to cause a significant reduction in the abundance of the xylan reducing end sequence, an effect opposite to that caused by *PoGT43B* RNAi downregulation in which the abundance of the xylan reducing end sequence is elevated (Fig. 5.11; Table 5.4). This finding indicates that PoGT8D is a functional ortholog of *Arabidopsis IRX8* involved in the bosynthesis of the xylan reducing sequence (Pena et al., 2007). Together with the previous studies showing that two other members of poplar wood-associated GTs, GT47C (Lee et al., 2009a) and GT8E/8F (Lee et al., 2009c), are functional orthologs of *Arabidopsis* FRA8 and PARVUS, respectively, that are required for the biosynthesis of xylan reducing end sequence,

these results indicate that the biochemical mechanisms underlying the biosynthesis of both xylan backbone and reducing end sequence are evolutionarily conserved between *Arabidopsis* and tree species.

Wood is a renewable, abundant forest product important for a myriad of commercial applications and a potential feedstock for biofuel production (Carroll and Somerville, 2009). Our findings that two functionally non-redundant groups of poplar GT43 members are involved in the biosynthesis of xylan backbone and that a poplar family GT8 member is implicated in the biosynthesis of the xylan reducing end sequence not only expands our understanding of the biochemical process of wood formation and but also provides additional tools for the genetic manipulation of wood components tailored to our needs. For example, we have demonstrated that alterations of xylan content and chain length in the *PoGT43B* RNAi lines lead to an apparent increase in the digestibility of wood by cellulase, which may have important implications in designing strategies for genetic modification of wood components for biofuel production. Further investigation of the biochemical activities of these xylan biosynthesis-related glycosyltransferases together with functional characterization of other wood-associated glycosyltransferases (Aspeborg et al., 2005) will undoubtedly help dissect the complex process of wood formation.

MATERIALS AND METHODS

Plant growth conditions

Arabidopsis thaliana, *Populus trichocarpa* (a gift from Dr. G.A. Tuskan) and *Populus alba* x *tremula* (a gift from Dr. S. Strauss) plants were grown in a greenhouse under 14-h-light/10-h-dark cycles. Common garden potting soil was used for growing plants with biweekly application of plant fertilizers.

In situ hybridization

Stems of *Populus trichocarpa* were fixed in 2.5% formaldehyde and 0.5% glutaraldehyde, embedded in paraffin, and sectioned for *in situ* mRNA localization according to Zhou et al. (2007). Digoxigenin-labeled antisense and sense RNA probes of *PtrGT43* cDNAs were generated using the DIG RNA labeling mix (Roche). Stem sections were hybridized with the antisense and sense probes and the hybridization signals were detected by incubating with alkaline phosphatase-conjugated antibodies against digoxygenin and subsequent color development with alkaline phosphatase substrates.

Subcellular localization

Yellow fluorescent protein (YFP)-tagged PtrGT43 fusion proteins and cyan fluorescent protein (CFP)-tagged Golgi marker (FRA8; Zhong et al., 2005) were co-transfected into carrot (*D. carota*) protoplasts to determine the subcellular localization of PtrGT43 proteins according to Liu et al. (1994). The full-length cDNAs of *PtrGT43* were fused in frame with the *YFP* cDNA and ligated between the CaMV 35S promoter and the nopaline synthase terminator in pBI221 (Clontech). Fluorescence signals in transfected protoplasts were visualized using a Leica TCs SP2 spectral confocal microscope (Leica Microsystems). At least 5 fluorescence-positive protoplasts were examined and the same subcellular localization pattern was observed for each construct. Images were saved and processed with Adobe Photoshop Version 7.0 (Adobe Systems).

Complementation analysis

The full-length *PtrGT43* cDNAs driven by the cauliflower mosaic virus (CaMV) 35S promoter were cloned into the pGPTV binary vector (Becker et al., 1992). The PtrGT43 overexpression constructs were introduced into the *Arabidopsis irx9* or *irx14* mutant by the

agrobacterium-mediated transformation (Bechtold and Bouchez, 1994). Transgenic plants were selected on hygromycin, and the first generation of transgenic plants was used for breaking strength and anatomical analyses. Basal parts of the main inflorescence of 10-week-old plants were measured for the breaking force using a digital force/length tester (Zhong et al., 1997). The breaking force was calculated as the force needed to break apart a stem segment. For each construct, at least 64 transgenic plants were generated and examined.

Histology

Stems were fixed in 2% formaldehyde and embedded in Low Viscosity (Spurr's) resin (Electron Microscopy Sciences) as described (Burk et al., 2006). For light microscopy, 1-µm-thick sections were cut with a microtome and stained with toluidine blue. For transmission electron microscopy, 85-nm-thick sections were cut, post-stained with uranyl acetate and lead citrate, and observed using a Zeiss EM 902A transmission electron microscope (Carl Zeiss). For each construct, stems from at least 8 transgenic plants were examined and representative data were shown.

Cellwall sugar composition analysis

Cell walls were isolated from stems of *Arabidopsis* and poplar plants according to Zhong et al. (2005). Neutral sugar composition of cell walls (as alditol acetates) was analyzed following the procedure described by Hoebler et al. (1989). The alditol acetates of the hydrolyzed cell wall sugars were determined on a PerkinElmer Clarus 500 gas-liquid chromatography equipped with a 30 m x 0.25 mm (i.d.) silica capillary column DB 225 (Alltech Assoc.). The minor fucose peak was not discerned due to its overlap with a noise peak.

Matrix-Assisted Laser-Desorption Ionization Time-of-Flight Mass Spectrometry (MALDI-TOF MS)

Xylan was solubilized from cell walls by incubation with 1 N KOH, and the solubilized xylan was digested with β-xylanase M6 (Megazyme) to release xylooligosaccharides as described (Zhong et al., 2005). The acidic xylooligosaccharides were analyzed using a MALDI-TOF mass spectrometer operated in the positive-ion mode with an accelerating voltage of 30 kV, an extractor voltage of 9 kV, and a source pressure of approximately 8 x 10^{-7} torr. The aqueous sample was mixed (1:1, v/v) with the MALDI matrix (0.2 M 2,5-dihydroxbenzoic acid and 0.06 M 1-hydroxyisoquinoline in 50% acetonitrile) and dried on the stainless steel target plate. Spectra are the average of 100 laser shots.

^{1}H-NMR Spectroscopy

NMR spectra of the acidic xylooligosaccharides from β-xylanase digestion were acquired at 20 ^{o}C on a Varian Inova 600 MHz spectrometer (599.7 MHz, ^{1}H) using a 5 mm cryogenic triple resonance probe (Varian). All NMR samples were prepared using 100% D_2O in 3 mm standard NMR tube. ^{1}H chemical shifts were referenced to DSS (2,2-dimethyl-2-silapentane-5-sulfonate sodium salt). For all experiments, 64 transients were collected using a spectral width of 6,000 Hz and an acquisition time of 5-seconds. The residual water resonance was suppressed by a 1-second presaturation pulse at a field strength of 40 Hz. 1D spectra were processed using MestReC (MestreC Research) with 0.2-Hz apodization followed by zero-filling to 128 k points. The ^{1}H NMR assignments were done by comparison with the NMR spectra data for *Arabidopsis* acidic xylooligosaccharides (Zhong et al., 2005; Peña et al., 2007).

Assay of xylosytransferase activity

Microsomes were isolated from the inflorescence stems of 7-week-old *Arabidopsis* plants and used for the xylosyltransferase activity assay (Kuroyama and Tsumuraya, 2001). For each assay, microsomes (100 μg) were incubated with the reaction mixture containing 50 mM

HEPES-KOH, pH 6.8, 5 mM $MnCl_2$, 1 mM dithiothritol, 0.5% Triton X-100, 0.1 mM cold UDP-Xyl (CarboSource Service), 0.2 μg/μl Xyl_6 (Megazyme) and UDP-[^{14}C]Xyl (0.1 μCi; American Radiolabeled Chemical). The reaction products were separated from UDP-[^{14}C]Xyl by paper chromatography according to Ishikawa et al. (2000) and counted for the amount of radioactivity with a PerkinElmer scintillation counter.

Generation of transgenic poplar plants

The *PoGT43B* and *PoGT8D* RNA interference (RNAi) constructs were generated by cloning their cDNAs into pBI121 in opposite orientations on both sides of the β-glucuronidase (GUS) spacer, which is located between the cauliflower mosaic virus (CaMV) 35S promoter and the nopaline synthase (NOS) terminator. The constructs were introduced into *Agrobacterium tumefacien* GV3101, which was further used to transform the hybrid poplar (*Populus tremula* X *Populus alba*) as described by Leple et al. (1992). The transgenic poplar seedlings were selected on Murashige and Skoog medium containing 100 μg/L kanamycin and 500 μg/L carbenicillin. After rooting, transgenic seedlings were transferred to soil and grown in the greenhouse. The wild-type control plants were transgenic poplar plants transformed with an empty vector.

Gene expression analysis

Total RNA from poplar stems was isolated with a Qiagen RNA isolation kit (Qiagen). First strand cDNA was synthesized from total RNA treated with DNase I and then used as a template for real-time quantitative PCR analysis with the QuantiTect SYBR Green PCR kit (Clontech). The PCR primers for *PoGT43A* are 5'-gttcgatcctttgggatcctgaga-3' and 5'-tcatagttttctcctgctagcatc-3', those for *PoGT43B* are 5'-ctcaatcctctgggatcctgagag-3' and 5'-catgtaaagaattgtaatctgctc-3', those for *PoGT8D* are 5'-tcgagcaaagccttggctagatatagc-3' and 5'-agatggcctaatatgacagcccttta-3', and those for *PoGT8D-2* are 5'-tcgagcaaagccttggctagatatagc-3'

and 5'-tcatgtcctaatatgacagcccgtaat-3'. The relative expression level was calculated by normalizing the PCR threshold cycle number of each gene with that of a poplar actin reference gene (Lee et al., 2009a). The data were the average of three replicates from three separate RNA extractions.

Immunodetection of xylan

Sections (1 μm thick) of poplar stems were subjected to immunodetection of xylan by incubating with the LM10 monoclonal xylan antibody (Plantprobes, Leeds, UK; McCartney et al., 2005) followed with fluorescein isothiocyanate-conjugated secondary antibodies (Sigma) according to Pena et al. (2007). The sections were observed for fluorescence signals using a Leica TCs SP2 spectral confocal microscope. Images from single optical sections were collected and processed with Adobe Photoshop.

Wood digestibility analysis

Poplar wood cell walls were digested with cellulase enzymes according to Chen and Dixon (2007). Briefly, the milled, ethanol-insoluble wood cell walls (equivalent to 100 mg of glucose) were incubated with cellulase (52 units; Celluclast 1.5L from Sigma) and Cellobiase (16 units; Sigma) in 0.1 M sodium acetate buffer (pH 4.8) at 37^{o}C for 72 h. Under the same conditions, the enzyme mixture was able to digest 90% of Whatmann No. 1 filter paper cellulose into glucose. The cellobiose released by cellulose was converted to glucose by the addition of cellobiase in the digestion solution. After centrifugation, the supernatant was used for quantitation of neutral sugars released from wood cellulose using gas chromatography as described above. The digestion of wood with cellulase and cellobiase resulted in little release of xylose. The enzyme mixture without the addition of wood cell walls was used as a blank. All samples were assayed independently twice.

Accession numbers

The GenBank accession numbers and gene models for poplar GT genes are as follows: PtrGT43A (JF518934; eugene3.00280138), PtrGT43B (JF518935; fgenesh1_kg.C_LG_XVI000045), PtrGT43C (JF518936; gw1.VII2855.1), PtrGT43D (JF518937; estExt_Genewise1_v1.C_LG_V4069), PtrGT43E (JF518938), PoGT43B (EF501825), and PoGT8D (EF501824). The *Arabidopsis* Genome Initiative locus identifiers for the *Arabidopsis* genes investigated in this study are IRX9 (At2g37090), I9H (At1g27600), IRX14 (At4g36890), and I14H (At5g67230).

ACKNOWLEDGMENTS

We thank two anonymous reviewers for their constructive comments and suggestions. This work was funded by the Division of Chemical Sciences, Geosciences, and Biosciences, Office of Basic Energy Sciences of the U.S. Department of Energy through Grant DE-FG02-03ER15415. This paper has been reviewed in accordance with the U.S. Environmental Protection Agency's peer and administrative review policies and approved for publication. Mention of trade names or commercial products does not constitute endorsement or recommendation for use. No conflict of interest declared.

REFERENCES

Andersson, S.-I., Samuelson, O., Ishihara, M., and Shimizu, K. (1983). Structure of the reducing end-groups in spruce xylan. Carbohydr. Res. 111, 283-288.

Andersson-Gunneras, S., Mellerowicz, E.J., Love, J., Segerman, B., Ohmiya, Y., Coutinho, P.M., Nilsson, P., Henrissat, B., Moritz, T., and Sundberg, B. (2006). Biosynthesis of cellulose-enriched tension wood in *Populus*: global analysis of transcripts and metabolites

identifies biochemical and developmental regulators in secondary wall biosynthesis. Plant J. 45, 144-165.

Aspeborg, H., Schrader, J., Coutinho, P.M., Stam, M., Kallas, A., Djerbi, S., Nilsson, P., Denman, S., Amini, B., Sterky, F., Master, E., Sandberg, G., Mellerowicz, E., Sundberg, B., Henrissat, B., and Teeri, T.T. (2005). Carbohydrate-active enzymes involved in the secondary cell wall biogenesis in hybrid aspen. Plant Physiol. 137, 983-997.

Bechtold, N., and Bouchez, D. (1994). In planta *Agrobacterium*-mediated transformation of adult *Arabidopsis thaliana* plants by vacuum infiltration. In Gene Transfer to Plants, Potrykus, I., Spangenberg, G., eds (Berlin:Springer-Verlag), pp. 19-23

Becker, D., Kemper, E., Schell, J., and Masterson, R. (1992). New plant binary vectors with selectable markers located proximal to the left T-DNA border. Plant Mol. Biol. 20, 1195-1197.

Bedon, F., Grima-Pettenati, J., and Mackay, J. (2007). Conifer R2R3-MYB transcription factors: sequence analyses and gene expression in wood-forming tissues of white spruce (*Picea glauca*). BMC Plant Biol. 7, 17.

Brown, D.M., Goubet, F., Wong, V. W., Goodacre, R., Stephens, E., Dupree, P., and Turner, S.R. (2007). Comparison of five xylan synthesis mutants reveals new insight into the mechanisms of xylan synthesis. Plant J. 52, 1154-1168.

Brown, D.M., Zeef, L.A.H., Ellis, J., Goodacre, R., and Turner, S.R. (2005). Identification of novel genes in *Arabidopsis* involved in secondary cell wall formation using expression profiling and reverse genetics. Plant Cell. 17, 2281-2295.

Brown, D.M., Zhang, Z., Stephens, E., Dupree, P., and Turner, S.R. (2009). Characterization of IRX10 and IRX10-like reveals an essential role in glucuronoxylan biosynthesis in *Arabidopsis*. Plant J. 57, 732-746.

Burk, D.H., Zhong, R., Morrison, W.H.III., and Ye, Z.-H. (2006). Disruption of cortical microtubules by overexpression of green fluorescent protein-tagged -tubulin 6 causes a marked reduction in cell wall synthesis. J. Integr. Plant Biol. 48, 85-98.

Campbell, J.A., Davies, G.J., Bulone, V., and Henrissat, B. (1997). A classification of nucleotide-diphospho-sugar glycosyltransferases based on amino acid sequence similarities. Biochem. J. 326, 929-939.

Carpita, N., and Vergara, C. (1998). A recipe for cellulose. Science. 279, 672-673.

Carroll, A., and Somerville, C. (2009). Cellulosic biofuels. Annu. Rev. Plant Biol. 60, 165-182.

Chen, F., and Dixon, R.A. (2007). Lignin modification improves fermentable sugar yields for biofuel production. Nat. Biotechnol. 25, 759-761.

Grant, E.H., Fujino, T., Beers, E.P., and Brunner, A.M. (2010). Characterization of NAC domain transcription factors implicated in control of vascular cell differentiation in Arabidopsis and Populus. Planta. 232, 337-352.

Harholt, J., Jensen, J.K., Sorensen, S.O., Orfila, C., Pauly, M., and Scheller, H.V. (2006). ARABINAN DEFICIENT 1 is a putative arabinosyltransferase involved in biosynthesis of pectin arabinan in Arabidopsis. Plant Physiol. 140, 49-58.

Himmel, M.E., Ding, S.Y., Johnson, D.K., Adney, W.S., Nimlos, M.R., Brady, J.W., and Foust, T.D. (2007). Biomass recalcitrance: engineering plants and enzymes for biofuels production. Science 315, 804-807.

Hoebler, C., Barry, J.L., David, A., and Delort-Laval, J. (1989). Rapid acid-hydrolysis of plant cell wall polysaccharides and simplified quantitative determination of their neutral monosaccharides by gas-liquid chromatography. J. Ag. Food Chem. 37, 360-367.

Ishikawa, M., Kuroyama, H., Takeuchi, Y., and Tsumuraya, Y. (2000). Characterization of pectin methyltransferase from soybean hypocotyls. Planta. 210, 782-791.

Jacobs, A., and Dahlman, O. (2001). Characterization of the molar masses of hemicelluloses from wood and pulps employing size exclusion chromatography and matrix-assisted laser desorption ionization time-of-flight mass spectrometry. Biomacromolecules. 2, 894-905.

Johansson, M.H., and Samuelson, O. (1977). Reducing end groups in birch xylan and their alkaline degradation. Wood Sci. Technol. 11, 251-263.

Joshi, C.P., Bhandari, S., Ranjan, P., Kalluri, U.C., Liang, X., Fujino, T., and Samuga, A. (2004). Genomics of cellulose biosynthesis in poplars. New Phytol. 164, 53-61.

Keppler, B.D., and Showalter, A.M. (2010). IRX14 and IRX14-LIKE, two glycosyl transferases involved in glucuronoxylan biosynthesis and drought tolerance in *Arabidopsis*. Mol. Plant. 3, 834-841.

Kuroyama, H., and Tsumuraya, Y. (2001). A xylosyltransferase that synthesizes -(1->4)-xylans in wheat (*Triticum aestivum* L.) seedlings. Planta. 213, 231-240.

Lee, C., O'Neill, M.A., Tsumuraya, Y., Darvill, A.G., and Ye, Z.-H. (2007a). The *irregular xylem9* mutant is deficient in xylan xylosyltransferase activity. Plant Cell Physiol. 48, 1624-1634.

Lee, C., Teng, Q., Huang, W., Zhong, R., and Ye, Z.-H. (2009a). Down-regulation of PoGT47C expression in poplar results in a reduced glucuronoxylan content and an increased wood digestibility by cellulase. Plant Cell Physiol. 50, 1075-1089.

Lee, C., Teng, Q., Huang, W., Zhong, R., and Ye, Z.-H. (2009b). The F8H glycosyltransferase is a functional paralog of FRA8 involved in glucuronoxylan biosynthesis in Arabidopsis. Plant Cell Physiol. 50, 812-827.

Lee, C., Teng, Q., Huang, W., Zhong, R., and Ye, Z.-H. (2009c). The poplar GT8E and GT8F glycosyltransferases are functional orthologs of Arabidopsis PARVUS involved in glucuronoxylan biosynthesis. Plant Cell Physiol. 50, 1982-1987.

Lee, C., Teng, Q., Huang, W., Zhong, R., and Ye, Z.-H. (2010). The Arabidopsis family GT43 glycosyltransferases form two functionally nonredundant groups essential for the elongation of glucuronoxylan backbone. Plant Physiol. 153, 526-541.

Lee, C., Zhong, R., Richardson, E.A., Himmelsbach, D.S., McPhail, B.T., and Ye, Z.-H. (2007b). The *PARVUS* gene is expressed in cells undergoing secondary wall thickening and is essential for glucuronoxylan biosynthesis. Plant Cell Physiol. 48, 1659-1672.

Leple, J.C., Brasileiro, A.C.M., Michel, M.F., Delmotte, F., and Jouanin, L. (1992). Transgenic poplars: expression of chimeric genes using four different constructs. Plant Cell Rep. 11, 137-141.

Liepman, A.H., Nairn, C.J., Willats, W.G., Sørensen, I., Roberts, A.W., and Keegstra, K. (2007). Functional genomic analysis supports conservation of function among cellulose synthase-like A gene family members and suggests diverse roles of mannans in plants. Plant Physiol. 143, 1881-1893.

Liu, Z. B., Ulmasov, T., Shi, X., Hagen, G., and Guilfoyle, T. J. (1994). Soybean GH3 promoter contains multiple auxin-inducible elements. Plant Cell. 6, 645-657.

Madson, M., Dunand, C., Li, X., Verma, R., Vanzin, G.F., Caplan, J., Shoue, D.A., Carpita, N.C., and Reiter, W.-D. (2003). The *MUR3* gene of Arabidopsis encodes a xyloglucan

galactosyltransferase that is evolutionarily related to animal exostosins. Plant Cell. 15, 1662-1670.

McCartney, L., Marcus, S.E., and Knox, J.P. (2005). Monoclonal antibodies to plant cell wall xylans and Arabinoxylans. J. Histochem. Cytochem. 53, 543-546.

Mellerowicz, E.J., and Sundberg, B. (2008). Wood cell walls: biosynthesis, developmental dynamics and their implications for wood properties. Curr. Opin. Plant Biol. 11, 293-300.

Page, R.D.M. (1996). TREEVIEW: An application to display phylogenetic trees on personal computers. Computer Appl. Biosci. 12, 357-358.

Pavy, N., Boyle, B., Nelson, C., Paule, C., Giguère, I., Caron, S., Parsons, L.S., Dallaire, N., Bedon, F., Bérubé, H., Cooke, J., and Mackay, J. (2008). Identification of conserved core xylem gene sets: conifer cDNA microarray development, transcript profiling and computational analyses. New Phytol. 180, 766-786.

Pena, M.J., Zhong, R., Zhou, G.-K., Richardson, E.A., O'Neill, M.A., Darvill, A.G., York, W.S., and Ye, Z.-H. (2007). *Arabidopsis irregular xylem8* and *irregular xylem9*: Implications for the complexity of glucuronoxylan biosynthesis. Plant Cell 19, 549-563.

Plomion, C., Leprovost, G., and Stokes, A. (2001). Wood formation in trees. Plant Physiol. 127, 1513-1523.

Prassinos, C., Ko, J.H., Yang, J., and Han, K.H. (2005). Transcriptome profiling of vertical stem segments provides insights into the genetic regulation of secondary growth in hybrid aspen trees. Plant Cell Physiol. 46, 1213-1225.

Shimizu, K., Ishihara, M., and Ishihara, T. (1976). Hemicellulases of brown rotting fungus, *Tyromyces palustris*. II. The oligosaccharides from the hydrolysate of a hardwood xylan by the intracellular xylanase. Mokuzai Gaikkashi. 22, 618-625.

Suzuki, S., Li, L., Sun, Y.-H., and Chiang, V.L. (2006). The cellulose synthase gene superfamily and biochemical functions of xylem-specific cellulose synthase-like genes in *Populus trichocarpa*. Plant Physiol. 142, 1233-1245.

Thompson, J.D., Higgins, D.G., and Gibson, T.J. (1994). CLUSTAL W: improving the sensitivity of progressive multiple sequence alignment through sequence weighting, position-specific gap penalties and weight matrix choice. Nuc. Acids Res. 22, 4673-4680.

Timell, T.E. (1967). Recent progress in the chemistry of wood hemicelluloses. Wood Sci. Technol. 1, 45-70

Tuskan, G.A., Difazio, S., Jansson, S. et al. (2006). The genome of black cottonwood, *Populus trichocarpa* (Torr. & Gray). Science. 313, 1596-1604.

Wilkins, O., Nahal, H., Foong, J., Provart, N.J., and Campbell, M.M. (2009). Expansion and diversification of the *Populus* R2R3-MYB family of transcription factors. Plant Physiol. 149, 981-993.

Wu, A.M., Hörnblad, E., Voxeur, A., Gerber, L., Rihouey, C., Lerouge, P., and Marchant, A. (2010). Analysis of the Arabidopsis IRX9/IRX9-L and IRX14/IRX14-L pairs of glycosyltransferase genes reveals critical contributions to biosynthesis of the hemicellulose glucuronoxylan. Plant Physiol. 153, 542-554.

Zhong, R., Lee, C., and Ye, Z.-H. (2010a). Functional characterization of poplar wood-associated NAC domain transcription factors. Plant Physiol. 152, 1044-1055.

Zhong, R., Lee C., and Ye, Z.-H. (2010b). Global analysis of direct targets of secondary wall NAC master switches in *Arabidopsis*. Mol. Plant 3, 1087-1103.

Zhong, R., Pena, M.J., Zhou, G.-K., Nairn, C.J., Wood-Jones, A., Richardson, E.A., Morrison, W.H., Darvill, A.G., York, W.S., and Ye, Z.-H. (2005). Arabidopsis *Fragile Fiber8*,

which encodes a putative glucuronyltransferase, is essential for normal secondary wall synthesis. Plant Cell. 17, 3390-3408.

Zhong, R., Taylor, J.J., and Ye, Z.-H. (1997). Disruption of interfascicular fiber differentiation in an *Arabidopsis* mutant. Plant Cell. 9, 2159-2170.

Zhong, R., and Ye, Z.-H. (2003). Unraveling the functions of glycosyltransferase family 47 in plants. Trends Plant Sci. 8, 565-568.

Zhou, G.K., Zhong, R., Richardson, E.A., Himmelsbach, D.S., McPhail, B.T., and Ye, Z.-H. (2007). Molecular characterization of PoGT8D and PoGT43B, two secondary wall-associated glycosyltransferases in poplar. Plant Cell Physiol. 48, 689-699.

Zhou, G.K., Zhong, R., Richardson, E.A., Morrison, W.H. 3rd., Nairn, C.J., Wood-Jones, A., and Ye, Z.-H. (2006). The poplar glycosyltransferase GT47C is functionally conserved with *Arabidopsis fragile fiber8.* Plant Cell Physiol. 47, 1229-1240.

Table 5.1. Cell wall composition analysis of stems of wild type, *irx9*, *irx14*, and the *irx9* and *irx14* plants overexpressing Poplar GT43 members

Sample	**Xylose**	**Glucose**	**Mannose**	**Galactose**	**Arabinose**	**Rhamnose**
Wild type	111.9 ± 14.0	415.7 ± 0.5	17.7 ± 2.0	13.9 ± 0.4	11.7 ± 1.0	10.9 ± 0.6
irx9	57.9 ± 3.3	333.3 ± 4.9	37.8 ± 1.4	31.6 ± 8.1	23.7 ± 5.1	15.1 ± 1.8
irx9 + PtrGT43A	88.9 ± 0.6	396.6 ± 20.2	18.4 ± 2.8	19.3 ± 1.9	15.9 ± 1.0	11.2 ± 0.8
irx9 + PtrGT43B	94.1 ± 4.5	386.3 ± 1.5	19.7 ± 0.9	18.7 ± 0.1	18.2 ± 0.6	13.0 ± 0.1
irx9 + PtrGT43C	53.8 ± 3.1	328.9 ± 8.9	28.1 ± 3.9	28.3 ± 2.0	26.8 ± 2.9	11.9 ± 0.8
irx9 + PtrGT43D	47.9 ± 3.4	316.1 ± 9.5	29.1 ± 0.1	27.5 ± 0.3	24.4 ± 0.5	12.0 ± 0.3
irx9 + PtrGT43E	81.1 ± 5.2	351.9 ± 13.0	19.2 ± 1.8	18.5 ± 1.6	16.1 ± 0.8	10.6 ± 0.7
irx9 + IRX9	120.1 ± 0.2	381.8 ± 1.7	15.4 ± 0.5	15.8 ± 0.2	14.8 ± 0.5	11.0 ± 0.9
irx14	55.4 ± 2.1	345.9 ± 2.6	24.8 ± 2.0	27.5 ± 7.0	14.8 ± 1.1	14.7 ± 0.6
irx14 + PtrGT43A	76.6 ± 2.4	415.4 ± 14.8	34.3 ± 0.7	23.8 ± 0.2	17.9 ± 0.1	14.9 ± 0.4
irx14 + PtrGT43B	70.5 ± 4.6	415.3 ± 11.4	33.2 ± 0.6	22.8 ± 0.5	18.4 ± 0.7	15.8 ± 0.2
irx14 + PtrGT43C	99.9 ± 0.2	375.1 ± 19.7	17.2 ± 1.0	14.6 ± 0.5	13.0 ± 0.5	11.1 ± 0.1
irx14 + PtrGT43D	96.7 ± 3.0	374.5 ± 9.8	17.4 ± 1.9	15.3 ± 1.7	13.4 ± 0.7	10.6 ± 0.4
irx14 + PtrGT43E	64.1 ± 0.1	399.0 ± 15.0	31.6 ± 2.3	21.5 ± 1.2	16.7 ± 0.5	14.8 ± 0.3
irx14 + IRX14	99.4 ± 5.2	384.1 ± 22.4	16.8 ± 1.5	16.4 ± 0.8	12.9 ± 0.7	10.1 ± 0.7

The wall residues for cell wall composition analysis were prepared from mature inflorescence stems. The data are means (mg/g dry cell wall) ± SE of duplicate assays.

Table 5.2. Relative abundance of the xylan reducing end sequence and the DP of xylan in wild type, *irx9*, *irx14*, and the *irx9* and *irx14* plants overexpressing Poplar GT43 members

Sample	Frequency of occurrence of GlcA and MeGlcA side chains[a]	Relative abundance of the reducing end sequence[b]	Average DP
Wild type	20.6%	100%	93
irx9	20.3%	335%	28
irx9 + PtrGT43A	17.4%	114%	82
irx9 + PtrGT43B	19.1%	130%	72
irx9 + PtrGT43C	16.6%	299%	31
irx9 + PtrGT43D	19.9%	287%	32
irx9 + PtrGT43E	18.3%	116%	80
irx9 + IRX9	20.3%	110%	85
irx14	22.1%	265%	35
irx14 + PtrGT43A	20.5%	229%	41
irx14 + PtrGT43B	20.6%	209%	44
irx14 + PtrGT43C	17.6%	96%	97
irx14 + PtrGT43D	19.3%	121%	77
irx14 + PtrGT43E	20.7%	222%	42
irx14 + IRX14	21.5%	137%	69

[a]The frequency of occurrence of glucuronic acid (GlcA) and methylated glucuronic acid (MeGlcA) side chains was calculated from the ratios of the NMR resonance of the branched β-Xyl to that of total β-Xyl. [b]The relative abundance of the reducing end sequence was determined from the ratios of the NMR resonance of the reducing end sequence to that of the branched β-Xyl. The abundance of the reducing end sequence in the wild type was taken as 100%. [c]The average degree of polymerization (DP) was calculated according to Pena et al. (2007).

Table 5.3. Cell wall composition analysis of the wood of control Poplar, *PoGT43B* and *PoGT8D* RNAi lines

Sample	Xylose	Glucose	Mannose	Galactose	Arabinose	Rhamnose
Control	127.0 ± 2.6	368.8 ± 6.7	17.5 ± 2.0	13.3 ± 0.2	17.1 ± 0.2	9.9 ± 0.4
PoGT43B-RNAi-3	88.9 ± 5.2	357.0 ± 5.4	18.0 ± 0.6	18.1 ± 0.6	20.2 ± 0.7	9.3 ± 0.1
PoGT43B-RNAi-5	77.0 ± 1.3	357.4 ± 0.4	21.3 ± 0.3	15.1 ± 0.2	25.1 ± 0.1	10.8 ± 0.1
PoGT43B-RNAi-11	73.3 ± 4.7	362.5 ± 6.5	21.6 ± 1.7	14.9 ± 0.4	22.2 ± 1.0	10.9 ± 0.3
PoGT43B-RNAi-32	92.3 ± 1.0	338.1 ± 4.7	16.4 ± 0.9	17.1 ± 0.4	20.8 ± 0.4	11.1 ± 0.5
PoGT8D-RNAi-1	69.4 ± 2.1	370.2 ± 5.3	19.1 ± 0.7	22.4 ± 0.5	11.3 ± 0.5	8.1 ± 0.3
PoGT8D-RNAi-5	92.7 ± 1.4	369.2 ± 8.0	14.0 ± 0.5	15.3 ± 0.5	8.2 ± 0.4	8.4 ± 0.2
PoGT8D-RNAi-15	99.8 ± 0.8	387.6 ± 2.7	17.7 ± 0.9	15.7 ± 0.9	11.5 ± 1.1	7.6 ± 0.7
PoGT8D-RNAi-26	79.5 ± 1.1	336.4 ± 26.4	14.5 ± 0.9	11.9 ± 1.2	10.4 ± 0.3	7.4 ± 0.2

The wall residues for cell wall composition analysis were prepared from stems. The data are means (mg/g dry cell wall) ± SE of duplicate assays.

Table 5.4. Relative abundance of the xylan reducing end sequence and the frequency of occurrence of side chains on the xylan backbone

Sample	Frequency of occurrence of MeGlcA side chains[a]	Relative abundance of the xylan reducing end sequence[b]
Control	20.5%	100%
PoGT8D-RNAi-1	23.9%	62%
PoGT8D-RNAi-26	24.3%	45%
PoGT43B-RNAi-3	22.4%	110%

[a]The frequency of occurrence of the MeGlcA side chains was calculated from the ratios of the NMR resonance of the branched β-Xyl to that of total β-Xyl.

[b]The relative abundance of the reducing end tetrasaccharide sequence was determined by the ratios of the NMR resonance of the reducing end sequence to that of the branched β-Xyl, and the abundance of the reducing end sequence in the control was taken as 100%.

Table 5.5. Lignin composition analysis of the wood of control Poplar, *PoGT43B* and *PoGT8D* RNAi lines

Sample	Guaiacyl lignin	Syringyl lignin
Control	6.7 ± 0.1	5.5 ± 0.4
PoGT43B-RNAi-3	3.4 ± 0.4	3.3 ± 0.3
PoGT43B-RNAi-5	1.7 ± 0.2	2.2 ± 0.2
PoGT43B-RNAi-11	1.7 ± 0.1	4.0 ± 0.5
PoGT43B-RNAi-32	6.1 ± 1.1	4.4 ± 0.5
PoGT8D-RNAi-1	4.5 ± 0.5	3.2 ± 0.3
PoGT8D-RNAi-5	3.8 ± 0.6	3.4 ± 0.4
PoGT8D-RNAi-15	5.8 ± 0.4	4.9 ± 0.7
PoGT8D-RNAi-26	6.8 ± 0.9	4.6 ± 0.7

Guaiacyl lignin is the sum of vanillin, acetovanillin and vanillic aicd. Syringyl lignin is the sum of syringaldehyde, acetosyringaldehyde and syringic acid. The data are means (mg/g dry cell wall) ± SE of two independent assays.

Figure 5.1. Phylogenetic and expression analysis of family GT43 members in *Populus trichocarpa*. **(A)** Phylogenetic relationship of PtrGT43 members together with the *Arabidopsis* GT43 members (IRX9, I9H, IRX14 and I14H). The amino acid sequences were aligned using the ClustlW program (Thompson et al., 1994) and the phylogenetic tree was shown using the TREEVIEW program (Page, 1996). The 0.1 scale indicates 10% change. **(B)** to **(E)** *In situ* mRNA localization of *PtrGT43* genes in the developing wood of poplar stems. Cross sections of stems were hybridized with digoxigenin-labeled antisense (B-D) or sense (E) RNA probes, and the hybridization signals were detected with alkaline phosphatase-conjugated antibodies and are shown as purple color. Note the strong hybridization signals for *PtrGT43A* (B), *PtrGT43C* (C), and *PtrGT43E* (D) in vessels, xylary fibers, and ray parenchyma in developing wood. The hybridization signals for *PtrGT43A* (B) and *PtrGT43C* (C) were also evident in phloem fibers. The section hybridized with the sense RNA probe of *PtrGT43A* exhibited no apparent hybridization signals (E). pf, phloem fiber; rp, ray parenchyma; ve, vessel; xf, xylary fiber. Bars = 81 μm.

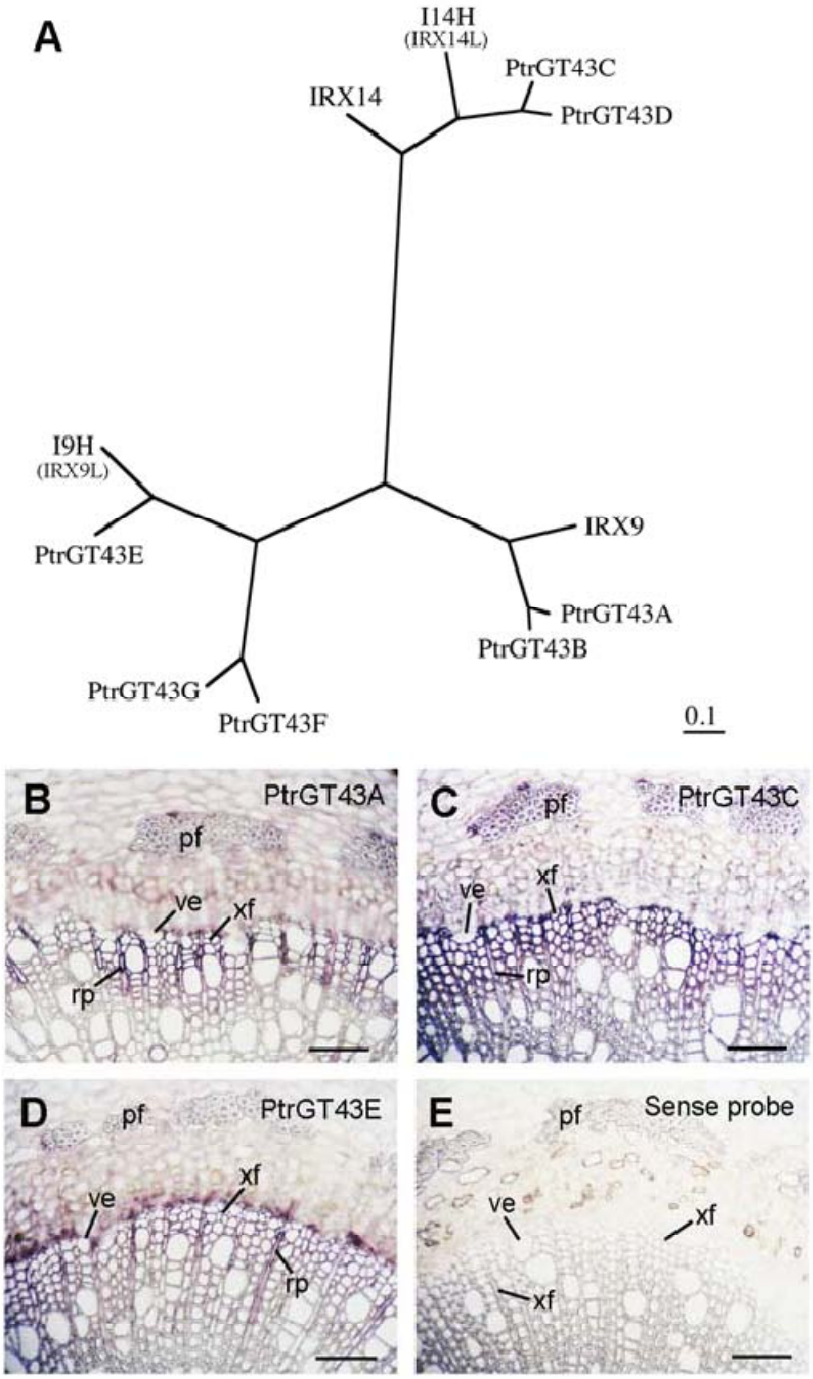
A
I14H
(IRX14L)
PtrGT43C
IRX14
PtrGT43D
I9H
(IRX9L)
IRX9
PtrGT43E
PtrGT43A
PtrGT43B
PtrGT43G
PtrGT43F
0.1
B
PtrGT43A
pf
ve
xf
rp
C
pf
PtrGT43C
ve
xf
rp
D
pf
PtrGT43E
xf
ve
rp
E
pf
Sense probe
ve
xf
xf

Figure 5.2. Subcellular localization of PtrGT43 proteins. Fluorescent protein-tagged fusion proteins were expressed in carrot protoplasts, and the fluorescent signals were detected with a laser confocal microscope. **(A)** to **(D)** PtrGT43 are type II membrane proteins as predicted by the TMHMM2.0 program. Inside, the cytoplasmic side of the membrane; outside, the noncytoplasmic side of the membrane. **(E)** and **(F)** A carrot protoplast (E; differential interference contrast image) expressing YFP alone showing the fluorescent signals throughout the cytoplasm (F). **(G)** to **(J)** A carrot protoplast (G) co-expressing PtrGT43A-YFP (H) and the Golgi-localized FRA8-CFP (I). **(K)** to **(N)** A carrot protoplast (K) co-expressing PtrGT43C-YFP (L) and FRA8-CFP (M). **(O)** to **(R)** A carrot protoplast (O) co-expressing PtrGT43D-YFP (P) and FRA8-CFP (Q). **(S)** to **(V)** A carrot protoplast (S) co-expressing PtrGT43E-YFP (T) and FRA8-CFP (U). Note the colocalization of PtrGT43A-YFP (J), PtrGT43C-YFP (N), PtrGT43D-YFP (R), and PtrGT43E (V) with the Golgi marker FRA8-CFP. Bars = 24 μm.

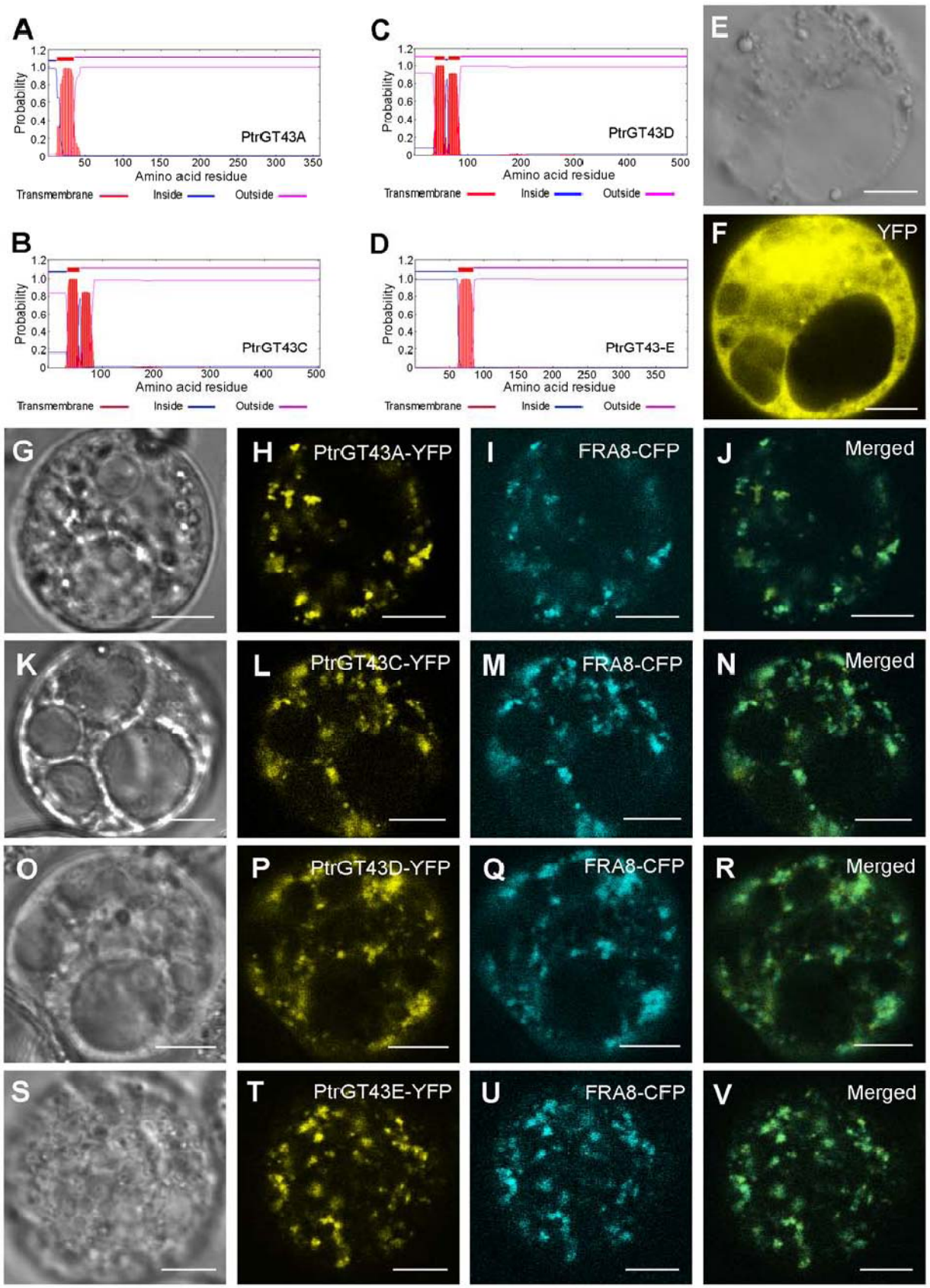
A
PtrGT43A
Probability
Amino acid residue
Transmembrane
Inside
Outside
B
PtrGT43C
C
PtrGT43D
D
PtrGT43-E
E
F
YFP
G
H
PtrGT43A-YFP
I
FRA8-CFP
J
Merged
K
L
PtrGT43C-YFP
M
FRA8-CFP
N
Merged
O
P
PtrGT43D-YFP
Q
FRA8-CFP
R
Merged
S
T
PtrGT43E-YFP
U
FRA8-CFP
V
Merged

Figure 5.3. Complementation analysis of PtrGT43 members in the *Arabidopsis irx9* and *irx14* mutants. The full-length *PtrGT43* cDNAs driven by the CaMV 35S promoter were introduced into *irx9* or *irx14* and the bottom parts of inflorescence stems of 10-week-old transgenic plants were examined for the stem breaking strength (A) and vessel morphology (B to Q). Bar in (B) = 58 μm in (B) to (Q). **(A)** Measurement of the breaking strength of stems of the wild type, *irx9*, *irx14*, and the mutants overexpressing PtrGT43 members. Each bar represents the breaking force of the inflorescence stem of individual plants. Note that the stem breaking strength of *irx9* was restored by overexpression of PtrGT43A/B/E and that of *irx14* was restored by overexpression of PtrGT43C/D. **(B)** to **(I)** The collapsed vessel phenotype (arrow) exhibited in the *irx9* mutant was rescued by overexpression of PtrGT43A/B/E but not PtrGT43C/D. **(J)** to **(Q)** The collapsed vessel phenotype (arrow) exhibited in the *irx14* mutant was rescued by overexpression of PtrGT43C/D but not PtrGT43A/B/E.

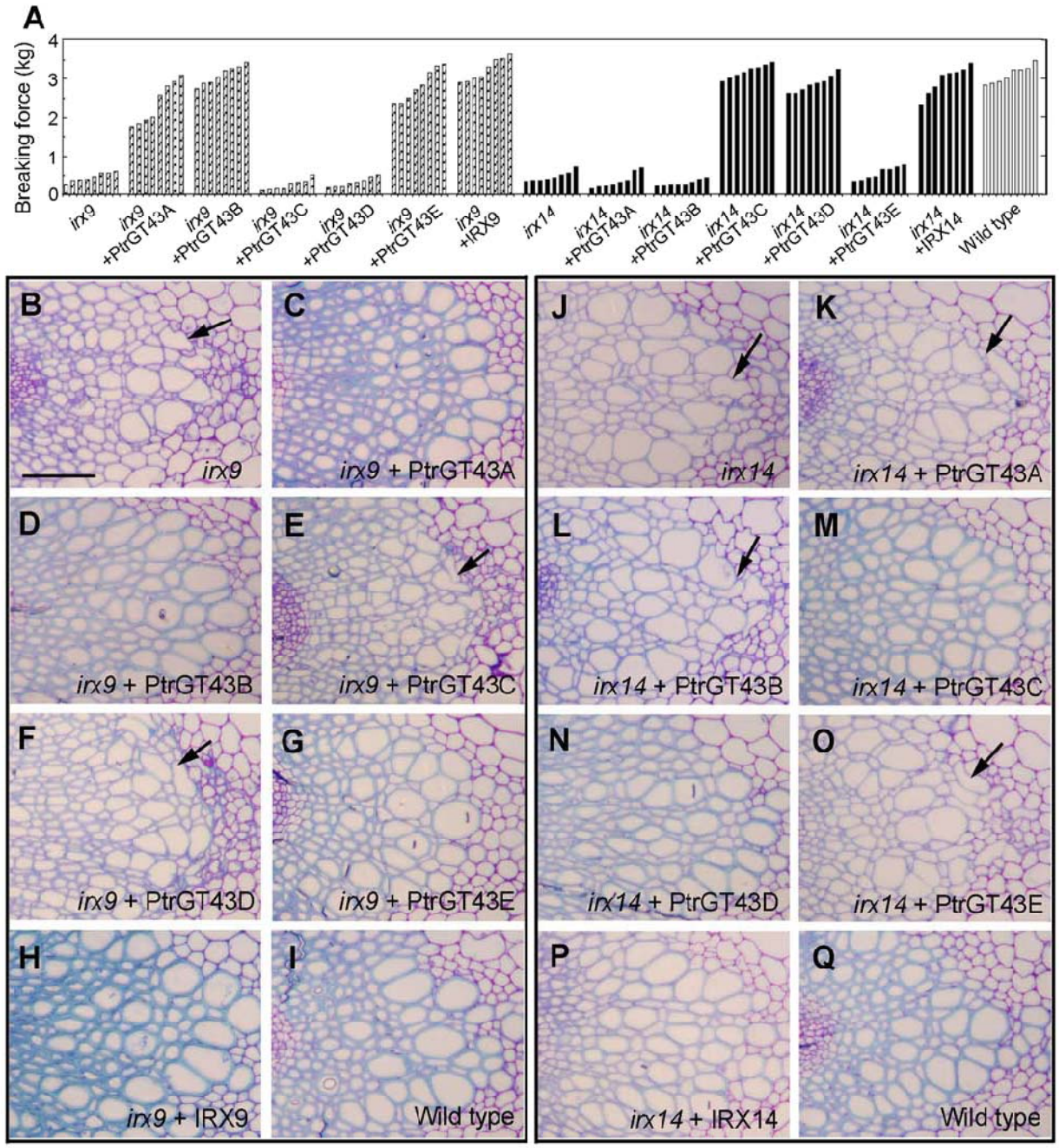
A
Breaking force (kg)
0
1
2
3
4
irx9
irx9 +PtrGT43A
irx9 +PtrGT43B
irx9 +PtrGT43C
irx9 +PtrGT43D
irx9 +PtrGT43E
irx9 +IRX9
irx14
irx14 +PtrGT43A
irx14 +PtrGT43B
irx14 +PtrGT43C
irx14 +PtrGT43D
irx14 +PtrGT43E
irx14 +IRX14
Wild type
B
irx9
C
irx9 + PtrGT43A
D
irx9 + PtrGT43B
E
irx9 + PtrGT43C
F
irx9 + PtrGT43D
G
irx9 + PtrGT43E
H
irx9 + IRX9
I
Wild type
J
irx14
K
irx14 + PtrGT43A
L
irx14 + PtrGT43B
M
irx14 + PtrGT43C
N
irx14 + PtrGT43D
O
irx14 + PtrGT43E
P
irx14 + IRX14
Q
Wild type

Figure 5.4. Transmission electron microscopic analysis of secondary walls in the *irx9* and *irx14* mutants overexpressing PtrGT43. The bottom parts of inflorescence stems of 10-week-old transgenic plants were examined for the secondary wall thickness of interfascicular fibers. Bar in (A) = 8.7 μm in (A) to (P). **(A)** to **(H)** Restoration of the secondary wall thickness of interfascicular fibers in the stems of the *irx9* mutant by overexpression of PtrGT43A/B/E but not PtrGT43C/D. **(I)** to **(P)** Restoration of the secondary wall thickness of interfascicular fibers in the stems of the *irx14* mutant by overexpression of PtrGT43C/D but not PtrGT43A/B/E.

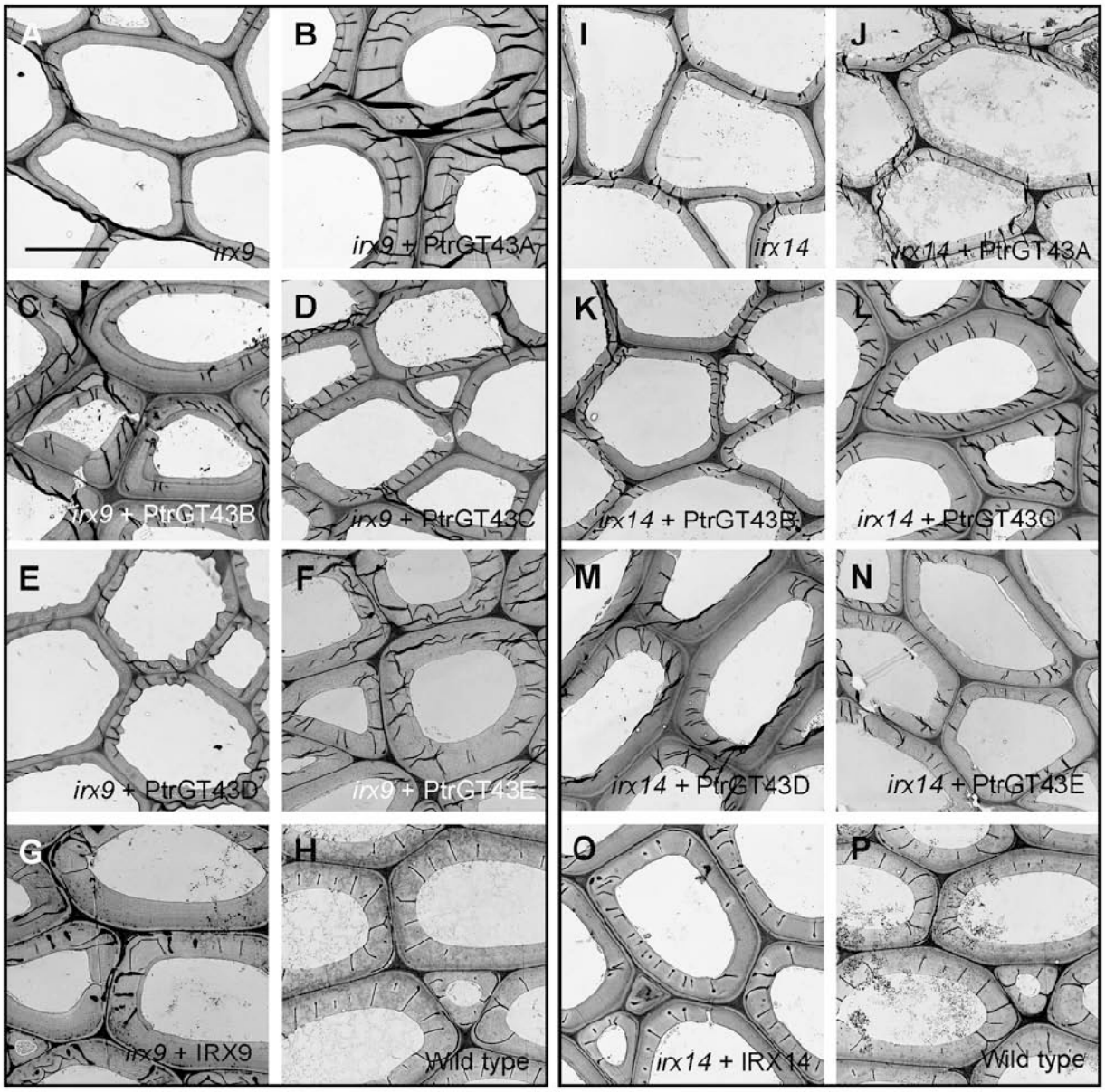
A
irx9
B
irx9 + PtrGT43A
I
irx14
J
irx14 + PtrGT43A
C
irx9 + PtrGT43B
D
irx9 + PtrGT43C
K
irx14 + PtrGT43B
L
irx14 + PtrGT43C
E
irx9 + PtrGT43D
F
irx9 + PtrGT43E
M
irx14 + PtrGT43D
N
irx14 + PtrGT43E
G
irx9 + IRX9
H
Wild type
O
irx14 + IRX14
P
Wild type

Figure 5.5. MALDI-TOF mass spectra of acidic xylooligosaccharides generated by β-endoxylanase digestion of xylan from stems of the wild type, *irx9*, *irx14*, and the mutants Overexpressing PtrGT43. The ions at *m/z* 745 and 759 correspond to xylotetrasaccharides bearing a GlcA residue (X_4G) or a methylated GlcA residue (X_4M). The ion at *m/z* 891 corresponds to xylopentasaccharide bearing a methylated GlcA residue (X_5M). **(A)** to **(H)** Restoration of the missing ion at *m/z* 745 corresponding to X_4G (arrows) in *irx9* by overexpression of PtrGT43A/B/E but not PtrGT43C/D. **(I)** to **(P)** Restoration of the missing ion at *m/z* 745 corresponding to X_4G (arrows) in *irx14* by overexpression of PtrGT43C/D but not PtrGT43A/B/E.

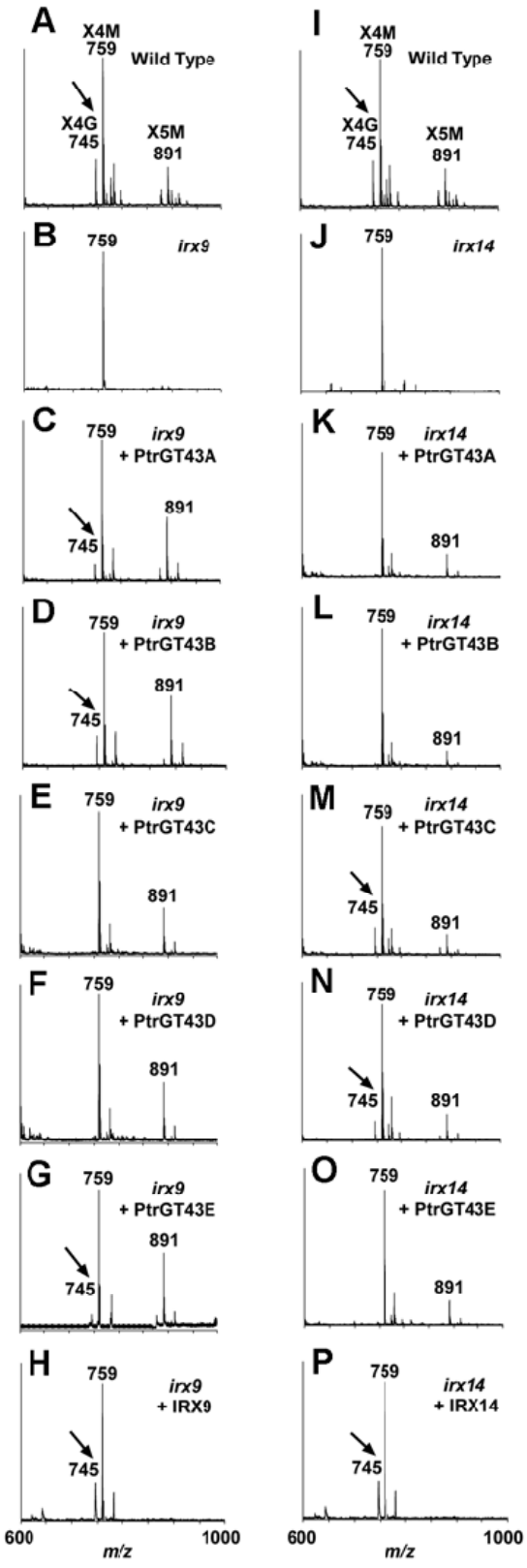
A
X4M
759
Wild Type
X4G
745
X5M
891
B
759
irx9
C
759
irx9
+ PtrGT43A
891
745
D
759
irx9
+ PtrGT43B
891
745
E
759
irx9
+ PtrGT43C
891
F
759
irx9
+ PtrGT43D
891
G
759
irx9
+ PtrGT43E
891
745
H
759
irx9
+ IRX9
745
600
1000
m/z
I
X4M
759
Wild Type
X4G
745
X5M
891
J
759
irx14
K
759
irx14
+ PtrGT43A
891
L
759
irx14
+ PtrGT43B
891
M
759
irx14
+ PtrGT43C
745
891
N
759
irx14
+ PtrGT43D
745
891
O
759
irx14
+ PtrGT43E
891
P
759
irx14
+ IRX14
745
600
1000
m/z

Figure 5.6. ^{1}H-NMR spectra of acidic xylooligosaccharides generated by β-endoxylanase digestion of xylan from stems of the wild type, *irx9*, *irx14*, and the mutants overexpressing PtrGT43. Resonances are labeled with the position of the assigned proton and the identity of the residue containing that proton. Note the restoration of the resonance of H1 of α-GlcA in *irx9* complemented with PtrGT43A/B/E and in *irx14* complemented with PtrGT43C/D (arrows). The resonances for the xylan reducing end tetrasaccharide sequence are shown as H1 of α-D-GalA, H1 of α-L-Rha, H1 of 3-linked β-D-Xyl, H4 of α-D-GalA, and H2 of α-L-Rha. Note that *irx 9* and *irx14* exhibit an elevated resonance intensity of the xylan reducing end tetrasaccharide sequence compared with the wild type and that this elevation is reduced in *irx9* overexpressing PtrGT43A/B/E and in *irx14* overexpressing PtrGT43C/D. The doublet resonance peak at 4.39 ppm in the wild type is assigned to H5 α-GlcA and that at 4.36 ppm is assigned to H5 Me-α-GlcA. The resonance shift of H5 proton in some of the other samples is likely attributed to its high sensitivity to a slight variation of pH and concentration of the samples because of its close proximity to the carboxyl group. HDO, hydrogen deuterium oxide.

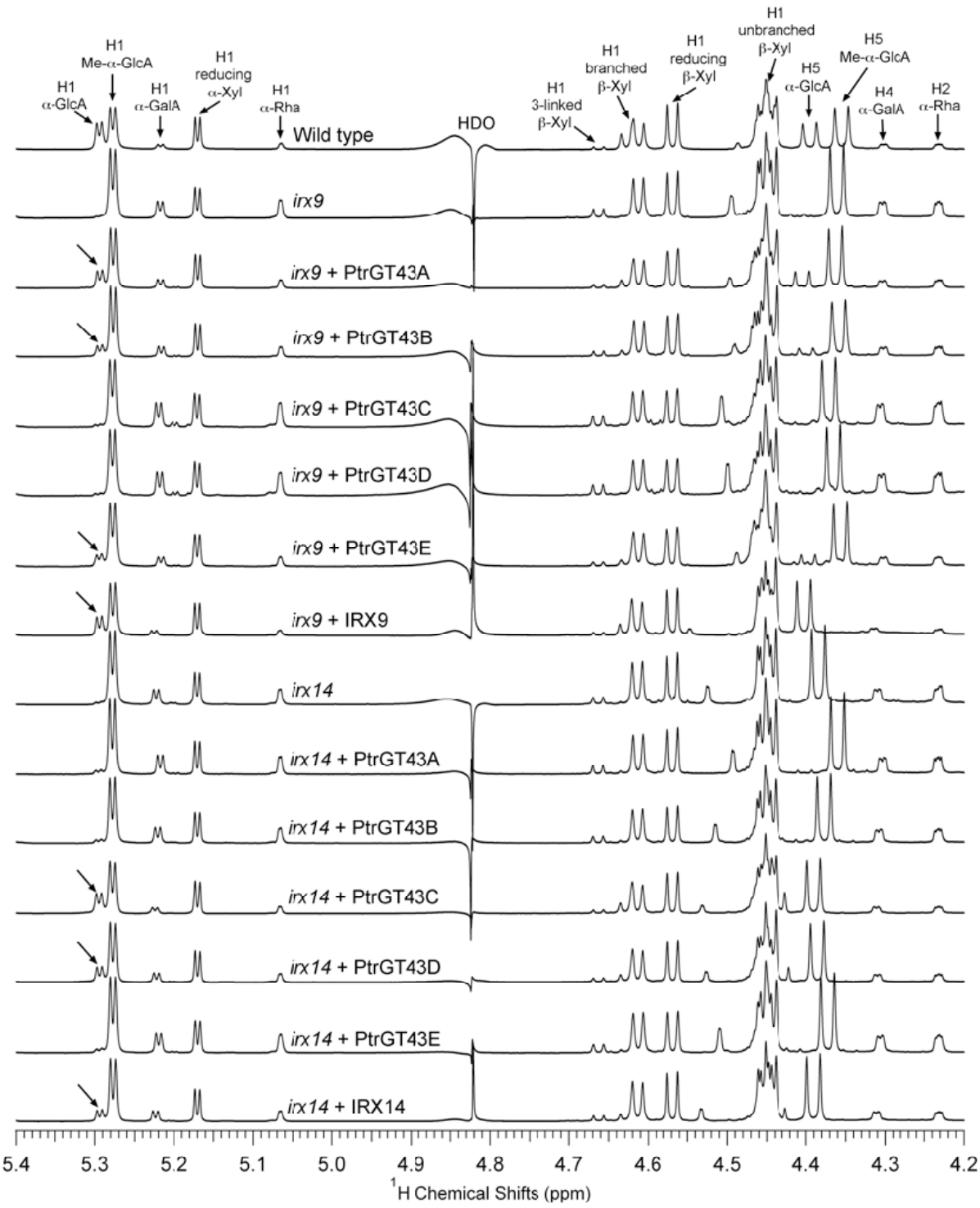
H1 α-GlcA
H1 Me-α-GlcA
H1 α-GalA
H1 reducing α-Xyl
H1 α-Rha
H1 3-linked β-Xyl
H1 branched β-Xyl
H1 reducing β-Xyl
H1 unbranched β-Xyl
H5 α-GlcA
H5 Me-α-GlcA
H4 α-GalA
H2 α-Rha
HDO
Wild type
irx9
irx9 + PtrGT43A
irx9 + PtrGT43B
irx9 + PtrGT43C
irx9 + PtrGT43D
irx9 + PtrGT43E
irx9 + IRX9
irx14
irx14 + PtrGT43A
irx14 + PtrGT43B
irx14 + PtrGT43C
irx14 + PtrGT43D
irx14 + PtrGT43E
irx14 + IRX14
5.4 5.3 5.2 5.1 5.0 4.9 4.8 4.7 4.6 4.5 4.4 4.3 4.2
1H Chemical Shifts (ppm)

Figure 5.7. Time course of the xylosyltransferase activity in the wild type, *irx9*, *irx14*, and the mutants overexpressing PtrGT43. Microsomes were isolated from inflorescence stems of 7-week-old *Arabidopsis* plants and subjected to the assay of xylosyltransferase activity using xylohexaose as an acceptor and UDP-[^{14}C]Xyl as a donor. **(A)** Partial restoration of the xylosyltransferase activity in *irx9* overexpressing PtrGT43A/B/E. A slight increase in the xylosyltransferase activity was also seen in *irx9* overexpressing PtrGT43C/D. **(B)** Partial restoration of the xylosyltransferase activity in *irx14* overexpressing PtrGT43C/D. Note that overexpression of PtrGT43E in *irx14* also resulted in an elevation in the xylosyltransferase activity.

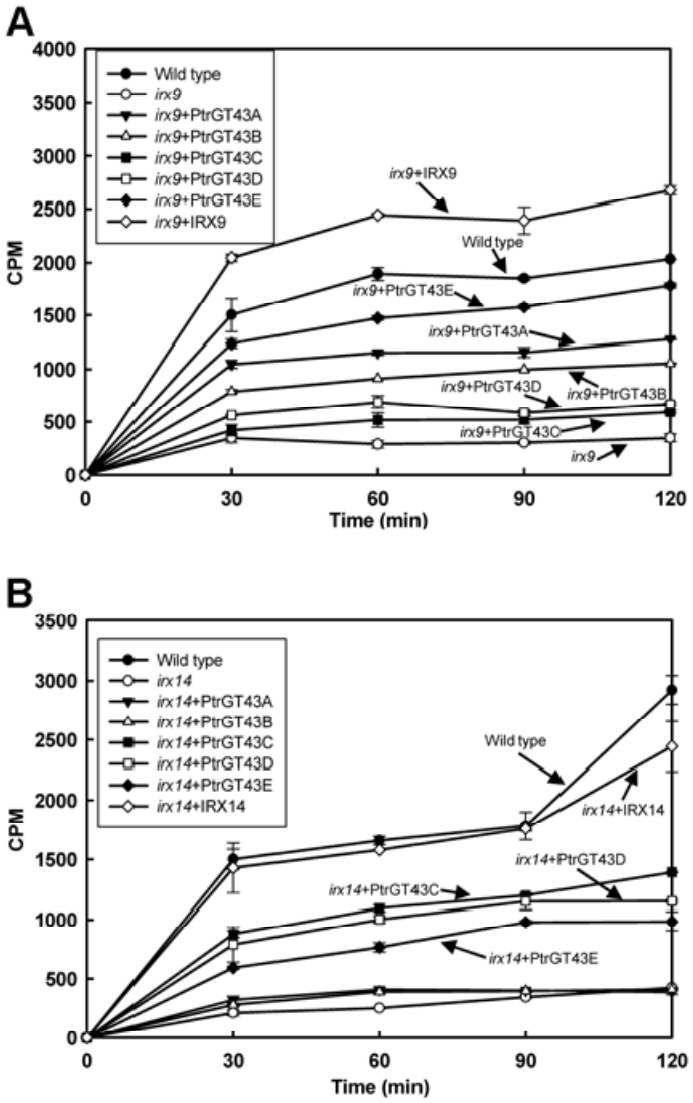
A
Wild type
irx9
irx9+PtrGT43A
irx9+PtrGT43B
irx9+PtrGT43C
irx9+PtrGT43D
irx9+PtrGT43E
irx9+IRX9
CPM
Time (min)
irx9+IRX9
Wild type
irx9+PtrGT43E
irx9+PtrGT43A
irx9+PtrGT43D
irx9+PtrGT43B
irx9+PtrGT43C
irx9
B
Wild type
irx14
irx14+PtrGT43A
irx14+PtrGT43B
irx14+PtrGT43C
irx14+PtrGT43D
irx14+PtrGT43E
irx14+IRX14
CPM
Time (min)
Wild type
irx14+IRX14
irx14+PtrGT43D
irx14+PtrGT43C
irx14+PtrGT43E

Figure 5.8. Effects of RNAi downregulation of expression of *PoGT43B* and *PoGT8D* on Poplar wood development. **(A)** Real-time quantitative PCR analysis showing a reduction in the expression of *PoGT43A/B* in *PoGT43B* RNA lines and that of *PoGT8D/8D-2* in *PoGT8D* RNA lines. The expression level of *PoGT43A/B* or *PoGT8D/8D-2* in the control is taken as 100. Error bars represent the SE of three independent replicates. **(B)** to **(F)** Cross sections of the secondary xylem of stems showing deformed vessel morphology (arrows) and thin walls of xylary fibers in the RNAi lines of *PoGT43B* (C and D) and *PoGT8D* (E and F) compared with the control (B). Stems from 9-month-old plants were sectioned and stained with toluidine blue for examination of wood cells. rp, ray parenchyma; ve, vessel; xf, xylary fiber. Bar in (B) = 73 μm for (B) to (F).

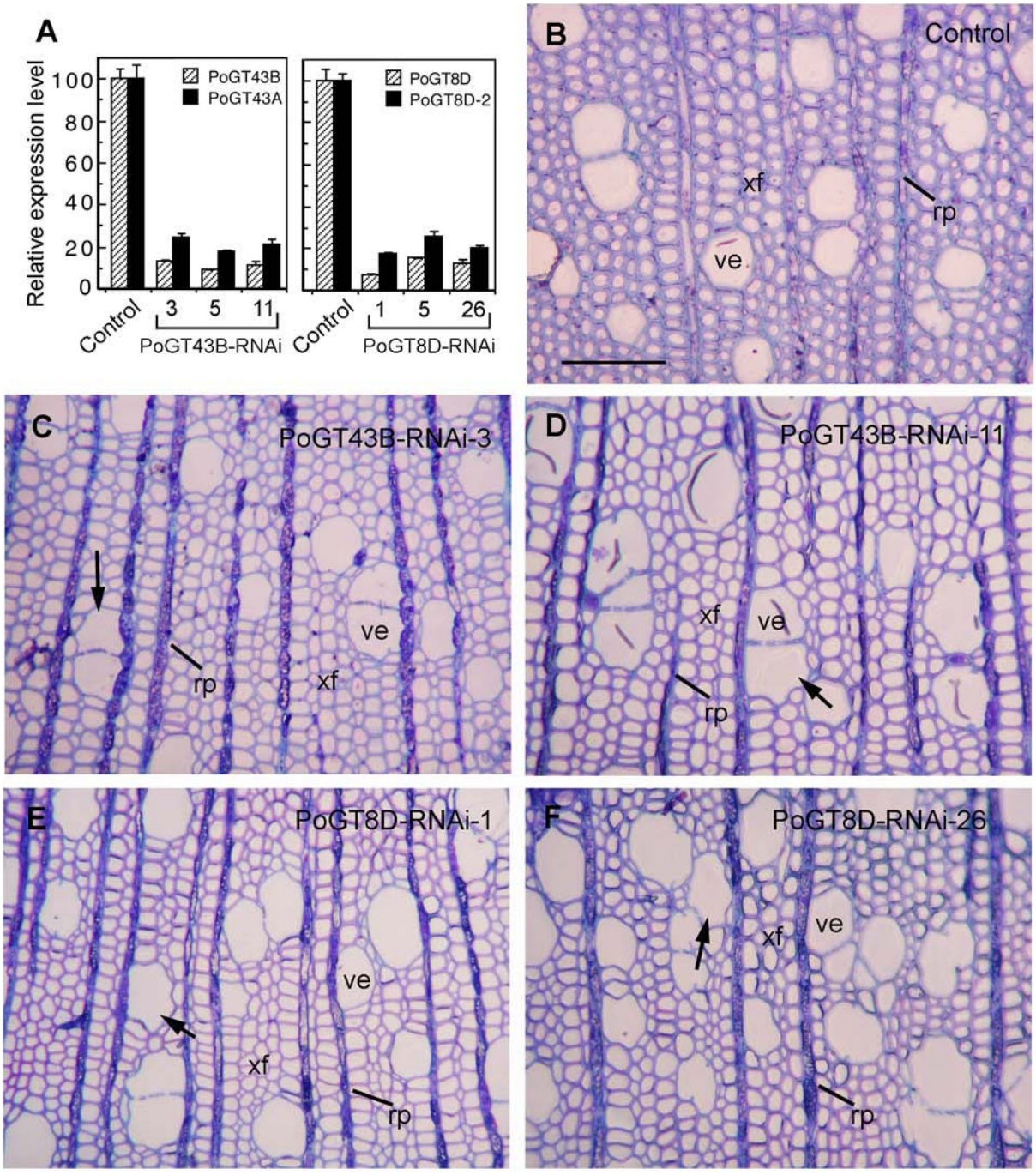
A
Relative expression level
100
80
60
40
20
0
PoGT43B
PoGT43A
PoGT8D
PoGT8D-2
Control
3
5
11
PoGT43B-RNAi
Control
1
5
26
PoGT8D-RNAi
B
Control
xf
rp
ve
C
PoGT43B-RNAi-3
ve
rp
xf
D
PoGT43B-RNAi-11
xf
ve
rp
E
PoGT8D-RNAi-1
ve
xf
rp
F
PoGT8D-RNAi-26
xf
ve
rp

Figure 5.9. Transmission electron microscopic analysis of the wood of the control, *PoGT43B*- and *PoGT8D*-RNAi lines. Note the significant reduction in the wall thickness of fibers in the RNAi lines of *PoGT43B* (B and C) and *PoGT8D* (D and E) compared with the control (A). Bar in (A) = 6.9 μm for (A) to (E).

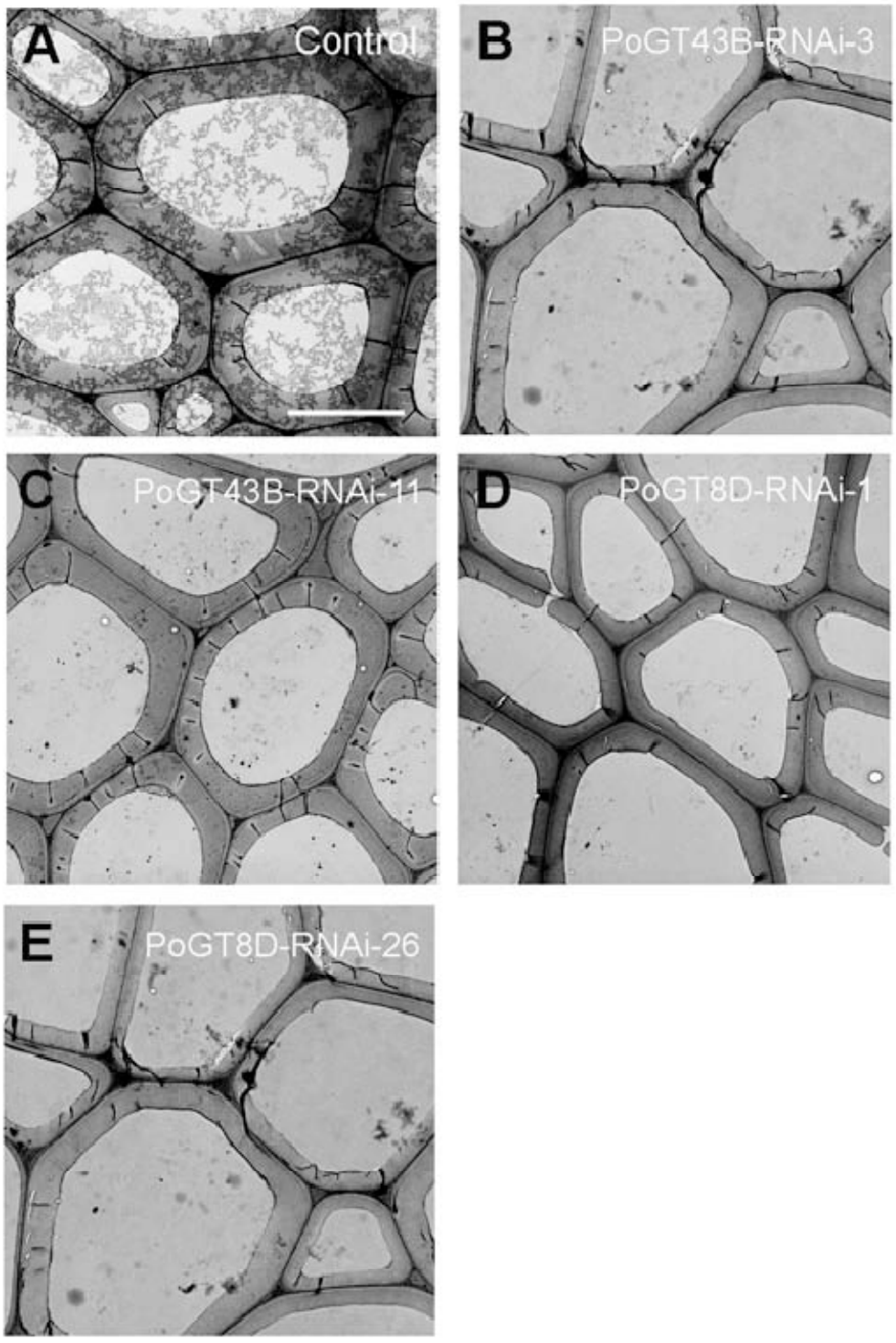
A
Control
B
PoGT43B-RNAi-3
C
PoGT43B-RNAi-11
D
PoGT8D-RNAi-1
E
PoGT8D-RNAi-26

Figure 5.10. Immunodetection of xylan in the wood of the control, *PoGT43B*- and *PoGT8D*-RNAi lines. Stems from 9-month-old wild type (A), *PoGT43B* (B) and *PoGT8D* (C) RNAi lines were sectioned and probed with the monoclonal xylan antibody LM10. Xylan signals were detected with fluorescein isothiocyanate-conjugated secondary antibodies and visualized with a laser confocal microscope. Note the drastic reduction in the xylan signals in the secondary xylem of *PoGT8D* RNAi line (C) compared with the control (A). pf, phloem fiber; sx, secondary xylem. Bar in (A) = 260 μm for (A) to (C).

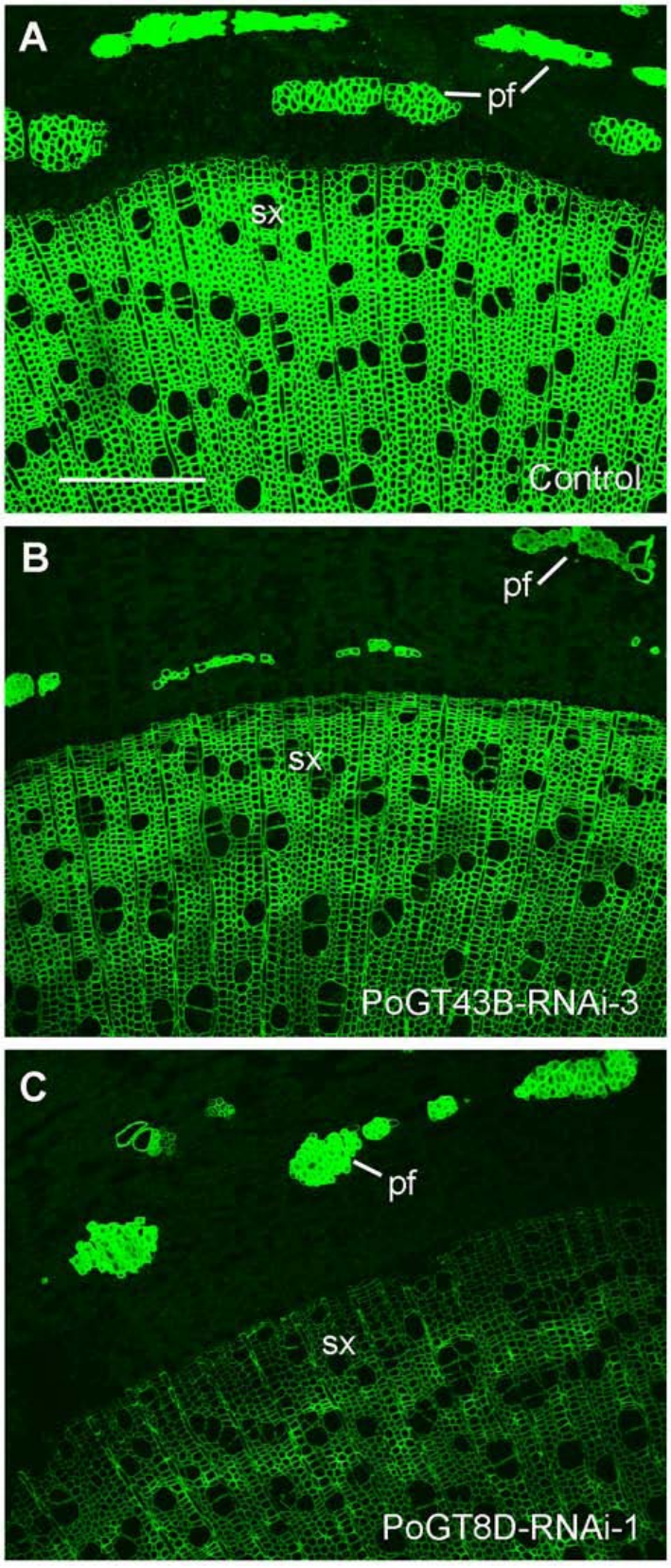
A
pf
sx
Control
B
pf
sx
PoGT43B-RNAi-3
C
pf
sx
PoGT8D-RNAi-1

Figure 5.11. ^{1}H-NMR spectra of xylooligosaccharides generated by β-endoxylanase digestion of xylan from the wood of the control, *PoGT43B*- and *PoGT8D*-RNAi lines. Resonances are labeled with the position of the assigned proton and the identity of the residue containing that proton. It is evident that compared with the control, the resonances of H1 of α-D-GalA, H1 of α-L-Rha, H1 of 3-linked β-D-Xyl, H4 of α-D-GalA, and H2 of α-L-Rha from the xylan reducing end sequence were reduced in *PoGT8D* RNAi lines but elevated in *PoGT43B-3* RNAi lines. The ^{1}H-NMR spectrum of xylooligosaccharides from *Arabidopsis* xylan is included for comparison. Note that the resonances of α-GlcA residues are prominent in *Arabidopsis* xylooligosaccharides (asterisks) but nearly absent in poplar xylooligosaccharides.

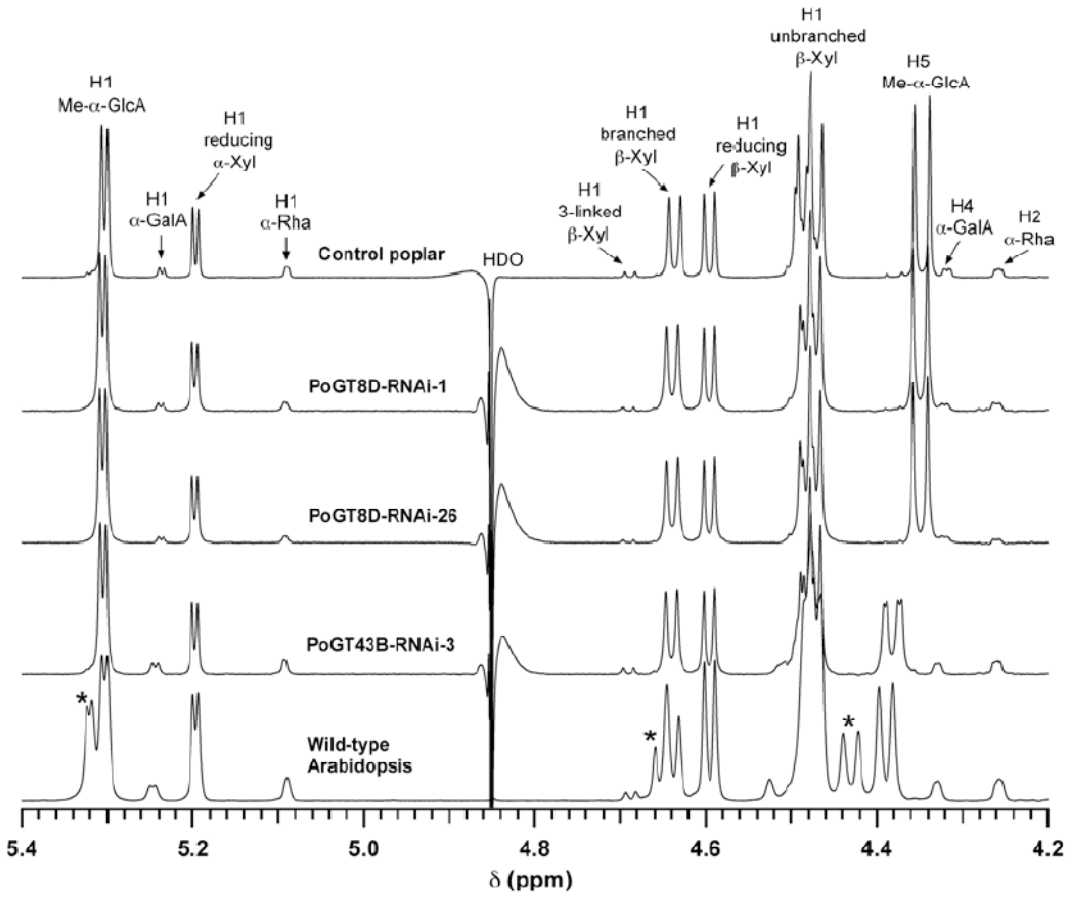
H1
Me-α-GlcA
H1
reducing
α-Xyl
H1
α-GalA
H1
α-Rha
Control poplar
HDO
H1
3-linked
β-Xyl
H1
branched
β-Xyl
H1
reducing
β-Xyl
H1
unbranched
β-Xyl
H5
Me-α-GlcA
H4
α-GalA
H2
α-Rha
PoGT8D-RNAi-1
PoGT8D-RNAi-26
PoGT43B-RNAi-3
Wild-type
Arabidopsis
*
*
*
5.4
5.2
5.0
4.8
4.6
4.4
4.2
δ (ppm)

Figure 5.12. Glucose release by cellulase enzymes from wood cell walls of the control, *PoGT43B* and *PoGT8D* RNAi lines. Wood cell walls of the control, *PoGT43B*- and *PoGT8D*-RNAi lines were incubated with cellulase and cellobiase. The enzymatic hydrolysis efficiency is presented by the percentage of glucose released by the enzymes over the total cellulose amount in the cell walls. Data are means ± SE of two separate assays and the quantitative difference of the data between the control and PoGT43-RNAi lines was found to be statistically significant using the Student's *t* test program (http://www.graphpad.com/quickcalcs/ttest1.cfm) ($p < 0.001$).

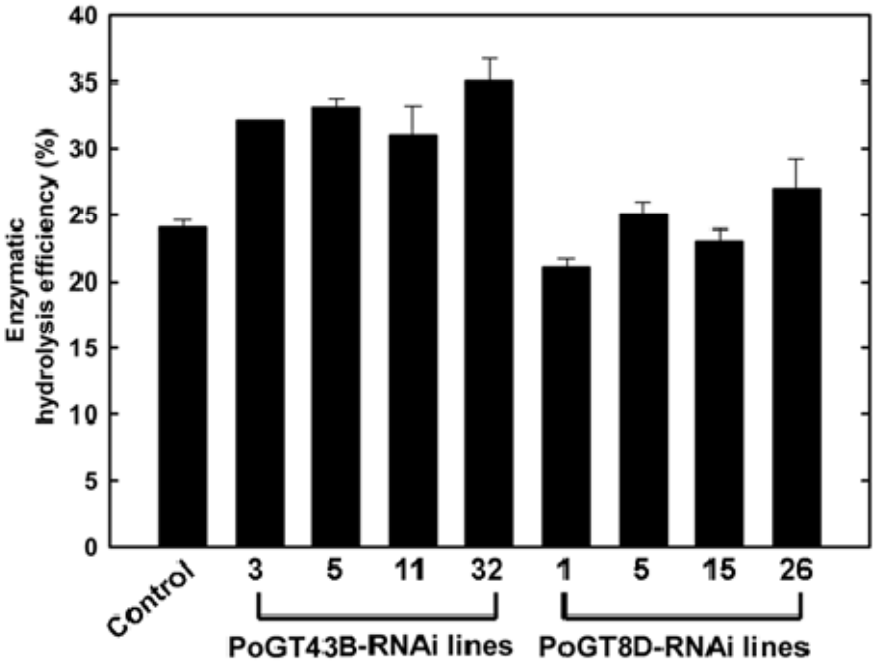
Enzymatic hydrolysis efficiency (%)
40
35
30
25
20
15
10
5
0
Control
3
5
11
32
1
5
15
26
PoGT43B-RNAi lines
PoGT8D-RNAi lines

CHAPTER 6

CONCLUSIONS

Xylan is an abundant hemicellulose and plays pivotal functions in the proper secondary cell wall formation. Xylan has recently attracted much attention since it might provide an important source of sugars for biofuel production from higher plants. Thus, understanding xylan biosynthesis is crucial not only to illuminate the basic features of cell wall biology, but also to lead us to design a better strategy for plant biotechnology.

The biosynthesis of xylan requires a number of glycosyltransferases and modifying enzymes. Given that more than 500 glycosyltransferases exist in the *Arabidopsis* genome, it is unrealistic to use traditional biochemical approaches to identify xylan biosynthetic enzymes. Recently, transcriptional profiling of genes specifically expressed in cells undergoing secondary cell wall deposition in *Arabidopsis* and Poplar has contributed to the identification of the candidate genes involved in xylan biosynthesis (Aspeborg et al., 2005; Brown et al., 2005). Detailed characterization of those T-DNA mutants has led to the identification of multiple glycosyltransferase that are essential for xylan biosynthesis. Among them, three proteins, FRA8, IRX8, and PARVUS appear to be responsible for the reducing end sequence (Pena et al., 2007; Lee et al., 2007a, 2010; Brown et al., 2007). Two functionally redundant glycosyltransferases, GUX1 and GUX2 in family GT8, seem to be required for the substitution of glucuronic acid (Mortimer et al., 2010).

Xylan backbone is composed of β-(1,4)-linked xylosyl residues in which each xylosyl residue is inverted nearly 180° with respect to each neighboring xylose. Thus, biosynthesis of xylan backbone needs to overcome this steric problem by either iterative addition of disaccharide units, β-(1,4)-linked xylose dimer, or involvement of at least two enzymes with opposing catalytic sites (Carpita, 2011). It was previously proposed that a member of the cellulose synthase-like (Csl) gene family may encode xylan backbone synthase (XylTase) because the only difference between glucose and xylose is the absence of the primary alcohol group at C6 in xylose (Richmond and Somerville, 2001; Lerouxel et al., 2006). However, heterologous expression of Csl proteins did not show the activity of XylTase (Liepman et al., 2005).

As an initial step to unambiguously identifying xylan backbone synthase, we established *in vitro* activity assay to detect XylTase activity from *Arabidopsis* stem microsomes. Early biochemical studies revealed that microsomal membrane fractions from different plants possess XylTase, which catalyzes the transfer of xylose from UDP-xylose to either an endogenous acceptor or exogenous xylooligosaccharide (Lee et al., 2007a). We determined that microsomes from *Arabidopsis* inflorescence stem, where xylan is actively synthesized, also contained XylTase, which is dependent on the presence of exogenous oligosaccharides. We confirmed that the reaction products are identical to the β-(1,4)-linked elongating oligomers by MALDI-TOF and endo- β-(1,4)-xylanase treatment.

We next determined if microsomes from any of xylan mutants (*fra8*, *irx8*, *irx9*, and *parvus*) are deficient in XylTase activity (Lee et al., 2007a). XylTase activities measured from *fra8*, *irx8*, and *parvus* mutant microsomes are comparable to that of wild type. In contrast, *irx9* exhibited a substantial reduction in XylTase activity, suggesting that IRX9 is essential for xylan chain elongation. These findings are consistent with the previous NMR data that the shortened

chain length of xylan backbone was found in *irx9*, whereas *fra8*, *irx8*, and *parvus* mutations resulted in the loss of reducing end sequence, but no effect on the xylan chain length.

In order to characterize the exact biochemical function of IRX9, we heterologously expressed IRX9 in yeast cells and Tobacco Bright Yellow-2 (BY-2) cells (Unpublished data). No XylTase activity was detected using recombinant IRX9 protein, leading to the possibility that more enzymatic/regulatory components are required for xylan backbone elongation.

Brown et al. identified an additional xylan biosynthetic gene *IRX14* encoding a member of family GT43 (Brown et al., 2007). Mutation of IRX14 resulted in similar defects in xylan chain length and XylTase activity as *irx9*. Thus, IRX14 is likely to have a role in xylan backbone elongation.

There exist four GT43 members in the *Arabidopsis* genome IRX9, I9H, IRX14, and I14H. Two (IRX9 and IRX14) of them appear to be essential for xylan backbone elongation. Thus, we questioned whether IRX9 and IRX14 perform the same biochemical function and whether the other two GT43 members are also involved in xylan biosynthesis. In order to address these questions, we performed comprehensive molecular and genetic studies of the role of all members of family GT43 (Lee et al., 2010). We found that I9H and I14H are redundant in function with IRX9 and IRX14, repectively, based on complementation tests and double mutant analysis. No xylan deficient phenotypes were observed in the single mutation of *I9H* and *I14H*, indicating that IRX9 and IRX14 are functionally dominant in xylan biosynthesis in vivo. We also found that IRX9 and IRX14 are two functionally nonredundant glycosyltransferases in xylan backbone elongation.

Multiple lines of evidence indicate that GTs involved in xylan biosynthesis are highly conserved between *Arabidopsis* and Poplar. First, all *Arabidopsis* GTs participating in xylan

biosynthesis have close homologs in Poplar. Previous transcriptional analysis in Poplar has shown that these homologs are specifically expressed in wood-forming tissues (Aspeborg et al., 2005; Ye et al., 2006). Second, overexpression of the Poplar homologs (PoGT47C, PoGT8D, PoGT43B, and PoGT8E/F) in the corresponding *Arabidopsis* mutants leads to the complete restoration of mutant phenotypes and chemotypes to wild type level (Zhou et al., 2006, 2007; Lee et al., 2009b). Third, down-regulation of PoGT47C, homologous to *Arabidopsis* FRA8, resulted in a reduction of the thickness of secondary walls, a decreased amount of xylose, and a reduction in the abundance of the reducing end sequence (Lee et al., 2009a). Fourth, considering the structural similarity of xylan polymer found in *Arabidopsis* and Poplar, it is conceivable that the overall enzymatic actions to complete xylan biosynthesis are performed by homologous GTs.

There exist seven members of GT43 family in the Poplar genome. Five of them are highly expressed during wood formation and their encoded proteins are targeted to the Golgi. Genetic complementation experiments demonstrated that PtrGT43 A/B/E are functional homologs of *Arabidopsis* IRX9, and PtrGT43 C/D are homologs of IRX14 (Lee et al., 2011). Downregulation of PtrGT43B expression through RNAi resulted in the xylan deficient phenotypes that included thin secondary cell walls and a reduced level of xylose content (Lee et al., 2011). Also, structural analysis of the xylan isolated from RNAi lines showed an elevation in the abundance of the xylan reducing end sequence, a chemontype similar to the *Arabidopsis irx9* mutant. Thus, our findings provide the genetic evidence that the poplar GT43 members form two functionally nonredundant groups, all of which are involved in the biosynthesis of xylan backbones.

Genetic studies and in vitro activity assay using mutant microsomes led to the hypothesis that *Arabidopsis* IRX9 or IRX14 function as xylan backbone synthase. However, polymerization

activity was not detected using the recombinant IRX9 or IRX14. Hence, we investigated whether the coexpression of IRX9 and IRX14 is required for xylan backbone polymerization. IRX9 and IRX14 were concomitantly expressed in tobacco BY-2 cells, and the resulting transformed lines were screened for in vitro xylan synthase activity. Notably, we detected an increased activity with the incorporation of four to five xylose residues into the acceptors (Lee, C and Ye, Z.H. manuscript in preparation). We confirmed that the reaction products are elongated β-(1,4)-linked xylooligomers by MALDI-TOF and endo- β-(1,4)-xylanase treatment. These findings will provide the first convincing biochemical evidence that successive addition of a xylose unit in β-(1,4) linkage into elongating xylooligosaccharide is cooperatively catalyzed by two golgi localized glycosyltransferases, IRX9 and IRX14, in *Arabidopsis*.

Glycosyltransferases (GTs) are a large famiy of enzymes that are essential to constructing sugar blocks in higher organisms (Lerouxel et al., 2006). Due to the presence of complex cell walls in plants, more GTs have been found (approximatedly 450 GTs in *Arabidopsis* and 800 GTs in Poplar). In order to make different complex polysaccharides found in the plant cell wall, it is apparent that the concerted and coordinated series of action of a number of GT are required. Given the fact that the classification of GTs into families is mainly derived from amino acid sequence similarities, not from catalytic activities, only limited information (fold types and stereochemical outcomes) can be obtained for the precise enzymatic roles. Genetic and molecular studies are indispensible to gain a better understanding of the possible roles of GTs and thereby design a better approach for its biochemical characterization.

In docot plants, secondary cell walls are predominantly composed of cellulose, xylan, mannan, and lignin. Molecular analysis of GT-encoding genes and detailed characterization of those T-DNA mutants have led to the identification of several xylan biosynthetic genes in

Arabidopsis. We showed the genetic and biochemical evidence that the coorperative activities of IRX9 and IRX14 are required for xylan backbone polymerization. However, the precise biochemical function of other GTs is presently still unknown. Thus, the next important challenge to increase our knowledge on the xylan biosynthesis is to provide biochemical evidence of FRA8, IRX8, PARVUS, GUX1/2, and IRX10/10L. In addition, understanding how the xylan polymers synthesized in the Golgi are transported and assembled during secondary cell wall formation is also an important issue that must be addressed.

REFERENCES

Aspeborg, H., Schrader, J., Coutinho, P.M., Stam, M., Kallas, A., Djerbi, S., Nilsson, P., Denman, S., Amini, B., Sterky, F., Master, E., Sandberg, G., Mellerowicz, E., Sundberg, B., Henrissat, B. and Teeri, T.T. (2005). Carbohydrate-Active Enzymes Involved in the Secondary Cell Wall Biogenesis in Hybrid Aspen. Plant Physiol. 137: 983-997.

Brown, D.M., Zeef, L.A.H., Ellis, J., Goodacre, R., and Turner, S.R. (2005). Identification of novel genes in Arabidopsis involved in secondary cell wall formation using expression profiling and reverse genetics. Plant Cell 17: 2281–2295.

Brown, D.M., Goubet, F., Wong, V.W., Goodacre, R., Stephens, E., Dupree, P., and Turner, S.R. (2007). Comparison of five xylan synthesis mutants reveals new insight into the mechanisms of xylan synthesis. Plant J 52:1154-1168.

Carpita, N.C. (2011). Update on Mechanisms of Plant Cell Wall Biosynthesis: How Plants Make Cellulose and Other (1→4)-β-d-Glycans. Plant Physiol. 155: 171-184.

Lee, C., O'Neill, M.A., Tsumuraya, Y., Darvill, A.G., and Ye, Z.H. (2007a). The irregular xylem9 mutant is deficient in xylan xylosyltransferase activity. Plant Cell Physiol 48: 1624–1634.

Lee, C., Zhong, R., Richardson, E.A., Himmelsbach, D.S., McPhail, B.T., and Ye, Z.H. (2007b). The PARVUS Gene is Expressed in Cells Undergoing Secondary Wall Thickening and is Essential for Glucuronoxylan Biosynthesis. Plant Cell Physiol 48: 1659-1672.

Lee, C., Teng, Q., Huang, W., Zhong, R., and Ye, Z.H. (2009a). Down-regulation of PoGT47C expression in poplar results in a reduced glucuronoxylan content and an increased wood digestibility by cellulase. Plant Cell Physiol 50: 1075–1089.

Lee, C., Teng, Q., Huang, W., Zhong, R., and Ye, Z.H. (2009b). The poplar GT8E and GT8F glycosyltransferases are functional orthologs of Arabidopsis PARVUS involved in glucuronoxylan biosynthesis. Plant Cell Physiol 50: 1982–1987.

Lee, C., Teng, Q., Huang, W., Zhong, R., and Ye, Z.H. (2010). The Arabidopsis family GT43 glycosyltransferases form two functionally nonredundant groups essential for the elongation of glucuronoxylan backbone. Plant Physiol. 153, 526–541.

Lerouxel, O., Cavalier, D.M., Liepman, A.H., and Keegstra, K. (2006). Biosynthesis of plant cell wall polysaccharides—A complex process. Curr. Opin. Plant Biol 9: 621–630.

Mortimer, J.C., Miles, G.P., Brown, D.M., Zhang, Z., Segura, M.P., Weimar, T., Yu, X., Seffen, K.A., Stephens, E., Turner, S.R., and Dupree, P. (2010). Absence of branches from xylan in Arabidopsis gux mutants reveals potential for simplification of lignocellulosic biomass. Proc Natl Acad Sci U S A. 107(40):17409-14.

Pena, M.J., Zhong, R., Zhou, G.-K., Richardson E.A., O'Neill, M.A., Darvill, A.G., York, W.S., and Ye, Z.H. (2007). Arabidopsis irregular xylem8 and irregular xylem9: implications for the complexity of glucuronoxylan biosynthesis. Plant Cell 19:549–563.

Ye, Z.H., York, W.S., and Darvill, A.G. (2006). Important new players in secondary wall synthesis. Trends Plant Sci. 11: 162–164.

Zhou, G.K., Zhong, R., Richardson, E.A., Himmelsbach, D.S., McPhail, B.T., and Ye, Z.-H. (2007). Molecular characterization of PoGT8D and PoGT43B, two secondary wall-associated glycosyltransferases in poplar. Plant Cell Physiol. 48, 689-699.

Zhou, G.K., Zhong, R., Richardson, E.A., Morrison, W.H. 3rd., Nairn, C.J., Wood-Jones, A., and Ye, Z.-H. (2006). The poplar glycosyltransferase GT47C is functionally conserved with *Arabidopsis fragile fiber8.* Plant Cell Physiol. 47, 1229-1240.